

2009

Controlled functionalization of crystalline polyolefins and their application in soluble polymer support

Jihoon Shin
University of Nevada Las Vegas

Follow this and additional works at: <https://digitalscholarship.unlv.edu/thesesdissertations>

 Part of the [Organic Chemistry Commons](#), and the [Polymer Chemistry Commons](#)

Repository Citation

Shin, Jihoon, "Controlled functionalization of crystalline polyolefins and their application in soluble polymer support" (2009). *UNLV Theses, Dissertations, Professional Papers, and Capstones*. 29.
<https://digitalscholarship.unlv.edu/thesesdissertations/29>

This Dissertation is protected by copyright and/or related rights. It has been brought to you by Digital Scholarship@UNLV with permission from the rights-holder(s). You are free to use this Dissertation in any way that is permitted by the copyright and related rights legislation that applies to your use. For other uses you need to obtain permission from the rights-holder(s) directly, unless additional rights are indicated by a Creative Commons license in the record and/or on the work itself.

This Dissertation has been accepted for inclusion in UNLV Theses, Dissertations, Professional Papers, and Capstones by an authorized administrator of Digital Scholarship@UNLV. For more information, please contact digitalscholarship@unlv.edu.

CONTROLLED FUNCTIONALIZATION OF CRYSTALLINE POLYOLEFINS AND
THEIR APPLICATION IN SOLUBLE POLYMER SUPPORT

by

Jihoon Shin

Bachelor of Engineering
Inha University
1995

Master of Engineering
Inha University
1999

A dissertation submitted in partial fulfillment
of the requirements for the

Doctor of Philosophy Degree in Chemistry
Department of Chemistry
College of Sciences

Graduate College
University of Nevada, Las Vegas
August 2009

ABSTRACT

Controlled Functionalization of Crystalline Polyolefins and Application in Soluble Polymer Support

by

Jihoon Shin

Dr. Chulsung Bae, Examination Committee Chair
Assistant Professor of Chemistry
University of Nevada, Las Vegas

Functionalization of polyolefins has been recognized as a useful methodology for the generation of new materials with a wide range of applications. Recently, crystalline or semi-crystalline polyolefins have drawn increasing attention in both industrial and academic fields as one of the most interesting engineering plastics, due to their remarkable physical and mechanical properties. This dissertation describes: (1) novel methods for the direct postfunctionalization of crystalline polyolefins to introduce functionality, (2) characterizations for the functionalized polymers to analyze their structures, molecular-weight properties, thermal properties, and hydrophilicity, and (3) an application of the modified crystalline polystyrene as a soluble polymer support for recyclable catalysts in green chemistry.

Chapter 1 describes the controlled iridium-catalyzed C–H activation of commercial polystyrenes having three types of tacticity. The resulting boronic group in the polymers was further converted into other versatile groups such as hydroxy and aryl groups via

subsequent modifications. Chapter 2 addresses the preparation of a soluble syndiotactic polystyrene-supported phosphine ligand. The Suzuki–Miyaura cross-coupling was effectively accomplished with the polymer-supported palladium complex, which was recovered quantitatively and recycled several times without any loss of activity and the addition of fresh base. In Chapter 3, controlled electronic aromatic bromination of syndiotactic polystyrene was studied. The brominated polymer could serve as a precursor for polyolefins having variable functionalities. Chapter 4 describes the synthesis of hydroxy-functionalized isotactic poly(1-butene) using controlled and regioselective rhodium-catalyzed C–H functionalization and subsequent oxidation. Atom transfer radical polymerization could generate a polar or amphiphilic graft copolymers from the functionalized crystalline polyolefin.

TABLE OF CONTENTS

ABSTRACT.....	iii
LIST OF FIGURES.....	viii
LIST OF SCHEMES.....	xi
LIST OF TABLES.....	xii
CHAPTER 1 CONTROLLED FUNCTIONALIZATION OF CRYSTALLINE POLYSTYRENES VIA ACTIVATION OF AROMATIC C–H BONDS.....	1
1.1. Abstract.....	1
1.2. Introduction.....	2
1.3. Results and Discussion.....	6
1.3.1. Screening Experiments for Standard Condition of sPS Functionalization..	6
1.3.2. Iridium–Catalyzed C–H Borylation of Crystalline Polystyrenes.....	8
1.3.3. Steric Effect in the C–H Borylation of sPS.....	21
1.3.4. Oxidation of Borylated Polystyrenes.....	22
1.3.5. Suzuki–Miyaura Coupling Reaction of Borylated Polystyrenes.....	27
1.3.6. Size Exclusion Chromatography.....	30
1.3.7. Thermal Analysis.....	33
1.4. Experimental.....	35
1.4.1. General Comments.....	35
1.4.2. Synthesis of Pinacol Boronic Ester–Functionalized Polystyrene.....	37
1.4.3. Synthesis of Hydroxy–Functionalized Polystyrene.....	40
1.4.4. Synthesis of <i>tert</i> -Butyldimethylsilyloxy–Functionalized Polystyrene...	41
1.5. Conclusion.....	43
CHAPTER 2 A HOMOGENEOUS PALLADIUM CATALYST SUPPORTED ON SYNDIOTACTIC POLYSTYRENE AND ITS APPLICATION IN SUZUKI– MIYAUURA CROSS–COUPLING REACTIONS.....	44
2.1. Abstract.....	44
2.2. Introduction.....	44
2.3. Results and Discussion.....	47
2.3.1. Solubility and Precipitation test of Functionalized sPS and aPS.....	47
2.3.2. Syndiotactic Polystyrene-Supported Triphenylphosphine (sPS–TPP)...	49
2.3.3. Effect of Base on the sPS–TPP-Supported Suzuki–Miyaura Reactions.	53
2.3.4. sPS–TPP-Supported Suzuki–Miyaura Reactions of Aryl Halides.....	54
2.3.5. Recovery/Recycling of sPS–TPP-Supported Palladium Catalyst.....	56

2.4. Experimental	58
2.4.1. General Comments.....	58
2.4.2. Synthesis of (4-Bromophenyl)diphenylphosphine (TPP-Br).....	60
2.4.3. Preparation of sPS-Supported Triphenylphosphine (sPS-TPP).....	60
2.4.4. General Procedure of Suzuki-Miyaura Reaction with sPS-TPP.....	61
2.4.5. Recycling Experiment of sPS-Supported Catalyst.....	65
2.4.6. Recycling Experiment without the Addition of Fresh Cs ₂ CO ₃	67
2.4.7. Product Characterization Data.....	67
2.5. Conclusion.....	76
CHAPTER 3 CONTROLLED FUNCTIONALIZATION OF SYNDIOTACTIC POLYSTYRENE BY A COMBINATION OF BROMINATION AND SUZUKI- MIYAUURA REACTION.....	77
3.1. Abstract.....	77
3.2. Introduction.....	77
3.3. Results and Discussion.....	80
3.3.1. Electrophilic Aromatic Bromination of sPS.....	80
3.3.2. Suzuki-Miyaura Coupling Reaction of sPS-Br.....	86
3.3.3. Molecular Weight Studies with Size Exclusion Chromatography.....	88
3.3.4. Thermal Properties.....	91
3.3.5. Water Contact Angles.....	93
3.4. Experimental.....	94
3.4.1. General Comments.....	94
3.4.2. Representative Synthesis of sPS-Br.....	96
3.4.3. General Suzuki-Miyaura Cross-Coupling Procedure for the Synthesis of sPS-FG..	97
3.4.4. NMR Spectra of Functionalized Polymer Products.....	101
3.5. Conclusion.....	108
CHAPTER 4 HYDROPHILIC GRAFT MODIFICATION OF A COMMERCIAL CRYSTALLINE POLYOLEFIN.....	109
4.1. Abstract.....	109
4.2. Introduction.....	110
4.3. Results and Discussion.....	112
4.3.1. Borylated and Hydroxylated Isotactic Poly(1-butene).....	112
4.3.2. Macroinitiator of Isotactic Poly(1-butene).....	121
4.3.3. Graft Copolymer PB- <i>g</i> -PtBA.....	124
4.3.4. Graft Copolymer PB- <i>g</i> -PAA.....	127
4.3.5. Size Exclusion Chromatography.....	129
4.3.6. Thermal Properties.....	130
4.3.7. Water Contact Angles.....	133
4.3.8. Graft Copolymer PB- <i>g</i> -PMMA.....	134
4.4. Experimental	139
4.4.1. General Comments.....	139
4.4.2. Synthesis of (Cp* <i>RhCl</i> ₂) ₂	141
4.4.3. Synthesis of [Cp* <i>Rh</i> (C ₆ Me ₆)](PF ₆) ₂	142
4.4.4. Synthesis of Cp* <i>Rh</i> (η ⁴ -C ₆ Me ₆).....	142

4.4.5. Synthesis of Isotactic PB-B(pin).....	143
4.4.6. Synthesis of Hydroxylated Isotactic Poly(1-butene).....	143
4.4.7. Synthesis of the Macroinitiator (PB-Br).....	144
4.4.8. Synthesis of PB-g-PtBA.....	145
4.4.9. Synthesis of PB-g-PAA.....	146
4.4.10. Synthesis of PB-g-PMMA.....	147
4.5. Conclusion.....	148
REFERENCES.....	149
VITA.....	168

LIST OF FIGURES

Figure 1.1.	^1H NMR spectrum of syndiotactic PS in CDCl_3	9
Figure 1.2.	^{13}C NMR spectrum of syndiotactic PS in CDCl_3	10
Figure 1.3.	^1H NMR spectrum of syndiotactic PS–B(pin) in CDCl_3	10
Figure 1.4.	^1H NMR spectrum of syndiotactic PS–B(pin) in C_6D_6	11
Figure 1.5.	^{13}C NMR spectrum of syndiotactic PS–B(pin) in CDCl_3	11
Figure 1.6.	^{13}C APT NMR spectrum of syndiotactic PS–B(pin) in CDCl_3	12
Figure 1.7.	^{11}B NMR spectrum of syndiotactic PS–B(pin) in CDCl_3	12
Figure 1.8.	^1H NMR spectrum of atactic PS in C_6D_6	13
Figure 1.9.	^{13}C NMR spectrum of atactic PS in CDCl_3	13
Figure 1.10.	^1H NMR spectrum of atactic PS–B(pin) in C_6D_6	14
Figure 1.11.	^{13}C NMR spectrum of atactic PS–B(pin) in CDCl_3	14
Figure 1.12.	^{11}B NMR spectrum of atactic PS–B(pin) in CDCl_3	15
Figure 1.13.	^1H NMR spectrum of isotactic PS in C_6D_6	15
Figure 1.14.	^1H NMR spectrum of isotactic PS–B(pin) in C_6D_6	16
Figure 1.15.	Expanded ^1H NMR spectra of (a) borylated cumene, (b) sPS–B(pin), (c) iPS–B(pin), and (d) aPS–B(pin) in C_6D_6	22
Figure 1.16.	FT-IR spectrum of syndiotactic PS–OH.....	24
Figure 1.17.	FT-IR spectrum of syndiotactic PS–OH.....	24
Figure 1.18.	^1H NMR spectrum of syndiotactic PS–OH in CDCl_3	25
Figure 1.19.	^{13}C NMR spectrum of syndiotactic PS–OH in 1,1,2,2-tetrachloroethane- d_2	25
Figure 1.20.	^1H NMR spectrum of atactic PS–OH in C_6D_6	26
Figure 1.21.	^{13}C NMR spectrum of atactic PS–OH in CDCl_3	26
Figure 1.22.	^1H NMR spectrum of syndiotactic PS–Ar in CDCl_3	28
Figure 1.23.	^{13}C NMR spectrum of syndiotactic PS–Ar in CDCl_3	28
Figure 1.24.	^1H NMR spectrum of atactic PS–Ar in C_6D_6	29
Figure 1.25.	^{13}C NMR spectrum of atactic PS–Ar in CDCl_3	29
Figure 1.26.	Size exclusion chromatography for atactic polystyrene (aPS), and aPS–B(pin)s.....	30
Figure 1.27.	High-temperature size exclusion chromatography for syndiotactic polystyrene (sPS), and sPS–B(pin)s.....	31
Figure 1.28.	Size exclusion chromatography for aPS, aPS–B(pin), aPS–OH, and aPS–Ar.....	32
Figure 1.29.	Differential scanning calorimetry scans of syndiotactic polystyrene (sPS), sPS–B(pin), sPS–OHs.....	33
Figure 2.1.	Precipitation of sPS–B(pin) and aPS–B(pin) by adding an <i>equal volume</i> of MeOH.....	48
Figure 2.2.	^1H NMR spectrum of (4-bromophenyl)diphenylphosphine.....	50

Figure 2.3.	^{13}C NMR spectrum of (4-bromophenyl)diphenylphosphine.....	51
Figure 2.4.	^{31}P NMR spectra of chlorodiphenylphosphine, (4-bromophenyl) diphenylphosphine, and sPS–TPP.....	52
Figure 2.5.	^1H NMR spectrum of sPS–supported triphenylphosphine.....	52
Figure 2.6.	^{13}C NMR spectrum of sPS-supported triphenylphosphine.....	53
Figure 2.7.	^1H NMR spectrum of biphenyl.....	67
Figure 2.8.	^{13}C NMR spectrum of biphenyl.....	68
Figure 2.9.	^1H NMR spectrum of 4-acetylbiphenyl.....	68
Figure 2.10.	^{13}C NMR spectrum of 4-acetylbiphenyl.....	69
Figure 2.11.	^1H NMR spectrum of 4-trifluoromethylbiphenyl.....	69
Figure 2.12.	^{13}C NMR spectrum of 4-trifluoromethylbiphenyl.....	70
Figure 2.13.	^1H NMR spectrum of 4-formylbiphenyl.....	70
Figure 2.14.	^{13}C NMR spectrum of 4-formylbiphenyl.....	71
Figure 2.15.	^1H NMR spectrum of 4-methylbiphenyl.....	71
Figure 2.16.	^{13}C NMR spectrum of 4-methylbiphenyl.....	72
Figure 2.17.	^1H NMR spectrum of 4-(hydroxymethyl)biphenyl.....	72
Figure 2.18.	^{13}C NMR spectrum of 4-(hydroxymethyl)biphenyl.....	73
Figure 2.19.	^1H NMR spectrum of 4-methoxybiphenyl.....	73
Figure 2.20.	^{13}C NMR spectrum of 4-methoxybiphenyl.....	74
Figure 2.21.	^1H NMR spectrum of (<i>N,N</i> -dimethylamino)biphenyl.....	74
Figure 2.22.	^{13}C NMR spectrum of (<i>N,N</i> -dimethylamino)biphenyl.....	75
Figure 2.23.	^1H NMR spectrum of 4-acetylbiphenyl (Cycle 1 in Table 5).....	75
Figure 2.24.	^{13}C NMR spectrum of 4-acetylbiphenyl (Cycle 1 in Table 5).....	76
Figure 3.1.	^1H NMR spectrum of brominated sPS.....	82
Figure 3.2.	^{13}C APT NMR spectrum of brominated sPS.....	83
Figure 3.3.	High-temperature size exclusion chromatography for syndiotactic polystyrene (sPS) and sPS–Brs.....	88
Figure 3.4.	Size exclusion chromatography for atactic polystyrene (aPS) and aPS–Brs.....	90
Figure 3.5.	High-temperature size exclusion chromatography for sPS–FGs.....	91
Figure 3.6.	DSC scans of sPS and sPS–Brs.....	92
Figure 3.7.	Water contact angles for sPS, sPS–Br, and sPS–FGs.....	94
Figure 3.8.	^1H NMR spectrum of sPS–COCH ₃	101
Figure 3.9.	^{13}C NMR spectrum of sPS–COCH ₃	102
Figure 3.10.	^1H NMR spectrum of sPS–OCH ₃	102
Figure 3.11.	^{13}C APT NMR spectrum of sPS–OCH ₃	103
Figure 3.12.	^1H NMR spectrum of sPS–OSi(CH ₃) ₂ C(CH ₃) ₃	103
Figure 3.13.	^{13}C APT NMR spectrum of sPS–OSi(CH ₃) ₂ C(CH ₃) ₃	104
Figure 3.14.	^1H NMR spectrum of sPS–COOCH ₃	104
Figure 3.15.	^{13}C APT NMR spectrum of sPS–COOCH ₃	105
Figure 3.16.	^1H NMR spectrum of sPS–CHO.....	105
Figure 3.17.	^{13}C APT NMR spectrum of sPS–CHO.....	106
Figure 3.18.	^1H NMR spectrum of sPS–NH ₂	106
Figure 3.19.	^{13}C APT NMR spectrum of sPS–NH ₂	107
Figure 3.20.	^1H NMR spectrum of sPS–CONH ₂	107
Figure 3.21.	^{13}C APT NMR spectrum of sPS–CONH ₂	108

Figure 4.1.	^1H NMR spectrum of PB–B(pin).....	114
Figure 4.2.	^{13}C NMR spectrum of PB–B(pin).....	115
Figure 4.3.	^{11}B NMR spectrum of PB–B(pin).....	115
Figure 4.4.	FT-IR spectrum of PB–OH.....	117
Figure 4.5.	^1H NMR spectrum of PB–OH.....	117
Figure 4.6.	^{13}C NMR spectrum of PB–OH.....	118
Figure 4.7.	^{13}C APT NMR spectrum of PB–OH.....	118
Figure 4.8.	^1H NMR spectrum of PB–Br.....	123
Figure 4.9.	^{13}C NMR spectrum of PB–Br.....	124
Figure 4.10.	FT-IR spectrum of PB- <i>g</i> -PtBA.....	125
Figure 4.11.	^1H NMR spectrum of PB- <i>g</i> -PtBA.....	125
Figure 4.12.	FT-IR spectrum of PB- <i>g</i> -PAA.....	128
Figure 4.13.	^1H NMR spectrum of PB- <i>g</i> -PAA in THF- <i>d</i> ₈	128
Figure 4.14.	Size exclusion chromatography for PB, PB–B(pin), PB–OH, PB–Br, and PB- <i>g</i> -PtBA.....	130
Figure 4.15.	DSC scans of PB and PB–OHs.....	132
Figure 4.16.	DSC scans of PB, PB–OH, PB–Br, PB- <i>g</i> -PtBA, and PB- <i>g</i> -PAA.....	133
Figure 4.17.	Water contact angles of PB–OHs and graft copolymers.....	134
Figure 4.18.	FT-IR spectra of PB–OH and PB- <i>g</i> -PMMA.....	136
Figure 4.19.	^1H NMR spectrum of PB- <i>g</i> -PMMA.....	136
Figure 4.20.	High-temperature size exclusion chromatography for PB, PB–Br, and PB- <i>g</i> -PMMA.....	139

LIST OF SCHEMES

Scheme 1.1.	C–H activation/borylation of polystyrenes with iridium catalyst.....	8
Scheme 1.2.	Oxidation of borylated polystyrenes.....	23
Scheme 1.3.	Suzuki–Miyaura coupling reaction of borylated styrenes.....	27
Scheme 2.1.	Synthesis of syndiotactic sPS–TPP.....	50
Scheme 3.1.	Bromination and subsequent Suzuki–Miyaura coupling of sPS.....	80
Scheme 4.1.	Regioselective functionalization of isotactic poly(1-butene).....	113
Scheme 4.2.	Preparation of macroinitiator, PB- <i>g</i> -PtBA, and PB- <i>g</i> -PAA.....	122
Scheme 4.3.	Preparation of PB- <i>g</i> -PMMA.....	135

LIST OF TABLES

Table 1.1.	Borylation of sPS with different iridium catalysts.....	7
Table 1.2.	Borylation of sPS and iPS with B ₂ (pin) ₂	18
Table 1.3.	Borylation of monodisperse aPS with B ₂ (pin) ₂	19
Table 1.4.	Borylation of sPS and aPS with HB(pin).....	20
Table 1.5.	Thermal properties of sPS and functionalized sPS.....	35
Table 2.1.	Solubility and precipitation test of sPS–B(pin).....	48
Table 2.2.	Solubility and precipitation test of aPS–B(pin).....	49
Table 2.3.	Effect of base on the sPS–TPP-supported Suzuki–Miyaura reactions of 4-bromoacetophenone and phenylboronic acid.....	54
Table 2.4.	sPS–TPP-supported Suzuki–Miyaura reactions of aryl halides with phenylboronic acid.....	55
Table 2.5.	Recovery/recycling of sPS–TPP-supported palladium catalyst in Suzuki–Miyaura reactions and the leaching of palladium.....	57
Table 2.6.	Recovery/Recycling of sPS–TPP-supported Palladium Catalyst in Suzuki–Miyaura Reactions and the Leaching of Palladium without adding fresh base.....	57
Table 3.1.	Bromination of syndiotactic polystyrene with bromine.....	84
Table 3.2.	Bromination of monodisperse atactic polystyrene.....	85
Table 3.3.	Suzuki–Miyaura reaction of Brominated sPS with phenylboronic acid.....	87
Table 3.4.	Thermal properties of sPS and brominated sPS.....	93
Table 4.1.	Regioselective C–H functionalization of PB with B ₂ (pin) ₂	120
Table 4.2.	Regioselective C–H functionalization of hPB with B ₂ (pin) ₂	121
Table 4.3.	Analytical results of PB- <i>g</i> -PtBAs and their precursor polymers.....	126
Table 4.4.	Analytical results of PB- <i>g</i> -PMMA and their precursor polymers....	137

CHAPTER 1

CONTROLLED FUNCTIONALIZATION OF CRYSTALLINE POLYSTYRENES VIA ACTIVATION OF AROMATIC C–H BONDS

1.1. Abstract

The functionalization of polystyrenes having three types of tacticity–syndiotactic (sPS), isotactic (iPS), and atactic (aPS)– is accomplished through the borylation of the C–H bonds in the aromatic ring using a commercially available iridium catalyst. The boronic ester group of the functionalized polymer was converted to more useful functional groups such as hydroxy and arene via subsequent oxidation and Suzuki–Miyaura cross–coupling reaction. There were no changes in the polymer chain length, molecular weight distribution and tacticity of the parent polymer after the functionalizations. The concentration of incorporated functional groups was easily tuned by adjusting the ratio of the diboron reagent, $B_2(\text{pin})_2$, to polymer repeating unit in the C–H borylation. The efficiency of C–H borylation was affected by the solubility of the polymer in reaction solvent and the ratio of the boron reagent with monomer unit, regardless of the tacticity.

It was found that the thermal properties of the functionalized sPS were greatly influenced by the size and concentration of the introduced functional groups. The crystallinity of sPS completely disappeared with even a small amount (< 5 mol %) of the

boronate ester group incorporated into the polymer, because the functional group in sPS–B(pin) is bulky. The high crystallinity and melting temperature of sPS were not significantly changed until 10 mol % of hydroxy group was introduced into the polymer, probably due to the small size of hydroxy group.

1.2. Introduction

Polyolefins account for more than 60% of total polymeric material consumption in the world, owing to good chemical stability, mechanical properties, processability and low production cost. These are materials made by polymerization of simple olefins such as ethylene, propylene, butane, isoprene, pentane, and styrene. Despite their favorable properties mentioned above, lack of polar functionality is still one of the most serious drawbacks of polyolefins and has prevented wider applications of the materials. The introduction of polar functionality into nonpolar polyolefins can address the limitation of surface properties and enhance adhesion to polar surfaces. However, a controlled selective mild functionalization of polyolefins has been one of the most difficult challenges in synthetic polymer chemistry.

Syndiotactic polystyrene (sPS) is a good example of a stereoregular polyolefin and has received a significant attention in polymer industry as well as academic field due to its intriguing physical properties such as a high degree of crystallinity and stable mechanical and chemical properties at high temperature.¹ Despite its unique properties, sPS has a few drawbacks for commercial applications as an engineering plastic. Because of its high melting point (~270 °C), excessively high melt-processing temperature >300 °C (close to the polymer degradation temperature) causes a major problem in processing

of the polymer. In addition, sPS has poor compatibility with polar materials and impact strength. To overcome these drawbacks, research has been conducted to introduce polar functional groups into sPS. So far, there are two methodologies employed to synthesize functionalized sPS. The first method is copolymerization with a second styrene monomer containing desired functional group. Unfortunately, as with other transition metal-catalyzed stereospecific olefin polymerization,² it is difficult to achieve comparable molecular weights and/or yields in the syndiospecific copolymerization of styrene with a functionalized monomer, compared with those afforded by the syndiospecific homopolymerization of styrene. Examples of the former approach include the copolymerization of styrene with a borane monomer and a silyloxy monomer which provide hydroxy functionalized syndiotactic polystyrenes.^{3,4}

The other method to prepare functionalized sPS is direct post-polymerization functionalization of sPS. Since a variety of polyolefins with different tacticities and variable molecular weights could be easily prepared with the significant development in homogeneous metallocene polymerization catalysts, the controlled postfunctionalization of such polyolefins could be an attractive alternative approach to yield functionalized polymers having variable molecular weight properties⁵ as well as to overcome the limitations of the copolymerization method. Because most postfunctionalizations of polyolefins are initiated by a highly reactive free radical, however, it is hard to control the molecular weight properties of the polymers. They can induce competitive side reactions which can break or couple chains of polymer and alter mechanical/physical properties of the parent polymer. Free radical mediated modification of sPS can also reduce the tacticity at the benzylic position of the polymer.

Atactic polystyrene (aPS), an amorphous material that has good solubility in a variety of solvents, can be readily functionalized by electrophilic aromatic substitution to introduce a high ratio of the polar functional group to the polymer.⁶ In sPS modification, however, very poor solubility of the crystalline polymer in most makes the postfunctionalization reaction conducted under heterogeneous condition, where it is difficult to introduce functional groups uniformly especially in a large scale reaction. To date, only a few examples of sPS modifications using carbon intermediates such as free radicals and carbocations have been reported with limited success.⁷⁻¹³ For example, only 3–12 mol % of the aromatic ring of sPS was functionalized with sulfonic acid group when electrophilic sulfonation of sPS under chlorinated solvents was conducted.⁷⁻¹⁰ Thus, a homogeneous controlled postfunctionalization of sPS highly desired.

Boron functionality in polymer can be used as a useful intermediate for generation of a variety of functionalized polymers, especially polyolefins.¹⁴ There are two methods to prepare boron-containing polymers. The first method is polymerization of boron-functionalized monomers and the second one is post-polymerization functionalization of a boron precursor polymer. It has been reported earlier that when aPS was directly borylated with haloboranes, it incorporated only a low content of boryl group while inducing significant side reactions under hard conditions.¹⁵ A boron moiety has also been introduced into the aromatic ring of polystyrene resin via several steps of post-functionalization.¹⁶ When this method was used for the preparation of soluble boron polymers, however, it caused significant cross-linking. It has recently been reported that soluble borylated polystyrene could be synthesized from the silylated precursor polymer through a silicon–boron exchange reaction. Although that modification was not a

catalytic process, it was an important example that showed controlled boron-functionalization with excellent chemo- and regioselectivity.^{17,18}

Polymer modification by transition metal-catalyzed C–H activation has emerged as a new polyolefin postfunctionalization methodology.¹⁹⁻²⁴ Unlike typical polyolefin modifications, which proceed through a highly reactive free radical or carbocation intermediate, this new method allows incorporation of functional groups into polyolefins with negligible changes in the polymer chain length, polydispersity and tacticity compared to those of the starting polymers. A representative example is functionalization of the side chain of saturated polyolefins by rhodium-catalyzed C–H borylation. The boron moiety of the polymer was conveniently converted to hydroxy and amine groups through simple organic reactions.²¹⁻²³ Unfortunately, some of these examples were conducted on amorphous polyolefins of relatively low molecular weight and required the preparation of special metal catalysts.¹⁹⁻²¹ Moreover, when semicrystalline polyolefins were functionalized via activation of C–H bonds, their efficiencies of the functionalization were very low.²²⁻²⁴

We herein report a highly efficient controlled aromatic C–H bond activation/functionalization of high-molecular-weight polystyrenes with different tacticities using a commercially available iridium catalyst (Scheme 1.1). We have found that up to 42 mol % of a boronate ester group can be incorporated by the iridium-catalyzed borylation of aromatic C–H bonds²⁵⁻²⁹ without affecting the molecular weight properties of the starting polymer. To our knowledge, this result reports the first example of crystalline polyolefin functionalization that affords a high degree of functionalization without any competitive side reactions. Because it is known that the iridium-catalyzed

aromatic C–H activation/borylation occur only at the aromatic ring of arenes,²⁵⁻²⁹ this functionalization would allow generation of borylated polystyrenes with different tacticities in a single step. We also demonstrate that the aryl boronate ester group of sPS can serve as a versatile synthetic precursor for a range of functionalized sPS products.

1.3. Results and Discussion

1.3.1. Screening Experiments for Standard Conditions of sPS Functionalization

We first tested suitable solvents that can dissolve the crystalline sPS at a reasonable concentration for optimized functionalization conditions of sPS under homogeneous conditions. sPS is known to be insoluble in most organic solvents except for hydrocarbon and chlorinated solvents at elevated temperatures. Thus, a solubility test of sPS was conducted with two hydrocarbon solvents having high boiling points, cyclooctane and 1,3,5-triisopropylbenzene, and two chlorinated solvents, chloroform and carbon tetrachloride. In the case of a mixture of sPS and solvent in a 1:6 molar ratio (sPS repeating unit to solvent), a homogeneous solution was observed under the following conditions: in cyclooctane at 150 °C, in 1,3,5-triisopropylbenzene at 200 °C, and in chloroform at 60 °C. The mixture of sPS and carbon tetrachloride still remained heterogeneous even at its boiling temperature. Although sPS was soluble in chloroform, it was found that cumene [C₆H₅–CH(CH₃)₂], a model small arene whose structure resembles that of sPS repeating unit, was not borylated in chloroform; thus we did not select it as a solvent for the C–H borylation of sPS. When we applied different transition metal catalyst/ligand systems—[IrCl(COD)]₂/dtbpy (COD = 1,5-cyclooctadiene; dtbpy = 4,4'-di-*tert*-butyl-2,2'-bipyridine), [Ir(OMe)(COD)]₂/dtbpy, [IrCl(COE)]₂/dtbpy (COE =

cyclooctene), and Cp*Rh(η^4 -C₆Me₆)–for the C–H activation of cumene with bis(pinacolato)diboron [B₂(pin)₂] in cyclooctane (in a 1:6 molar ratio of cumene and solvent) at its boiling temperature, all iridium catalyst/ligand systems were much more effective than the rhodium catalyst. When different iridium catalysts such as [IrCl(COE)₂]₂, [Ir(OMe)(COD)]₂, and [IrCl(COD)]₂ were used for the C–H activation of sPS with B₂(pin)₂, [IrCl(COD)]₂/dtbpy was slightly more reactive compared with two other catalysts (Table 1.1). Moreover, the lower cost of [IrCl(COD)]₂ compared to those of [IrCl(COE)₂]₂ and [Ir(OMe)(COD)]₂ makes [IrCl(COD)]₂ be more preferred catalyst of sPS functionalization. Thus, we selected the experimental condition of [IrCl(COD)]₂ (3 mol % iridium) and dtbpy ligand (3 mol %) in cyclooctane at 150 °C as the standard condition for the C–H borylation of sPS.

Table 1.1. Borylation of syndiotactic polystyrene with different iridium catalysts^a.

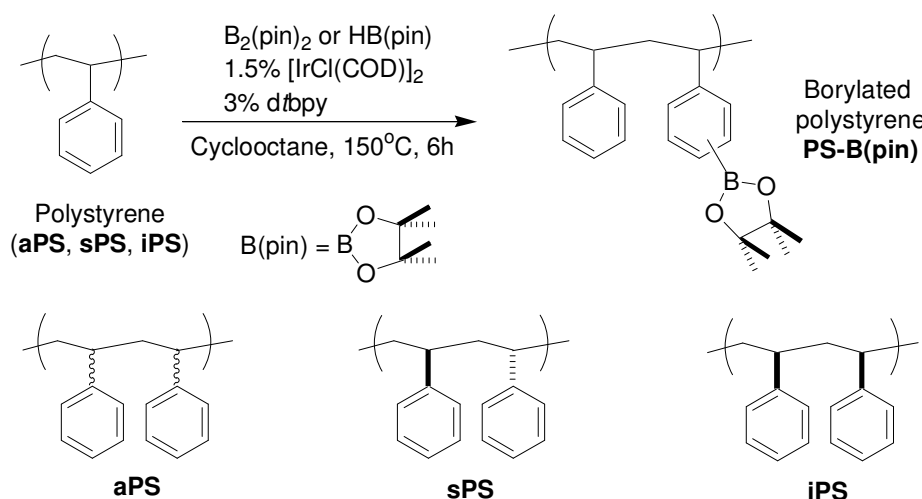
entry	PS	Iridium catalyst	[B ₂ (pin) ₂]/ [monomer]	sPS–B(pin)	
				B(pin) (%) ^b	effic (%) ^c
1	sPS	[IrCl(COE) ₂] ₂	0.05	4.2	42
2	sPS	[Ir(OMe)(COD)] ₂	0.05	5.5	55
3	sPS	[IrCl(COD)] ₂	0.05	5.9	59
4	sPS	[IrCl(COE) ₂] ₂	0.1	12.4	62
5	sPS	[Ir(OMe)(COD)] ₂	0.1	14.7	74
6	sPS	[IrCl(COD)] ₂	0.1	16.4	82

^a C–H borylation was conducted on 200 mg of polymer with 3 mol % of iridium catalyst and 3 mol % of dtbpy relative to B₂(pin)₂ in cyclooctane (in a 1:6 molar ratio of polystyrene repeating unit to solvent) at 150 °C for 6 h. ^b The mol % of B(pin) functionalized styrene unit calculated from the ¹H NMR spectrum. ^c Efficiency of

functionalization (i.e., the percentage of functionalized styrene unit relative to boron atoms added).

1.3.2. Iridium-Catalyzed C–H Borylation of Crystalline Polystyrenes

The iridium-catalyzed reaction of commercial polystyrenes [syndiotactic (sPS), atactic (aPS), and Isotactic (iPS)] with a boron reagent such as $B_2(\text{pin})_2$ or pinacolborane [HB(pin)] in cyclooctane generated the corresponding borylated polymers [PS-B(pin)] (Scheme 1.1).



Scheme 1.1. C–H activation/borylation of polystyrenes with iridium catalyst.

In ^1H NMR spectra of all PS–B(pin), a distinct new peak was found at 1.20–1.35 ppm for the methyl groups of pinacolboronate ester [B(pin)]: 1.35 ppm for sPS–B(pin) in CDCl_3 (Figure 1.3); 1.20 ppm for sPS–B(pin), aPS–B(pin), and iPS–B(pin) in C_6D_6 (Figures 1.4, 1.10 and 1.14). The two proton resonances from $-\text{CH}_2-$ and $-\text{CH}-$ of the polystyrene main chain maintained a ratio of 2:1, confirming that the methylene and

methine groups of polystyrene were intact during the borylation. In ^{13}C NMR spectra, new sharp peaks were also shown at 83.5 and 24.0 for the aryl-B(pin) moiety of the polymer (Figures 1.5 and 1.11). ^{13}C NMR attached proton test (APT) spectroscopy of sPS-B(pin) confirmed that those two resonances corresponded to the methyl and the quaternary carbon atoms of the B(pin) structure (Figure 1.6). The ^{11}B NMR spectrum of sPS-B(pin) showed a broad peak at 27 ppm, which is consistent with the boron chemical shift of previously reported B(pin)-functionalized aPS homopolymer (Figures 1.7 and 1.12).¹⁸

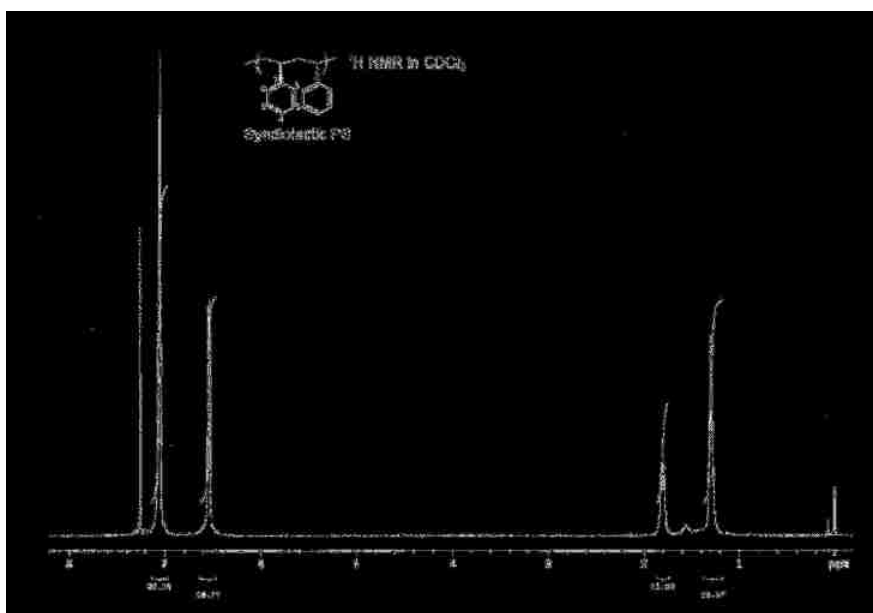


Figure 1.1. ^1H NMR spectrum of syndiotactic PS [10 mg/mL in CDCl_3 at $25\text{ }^\circ\text{C}$].

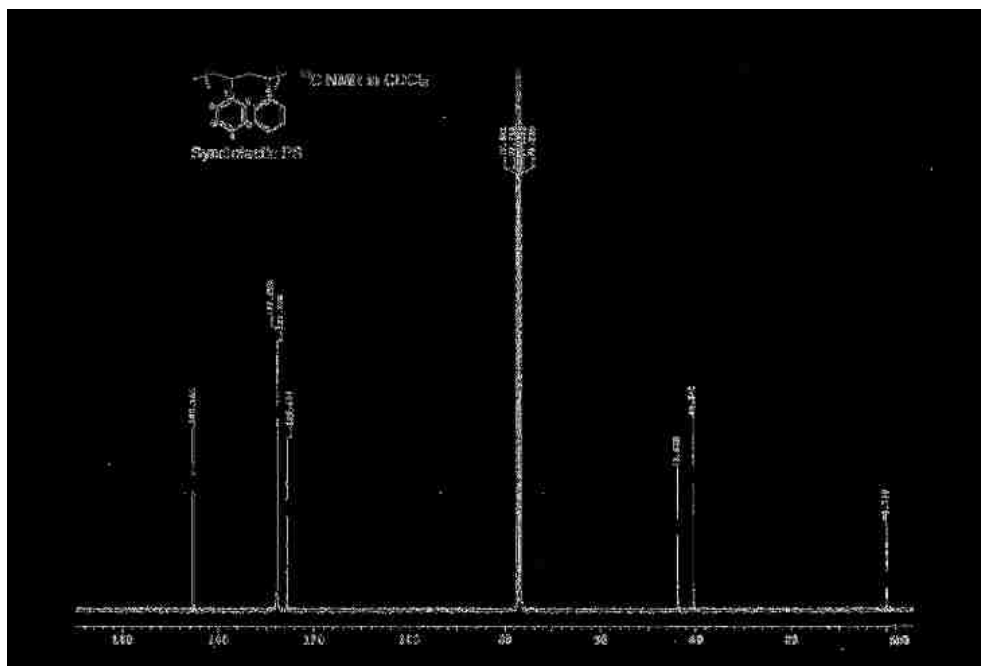


Figure 1.2. ^{13}C NMR spectrum of syndiotactic PS [20 mg/mL in CDCl_3 at 25°C].

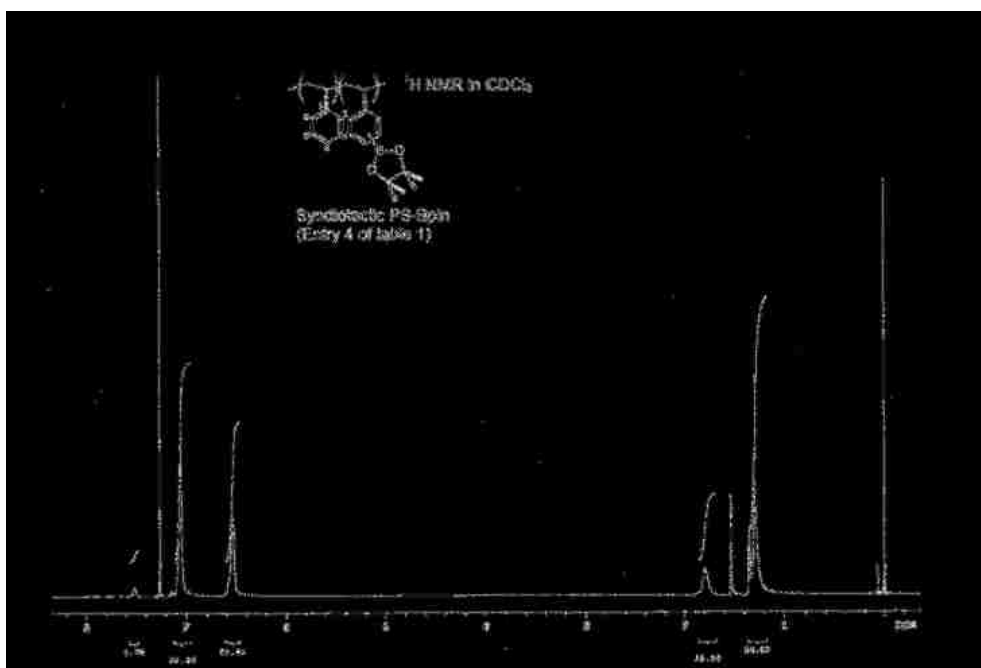


Figure 1.3. ^1H NMR spectrum of syndiotactic PS-B(pin) [10 mg/mL in CDCl_3 at 25°C].

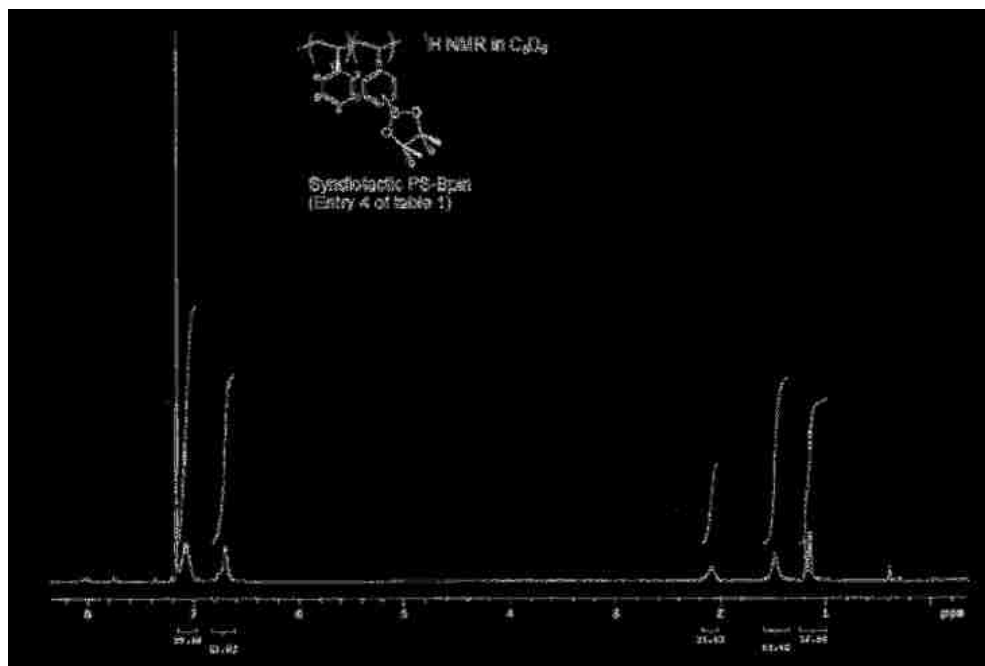


Figure 1.4. ¹H NMR spectrum of syndiotactic PS-B(pin) [10 mg/mL in C₆D₆ at 25 °C].

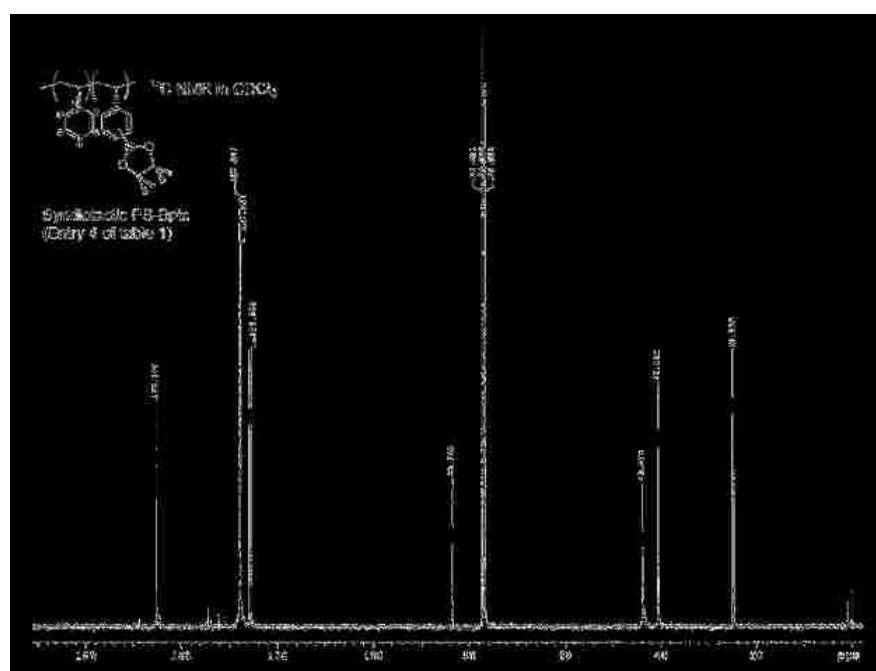


Figure 1.5. ¹³C NMR spectrum of syndiotactic PS-B(pin) [30 mg/mL in CDCl₃ at 25 °C].

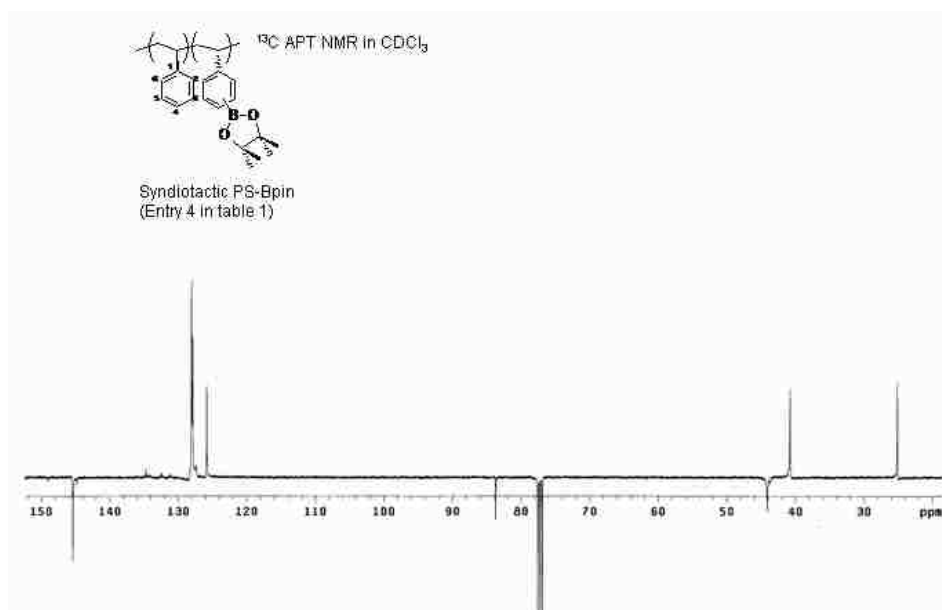


Figure 1.6. ^{13}C APT NMR spectrum of syndiotactic PS-B(pin) [30 mg/mL in CDCl_3 at 25 $^\circ\text{C}$].

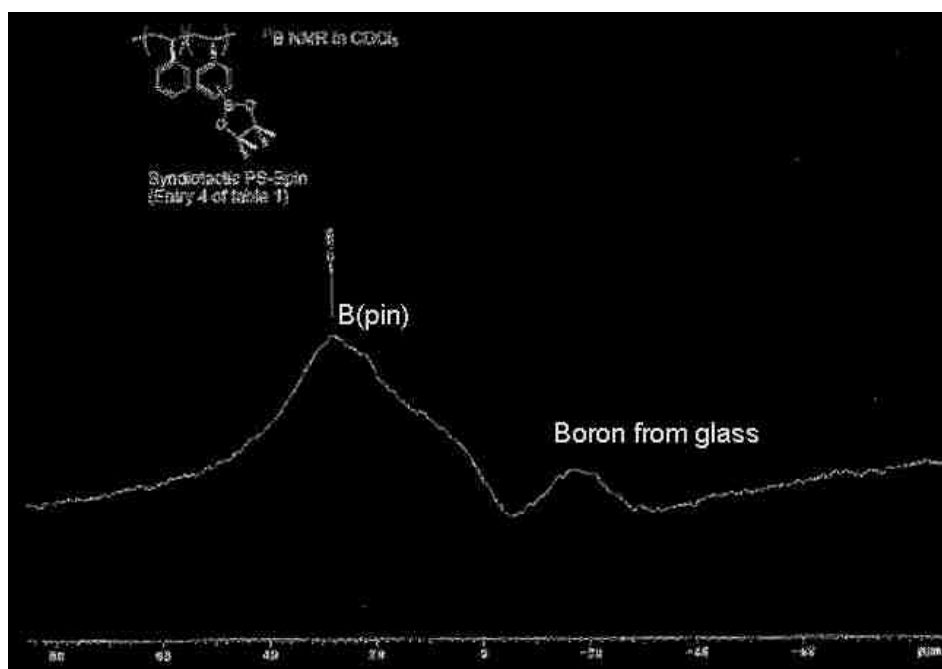


Figure 1.7. ^{11}B NMR spectrum of syndiotactic PS-B(pin) [30 mg/mL in CDCl_3 at 25 $^\circ\text{C}$].

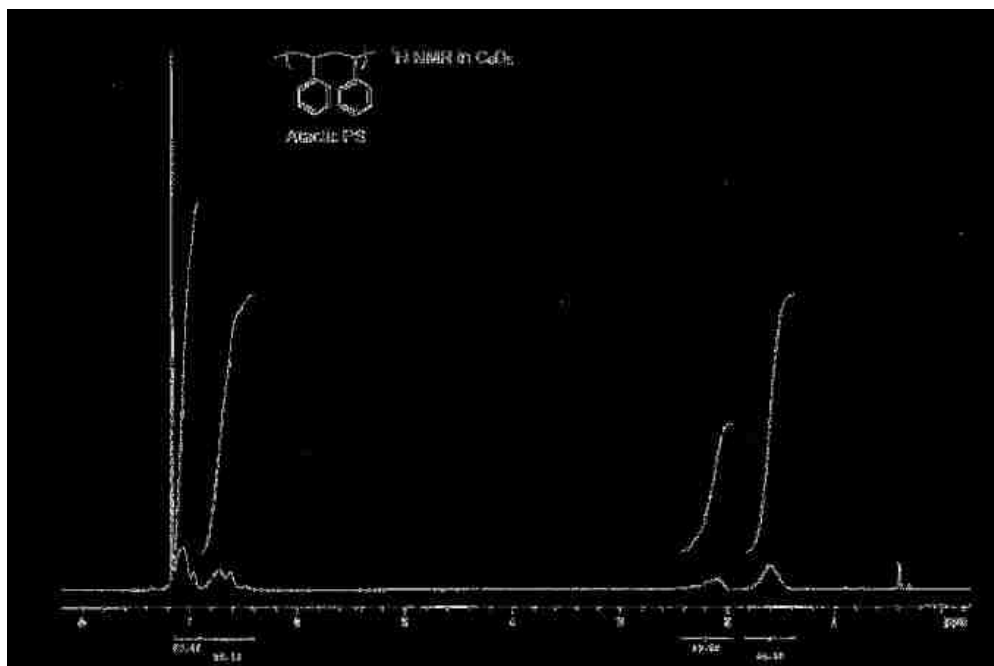


Figure 1.8. ^1H NMR spectrum of atactic PS [10 mg/mL in C_6D_6 at 25 °C].

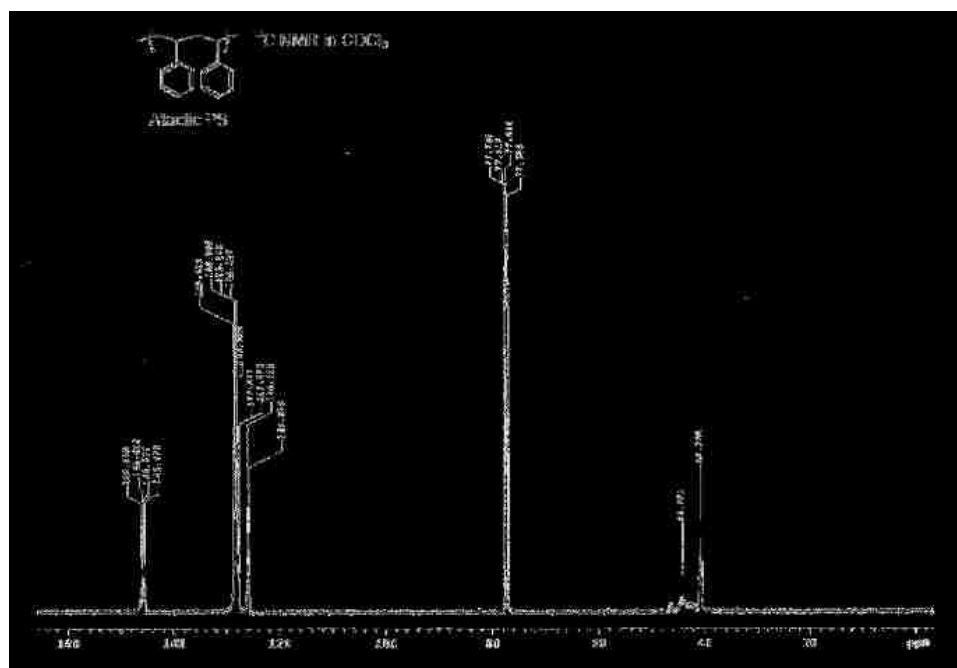


Figure 1.9. ^{13}C NMR spectrum of atactic PS [30 mg/mL in CDCl_3 at 25 °C].

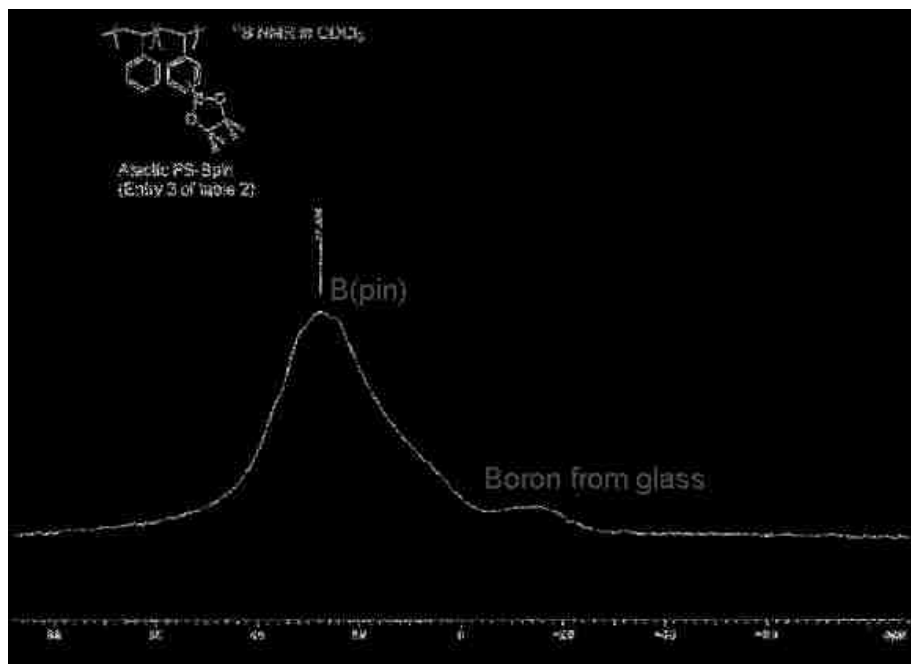


Figure 1.12. ¹¹B NMR spectrum of atactic PS-B(pin) [30 mg/mL in CDCl₃ at 25 °C].

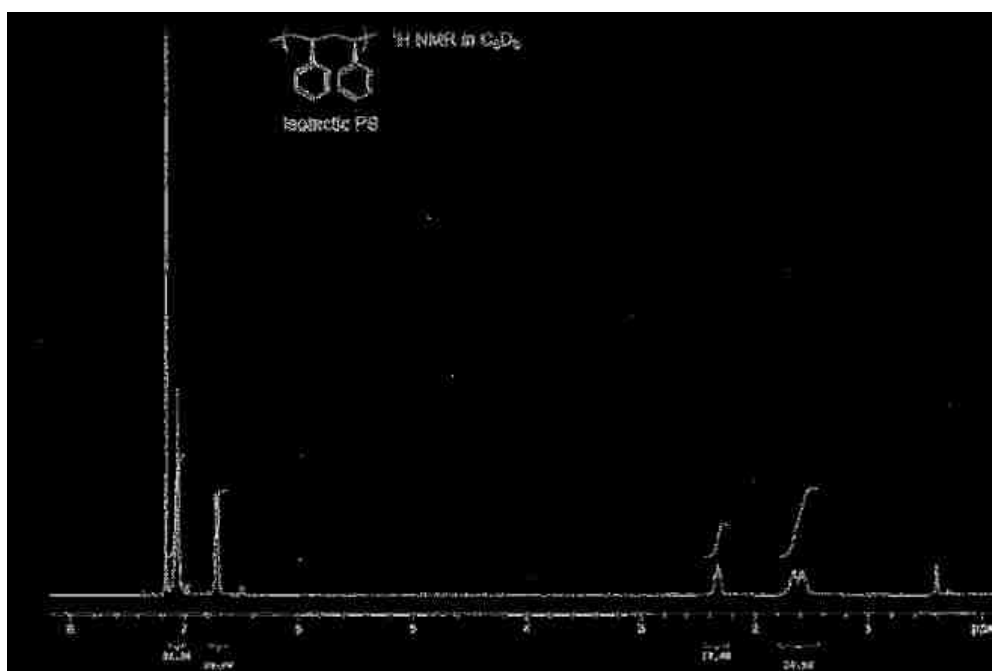


Figure 1.13. ¹H NMR spectrum of isotactic PS [10 mg/mL in C₆D₆ at 25 °C].

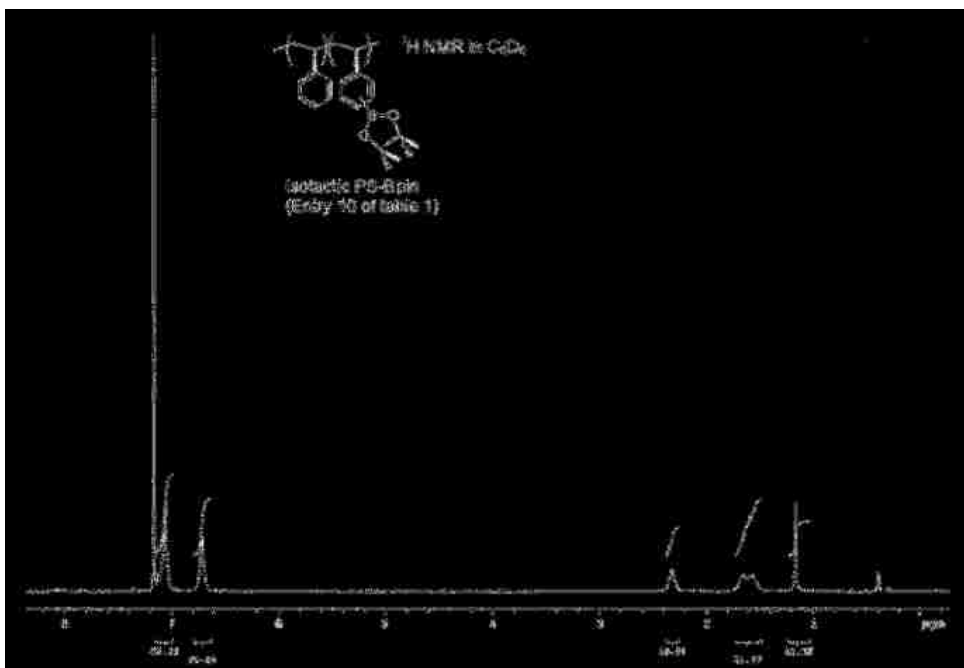


Figure 1.14. ^1H NMR spectrum of isotactic PS-B(pin) [10 mg/mL in C_6D_6 at 25 $^\circ\text{C}$].

We calculated the mol % of the borylated styrene repeating unit from the ^1H NMR spectrum by comparing the ratio of the methine proton of the polystyrene main chain and the methyl groups of the B(pin) group. These results are summarized in Tables 1.2 and 1.3. Note that the efficiency of functionalization in Tables 1.2 and 1.3 is defined as the percentage of borylated styrene units relative to added *boron atoms*. All polystyrenes could be efficiently functionalized with varying numbers of boryl groups without any influence on polymer tacticity. Except for the functionalizations of sPS with a very low ratio of added $\text{B}_2(\text{pin})_2$ to monomer unit (ratios <0.1 ; Table 1.2, Entries 1–3), both sPS and aPS generally showed decreased efficiency of functionalization as the added diboron amount was increased (Table 1.2, Entries 4–8 for sPS; Table 1.3, Entries 1–7 for aPS). The explanation for the sPS exceptions is not clearly understood and needs further investigation. Although efficiency of C–H borylation steadily decreases as more $\text{B}_2(\text{pin})_2$

is added to the styrene unit, up to 42 mol % of styrene repeating units of sPS and aPS can be easily borylated using 3 mol % of the commercially available iridium catalyst and the ligand using this method (Table 1.2, Entry 7 for sPS; Table 1.3, Entry 6 for aPS). We also observed that the effect of solubility has an influence on the efficiency of functionalization in the case of iPS borylation. Since the commercial iPS that we studied has an extremely high molecular weight ($M_n = 309$ kg/mol, PDI = 6.42), homogeneous dissolution at 150 °C was achieved by adding more solvent (i.e., in a 1:10 molar ratio of iPS repeating unit to solvent). The solvent dilution induced a decrease in efficiency compared with that of the standard conditions for sPS–B(pin) (Table 1.2, Entries 4 and 9). Similarly, the borylation of sPS under the identical diluted condition (i.e., in a 1:10 molar ratio of sPS repeating unit to cyclooctane) also resulted in a slightly reduced efficiency compared with that under the standard condition (Table 1.2, Entries 4 and 10). Unlike other transition metal-catalyzed polyolefin C–H functionalizations,¹⁹⁻²⁴ the iridium-catalyzed borylation of sPS was highly effective even with low catalyst loading (i.e., 0.5 mol % iridium catalyst loading for Table 1.2, Entry 11).

Table 1.2. Borylation of crystalline polystyrene [syndiotactic (sPS) and isotactic (iPS)] with bis(pinacolato)diboron [B₂(pin)₂]^a.

entry	PS	M_n^b	PDI ^b (M_w/M_n)	[B ₂ (pin) ₂]/ [monomer]	PS–B(pin)			
					M_n^b	PDI ^b (M_w/M_n)	B(pin) (%) ^c	Effic. (%) ^d
1	sPS	127	2.64	0.03	133	2.37	2.5	42
2	sPS	127	2.64	0.05	116	2.74	5.9	59
3	sPS	127	2.64	0.07	116	2.53	9.9	71
4	sPS	127	2.64	0.1	90.0	2.50	16.4	82
5	sPS	127	2.64	0.2	124	2.40	23.6	59
6	sPS	127	2.64	0.4	97.0	2.55	34.2	43
7	sPS	127	2.64	0.8	<i>g</i>	<i>g</i>	41.1	26
8	sPS	127	2.64	1.2	<i>g</i>	<i>g</i>	42.1	18
9 ^e	iPS	309	6.42	0.1	418	5.00	10.6	50
10 ^e	sPS	127	2.64	0.1	<i>g</i>	<i>g</i>	13.7	69
11 ^f	sPS	127	2.64	0.1	<i>g</i>	<i>g</i>	12.9	65

^a B(pin) = pinacolboronate ester. PS = polystyrene. Unless otherwise specified, C–H borylation was conducted on 200–260 mg of polymer with 3 mol % of iridium and 3 mol % of ligand relative to B₂(pin)₂ in cyclooctane (in a 1:6 molar ratio of polystyrene repeating unit to solvent) at 150 °C for 6 h. sPS = syndiotactic polystyrene; iPS = isotactic polystyrene. ^b Number-average molecular weight (M_n) in kg/mol and polydispersity index (PDI) measured with high-temperature size-exclusion chromatography in 1,2,4-trichlorobenzene at 160 °C relative to polystyrene standards. ^c The mol % of B(pin) functionalized styrene unit calculated from the ¹H NMR spectrum. ^d Efficiency of functionalization (i.e., the percentage of functionalized styrene unit relative to boron atoms added). ^e Borylation conducted in cyclooctane in a 1:10 molar ratio of

polystyrene repeating unit to solvent.^f 0.5 mol % of iridium and 0.5 mol % of ligand were used.^g Not measured.

Table 1.3. Borylation of monodisperse atactic polystyrene (aPS) with bis(pinacolato) diboron [B₂(pin)₂]^a.

entry	PS	M_n^b	PDI ^b (M_w/M_n)	[B ₂ (pin) ₂]/ [monomer]	PS-B(pin)			
					M_n^b	PDI ^b (M_w/M_n)	B(pin) (%) ^c	Effic. (%) ^d
1	aPS	25.1	1.09	0.05	26.5	1.09	8.4	84
2	aPS	25.1	1.09	0.07	27.0	1.09	11.1	80
3	aPS	25.1	1.09	0.1	27.9	1.10	16.4	82
4	aPS	25.1	1.09	0.2	29.2	1.10	22.4	56
5	aPS	25.1	1.09	0.4	30.1	1.11	32.8	41
6	aPS	25.1	1.09	0.8	30.9	1.12	42.3	26
7	aPS	25.1	1.09	1.2	31.1	1.14	41.1	17
8	aPS	247	1.07	0.1	256	1.05	16.9	85

^a B(pin) = pinacolboronate ester. PS = polystyrene. C–H borylation was conducted on 200 mg of polymer with 3 mol % of iridium and 3 mol % of ligand relative to B₂(pin)₂ in cyclooctane (in a 1:6 molar ratio of polystyrene repeating unit to solvent) at 150 °C for 6 h. ^b M_n in kg/mol and PDI measured with SEC in THF at 40 °C relative to polystyrene standards. ^c The mol % of B(pin) functionalized styrene unit calculated from the ¹H NMR spectrum. ^d Efficiency of functionalization.

The iridium-catalyzed C–H borylation of sPS and aPS can also be accomplished with HB(pin) as the boron reagent (Table 1.4). Although the efficiency of functionalization with HB(pin) was lower than that with B₂(pin)₂, the borylation using various ratios of

HB(pin) to styrene repeating unit produced 1–10 mol % B(pin)-functionalized sPS and aPS. The C–H borylation results of aPS showed that the polymer chain lengths after the post-functionalization were unchanged from those of the starting polymers.

Table 1.4. Borylation of polystyrene [syndiotactic (sPS) and atactic (aPS)] with pinacolborane [HB(pin)]^a.

entry	PS ^b	M_n^c	PDI ^c (M_w/M_n)	[HB(pin)]/ [monomer]	PS–B(pin)			
					M_n^c	PDI ^c (M_w/M_n)	B(pin) (%) ^c	Effic. (%) ^e
1	sPS	127 ^f	2.64 ^f	0.05	– ^g	– ^g	2.6	52
2	sPS	127 ^f	2.64 ^f	0.1	– ^g	– ^g	4.5	45
3	sPS	127 ^f	2.64 ^f	0.2	82.1 ^f	2.65 ^f	7.1	36
4	sPS	127 ^f	2.64 ^f	0.4	93.8 ^f	2.38 ^f	9.8	25
5	aPS	25.1	1.09	0.1	25.7	1.09	4.0	40
6	aPS	25.1	1.09	0.4	26.0	1.10	5.9	15
7	aPS	247	1.07	0.1	259	1.07	4.0	40
8	aPS	247	1.07	0.4	262	1.05	5.6	14

^a B(pin) = pinacolboronate ester. PS = polystyrene. borylations were conducted on 200–260 mg of polymer with 3 mol % of iridium and 3 mol % of ligand relative to HB(pin) in cyclooctane (in a 1:6 molar ratio of polystyrene repeating unit to solvent) at 150 °C for 6 h. ^b PS = polystyrene. aPS [M_n = 25.1 kg/mol, PDI = 1.09; and M_n = 247 kg/mol, PDI = 1.07]; sPS [M_n = 127 kg/mol, PDI = 2.64]. ^c M_n in kg/mol and polydispersity index (PDI) measured with size-exclusion chromatography in THF at 40 °C relative to polystyrene standards unless otherwise specified. ^d The mol % of B(pin) functionalized styrene unit calculated from the ¹H NMR spectrum. ^e Efficiency of functionalization (i.e., the percentage of functionalized styrene unit relative to boron atoms added). ^f M_n in kg/mol

and PDI measured with high-temperature size-exclusion chromatography in 1,2,4-trichlorobenzene at 160 °C relative to polystyrene standards.⁸ Not measured.

1.3.3. Steric Effect in the C–H Borylation of sPS

When cumene was borylated with $B_2(\text{pin})_2$ under the standard condition for the C–H functionalization of sPS, a mixture of *meta*- and *para*- substituted cumene–B(pin) isomers in an approximate ratio of 7:3 was generated, because this reaction is controlled by steric hindrance (Figure 1.15a). A related iridium-catalyzed C–H activation of mono-substituted arene shows similar results.²⁹ Surprisingly, when we studied the ratio of regioisomers of borylated polymer products, we found the ratio of *meta*- and *para*-borylated polymers to be approximately 4:3 based on the resonances at 7.50–8.50 ppm on the ^1H NMR spectrum of sPS–B(pin). The ^1H NMR spectra of both sPS–B(pin) and iPS–B(pin) in C_6D_6 showed distinctive resonances for their *meta*- and *para*- isomers (Figure 1.15b,c). Although it was difficult to determine the isomer ratio of aPS–B(pin), because stereoregularity in the polymer chain was absent and the resulting peaks at 7.50–8.50 ppm region of the ^1H NMR spectrum were very broad in Figure 1.15d, we can assume that it possesses a similar ratio of isomers. It is believed that the higher ratio of *para*-isomer in the borylated polystyrene compared with that of borylated cumene results from reduced steric accessibility of the iridium catalyst for the *meta*- site of the polymer in the reaction medium. Since aromatic rings are attached to every other carbon of the polystyrene main chain, the available space for the active iridium catalyst to insert into the *meta*- C–H bond of the aromatic rings in the polystyrene chain is much smaller compared with that in the C–H borylation of cumene.

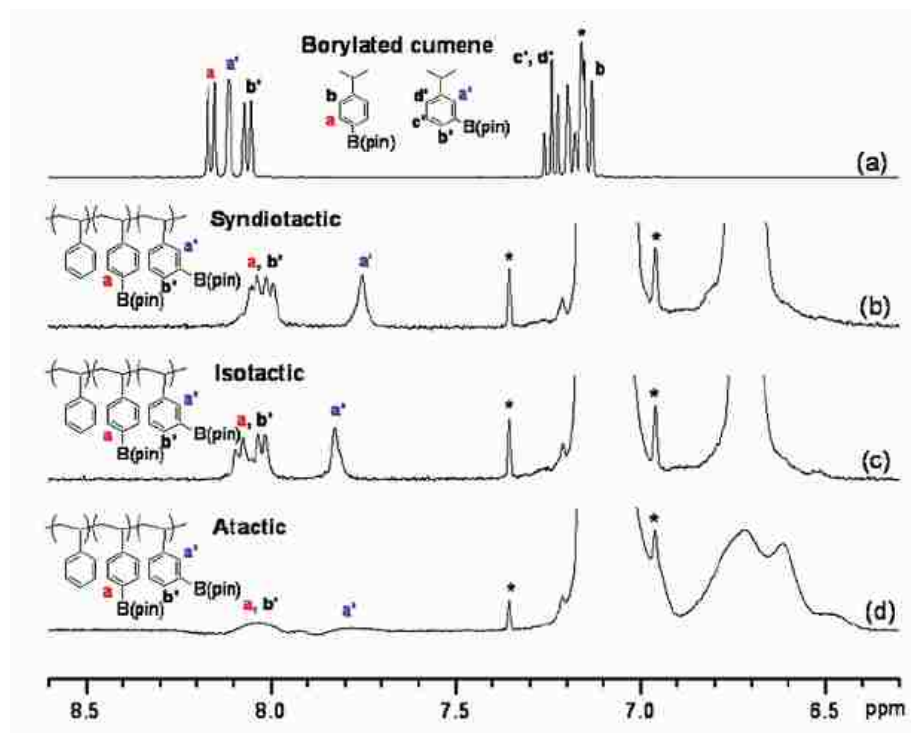
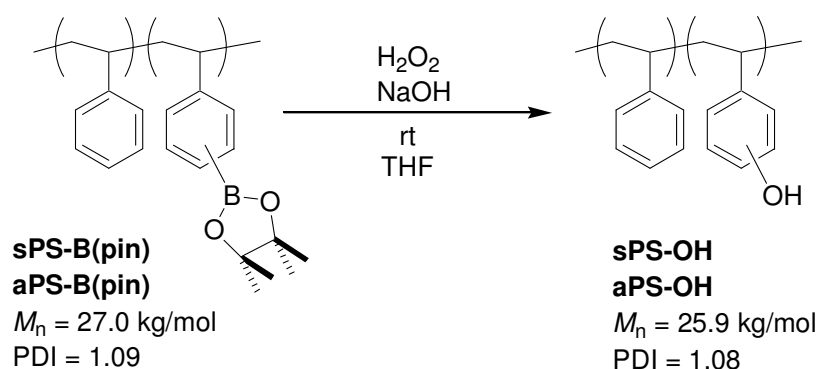


Figure 1.15. Expanded ^1H NMR spectra of (a) borylated cumene, (b) sPS-B(pin), (c) iPS-B(pin), and (d) aPS-B(pin) in C_6D_6 . An asterisk denotes resonances from the deuterated NMR solvent.

1.3.4. Oxidation of Borylated Polystyrenes

The boronic ester group of sPS-B(pin) (Table 1.2, Entries 1–6) and aPS-B(pin) (Table 1.3, Entry 2) was oxidized to hydroxy group with $\text{NaOH}/\text{H}_2\text{O}_2$ in THF to give the corresponding polar polymers, sPS-OH and aPS-OH, respectively (Scheme 1.2). It is known that a hydroxy-functionalized sPS could be synthesized through copolymerization with functionalized styrenes.³ However, its molecular weight and concentration of hydroxy group in the functionalized sPS were low ($M_n = 9.2$ kg/mol, 1.8 mol % OH group).³ In another example, when a borane-functionalized styrene monomer containing long alkylene spacers between the borane group and the aromatic ring was used in

syndiospecific polymerization with styrene, a higher concentration of hydroxy group could be incorporated into sPS after oxidation. Similar to the previous example of hydroxylated sPS,³ however, the polymerization resulted in decreased molecular weights and reduced degrees of crystallinity for the polymers compared with those of an sPS homopolymer.⁴



Scheme 1.2. Oxidation of borylated polystyrenes [Entries 1–6 of Table 1.2 for sPS–B(pin) and Entry 2 of Table 1.3 for aPS–B(pin)].

In our study, the hydroxy group was directly incorporated into the aromatic ring of sPS. The hydroxy group of sPS–OH and aPS–OH could be easily identified by a strong O–H stretching band at 3477 cm^{-1} and 3485 cm^{-1} in the IR spectrum, respectively (Figures 1.16 and 1.17). The resonances of B(pin) unit in the polymer chain disappeared completely in the ^1H and ^{13}C NMR spectra of sPS–OH and aPS–OH (Figures 1.18, 1.19, 1.20 and 1.21). Thus, the iridium-catalyzed borylation of aromatic C–H bonds and subsequent oxidation is a convenient method for introducing a hydroxy group directly into the aromatic ring of sPS.

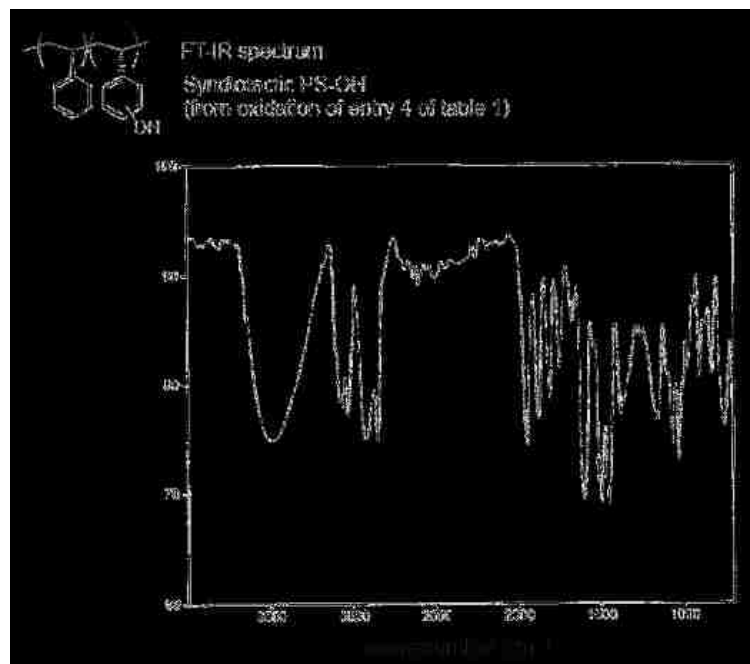


Figure 1.16. FT-IR spectrum of syndiotactic PS-OH.

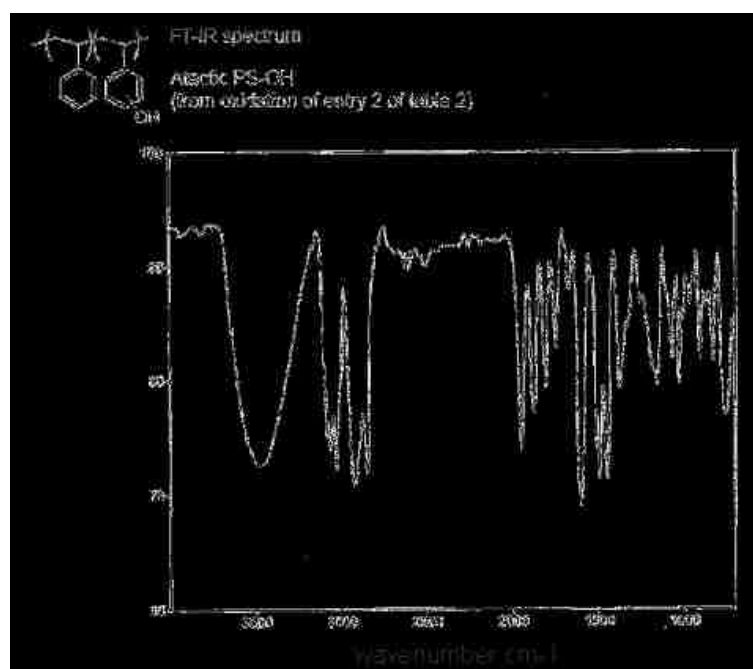


Figure 1.17. FT-IR spectrum of syndiotactic PS-OH.

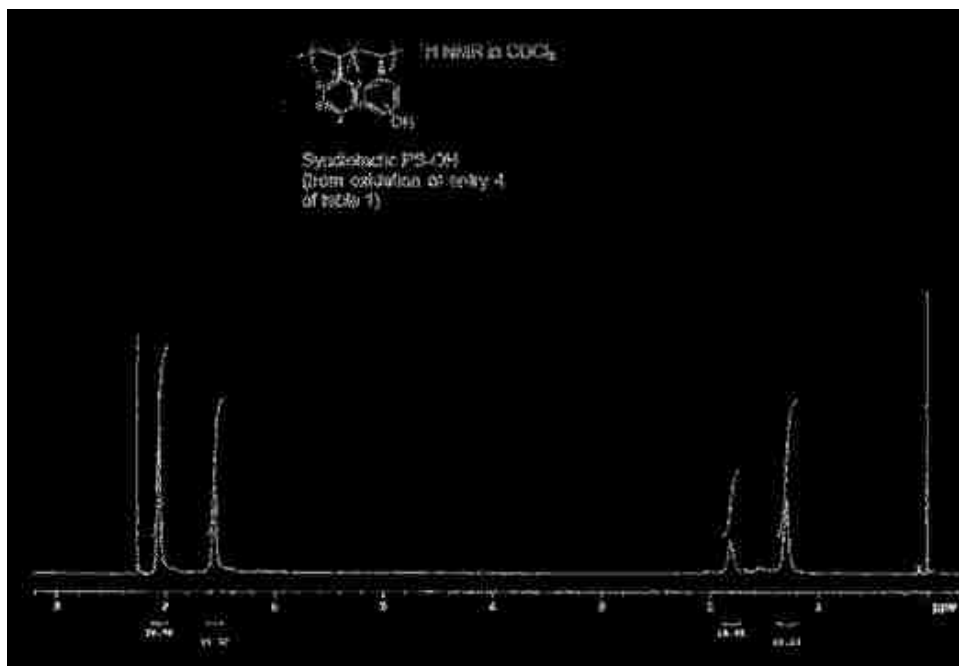


Figure 1.18. ¹H NMR spectrum of syndiotactic PS-OH [10 mg/mL in CDCl₃ at 25 °C].

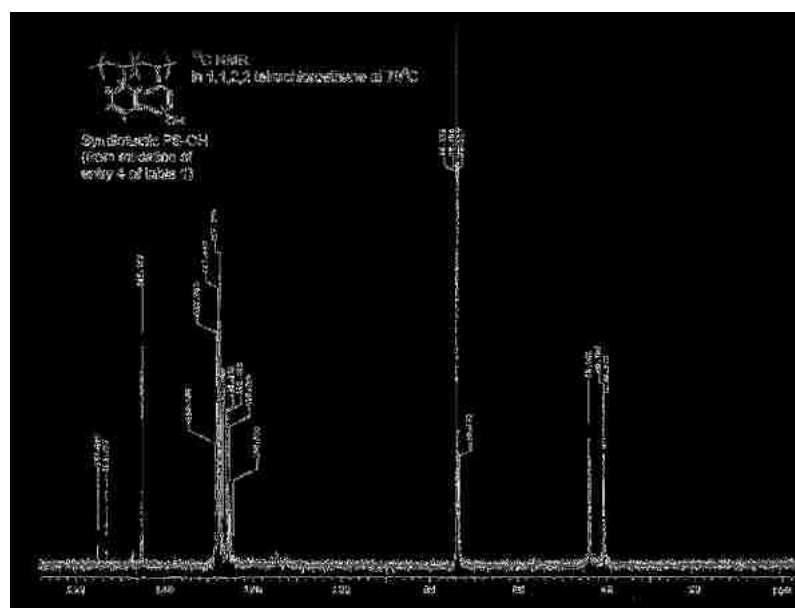


Figure 1.19. ¹³C NMR spectrum of syndiotactic PS-OH [30 mg/mL in 1,1,2,2-tetrachloroethane-*d*₂ at 70 °C].

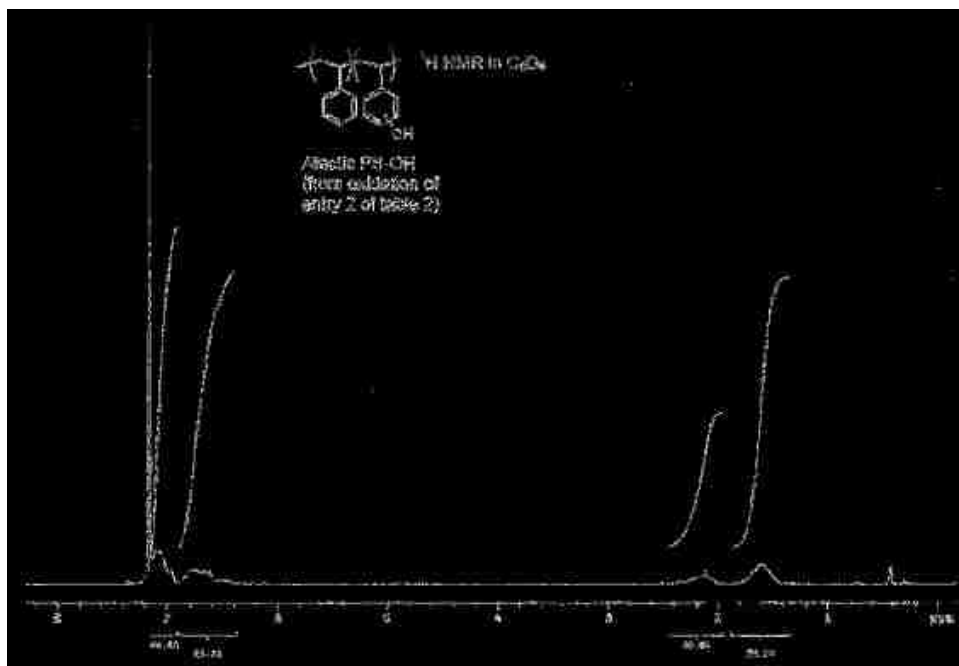


Figure 1.20. ¹H NMR spectrum of atactic PS-OH [10 mg/mL in C₆D₆ at 25 °C].

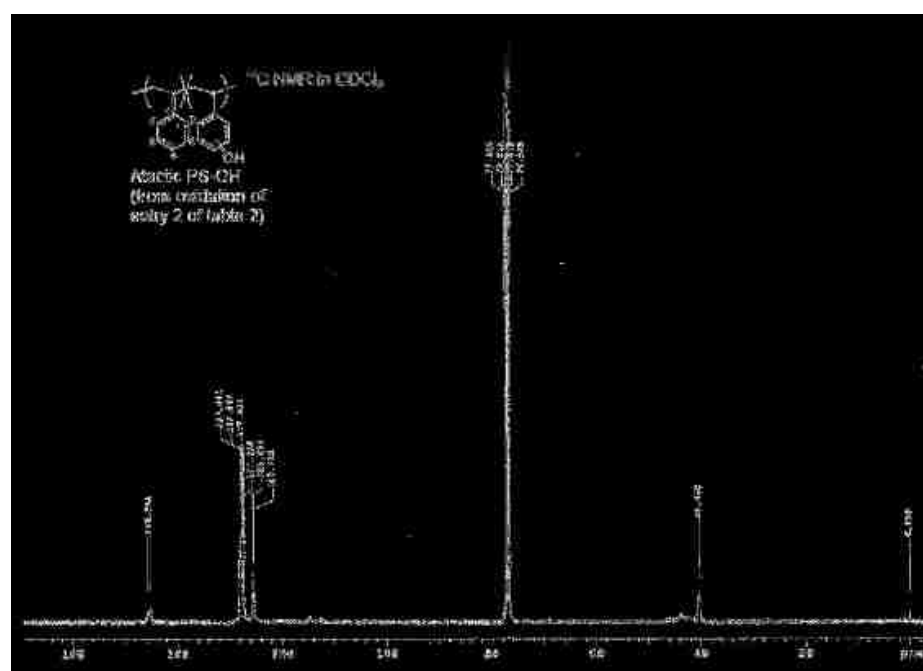
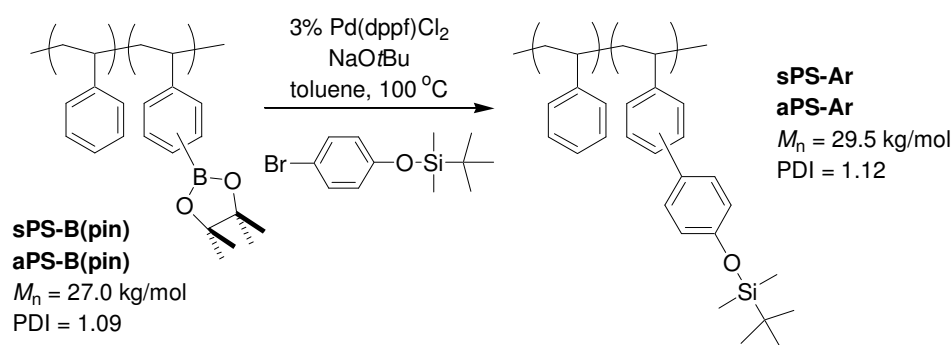


Figure 1.21. ¹³C NMR spectrum of atactic PS-OH [30 mg/mL in CDCl₃ at 25 °C].

1.3.5. Suzuki–Miyaura Coupling Reaction of Borylated Polystyrenes

Suzuki–Miyaura coupling reaction allows biaryl C–C bond formation through a cross-coupling reaction of aryl boron compound and an aryl halide in presence of a palladium catalyst. The cross reaction is widely used in organic synthesis owing to its good compatibility with various functional groups.³⁰ The coupling reaction of the polymer B(pin) groups with a functionalized aryl halide can install various functional groups at the polymer side chain. As shown in Scheme 1.3, (4-bromophenoxy)-*tert*-butyldimethylsilane coupled with PS–B(pin) to form arene-functionalized polystyrenes (sPS–Ar and aPS–Ar in Scheme 1.3) using 3 mol % of palladium catalyst.



Scheme 1.3. Suzuki–Miyaura coupling reaction of borylated polystyrenes [Entries 1–6 in Table 1.2 for sPS–B(pin) and Entry 2 in Table 1.3 for aPS–B(pin)].

Upon the Suzuki–Miyaura coupling reaction, the B(pin) group in the polymer disappeared completely and new *tert*-butyldimethylsilyl group appeared with a similar concentration in the ¹H and ¹³C NMR spectra of the coupled products (Figures 1.22, 1.23, 1.24 and 1.25).

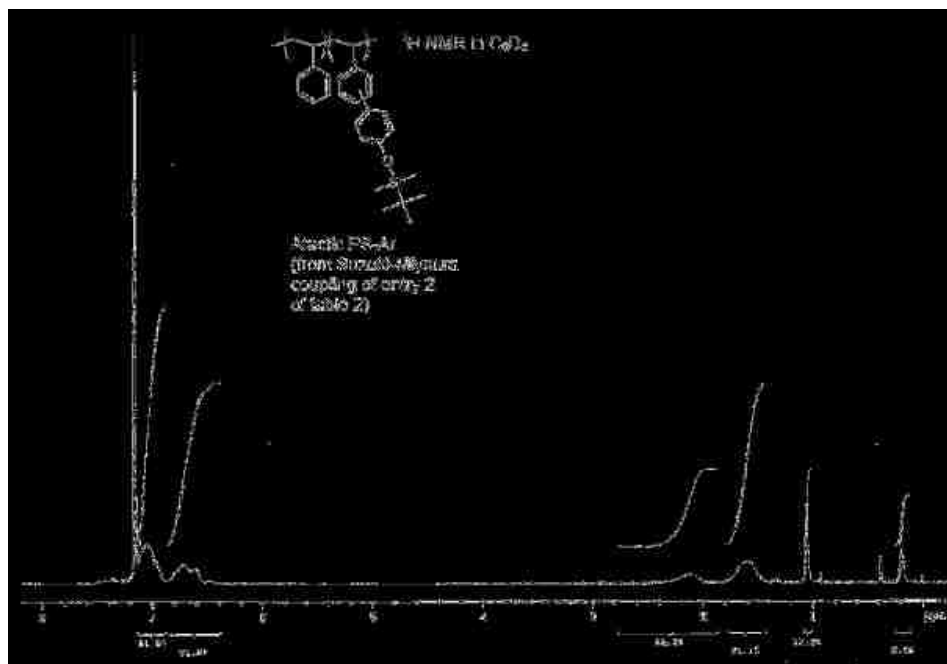


Figure 1.24. ¹H NMR spectrum of atactic PS-Ar [10 mg/mL in C₆D₆ at 25 °C].

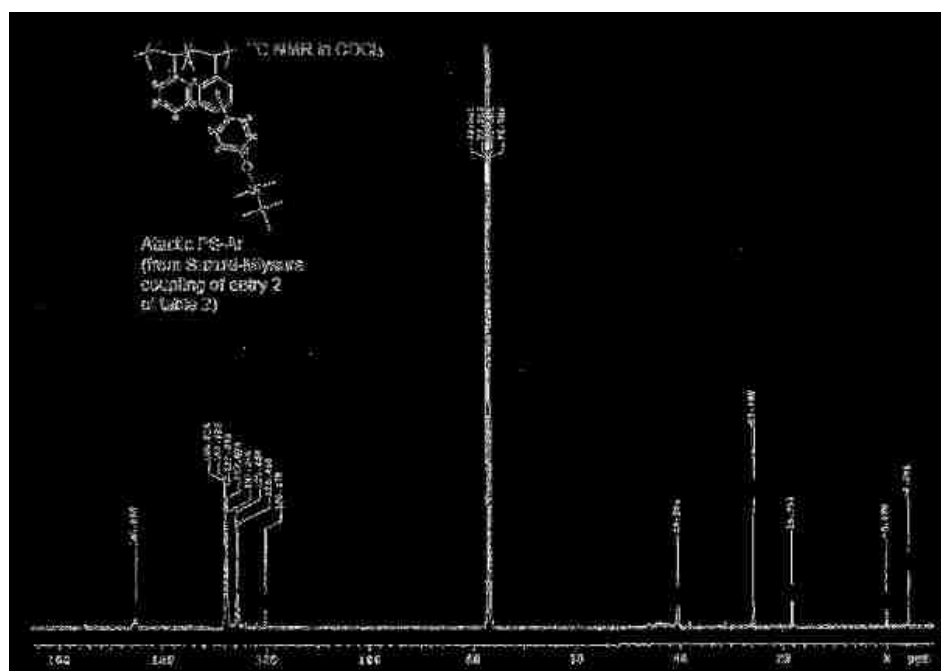


Figure 1.25. ¹³C NMR spectrum of atactic PS-Ar [30 mg/mL in CDCl₃ at 25 °C].

1.3.6. Size Exclusion Chromatography

To study whether there is any change in M_n and PDI during the C–H activation process in detail, we subjected two model aPS materials with narrow molecular weight distributions (M_n of 25.1 kg/mol with a PDI of 1.09, and M_n of 247 kg/mol with a PDI of 1.07) to the standard borylation condition. It was found that an increase in the ratio of $B_2(\text{pin})_2$ to monomer resulted in an M_n increase owing to the incorporation of more B(pin) group into aPS–B(pin) (Entries 1–8 of Table 1.3 and Figure 1.26). All PDI values remained ~ 1.10 , however, even with the incorporation of 41 mol % of B(pin) group (Table 1.3, Entry 7). This data clearly indicate that the iridium-catalyzed arene C–H activation process does not induce any deleterious side reactions leading to cleavage or coupling of polymer chains.

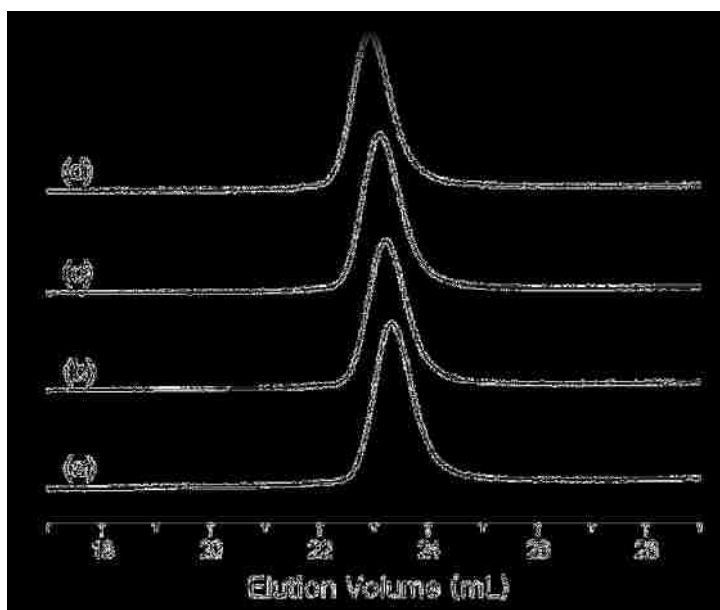


Figure 1.26. Size exclusion chromatography for (a) atactic polystyrene (aPS) [$M_n = 25.1$ kg/mol; PDI = 1.09]; (b) aPS–B(pin) [$M_n = 26.5$ kg/mol; PDI = 1.09] (Table 1.3, Entry 1); (c) aPS–B(pin) [$M_n = 27.8$ kg/mol; PDI = 1.10] (Table 1.3, Entry 3); and (d) aPS–

B(pin) [$M_n = 30.1$ kg/mol; PDI = 1.11] (Table 1.3, Entry 5). M_n relative to polystyrene standards.

Although the molecular weight data of sPS (Table 1.2, Entries 1–6) and iPS (Table 1.2, Entry 9) apparently show slight deviation from those of unfunctionalized crystalline polymers (i.e., $M_n = 127$ kg/mol, PDI = 2.64 for sPS; $M_n = 309$ kg/mol, PDI = 6.42 for iPS), these values may be due to the nature of the relatively broader molecular weight distributions of the polymers. When examined using high-temperature size exclusion chromatography (SEC) in 1,2,4-trichlorobenzene at 160 °C, their SEC traces did not show any sign of polymer chain degradation or coupling (Figure 1.27).

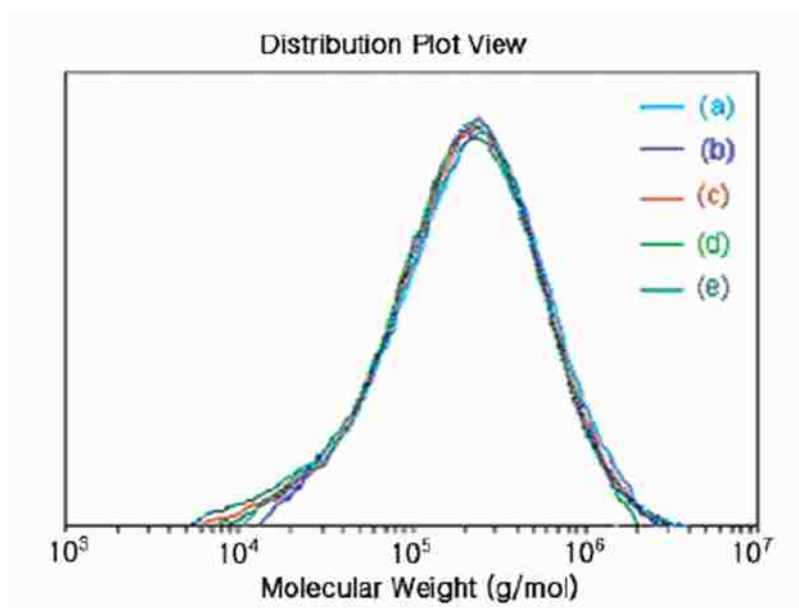


Figure 1.27. High-temperature size exclusion chromatography for (a) syndiotactic polystyrene (sPS) [$M_n = 127$ kg/mol; PDI = 2.64]; (b) sPS–B(pin) [$M_n = 132$ kg/mol; PDI = 2.37] (Table 1.2, Entry 1); (c) sPS–B(pin) [$M_n = 116$ kg/mol; PDI = 2.74] (Table 1.2, Entry 2); (d) sPS–B(pin) [$M_n = 116$ kg/mol; PDI = 2.53] (Table 1.2, Entry 3); and (e)

sPS-B(pin) [$M_n = 97.0$ kg/mol; PDI = 2.55] (Table 1.2, Entry 6). M_n relative to polystyrene standards.

The molecular weight changes from the borylation-oxidation sequence, which was studied in depth with model aPS, were negligible (Figure 1.28: aPS: $M_n = 25.1$ kg/mol, PDI = 1.09; aPS-B(pin): $M_n = 27.0$ kg/mol, PDI = 1.09; aPS-OH: $M_n = 25.9$ kg/mol, PDI = 1.08), highlighting the mildness of this protocol. The molecular weight distribution of the Suzuki coupling product, which was studied in depth with the model aPS, was again found to be unchanged from that of the precursor polymer (Figure 1.28: aPS-B(pin): $M_n = 27.0$ kg/mol, PDI = 1.09; aPS-Ar: $M_n = 29.5$ kg/mol, PDI = 1.12).

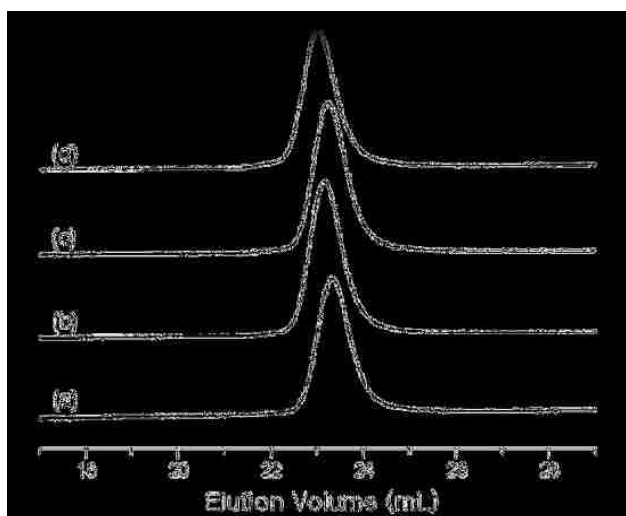


Figure 1.28. Size-exclusion chromatography for (a) aPS [$M_n = 25.1$ kg/mol, PDI = 1.09], (b) aPS-B(pin) [$M_n = 27.0$ kg/mol, PDI = 1.09] (Table 1.3, Entry 2), and (c) aPS-OH [$M_n = 25.9$ kg/mol, PDI = 1.08] (Scheme 1.2), (d) aPS-Ar [$M_n = 29.5$ kg/mol, PDI = 1.12] (Scheme 1.3). M_n relative to polystyrene standards.

1.3.7. Thermal Analysis

The thermal properties of sPS, sPS–B(pin) and sPS–OH are shown in Figure 1.29. sPS is known to possess a complex polymorphism. The most stable α and β crystalline forms have similar melting temperatures approximately at 270 °C, and their crystallization behaviors strongly depend on experimental conditions,³¹⁻³³ which may explain why the unfunctionalized sPS exhibits more than one melting transition in our study (Figure 1.29a). Despite high crystallinity in unfunctionalized sPS, the melting point and crystallinity of sPS were strongly affected by the size and concentration of functional group incorporated on the polymer (Figure 1.29 and Table 1.5).

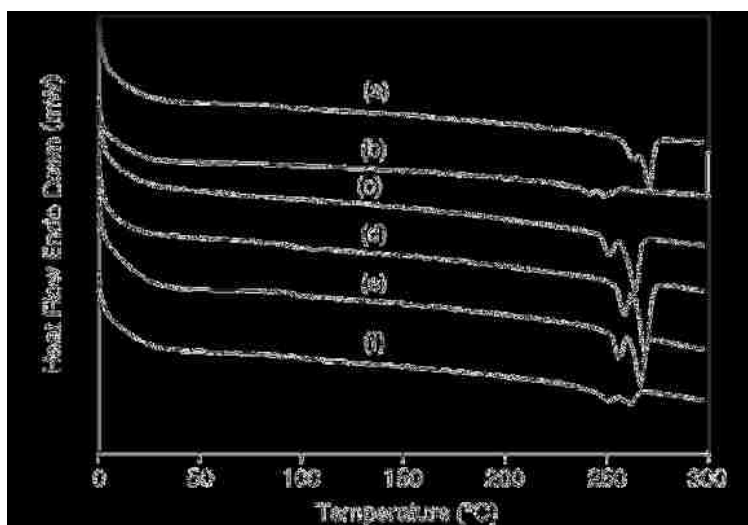


Figure 1.29. Differential scanning calorimetry scans of (a) syndiotactic polystyrene (sPS); (b) 2.5 mol % B(pin)-functionalized sPS–B(pin) (Table 1.2, Entry 1); (c) 2.5 mol % OH-functionalized sPS–OH (from oxidation of Entry 1 of Table 1.2); (d) 5.9 mol % OH-functionalized sPS–OH (from oxidation of Entry 2 of Table 1.2); (e) 9.9 mol % OH-functionalized sPS–OH (from oxidation of Entry 3 of Table 1.2); (f) 16.4 mol % OH-functionalized sPS–OH (from oxidation of Entry 4 of Table 1.2).

For example, the sPS–B(pin) containing 5.9 mol % B(pin) group (Table 1.2, Entry 2) lost crystallinity completely because the bulky B(pin) group disrupted crystallization. This result is consistent with a report that the attached sulfonic acid group sharply decreases the melting point and degree of crystallinity of sPS even in lightly (i.e., <5 mol %) sulfonated sPS.⁸ After oxidation, however, even sPS–OH containing 9.9 mol % group (from oxidation of Entry 3 of Table 1.2) recovered high crystallinity and showed a slightly lower melting temperature (267 °C) compared with those of unfunctionalized sPS (40% and 271 °C) (Figure 1.29e and Table 1.5). It is believed that the smaller hydroxy group in the polymer did not interfere with the crystallization as much as the bulky boronic ester group did in sPS–B(pin). Overall, the sequence of borylation-oxidation process can generate polar group-functionalized sPS that has a slightly lower melting point without inducing degradation or cross-linking of the parent polymer.

Table 1.5. Thermal properties of syndiotactic polystyrene (sPS) and functionalized sPS^a.

Polymer	Functional group	T_g (°C) ^b	T_m (°C) ^c	ΔH_f (J/g) ^d	Crystallinity ^e (%)
sPS	none	99	271	21.1	40
sPS-B(pin)	2.5 mol % B(pin)	95	249	3.1	6
sPS-B(pin)	5.9 mol % B(pin)	109	^f	-	-
sPS-OH	2.5 mol % OH	^f	264	19.5	37
sPS-OH	5.9 mol % OH	100	269	17.2	34
sPS-OH	9.9 mol % OH	104	267	19.2	36
sPS-OH	16.4 mol % OH	106	261	8.3	16
sPS-OH	23.6 mol % OH	118	260	0.9	2
sPS-OH	34.2 mol % OH	129	^f	-	-

^a Differential scanning calorimetry (DSC) measurements conducted using heating/cooling rates of 10 °C/min. The OH mol % is based on the assumption of quantitative conversion of B(pin) group without formation of other deborylated byproducts. ^b Glass transition temperature in °C. ^c Melting point of polymer in °C. ^d Heat of fusion of polymer in J/g. ^e The percent of crystallinity based on the theoretical heat of fusion calculated for 100% crystalline sPS (i.e., $\Delta H_f^0 = 53.3$ J/g; from reference 1). ^f Not detected.

1.4. Experimental

1.4.1. General Comments

[IrCl(COD)]₂, d/bpy, HB(pin), hydrogen peroxide, tetrahydrofuran (THF), sodium hydroxide, and chloroform were reagent grade and used without further purification. B₂(pin)₂ was obtained from Frontier Scientific Co. and used after recrystallization from hexane. Cyclooctane was dried using sodium and benzophenone, distilled under reduced pressure, and stored in a nitrogen-filled glovebox. sPS ($M_n = 127$ kg/mol with PDI =

2.64) and two model aPS of narrow molecular distributions ($M_n = 25.1$ kg/mol with PDI = 1.09 and $M_n = 247$ kg/mol with PDI = 1.07) were obtained from LG Chem Ltd., Daejeon, South Korea, and Sigma Aldrich Co., respectively, and used as received. To improve the solubility of iPS ($M_n = 309$ kg/mol, PDI = 6.42, 90% isotactic from Sigma Aldrich Co.) in the borylation medium, the following procedure was performed. One gram of the polymer was placed in a two-neck round-bottom flask, and then the flask was evacuated and backfilled with nitrogen three times. 1,2-Dichlorobenzene (30 mL) was added to this flask and the mixture was refluxed at 180 °C under nitrogen for 30 min to dissolve all iPS. The solution was then cooled to 140 °C and poured into cold methanol (300 mL). The precipitate was filtered and dried under vacuum at 60 °C.

^1H NMR spectra were obtained using a 400 MHz Varian NMR spectrometer at room temperature and chemical shifts were referenced to TMS. The NMR samples were prepared by applying gentle heat to dissolve polymer in CDCl_3 (for sPS) or C_6D_6 (for sPS, aPS, and iPS). The ^1H NMR samples were prepared at a concentration of 10 mg/mL. The B(pin) mol % of PS-B(pin) was determined based on the relative intensity of $-\text{CH}-$ in polystyrene main chain ($\delta = 1.81$ in CDCl_3 ; $\delta = 2.10\text{--}2.30$ in C_6D_6) to $-\text{CH}_3$ of B(pin) ($\delta = 1.35$ in CDCl_3 ; $\delta = 1.15\text{--}1.20$ in C_6D_6) in the spectra and provided in Tables 1.2–4. For molecular weight characterization of aPS materials, size exclusion chromatography (SEC) analysis was conducted using a VISCOTEK chromatograph equipped with three visco-GEL I Series columns and tetra detector array (UV/vis, low and right angle light scattering, refractive index, and viscometer) at 40 °C. THF was used as the mobile phase and the flow rate was set at 1.0 mL/min. High-temperature size exclusion chromatography analysis for the molecular weight measurement of sPS and iPS was

obtained using a Polymer Laboratory GPC-220 high-temperature size exclusion chromatography at 160 °C. 1,2,4-Trichlorobenzene was used as the mobile phase and the flow rate was set at 1.0 mL/min. Both instruments were calibrated using polystyrene standards. The differential scanning calorimetry (DSC) measurement was conducted on a Perkin-Elmer Pyris 6 DSC series under a nitrogen atmosphere. The polymer samples were heated to 300 °C, with a hold at 300 °C for 1 min in order to remove the influence of thermal history, cooled to 0 °C, held at 0 °C for 1 min, and then reheated to 300 °C, cooling and heating at a rate of 10 °C/min. All DSC curves in Figure 1.29 were obtained from the second heating. The temperatures (T_g and T_m) and enthalpy (ΔH_f) were obtained after calibration with high-purity indium and zinc standards.

sPS: ^1H NMR (400 MHz, CDCl_3) δ = 1.30 (2H, $-\text{CH}_2-$), 1.81 (1H, $-\text{CH}-$), 6.55 (2H, H_{arom}), 7.06 (3H, H_{arom}). ^{13}C NMR (100 MHz, CDCl_3) δ = 40.54 ($-\text{CH}-$), 43.84 ($-\text{CH}_2-$), 125.60 ($\text{C}_6\text{H}_5-\text{C}4$), 127.60 ($\text{C}_6\text{H}_5-\text{C}2,6$), 127.86 ($\text{C}_6\text{H}_5-\text{C}3,5$), 145.19 ($\text{C}_6\text{H}_5-\text{C}1$).

aPS: ^1H NMR (400 MHz, C_6D_6) δ = 1.60 (br, 2H, $-\text{CH}_2-$), 2.10 (br, 1H, $-\text{CH}-$), 6.41–6.88 (2H, H_{arom}), 6.91–7.28 (3H, H_{arom}). ^{13}C NMR (100 MHz, CDCl_3) δ = 40.74 ($-\text{CH}-$), 41.3–47.2 ($-\text{CH}_2-$), 126.02 ($\text{C}_6\text{H}_5-\text{C}4$), 128.02 ($\text{C}_6\text{H}_5-\text{C}2,6$), 128.34 ($\text{C}_6\text{H}_5-\text{C}3,5$), 145.70 ($\text{C}_6\text{H}_5-\text{C}1$).

iPS: ^1H NMR (400 MHz, C_6D_6) δ = 1.59 and 1.65 (2H, $-\text{CH}_2-$), 2.33 (1H, $-\text{CH}-$), 6.77 (2H, H_{arom}), 7.08 (3H, H_{arom}). ^{13}C NMR spectrum could not be obtained due to lack of solubility of the polymer in C_6D_6 or CDCl_3 .

1.4.2. Synthesis of Pinacol Boronic Ester-Functionalized Polystyrene

Preparation of sPS-B(pin) using $\text{B}_2(\text{pin})_2$ (Entry 4 of Table 1.2). In a nitrogen-filled glovebox, a mixture of sPS (260 mg, 2.50 mmol polystyrene repeating unit), $\text{B}_2(\text{pin})_2$

(63.0 mg, 0.25 mmol), [IrCl(COD)]₂ (2.5 mg, 3 mol % iridium based on the amount of B₂(pin)₂), dtbpy (2.0 mg, 3 mol % based on the amount of B₂(pin)₂), and cyclooctane (1.68 g, 15.0 mmol) and a magnetic stirring bar were placed into a vial and capped with a Teflon-lined septum. The vial was removed from the glovebox and placed in an oil bath at 150 °C for 6 h. After cooling to room temperature, the mixture was diluted with chloroform (30 mL) and filtered through a short plug of silica to remove the catalyst. The filtrate was concentrated by a rotary evaporator to approximately 5 mL, and cold methanol (25 mL) was added to precipitate the polymer. The dissolution and precipitation process was repeated one more time to ensure complete removal of any small molecules trapped in the polymer. The borylated polymer was filtered as a white solid and dried under vacuum at 60 °C (281 mg, 108% yield based on polymer weight): ¹H NMR (400 MHz, CDCl₃) δ = 1.30 (2H, -CH₂-), 1.35 (s, BOCCH₃), 1.80 (1H, -CH-), 6.54 (2H, H_{arom}), 7.05 (3H, H_{arom}), 7.56 (H_{arom} from C₆H₄-B(pin)); ¹H NMR (400 MHz, C₆D₆) δ = 1.15 and 1.19 (BOCCH₃), 1.49 (2H, -CH₂-), 2.08 (1H, -CH-), 6.07 (2H, H_{arom}), 7.05 (3H, H_{arom}), 7.75 [H_{arom} from C₆H₄-B(pin)], 8.00 [H_{arom} from C₆H₄-B(pin)], 8.04 [H_{arom} from C₆H₄-B(pin)]. ¹³C NMR (100 MHz, CDCl₃) δ = 24.9 (BOCCH₃), 40.5 (-CH-), 43.8 (-CH₂-), 83.5 (BOCCH₃), 125.6 (C₆H₅-C₄), 127.2 [C_{arom} from C₆H₄-B(pin)], 127.7 (C₆H₅-C_{2,6}), 127.9 (C₆H₅-C_{3,5}), 130.9 [C_{arom} from C₆H₄-B(pin)], 132.3 [C_{arom} from C₆H₄-B(pin)], 134.0 [C_{arom} from C₆H₄-B(pin)], 134.5 [C_{arom} from C₆H₄-B(pin)], 144.6 [C_{arom} from C₆H₄-B(pin)], 145.18 (C₆H₅-C₁), 148.79 [C_{arom} from C₆H₄-B(pin)]. ¹¹B NMR (128.3 MHz, CDCl₃) δ = 28.0 (br).

Preparation of sPS-B(pin) using HB(pin) (Entry 2 of Table 1.4). In a nitrogen-filled glovebox, a mixture of sPS (260 mg, 2.50 mmol polystyrene repeating unit), HB(pin)

(32.0 mg, 0.25 mmol), [IrCl(COD)]₂ [2.5 mg, 3 mol % iridium based on the amount of HB(pin)], dtbpy [2.0 mg, 3 mol % based on the amount of HB(pin)], and cyclooctane (1.68 g, 15.0 mmol) and a magnetic stirring bar were placed into a vial and capped with a Teflon-lined septum. The vial was removed from the glovebox and placed in an oil bath at 150 °C for 16 h. After cooling to room temperature, the mixture was diluted with chloroform (30 mL) and filtered through a short plug of silica to remove the catalyst. The filtrate was concentrated by a rotary evaporator to approximately 5 mL, and cold methanol (25 mL) was added to precipitate the polymer. The dissolution and precipitation process was repeated one more time to ensure complete removal of any small molecules trapped in the polymer. The borylated polymer was filtered as a white solid and dried under vacuum at 60 °C (255 mg, 98% yield based on polymer weight).

Preparation of aPS-B(pin) using B₂(pin)₂. Borylated atactic polystyrene with the different ratios of B₂(pin)₂/monomer reported in Table 1.3 was prepared in a 200 mg scale (1.92 mmol polystyrene repeating unit) according to the procedure described for the preparation of sPS-B(pin) using B₂(pin)₂: ¹H NMR (400 MHz, C₆D₆) δ = 1.17 (s, BOCCH₃), 1.58 (br, 2H, -CH₂-), 2.09 (br, 1H, -CH-), 6.41–6.88 (2H, *H_{arom}*), 6.91–7.28 (3H, *H_{arom}*), 8.03 [br, *H_{arom}* from C₆H₄-B(pin)]. ¹³C NMR (100 MHz, CDCl₃) δ = 24.9 (-BOCCH₃), 40.3 (-CH-), 41.3–47.2 (-CH₂-), 83.5 (-BOCCH₃), 125.6 (C₆H₅-C4), 127.6 (C₆H₅-C2,6), 127.94 (C₆H₅-C3,5), 131.02 [*C_{arom}* from C₆H₄-B(pin)], 132.39 [*C_{arom}* from C₆H₄-B(pin)], 134.66 [*C_{arom}* from C₆H₄-B(pin)], 145.31 (C₆H₅-C1). ¹¹B NMR (128.3 MHz, CDCl₃) δ = 27.5 (br).

Preparation of aPS-B(pin) using HB(pin). Borylated atactic polystyrene with the different ratios of HB(pin)/monomer reported in Table 1.4 was prepared in a 200 mg

scale (1.92 mmol polystyrene repeating unit) according to the procedure described for preparation of sPS–B(pin) using HB(pin).

Preparation of iPS–B(pin) using B₂(pin)₂ (Entry 9 of Table 1.2). In a nitrogen-filled glovebox, a mixture of iPS (200 mg, 1.92 mmol polystyrene repeating unit), B₂(pin)₂ (48.3 mg, 0.192 mmol), [IrCl(COD)]₂ (1.9 mg, 3 mol % iridium based on the amount of B₂(pin)₂), dtbpy [1.5 mg, 3 mol % based on the amount of B₂(pin)₂], cyclooctane (2.15 g, 19.2 mmol) and a magnetic stirring bar were placed into a vial and capped with a Teflon-lined septum. The vial was removed from the glovebox and placed in an oil bath at 150 °C for 6 h. After cooling to room temperature, the mixture was diluted with chloroform (40 mL). (Because of high viscosity of the solution, filtration through silica was avoided). The solution was concentrated by a rotary evaporator to approximately 5 mL, and cold methanol (25 mL) was added to precipitate the polymer. The dissolution and precipitation process was repeated one more time to ensure complete removal of any small molecules trapped in the polymer. The precipitated solid was filtered and dried under vacuum at 60 °C (203 mg, 102% yield based on polymer weight from iPS): ¹H NMR (400 MHz, C₆D₆) δ = 1.16 (s, BOCCH₃), 1.59 and 1.65 (2H, –CH₂–), 2.33 (1H, –CH–), 6.71 (2H, *H_{arom}*), 7.06 (3H, *H_{arom}*), 7.83 [*H_{arom}* from C₆H₄–B(pin)], 8.03 [*H_{arom}* from C₆H₄–B(pin)], 8.08 [*H_{arom}* from C₆H₄–B(pin)]. ¹³C NMR spectrum could not be obtained due to lack of solubility of the polymer in C₆D₆ or CDCl₃.

1.4.3. Synthesis of Hydroxy-Functionalized Polystyrene

Preparation of sPS–OH. sPS–B(pin) (100 mg, Entry 4 of Table 1.2) was dissolved in THF (100 mL) in a 250 mL flask by applying gentle heat and then cooled to room temperature. A mixture of aqueous 3M NaOH (1 mL) and 30% H₂O₂ (1 mL) was slowly

added to the polymer solution at room temperature. The resulting solution was stirred at room temperature for 12 h. The solution was concentrated by a rotary evaporator to approximately 5 mL, and a mixture of methanol and water (10 mL/40 mL) was added. The heterogeneous suspension was stirred for 20 min and filtered. The collected white solid was washed with water (3 × 10 mL) and methanol (3 × 5 mL). The solid was dried under vacuum at 60 °C [87 mg, 87% yield based on polymer weight from sPS-B(pin)]: ¹H NMR (400 MHz, CDCl₃) δ = 1.30 (2H, -CH₂-), 1.80 (1H, -CH-), 6.54 (2H, *H*_{arom}), 7.05 (3H, *H*_{arom}). ¹³C NMR (100 MHz, 1,1,2,2-tetrachloroethane-*d*₂ at 70 °C) δ = 40.7 (-CH-), 43.8 (-CH₂-), 112.4 (*C*_{arom} from C₆H₄-OH), 114.7 (*C*_{arom} from C₆H₄-OH), 120.1 (*C*_{arom} from C₆H₄-OH), 125.6 (C₆H₅-C4), 127.6 (C₆H₅-C2,6), 127.9 (C₆H₅-C3,5), 124.0–129.2 (multiple *C*_{arom} from C₆H₄-OH), 137.5 (*C*_{arom} from C₆H₄-OH), 145.2 (C₆H₅-C1), 147.2 (*C*_{arom} from C₆H₄-OH), 153.0 (HO-*p*-C₆H₄-C4), 154.9 (HO-*m*-C₆H₄-C3). FT-IR (film) ν = 3477 cm⁻¹ (O-H).

Preparation of aPS-OH. Hydroxylated atactic polystyrene was prepared in a 100 mg scale according to the procedure described for the preparation of sPS-OH: ¹H NMR (400 MHz, C₆D₆) δ = 1.60 (2H, -CH₂-), 2.11 (1H, -CH-), 6.41–6.88 (2H, *H*_{arom}), 6.91–7.28 (3H, *H*_{arom}). ¹³C NMR (100 MHz, CDCl₃) δ = 40.3 (-CH-), 41.3–47.2 (-CH₂-), 125.7 (C₆H₅-C4), 127.7 (C₆H₅-C2,6), 112.7 (*C*_{arom} from C₆H₄-OH), 114.8 (*C*_{arom} from C₆H₄-OH), 128.1 (C₆H₅-C3,5), 129.2 (*C*_{arom} from C₆H₄-OH), 145.2 (C₆H₅-C1), 153.3 (HO-*p*-C₆H₄-C4), 155.2 (HO-*m*-C₆H₄-C3). FT-IR (film) ν = 3472 cm⁻¹ (O-H).

1.4.4. Synthesis of *tert*-Butyldimethylsilyloxy-Functionalized Polystyrene

Preparation of sPS-Ar by Suzuki-Miyaura Cross-Coupling of sPS-B(pin) (from Entry 3 of Table 1.3). In a nitrogen-filled glovebox, a mixture of sPS-B(pin) [50 mg,

0.043 mmol B(pin)], (4-bromophenoxy)-*tert*-butyldimethylsilane (62.0 mg, 0.215 mmol), dichloro[1,1'-bis(diphenylphosphino)ferrocene] palladium(II) [1.1 mg, 3 mol % based on the amount of boron concentration in sPS-B(pin)], sodium *tert*-butoxide [12.4 mg, 0.129 mmol, 3 equiv to the amount of boron concentration in sPS-B(pin)], and toluene (1 mL) and a magnetic stirring bar were placed into a vial and capped with Teflon-lined septum. The vial was removed from the glovebox and placed in an oil bath at 100 °C for 22 h. After cooling, the mixture was diluted with chloroform (30 mL) and filtered through a short plug of silica. The filtrate was concentrated by a rotary evaporator to approximately 5 mL, and cold methanol (25 mL) was added to precipitate the polymer. The dissolution and precipitation process was repeated one more time to ensure complete removal of any small molecules trapped in the polymer. The polymer product was filtered as a white solid and dried under vacuum at 60 °C [45 mg, 90% yield based on polymer weight from sPS-B(pin)]: ¹H NMR (400 MHz, CDCl₃) δ = 0.24 [s, Si(CH₃)₂C(CH₃)₃], 1.02 [s, Si(CH₃)₂C(CH₃)₃], 1.30 (2H, -CH₂-), 1.80 (1H, -CH-), 6.54 (*H_{arom}*), 7.06 (*H_{arom}*). ¹³C NMR (100 MHz, CDCl₃) δ = -4.4 [Si(CH₃)₂C(CH₃)₃], 18.3 [Si(CH₃)₂C(CH₃)₃], 25.7 [Si(CH₃)₂C(CH₃)₃], 40.5 (-CH-), 43.8 (-CH₂-), 120.2 (*C_c*), 124.1 (*C_{arom}* from C₆H₄-Ar), 125.6 (C₆H₅-C₄), 126.1 (*C_{arom}* from C₆H₄-Ar), 127.7 (C₆H₅-C_{2,6}), 127.9 (C₆H₅-C_{3,5}), 128.0 (*C_b*), 134.6 (*C_a*), 145.2 (C₆H₅-C₁), 155.0 (*C_d*).

Preparation of aPS-Ar by Suzuki-Miyaura Cross-Coupling of aPS-B(pin) (from Entry 2 of Table 1.3). Arene functionalized atactic polystyrene was prepared from aPS-B(pin) [50 mg, 0.043 mmol B(pin)] according to the procedure described for the preparation of sPS-Ar: ¹H NMR (400 MHz, C₆D₆) δ = 0.19 [s, Si(CH₃)₂C(CH₃)₃], 1.06 [s, Si(CH₃)₂C(CH₃)₃], 1.60 (2H, -CH₂-), 2.11 (1H, -CH-), 6.41–6.88 (*H_{arom}*), 6.91–7.28

(H_{arom}). ^{13}C NMR (100 MHz, CDCl_3) δ = -4.3 [$\text{Si}(\text{CH}_3)_2\text{C}(\text{CH}_3)_3$], 18.3 [$\text{Si}(\text{CH}_3)_2\text{C}(\text{CH}_3)_3$], 25.8 [$\text{Si}(\text{CH}_3)_2\text{C}(\text{CH}_3)_3$], 40.4 (-CH-), 41.3–47.2 (-CH₂-), 120.2 (C_c), 124.1 (C_{arom} from $\text{C}_6\text{H}_4\text{-Ar}$), 125.7 ($\text{C}_6\text{H}_5\text{-C4}$), 126.2 (C_{arom} from $\text{C}_6\text{H}_4\text{-Ar}$), 127.6 ($\text{C}_6\text{H}_5\text{-C2,6}$), 128.0 ($\text{C}_6\text{H}_5\text{-C3,5}$), 134.6 (C_a), 145.3 ($\text{C}_6\text{H}_5\text{-C1}$), 155.0 (C_d).

1.5. Conclusion

In summary, the iridium-catalyzed functionalization of the aromatic C–H bond of commercial polystyrenes with three types of tacticities (syndiotactic, isotactic, and atactic) using boron reagents was accomplished. The introduction of a boronic ester group was controlled up to 42 mol % without negatively influencing the chain length or tacticity of the parent polymer. The amount of the incorporated boryl group can be easily controlled by changing the ratio of boron reagent to polymer repeating unit with as low as 0.5 mol % of catalyst loading. The boronic ester group in the polymer was further converted to other versatile groups by subsequent oxidation and Suzuki-Miyaura cross-coupling reaction. It was shown that sPS–OH containing up to 10 mol % of hydroxy group still kept high crystallinity with a high melting temperature in the thermal analysis. This study has shown a facile route to install functional groups into crystalline polystyrenes for further applications of these important polymers.

CHAPTER 2

A HOMOGENEOUS PALLADIUM CATALYST SUPPORTED ON SYNDIOTACTIC POLYSTYRENE AND ITS APPLICATION IN SUZUKI-MIYAJIMA CROSS- COUPLING REACTIONS

2.1. Abstract

Soluble syndiotactic polystyrene-supported triphenylphosphine (sPS-TPP) was prepared from boronated syndiotactic polystyrene [sPS-B(pin)] and (4-bromophenyl)diphenylphosphine (TPP-Br). We studied the reactivity of a palladium complex supported on sPS-TPP as a catalyst for Suzuki-Miyajima coupling reactions of aryl halides under homogeneous conditions. The polymer-supported palladium complex ligand was quantitatively recovered from the reaction mixture through precipitation by adding a poor solvent of the polymer and recycled in four consecutive runs without significant loss of activity.

2.2. Introduction

Although homogeneous catalysts have been widely used in chemical synthesis due to better efficiency and selectivity than the heterogeneous counterparts, they require tedious, time-consuming, and laborious purification steps such as chromatography, distillation, or crystallization to separate product from the catalyst in reaction mixture.

Thus, recovery and recycling of homogenous catalysts are difficult.³⁴ Since Merrifield resin was introduced for peptides synthesis in the 1960s, cross-linked polystyrene-supported catalysts have been widely used in numerous organic reactions to make product purification and catalyst recovery simpler.³⁵ Catalysts have also been supported on insoluble materials such as activated carbon,³⁶ zeolite,³⁷ metal oxide,³⁸ insoluble polymer resin,³⁹ and mesoporous silica nano particles.⁴⁰ Despite the well-known advantage of insoluble supports—convenient separation—they generally suffer from slow diffusion rates caused by interfacial mass transfer limitation, difficult characterization, metal leaching, and lower activity and selectivity owing to the nature of heterogeneous reaction conditions.⁴¹

To overcome the problems of insoluble supports, soluble polymer supports have recently gained a significant attention as an alternative catalyst recovery method. Soluble polymer supports allow convenient transfer of solution-based synthetic protocols that are commonly used in traditional solution-organic chemistry, thus additional optimization process often required in the heterogeneous reactions is not necessary.

Soluble polymer supports include polyethylene glycol, polyacrylic ester, polyvinyl alcohol, polyethylene imine, polyacrylamide, polyethylene, polypropylene (PP), polyacrylic acid, cellulose, and atactic polystyrene. Among them, oligomeric polyethylene glycol (PEG, $M_n = 3\text{--}5$ kg/mol),⁴² oligomeric polyethylene (PE, $M_n \sim 3$ kg/mol),⁴³ and non-cross-linked (atactic) polystyrene (aPS)⁴⁴ are the most representative soluble polymeric supports used in organic synthesis and combinatorial chemistry. However, these supports also have some drawbacks needed to be

overcome. First, because PEG is soluble in water, it is not suitable for an organic reaction that needs an aqueous workup process. Second, PEG and PE are end-functionalized polymer supports which have the limitation on loading capacity. Typical loading capacity is less than 0.3 mmol/g for PEG and 0.1 mmol/g for PE. Lastly, soluble polymer supports are often isolated as a viscous gooey or gummy material (for example aPS, see Figure 2.1b), making them difficult to be recovered in high yields via simple precipitation methods. Thus, studies of recovery yields of soluble polymer support have often been omitted.⁴⁵

Herein, we introduce a new type of soluble polymer support derived from crystalline syndiotactic polystyrene (sPS). aPS has good solubility in most solvents due to its amorphous nature, which often results in low or non-quantitative recovery yield. To recover aPS support in high yield, it is required to add excess of cold poor solvent. Compared to aPS, sPS and functionalized sPS show a more restrictive solubility profile because of high stereoregular configuration of phenyl rings along the polymer main chain and the resulting tendency toward crystallization.⁴⁶ We assumed that the relationship between solubility and recovery of crystalline polymer can induce better recovery yield of sPS support when precipitated with addition of poor solvent.

In Chapter 1 we reported that a controlled functionalization of sPS by an iridium-catalyzed activation/borylation of aromatic C–H bonds. This functionalization allowed the introduction of a pinacolboronate ester [B(pin)] group in a quantity of up to 42 mol %.⁴⁷ Developing a controlled functionalization of sPS ($M_n = 48.6$ kg/mol, $M_w/M_n = 2.90$) has allowed us to prepare sPS supports of variable loading capacity

without sacrificing molecular weight and recovery yield.

Triphenylphosphine (TPP) is widely used in organic synthesis including Staudinger reduction, Mitsunobu reaction, Wittig reaction, halogenation of alcohols and carbon-carbon coupling reactions (Sonogashira, Suzuki–Miyaura, and Heck).⁴⁸ We decided to synthesize sPS-supported TPP (sPS-TPP; Scheme 2.1) and investigate its catalytic activity and reusability in palladium-catalyzed Suzuki–Miyaura cross-coupling reactions of aryl halides and arylboronic acid.⁴⁹ Recently there has been considerable interest in developing heterogeneous catalyst systems⁵⁰ and recoverable homogeneous catalysts⁵¹ for Suzuki–Miyaura reactions. This is the first example of a sPS-supported palladium catalyst and its use in Suzuki–Miyaura cross-coupling reactions.

2.3. Results and Discussion

2.3.1. Solubility and Precipitation Test of Functionalized sPS and aPS

It was reported in Chapter 1 that a controlled functionalization of sPS was accomplished by the iridium-catalyzed activation/borylation of aryl C–H bonds. The functionalization allowed introduction of a boronate ester group (up to 42 mol %) into the aromatic ring of polystyrene.⁴⁷ While working on the functionalization of sPS, we found that a functionalized sPS such as pinacolboronate ester–functionalized sPS [sPS–B(pin)], (50 mg) can be recovered *quantitatively* as a fine powder when dissolved in good solvent (CHCl₃, 2.5 mL) and precipitated by adding an *equal volume* of poor solvent (methanol, 2.5 mL). The recovery yield of sPS–B(pin) was over 99%, whereas the yield of borylated atactic polystyrene [aPS–B(pin)] was 55% under the same conditions (Figure 2.1 and

Table 2.1). Additional solubility/recovery data of sPS-B(pin) and aPS-B(pin) using different organic solvents were are summarized in Tables 2.1 and 2.2.



Figure 2.1. Precipitation results when precipitated by adding an *equal volume* of MeOH: (a) sPS-B(pin) in fine power and (b) aPS-B(pin) in suspension solution.

Table 2.1. Solubility and precipitation test of sPS-B(pin)^a.

Good solvent	CHCl ₃	Toluene	THF	Dioxane
Polymer	sPS-B(pin)	sPS-B(pin)	sPS-B(pin)	sPS-B(pin)
M_n	48,600	48,600	48,600	48,600
Solution	100 mg/5 mL	100 mg/5 mL	50 mg/2.5 mL	50 mg/2.5 mL
Concentration	20 mg/mL	20 mg/mL	20 mg/mL	20 mg/mL
Poor solvent	5 mL MeOH	5 mL MeOH	2.5 mL MeOH	2.5 mL MeOH
Good/poor solvent ratio	5/5 (v/v)	5/5 (v/v)	2.5/2.5 (v/v)	2.5/2.5 (v/v)
Precip. type	small particles	small particles	small particles	small particles
Recov. yield	99%	98%	98%	99%

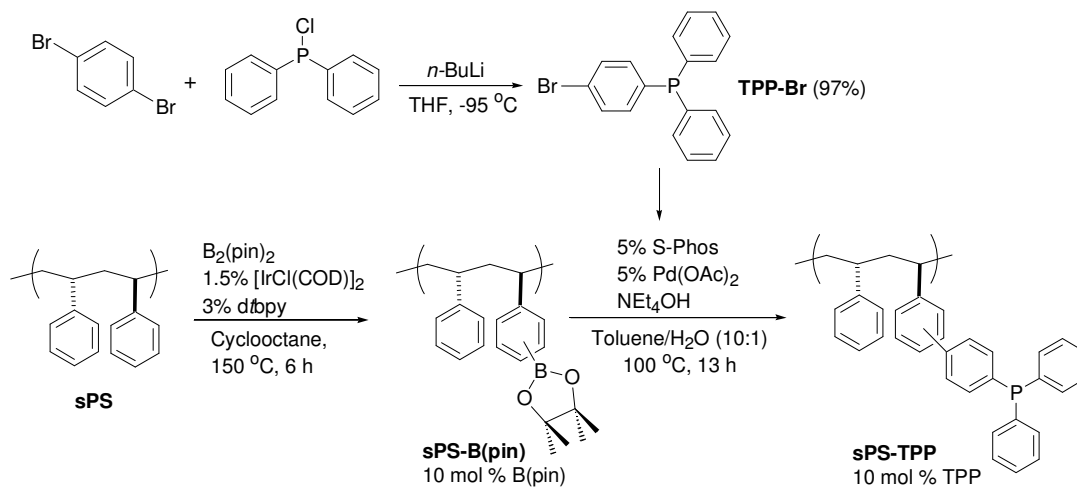
^a Recovery yield for other solvents: CH₂Cl₂ (98%), Digylme (99%), DME (99%), DMA (99%), DMF (99%)

Table 2.2. Solubility and precipitation test of aPS–B(pin).

Good solvent	CHCl ₃	Toluene	THF
Polymer	aPS–B(pin)	aPS–B(pin)	aPS–B(pin)
<i>M_n</i>	212,000	212,000	212,000
Solution	100 mg/5 mL	100 mg/5 mL	50 mg/2.5 mL
Concentration	20 mg/mL	20 mg/mL	20 mg/mL
Poor solvent	5 mL MeOH	5 mL MeOH	2.5 mL MeOH
Good/poor solvent ratio	5/5 (v/v)	5/5 (v/v)	2.5/2.5 (v/v)
Precipitation type	Suspension and gummy/viscous substance	Suspension and gummy/viscous substance	Suspension and gummy/viscous substance
Recov. yield	55%	60%	33%

2.3.2. Syndiotactic Polystyrene-Supported Triphenylphosphine (sPS–TPP).

As shown in Scheme 2.1, (4-bromophenyl)diphenylphosphine (TPP–Br) was synthesized in 97% yield from the reaction of 1,4-dibromobenzene and chlorodiphenylphosphine in THF. The chemical shift assignment in ¹H and ¹³C NMR spectra of TPP–Br matched well with the structure of the compound (Figures 2.2 and 2.3). The ³¹P NMR spectrum of TPP–Br displayed a new resonance at –5.3 ppm of the arylphosphine (Figure 2.4b). The resonance at 82.8 ppm from chlorodiphenylphosphine in the NMR data disappeared completely. We prepared 10 mol % functionalized sPS–B(pin) via iridium-catalyzed C–H borylation according to literature method.¹⁴ TPP was immobilized to sPS via the Suzuki–Miyaura coupling reaction of TPP–Br and sPS–B(pin), and the immobilized polymer support, sPS–TPP, was fully characterized using NMR spectroscopies.



Scheme 2.1. Synthesis of syndiotactic polystyrene-supported triphenylphosphine (sPS-TPP).

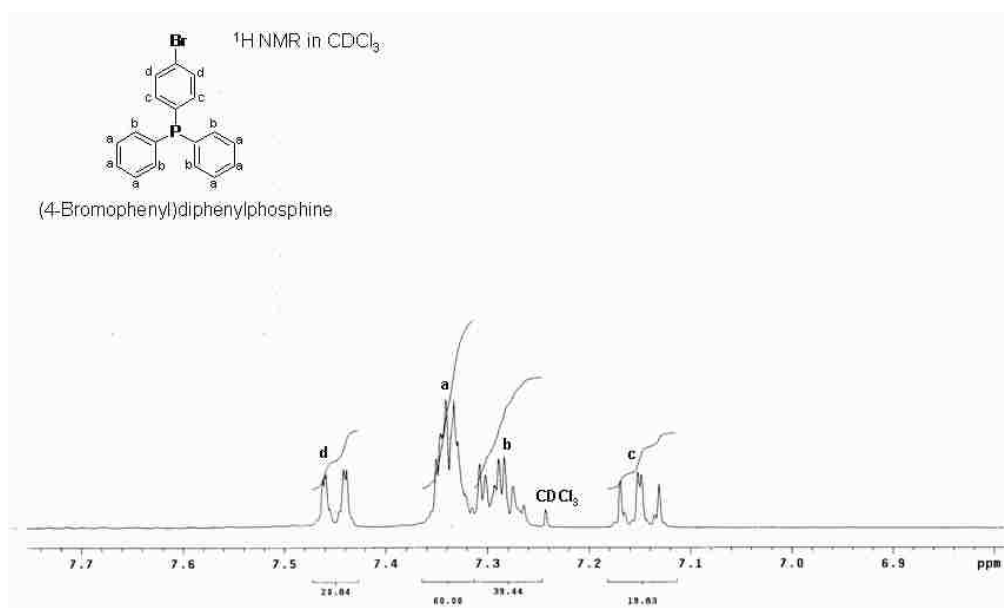


Figure 2.2. ^1H NMR spectrum of (4-bromophenyl)diphenylphosphine [10 mg/mL in CDCl_3 at $25\text{ }^\circ\text{C}$].

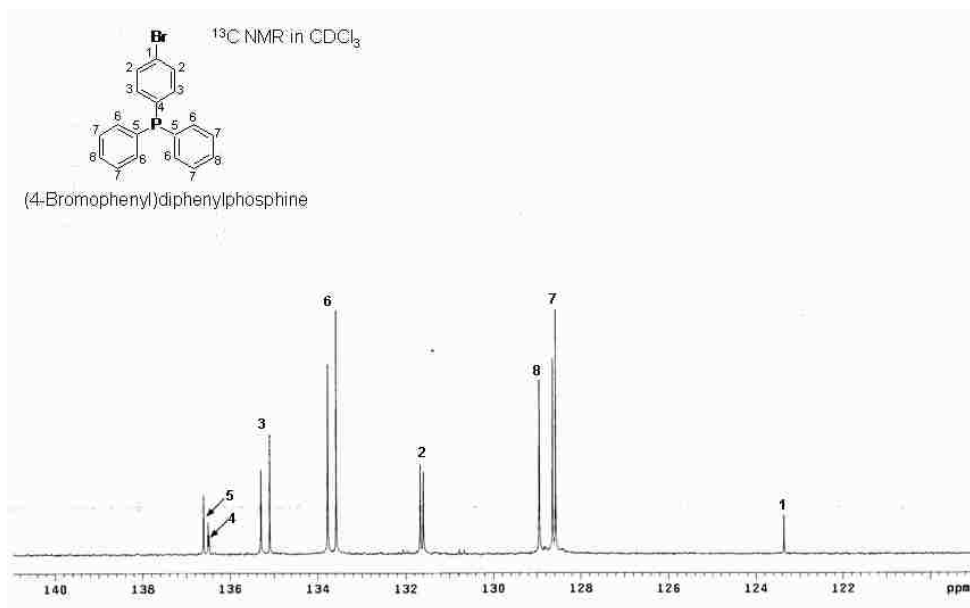


Figure 2.3. ¹³C NMR spectrum of (4-bromophenyl)diphenylphosphine [20 mg/mL in CDCl₃ at 25 °C].

The successful incorporation of the TPP moiety was confirmed in the ³¹P NMR spectrum, which revealed a resonance at −5.0 ppm (Figure 2.4c). The ³¹P NMR spectrum did not show any resonance that could have resulted from arylphosphine oxide. In addition, the ¹H NMR spectrum of sPS–TPP showed two new resonances at 7.34 and 7.51 ppm, which correlate to the phenyl groups of the attached TPP moiety (Figure 2.5). The attached aromatic moiety of the polymer showed new sharp resonances at 137.4, 133.7, 128.7, and 128.5 ppm in the ¹³C NMR spectrum (Figure 2.6). The phosphine loading level of sPS–TPP determined by ¹H NMR was 0.71 mmol/g (i.e., 10 mol %). Unlike that of end-functionalized polymer supports, this loading capacity can be easily tuned by adjusting the pinacolboronate ester concentration in the C–H borylation step without affecting the solubility and recovery of the polymer.

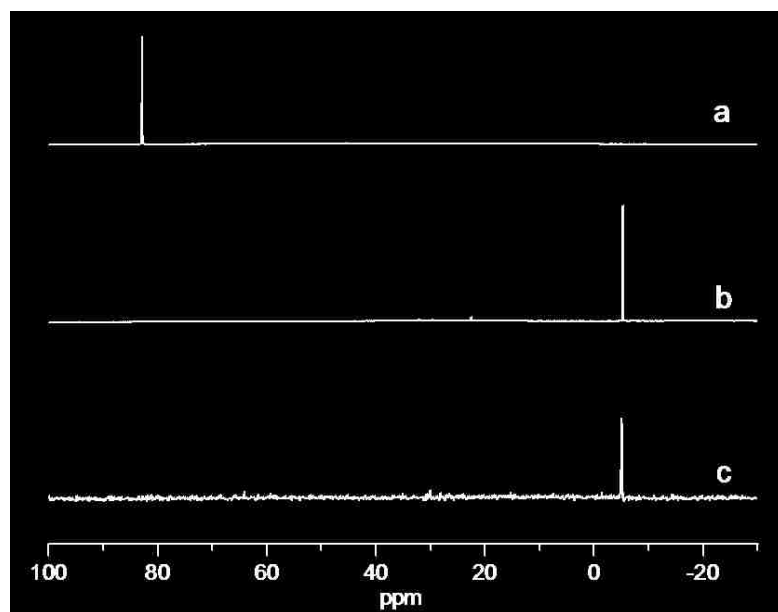


Figure 2.4. ^{31}P NMR spectra of (a) chlorodiphenylphosphine ($\delta = 82.8$ ppm), (b) (4-bromophenyl)diphenylphosphine ($\delta = -5.3$ ppm), and (c) sPS-TPP ($\delta = -5.0$ ppm).

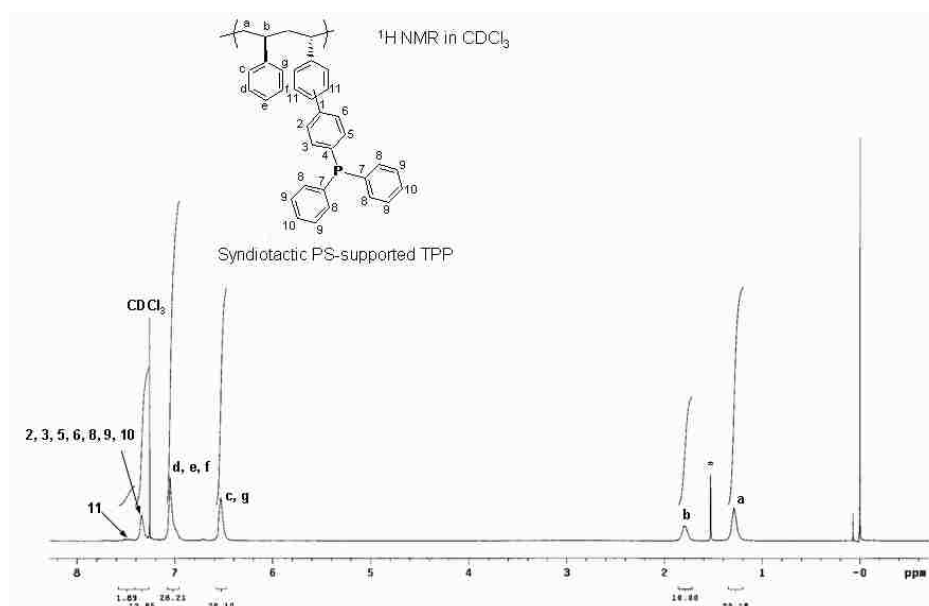


Figure 2.5. ^1H NMR spectrum of sPS-supported triphenylphosphine (An asterisk indicates H_2O from CDCl_3).

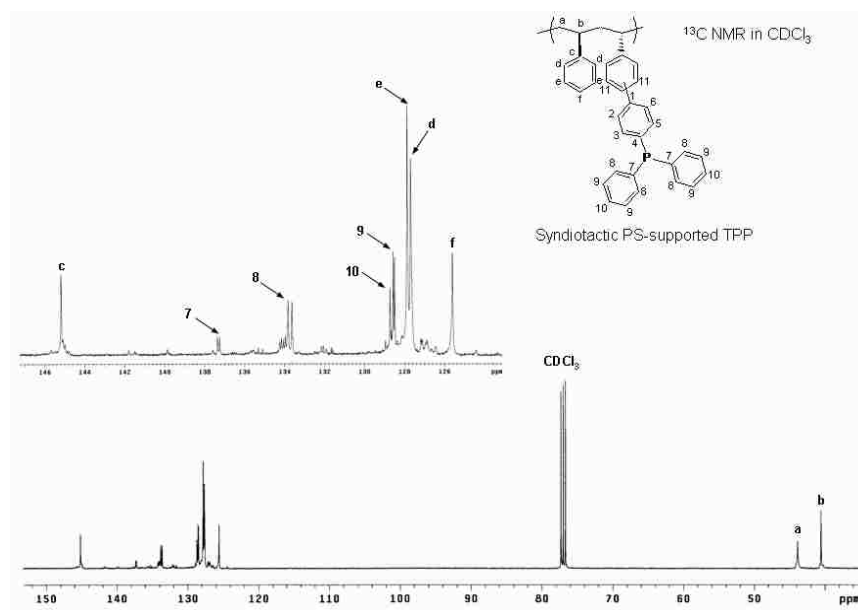


Figure 2.6. ^{13}C NMR spectrum of syndiotactic polystyrene-supported triphenylphosphine [20 mg/mL in CDCl_3 at 25 $^\circ\text{C}$].

sPS–TPP is readily soluble in common organic solvents including toluene, THF, dioxane, diglyme, DME, DMF, DMA, CH_2Cl_2 , and CHCl_3 when heated gently and is insoluble in hexane, diethyl ether, and methanol. Unlike aPS support, which requires the addition of an excess of cold poor solvent (e.g., 10-fold volume of $-30\text{ }^\circ\text{C}$ methanol) for polymer recovery in high yield, support with sPS–TPP requires only the addition of *an equal volume* of methanol for *quantitative* precipitation of the polymer.

2.3.3. Effect of Base on the sPS–TPP-Supported Suzuki–Miyaura Reactions

The catalyst activity of the soluble polymer-supported ligand was tested for the Suzuki–Miyaura coupling reactions of aryl bromides and chlorides with phenylboronic acid. The coupling of 4-bromoacetophenone (1 equiv) and phenylboronic acid (1.5 equiv) in toluene was performed as a model reaction under varying reaction conditions using a palladium catalyst/ligand system generated in situ from the complexation of sPS–TPP (1

mol %) and Pd(OAc)₂ (1 mol %) (Table 2.3). Among six different bases tested (Cs₂CO₃, K₃PO₄, K₂CO₃, NEt₃OH, NaOH, and NaOtBu), Cs₂CO₃ gave the highest conversion (99%) within 1 h (Table 2.3, Entry 1). Thus, Cs₂CO₃ was selected as the base for polymer-catalyzed Suzuki-Miyaura reactions of various aryl halides with phenylboronic acid (Table 2.4).

Table 2.3. Effect of base on the sPS-TPP-supported Suzuki-Miyaura reactions of 4-bromoacetophenone and phenylboronic acid.^a

Entry	Base	Time (h)	Temp (°C)	Conv. ^b (%)
1	Cs ₂ CO ₃	1	110	99
2	K ₃ PO ₄	1	110	92
3	K ₂ CO ₃	1	110	94
4	NEt ₄ OH	1	110	18
5	NaOH	1	110	91
6	NaOtBu	1	110	52

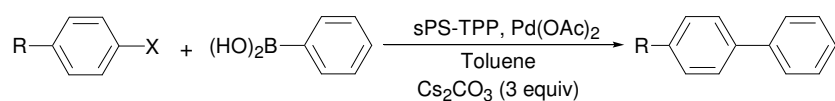
^a 4-Bromoacetophenone (0.044 mmol), phenylboronic acid (0.066 mmol), sPS-TPP (1 mol %), Pd(OAc)₂ (1 mol %), toluene (1 mL). ^b Conversion to coupled product determined using GC-MS.

2.3.4. sPS-TPP-Supported Suzuki-Miyaura Reactions of Aryl Halides

As shown in Table 2.4, Suzuki-Miyaura reactions of both electron-rich and electron-deficient aryl bromides proceed with high yields at 70 °C under homogeneous conditions. As expected, the reaction rates of electron-deficient aryl bromides were faster than those of electron-rich aryl bromides (Entries 2–4 of Table 2.4) which required a slightly longer

reaction time (i.e., 4 h) to achieve over 80% yield (Entries 5–7 of Table 2.4). When conducted at 110 °C, all aryl bromides except for *p*-(*N,N*-dimethylamino)phenyl bromide afforded more than 99% conversion within 1 h and their products could be conveniently isolated by simple precipitation of the sPS–TPP-supported palladium catalyst and removal of the supported catalyst. Aryl chlorides are known to be much less reactive when TPP is used a ligand.⁵² Although the sPS–TPP-supported palladium catalyst furnished the Suzuki–Miyaura reaction products of aryl chlorides, it did so in low yields even after 24 h at 110 °C (7–28%; Table 2.4, Entries 9–12).

Table 2.4. sPS–TPP-supported Suzuki–Miyaura reactions of aryl halides with phenylboronic acid.^a



Entry	R	X	Temp (°C)	Time (h)	Yield ^b (Conv.) ^c (%)
1	H	Br	70	1	84 (93)
2	COCH ₃	Br	70	1	84 (94)
3	CF ₃	Br	70	1	82 (93)
4	CHO	Br	70	1	83 (95)
5	CH ₃	Br	70	4	82 (90)
6	CH ₂ OH	Br	70	4	79 (89)
7	OCH ₃	Br	70	4	81 (87)
8	NMe ₂	Br	70	4	11 (20)
9	H	Cl	110	24	11 (20)
10	CHO	Cl	110	24	28 (41)
11	COCH ₃	Cl	110	24	17 (25)
12	CH ₃	Cl	110	24	7 (18)

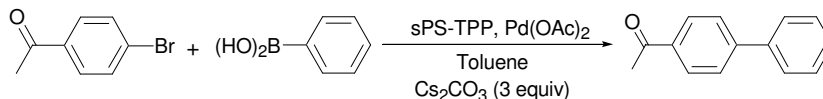
^a 4-Bromoacetophenone (0.88 mmol), phenylboronic acid (1.32 mmol), sPS–TPP (1

mol %), Pd(OAc)₂ (1 mol %), toluene (2 mL). ^b Isolated yield obtained by column chromatography. ^c Conversion to coupled product determined using GC-MS.

2.3.5. Recovery/Recycling of sPS–TPP-Supported Palladium Catalyst

Adding methanol allowed us to recover sPS–TPP quantitatively, enabling us to perform a recycling experiment with the sPS-supported palladium catalyst (Table 2.5). After filtering the base and polymer-supported catalyst in the first run, we evaporated the volatile liquid from the filtrate and retrieved the pure coupled product in 96% isolated yield. No additional purification process such as column chromatography or recrystallization was necessary. Washing the filtered solids with water removed any remaining base and allowed measurement of the recovered polymer support. As shown in Table 2.5, the recovery yield of polymer support is *quantitative* in each cycle, demonstrating the great potential of the soluble support for use as a recoverable catalyst or reagent. The recovered polymer-supported catalyst was reused for the next cycle with fresh Cs₂CO₃ (Table 2.5). Alternatively, the filtered solid (i.e., a mixture of polymer-supported catalyst and base) can be reused for each cycle without adding fresh base (Table 2.6).

Table 2.5. Recovery/recycling of sPS–TPP-supported palladium catalyst in Suzuki–Miyaura reactions and the leaching of palladium.^a



Cycle ^b	1st	2nd	3rd	4th	5th
Conversion (%) ^c	99	96	99	98	66
Yield of product (%) ^d	96	96	97	95	— ^h
Purity (%) ^e	>99	>99	>99	>99	— ^h
Recovery yield of polymer support (%) ^f	99	98	98	99	99
Leaching of Pd (%) ^g	0.6	0.5	0.4	0.4	0.4

^a 4-Bromoacetophenone (14.2 mmol), phenylboronic acid (21.3 mmol), sPS–TPP (1 mol %), and Pd(OAc)₂ (1 mol%) at 110 °C for 1h. ^b No additional Pd(OAc)₂ was added in the recycling experiments. ^c Conversion to the coupled product determined using GC-MS based on an average of two experiments. ^d Isolated yield of product based on an average of two experiments. ^e Determined from ¹H NMR spectrum. ^f Recovered yield (weight %) of polymer support when precipitated by adding methanol and washed with H₂O. ^g Percentage of original Pd leached into the product solution. ^h Not measured.

Table 2.6. Recovery/recycling of sPS–TPP-supported palladium catalyst in Suzuki–Miyaura reactions and the leaching of palladium without adding fresh base^a

Cycle ^b	1st	2nd	3rd	4th	5th
Conversion (%) ^c	99	99	99	99	60
Yield of product (%) ^d	96	96	97	95	— ^f
Leaching of Pd (%) ^e	1.0	0.6	0.7	0.9	0.4

^a 4-Bromoacetophenone (14.2 mmol), phenylboronic acid (21.3 mmol), sPS-TPP (1 mol%), and Pd(OAc)₂ (1 mol%) at 110 °C for 1 h. ^b No additional Pd(OAc)₂ and Cs₂CO₃ were added in the recycling experiments. ^c Conversion to coupled product determined using GC-MS. ^d Isolated yield of product. ^e Percentage of Pd leached into the product solution. ^f Not measured.

The recycled sPS-supported palladium catalyst did not show any loss of catalytic activity up to a fourth cycle. When we investigated the leaching of the palladium into the product solution after precipitation of the polymer support, however, we found that a very small percent of the total amount of the original palladium species was lost to the product solution in each cycle (0.6%, 0.5%, 0.4%, 0.4%, and 0.4%, measured using ICP-AES). Considering the initial loading of Pd(OAc)₂ in the first run of the reaction (1 mol %) and the convenience of product purification (just precipitation and filtration), the amount of palladium found in the product is very small (an average of 46 ppm of palladium each cycle).

2.4. Experimental

2.4.1. General Comments

1,4-Dibromobenzene, *n*-butyllithium (1.6 M in hexane), chlorodiphenyl phosphine, chloro-1,5-cyclooctadiene iridium(I) dimer ([IrCl(COD)]₂), 4,4'-di-*tert*-butyl-2,2'-dipyridyl (dtbpy), Pd(OAc)₂, 2-dicyclohexylphosphino-2',6'-dimethoxy-1,1'-biphenyl (S-Phos), tetraethylammonium hydroxide (NEt₄OH, 35 wt% solution in water), 4-bromobenzene, 4-bromoacetophenone, 4-bromobenzotrifluoride, 4-bromobenzaldehyde, 4-bromotoluene, 4-bromobenzyl alcohol, 4-bromoanisole, 4-bromo-*N,N*-dimethylaniline,

4-chlorotoluene, 4-chloroacetophenone, 4-chlorobenzene, 4-chlorobenzaldehyde, phenylboronic acid, cesium carbonate (Cs_2CO_3), methanol, and chloroform were purchased from commercial vendors and used without further purification. Bis(pinacolato)diboron [$\text{B}_2(\text{pin})_2$] was obtained from Frontier Scientific Co. and used after recrystallization from hexane. Anhydrous THF and toluene were obtained from EMD Chemicals (EM Recycler[®] Container System) and collected from the containers using a positive pressure of nitrogen. Cyclooctane was dried using sodium and benzophenone, distilled under reduced pressure, and stored in a nitrogen-filled glovebox. Syndiotactic polystyrene (sPS) was obtained from LG Chem Ltd., Daejeon, South Korea. Pinacolboronic ester-functionalized syndiotactic polystyrene [sPS-B(pin)] was synthesized according to a literature method.⁴⁷

^1H and ^{13}C NMR spectra were obtained using a Varian NMR spectrometer (400 MHz for ^1H and 100 MHz for ^{13}C) at room temperature, and chemical shifts were referenced to tetramethylsilane (TMS). ^{31}P NMR spectra were obtained using a 161.82 MHz Varian NMR spectrometer at room temperature. Chemical shifts of ^{31}P NMR spectra were referenced to 85% H_3PO_4 . ^1H and ^{13}C NMR samples were prepared at a concentration of 10 and 20 mg/mL, respectively. GC-MS analysis was conducted using a Shimadzu QP2010S equipped with a 30 m x 0.25 mm SHR-XLB GC column and an EI ionization MS detector. The amount of palladium leached to product solution in each recycling cycle was measured by inductively coupled plasma atomic emission spectroscopic (ICP-AES) analysis using a Thermo Scientific iCAP 6500 Duo.

2.4.2. Synthesis of (4-bromophenyl)diphenylphosphine (TPP-Br)⁵³

A solution of 1,4-dibromobenzene (3.00 g; 12.7 mmol) in THF (75 mL) was cooled to

-95 °C using a toluene/liquid nitrogen bath under a nitrogen atmosphere. *n*-BuLi (8.10 mL of 1.6 M in hexane; 12.7 mmol) was added slowly and the resulting solution was stirred at -95 °C. After 1 h, chlorodiphenylphosphine (2.81 g; 12.7 mmol) was added. The solution was allowed to warm to room temperature, stirred overnight, and filtered through a short plug of Celite. The filtrate was evaporated under reduced pressure, and the remaining solid was extracted with hexane (300 mL) and filtered through a short plug of silica gel. Evaporation of solvent from the filtrate afforded a pure, air-stable white solid (4.21 g; 97% yield). ¹H NMR (400 MHz, CDCl₃, ppm) δ = 7.45 (dd, 2H, *J* = 1.2 and 8.0 Hz), 7.36–7.32 (m, 6H), 7.31–7.26 (m, 4H), 7.15 (dd, 2H, *J* = 6.9 and 8.0 Hz). ¹³C NMR (100 MHz, CDCl₃, ppm) δ = 136.6 (d, C₅, *J* = 10.5 Hz), 136.5 (d, C₄, *J* = 12.7 Hz), 135.2 (d, C₃, *J* = 20.2 Hz), 133.7 (d, C₆, *J* = 19.4 Hz), 131.6 (d, C₂, *J* = 7.5 Hz), 129.0 (s, C₈), 128.6 (d, C₇, *J* = 6.7 Hz), 123.4 (s, C₁). ³¹P NMR (161.8 MHz, CDCl₃, ppm) δ = -5.32 (s).

2.4.3. Preparation of sPS-Supported Triphenylphosphine (sPS-TPP)

In a nitrogen-filled glovebox, sPS-B(pin) [500 mg; 0.470 mmol B(pin)], (4-bromophenyl)diphenylphosphine [1.30 g; 3.79 mmol; 8 equiv based on the amount of boron concentration of sPS-B(pin)], Pd(OAc)₂ [5.3 mg; 0.024 mmol; 5 mol % based on the amount of boron concentration of sPS-B(pin)], S-Phos [11.0 mg; 0.0240 mmol; 5 mol % based on the amount of boron concentration of sPS-B(pin)], toluene (10 mL), and a magnetic stirring bar were placed in a vial. The vial was capped with a Teflon-lined septum and removed from the glovebox. NEt₄OH solution [0.6 mL of 35% solution; 1.42 mmol, 3 equiv based on the amount of boron concentration of sPS-B(pin)] and water (1 mL) were added to the vial. The vial was placed in an oil bath at 100 °C for 13 h. After

cooling, the reaction mixture was diluted with chloroform (50 mL), dried with anhydrous magnesium sulfate, and filtered through a short plug of Celite. The filtrate was concentrated using a rotary evaporator to approximately 7 mL, and methanol (7 mL) was added to precipitate polymer. The precipitated polymer was filtered and dried under vacuum at 60 °C for 12 h (589 mg, 103% yield based on polymer weight). ¹H NMR (400 MHz, CDCl₃, ppm) δ = 1.29 (2H, -CH₂- of sPS main chain), 1.80 (1H, -CH- of sPS main chain), 6.53 (2H, *H_c* and *H_g* of C₆H₅ in sPS side chain), 7.05 (3H, *H_d*, *H_e*, and *H_f* of C₆H₅ in sPS side chain), 7.34 (14H, *H_{2,3,5,6,8,9,10}* of triphenylphosphine moiety in the polymer), 7.51 (2H, *H₁₁* of triphenylphosphine moiety in the polymer). ¹³C NMR (100 MHz, CDCl₃, ppm) δ = 145.2 (*C_c* of C₆H₅ in sPS side chain), 137.3 (d, *C₇*, *J* = 10.5 Hz), 133.7 (d, *C₈*, *J* = 18.7 Hz), 128.7 (s, *C₁₀*), 128.5 (d, *C₉*, *J* = 7.5 Hz), 127.9 (*C_e* of C₆H₅ in sPS side chain), 127.7 (*C_d* of C₆H₅ in sPS side chain), 125.6 (*C_f* of C₆H₅ in sPS side chain), 43.9 (-CH₂- of sPS main chain), 40.6 (-CH- of sPS main chain). ³¹P NMR (161.8 MHz, CDCl₃, ppm) δ = -5.04 (s).

2.4.4. General Procedure of Suzuki–Miyaura Reaction with sPS–TPP.

In a nitrogen-filled glovebox, aryl halide (0.880 mmol; 1 equiv), phenylboronic acid (161 mg; 1.32 mmol; 1.5 equiv), Pd(OAc)₂ (2.0 mg; 0.0088 mmol; 1 mol % based on the amount of aryl halide), Cs₂CO₃ (860 mg; 2.64 mmol; 3 equiv), and a magnetic stirring bar were placed in a vial. sPS–TPP (12.4 mg; 0.00880 mmol TPP, 1 mol % based on the amount of aryl halide) and toluene (2 mL) were placed in another vial. Both vials were capped with Teflon-lined septa and removed from the glovebox. sPS–TPP was dissolved in toluene by applying gentle heat. The sPS–TPP solution was transferred to the aryl halide solution using a syringe, and the reaction mixture was stirred in an oil bath under

the specified conditions in Table 2.4 (70 °C for aryl bromide and 110 °C for aryl chloride). The reaction mixture was cooled to room temperature, diluted with chloroform (2 mL), and filtered through a short plug of Celite. The filtrate was concentrated by a rotary evaporator to approximately 2 mL. Methanol (2 mL) was added to precipitate polymer. The precipitated polymer was removed by filtration through a short plug of Celite. The filtrate was dried under vacuum and analyzed using GC-MS to check conversion of the coupled product. Isolation by column chromatography afforded a pure product.

Biphenyl from aryl bromide (Table 2.4, Entry 1). The crude product was purified with column chromatography (ethyl acetate:hexane = 2:98). Yield: 84%. ¹H NMR (400 MHz, CDCl₃, ppm) δ = 7.59 (d, 4H, *J* = 7.4 Hz), 7.44 (t, 4H, *J* = 7.5 Hz), 7.34 (t, 2H, *J* = 7.3 Hz). ¹³C NMR (100 MHz, CDCl₃, ppm) δ = 141.5, 129.0, 127.5, 127.4. Spectra agree with those reported in literature.⁵⁴

4-Acetylbiphenyl from aryl bromide (Table 2.4, Entry 2). The crude product was purified with column chromatography (ethyl acetate:hexane = 2:98). Yield: 84%. ¹H NMR (400 MHz, CDCl₃, ppm) δ = 8.04 (d, 2H, *J* = 8.0 Hz), 7.69 (d, 2H, *J* = 8.0 Hz), 7.63 (d, 2H, 7.2 Hz), 7.48 (t, 2H, *J* = 7.4 Hz), 7.42 (t, 1H, *J* = 6.8), 2.65 (s, 3H). ¹³C NMR (100 MHz, CDCl₃, ppm) δ = 197.7, 145.8, 139.9, 135.9, 129.0, 128.9, 128.2, 127.3, 127.2, 26.7. Spectra agree with those reported in literature.⁵⁵

4-Methylbiphenyl from aryl bromide (Table 2.4, Entry 5). The crude product was purified with column chromatography (ethyl acetate:hexane = 2:98). Yield: 82%. ¹H NMR (400 MHz, CDCl₃, ppm) δ = 7.58 (d, 2H, *J* = 7.2 Hz), 7.50 (d, 2H, *J* = 8.2 Hz), 7.43 (t, 2H, *J* = 7.4 Hz), 7.33 (t, 1H, *J* = 7.6 Hz), 7.25 (d, 2H, *J* = 8.2 Hz), 2.35 (s, 3H). ¹³C NMR (100 MHz, CDCl₃, ppm) δ = 141.1, 138.6, 137.3, 129.7, 129.0, 127.3, 127.2,

21.4. Spectra agree with those reported in literature.⁵⁵

4-Trifluoromethylbiphenyl from aryl bromide (Table 2.4, Entry 3). The crude product was purified with column chromatography (ethyl acetate:hexane = 2:98). Yield: 82%. ¹H NMR (400 MHz, CDCl₃, ppm) δ = 7.69 (s, 4H), 7.61 (m, 2H), 7.48 (m, 2H), 7.41 (m, 1H). ¹³C NMR (100 MHz, CDCl₃, ppm) δ = 145.0, 140.0, 129.6 (q, J_{CF} = 32.2 Hz), 129.2, 128.4, 127.7, 127.5, 126.0 (q, J_{CF} = 3.7 Hz), 124.6 (q, J_{CF} = 272.3 Hz). Spectra agree with those reported in literature.⁵⁶

4-Formylbiphenyl from aryl bromide (Table 2.4, Entry 4). The crude product was purified with column chromatography (ethyl acetate:hexane = 2:98). Yield: 83%. ¹H NMR (400 MHz, CDCl₃, ppm) δ = 10.06 (s, 1H), 7.96 (d, 2H, J = 8.4 Hz), 7.76 (d, 2H, J = 8.2 Hz), 7.64 (d, 2H, J = 7.1 Hz), 7.49 (t, 2H, J = 7.2 Hz), 7.42 (t, 1H, J = 7.2 Hz). ¹³C NMR (100 MHz, CDCl₃, ppm) δ = 192.1, 147.4, 140.0, 135.4, 130.5, 129.3, 128.7, 127.9, 127.6. Spectra agree with those reported in literature.⁵⁷

4-(Hydroxymethyl)biphenyl from aryl bromide (Table 2.4, Entry 6). The crude product was purified with column chromatography (ethyl acetate:hexane = 2:98). Yield: 79%. ¹H NMR (400 MHz, CDCl₃, ppm) δ = 7.59 (d, 4H, J = 8.2 Hz), 7.44 (t, 4H, J = 7.8 Hz), 7.35 (t, 1H, J = 7.2 Hz), 4.73 (s, 2H). ¹³C NMR (100 MHz, CDCl₃, ppm) δ = 140.8, 140.6, 139.9, 128.8, 127.5, 127.3, 127.2, 127.1, 65.1. Spectra agree with those reported in literature.⁵⁸

4-Methoxybiphenyl from aryl bromide (Table 2.4, Entry 7). The crude product was purified with column chromatography (ethyl acetate:hexane = 2:98). Yield: 81%. ¹H NMR (400 MHz, CDCl₃, ppm) δ = 7.54 (t, 4H, J = 7.6 Hz), 7.42 (t, 2H, J = 7.6 Hz), 7.30 (t, 1H, J = 7.2 Hz), 6.98 (d, 2H, J = 8.8 Hz), 3.85 (s, 3H). ¹³C NMR (100 MHz, CDCl₃,

ppm) δ = 159.4, 141.1, 134.0, 128.9, 128.4, 127.0, 126.9, 114.4, 55.6. Spectra agree with those reported in literature.⁵⁴

4-(*N,N*-Dimethylamino)biphenyl from Aryl Bromide (Table 2.4, Entry 8). The crude product was purified with column chromatography (ethyl acetate:hexane = 2:98). Yield: 11%. ¹H NMR (400 MHz, CDCl₃, ppm) δ = 7.55 (d, 2H, *J* = 7.2 Hz), 7.50 (d, 2H, *J* = 9.2 Hz), 7.38 (t, 2H, *J* = 8.0 Hz), 7.26 (t, 1H, *J* = 7.6 Hz), 6.80 (d, 2H, *J* = 8.8 Hz), 2.99 (s, 6H). ¹³C NMR (100 MHz, CDCl₃, ppm) δ = 150.0, 141.2, 129.3, 128.6, 127.7, 126.3, 126.0, 112.8, 40.6. Spectra agree with those reported in literature.⁵⁵

Biphenyl from aryl chloride (Table 2.4, Entry 9). The crude product was purified with column chromatography (ethyl acetate:hexane = 2:98). Yield: 11%. ¹H NMR (400 MHz, CDCl₃, ppm) δ = 7.59 (d, 4H, *J* = 7.4 Hz), 7.44 (t, 4H, *J* = 7.5 Hz), 7.34 (t, 2H, *J* = 7.3 Hz). ¹³C NMR (100 MHz, CDCl₃, ppm) δ = 141.5, 129.0, 127.5, 127.4. Spectra agree with those reported in literature.⁵⁴

4-Formylbiphenyl from aryl chloride (Table 2.4, Entry 10). The crude product was purified with column chromatography (ethyl acetate:hexane = 2:98). Yield: 28%. ¹H NMR (400 MHz, CDCl₃, ppm) δ = 10.06 (s, 1H), 7.96 (d, 2H, *J* = 8.4 Hz), 7.76 (d, 2H, *J* = 8.2 Hz), 7.64 (d, 2H, *J* = 7.1 Hz), 7.49 (t, 2H, *J* = 7.2 Hz), 7.42 (t, 1H, *J* = 7.2 Hz). ¹³C NMR (100 MHz, CDCl₃, ppm) δ = 192.1, 147.4, 140.0, 135.4, 130.5, 129.3, 128.7, 127.9, 127.6. Spectra agree with those reported in literature.⁵⁷

4-Acetylbiphenyl from aryl chloride (Table 2.4, Entry 11). The crude product was purified with column chromatography (ethyl acetate:hexane = 2:98). Yield: 17%. ¹H NMR (400 MHz, CDCl₃, ppm) δ = 8.04 (d, 2H, *J* = 8.0 Hz), 7.69 (d, 2H, *J* = 8.0 Hz), 7.63 (d, 2H, 7.2 Hz), 7.48 (t, 2H, *J* = 7.4 Hz), 7.42 (t, 1H, *J* = 6.8), 2.65 (s, 3H). ¹³C NMR

(100 MHz, CDCl_3 , ppm) δ = 197.7, 145.8, 139.9, 135.9, 129.0, 128.9, 128.2, 127.3, 127.2, 26.7. Spectra agree with those reported in literature.⁵⁵

4-Methylbiphenyl from aryl choride (Table 2.4, Entry 12). The crude product was purified with column chromatography (ethyl acetate:hexane = 2:98). Yield: 7%. ^1H NMR (400 MHz, CDCl_3 , ppm) δ = 7.58 (d, 2H, J = 7.2 Hz), 7.50 (d, 2H, J = 8.2 Hz), 7.43 (t, 2H, J = 7.4 Hz), 7.33 (t, 1H, J = 7.6 Hz), 7.25 (d, 2H, J = 8.2 Hz), 2.35 (s, 3H). ^{13}C NMR (100 MHz, CDCl_3 , ppm) δ = 141.1, 138.6, 137.3, 129.7, 129.0, 127.3, 127.2, 21.4. Spectra agree with those reported in literature.⁵⁵

2.4.5. Recycling Experiment of sPS-Supported Catalyst

In a nitrogen-filled glovebox, 4-bromoacetophenone (2.83 g, 14.2 mmol, 1 equiv), phenylboronic acid (2.60 g, 21.3 mmol, 1.5 equiv), Cs_2CO_3 (13.9 g; 42.6 mmol; 3 equiv), $\text{Pd}(\text{OAc})_2$ (31.8 mg; 0.142 mmol; 1 mol %), sPS-TPP (184 mg; 0.142 mmol TPP; 1 mol %), toluene (33 mL), and a magnetic stirring bar were placed in a 250 mL flask. The flask was removed from the glovebox and placed in an oil bath at 110 °C for 1 h. The reaction mixture was cooled to room temperature, filtered, and washed with hot toluene (100 mL). The filtered solid, which contains base and polymer-supported palladium catalyst, was washed with additional hot toluene (20 mL \times 2) and dried under vacuum. The filtrate was concentrated by a rotary evaporator to approximately 10 mL, then methanol (10 mL) was added to precipitate the remaining polymer support which was collected by centrifugation (~30 mg of polymer was recovered). Although the remaining polymer precipitated quantitatively with the addition of 10 mL of methanol, additional methanol (300 mL) was added to the toluene/methanol solution to prevent co-precipitation of the product with the polymer during centrifugation—because the solubility

of the product in methanol for the centrifugation process was found to be ~10 mg/mL and the expected weight of the product was 2.78 g, it was necessary to add 300 mL of methanol to prevent co-precipitation of the product. After removal of the precipitated polymer, evaporation of the centrifuged methanol solution afforded pure product (96% yield), which was analyzed by ^1H and ^{13}C NMR spectroscopies to check the purity and subjected to ICP-AES to determine the amount of leached palladium. The recovered polymer from the centrifugation was dried, combined with the initially filtered base and polymer-supported palladium catalyst mixture, and washed with water (400 mL) to remove the base. The resulting brownish polymer solid was filtered, washed with water (50 mL \times 2) and methanol (10 mL \times 1), and dried under vacuum. The weight percent of the brownish polymer relative to the initial weight of sPS-TPP is provided as the recovery yield of polymer support in Table 2.5. Fresh Cs_2CO_3 (3 equiv), 4-bromoacetophenone (2.83 g, 14.2 mmol, 1 equiv), phenylboronic acid (2.60 g, 21.3 mmol, 1.5 equiv), and toluene (33 mL) were added to the recovered polymer support and were used for the next run.

4-Acetylbiphenyl (Table 2.6, cycle 1). ^1H NMR (400 MHz, CDCl_3 , ppm) δ = 8.04 (d, 2H, J = 8.6 Hz), 7.69 (d, 2H, J = 8.4 Hz), 7.63 (d, 2H, 7.4 Hz), 7.48 (t, 2H, J = 7.2 Hz), 7.42 (t, 1H, J = 7.2), 2.64 (s, 3H). ^{13}C NMR (100 MHz, CDCl_3 , ppm) δ = 198.0, 146.0, 140.1, 136.1, 129.2, 129.1, 128.5, 127.5, 127.4, 26.9. Spectra agree with those reported in literature.⁵⁵

2.4.6. Recycling Experiment without the Addition of Fresh Cs_2CO_3

The same reaction scale and experimental procedure of the above recycling procedure were used until the centrifugation step of methanol solution. The recovered polymer from

the centrifugation (~30 mg) was dried, combined with the initially filtered base and polymer-supported palladium catalyst mixture, and used for the next run without removing the base. Almost identical results of Table 2.5 were obtained (Table 2.6).

2.4.7. Product Characterization Data

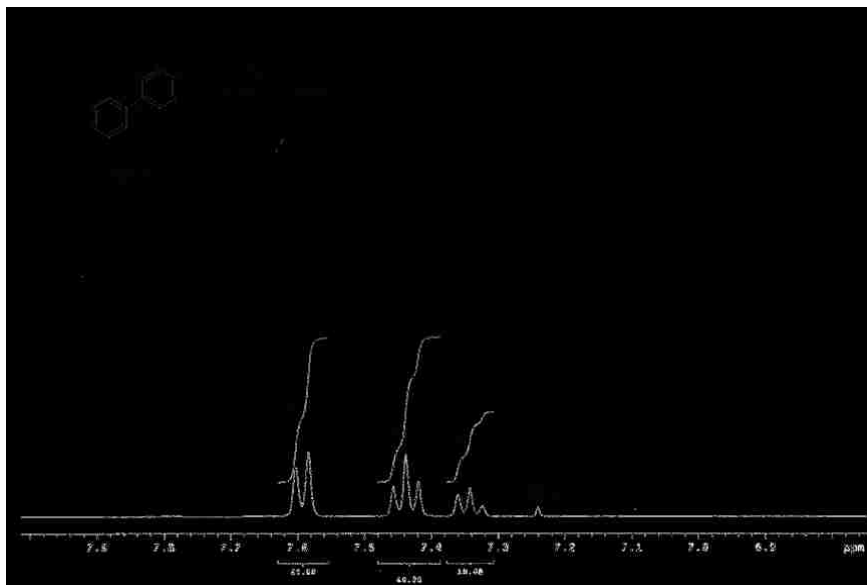


Figure 2.7. ¹H NMR spectrum of biphenyl (Entry 1 of Table 2.4).

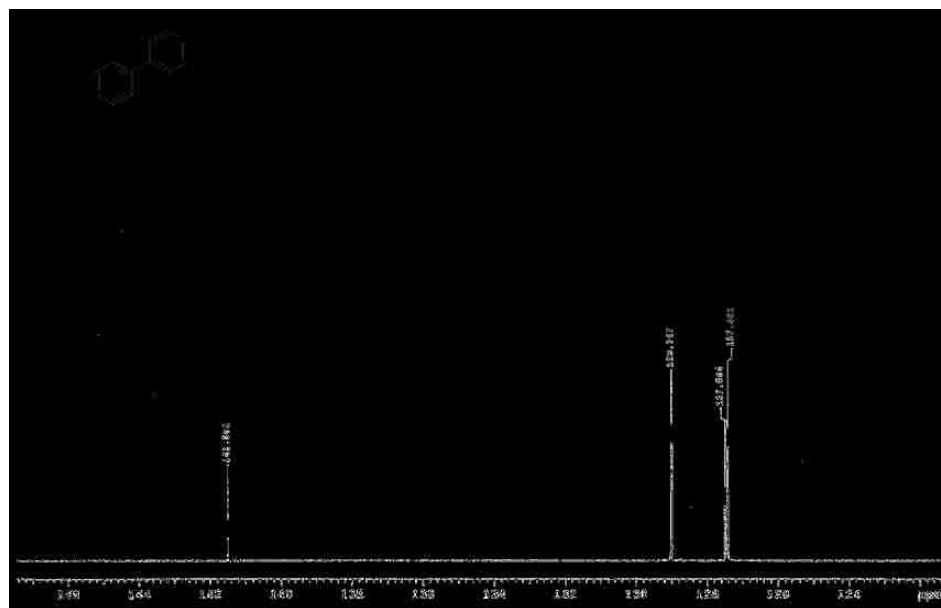


Figure 2.8. ^{13}C NMR spectrum of biphenyl (20 mg/mL in CDCl_3 at 25 $^\circ\text{C}$) (Entry 1 of Table 2.4).

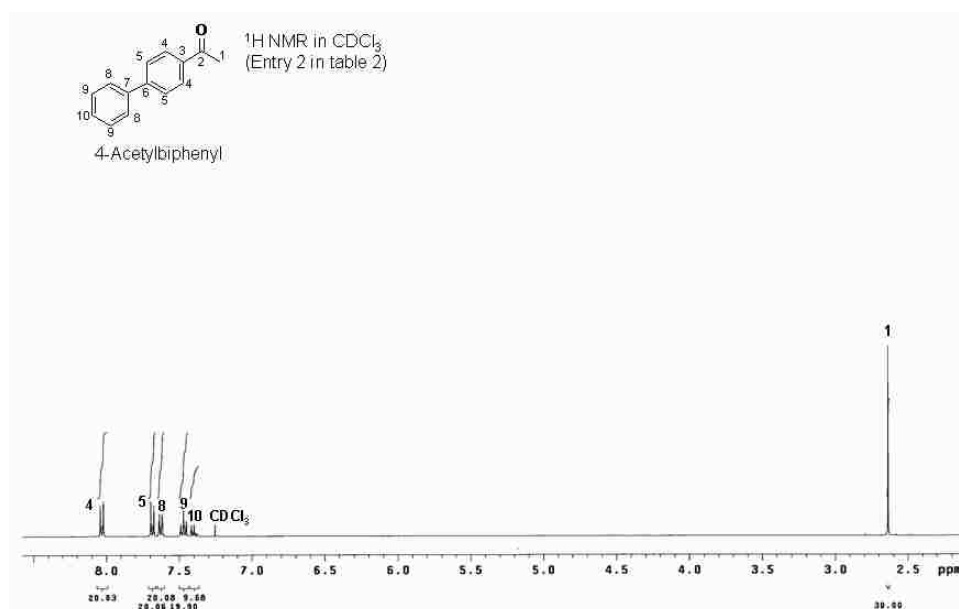


Figure 2.9. ^1H NMR spectrum of 4-acetylbiphenyl (10 mg/mL in CDCl_3 at 25 $^\circ\text{C}$) (Entry 2 of Table 2.4).

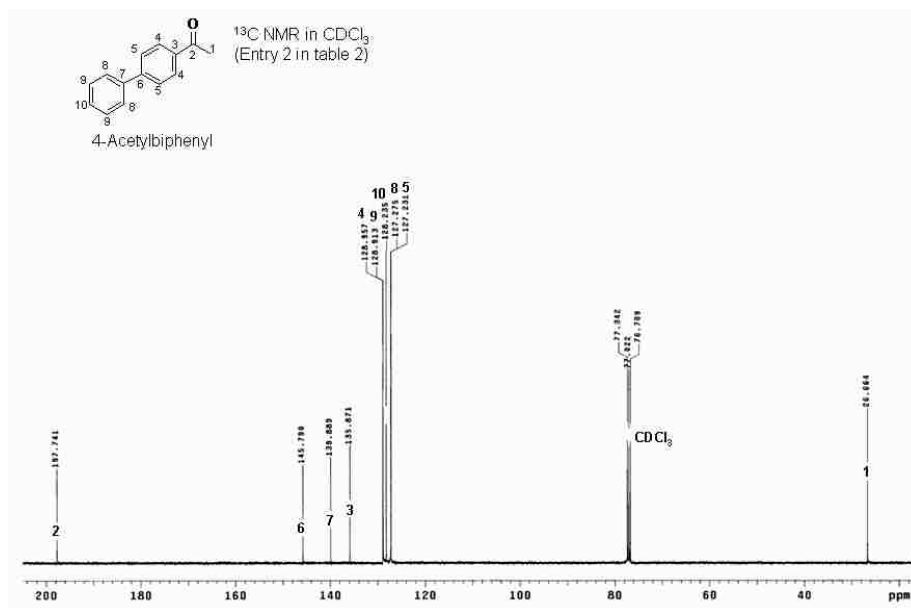


Figure 2.10. ¹³C NMR spectrum of 4-acetylbiphenyl (20 mg/mL in CDCl₃ at 25 °C) (Entry 2 of Table 2.4).

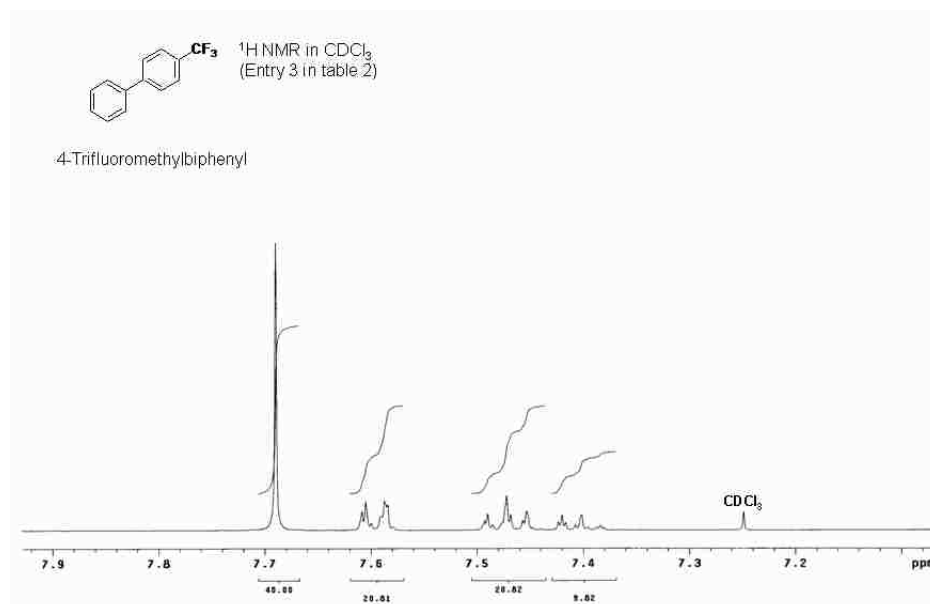


Figure 2.11. ¹H NMR spectrum of 4-trifluoromethylbiphenyl (10 mg/mL in CDCl₃ at 25 °C) (Entry 3 of Table 2.4).

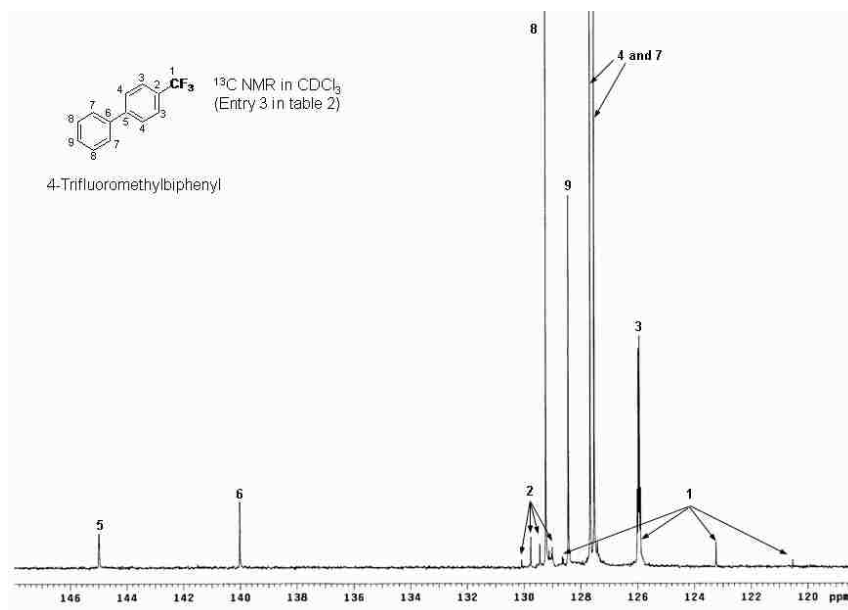


Figure 2.12. ^{13}C NMR spectrum of 4-trifluoromethylbiphenyl (20 mg/mL in CDCl_3 at 25 $^\circ\text{C}$) (Entry 3 of Table 2.4).

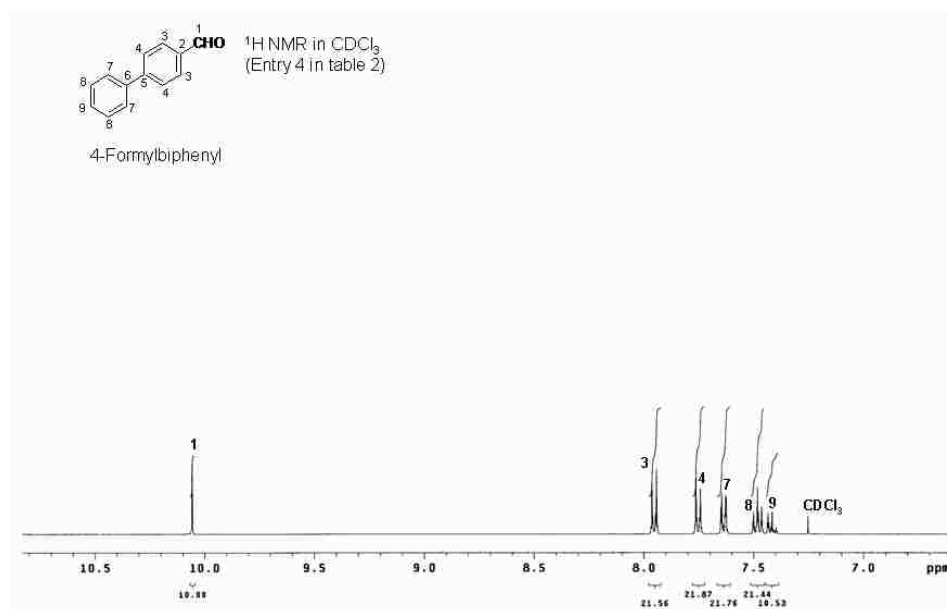


Figure 2.13. ^1H NMR spectrum of 4-formylbiphenyl (10 mg/mL in CDCl_3 at 25 $^\circ\text{C}$) (Entry 4 of Table 2.4).

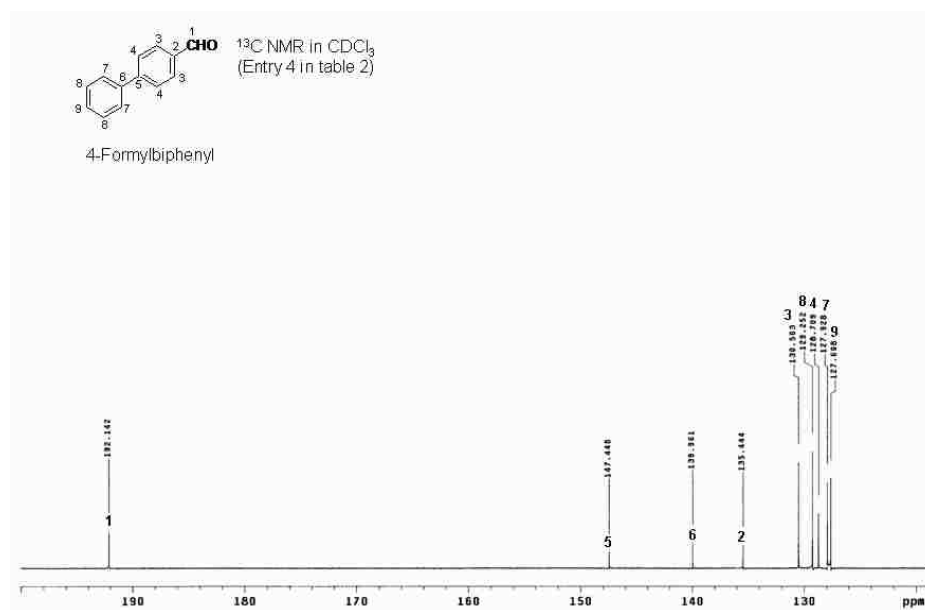


Figure 2.14. ¹³C NMR spectrum of 4-formylbiphenyl (20 mg/mL in CDCl₃ at 25 °C) (Entry 4 of Table 2.4).

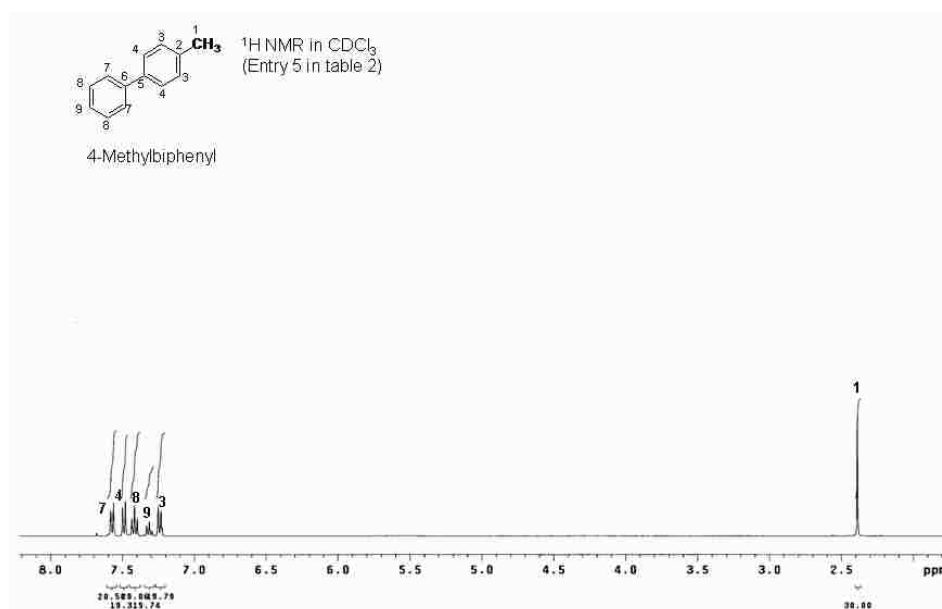


Figure 2.15. ¹H NMR spectrum of 4-methylbiphenyl (10 mg/mL in CDCl₃ at 25 °C) (Entry 5 of Table 2.4).

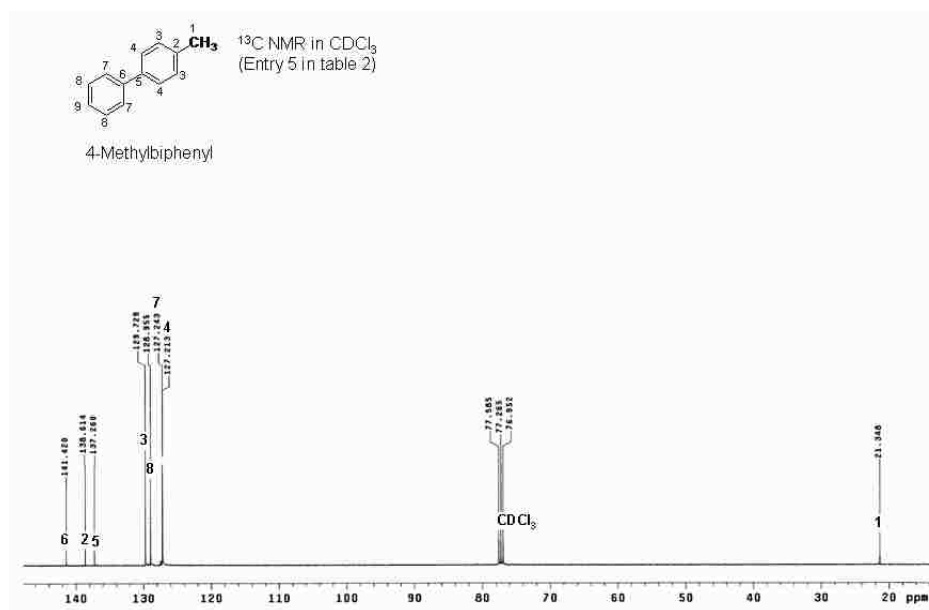


Figure 2.16. ¹³C NMR spectrum of 4-methylbiphenyl (20 mg/mL in CDCl₃ at 25 °C) (Entry 5 of Table 2.4).

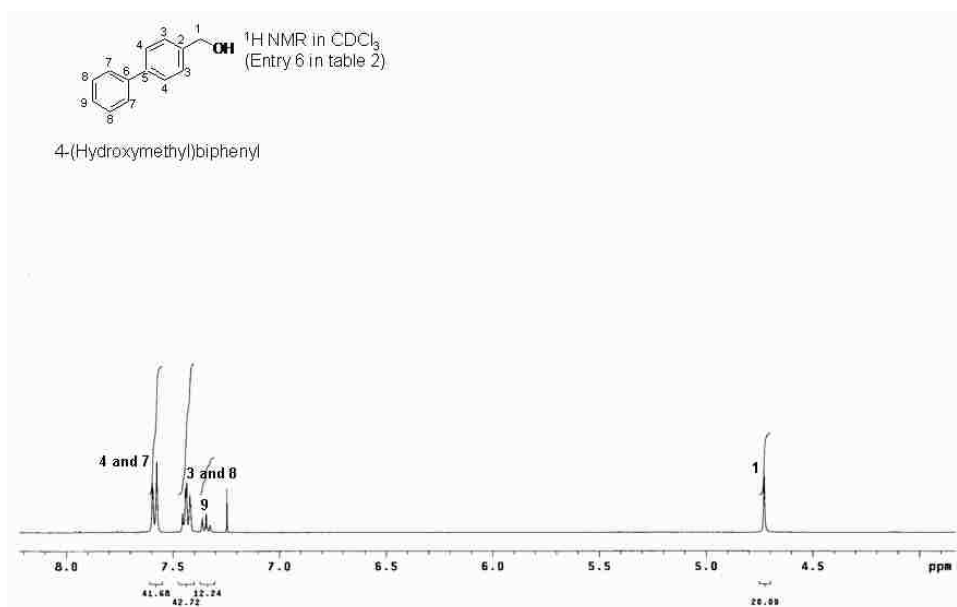


Figure 2.17. ¹H NMR spectrum of 4-(hydroxymethyl)biphenyl (10 mg/mL in CDCl₃ at 25 °C) (Entry 6 of Table 2.4).

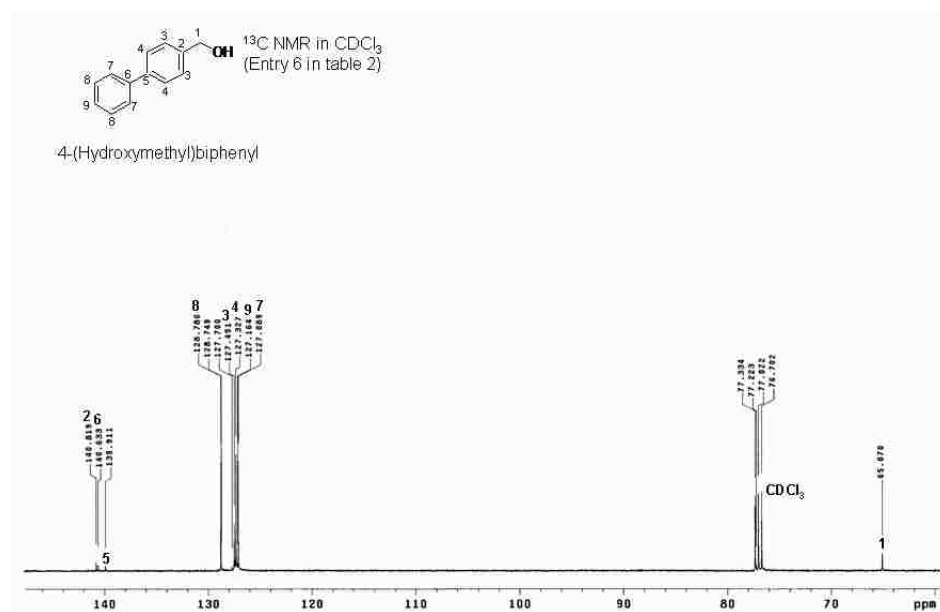


Figure 2.18. ¹³C NMR spectrum of 4-(hydroxymethyl)biphenyl (20 mg/mL in CDCl₃ at 25 °C) (Entry 6 of Table 2.4).

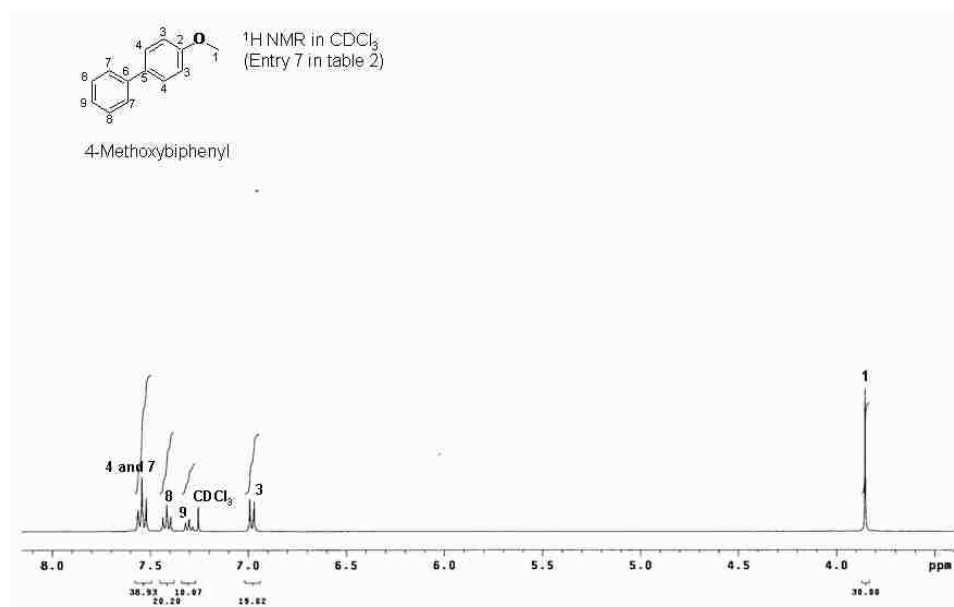


Figure 2.19. ¹H NMR spectrum of 4-methoxybiphenyl (10 mg/mL in CDCl₃ at 25 °C) (Entry 7 of Table 2.4).

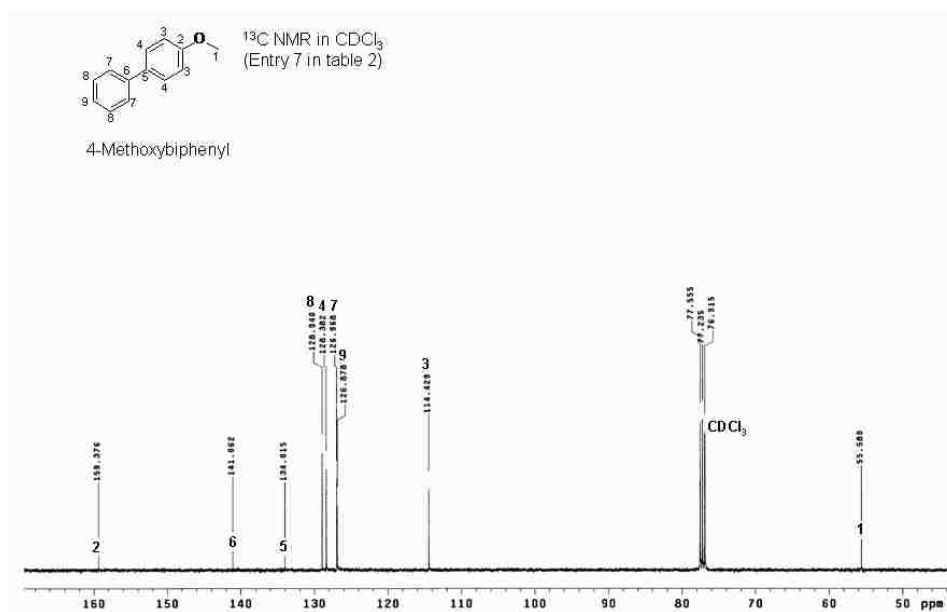


Figure 2.20. ¹³C NMR spectrum of 4-methoxybiphenyl (20 mg/mL in CDCl₃ at 25 °C) (Entry 7 of Table 2.4).

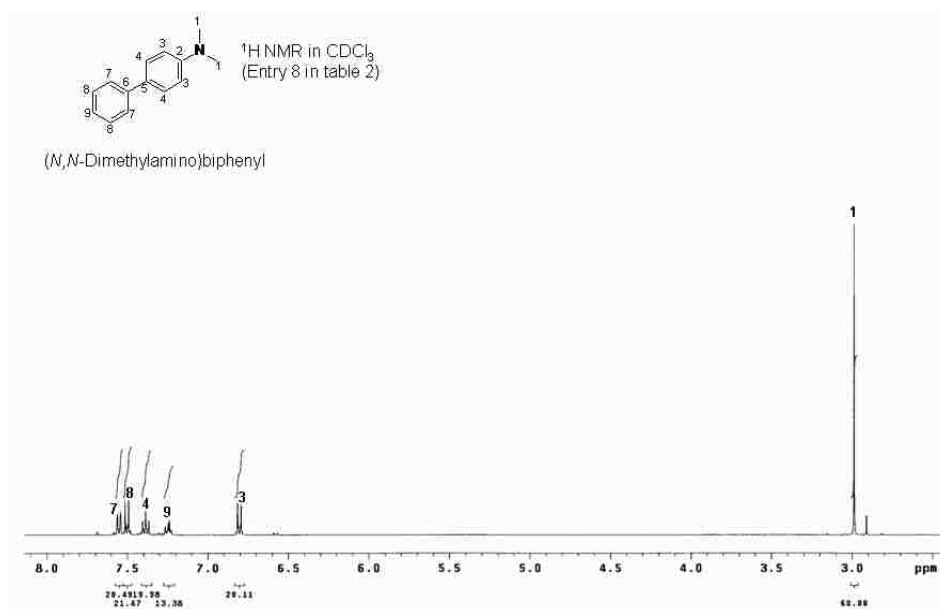


Figure 2.21. ¹H NMR spectrum of (*N,N*-diméthylamino)biphenyl (10 mg/mL in CDCl₃ at 25 °C) (Entry 8 of Table 2.4).

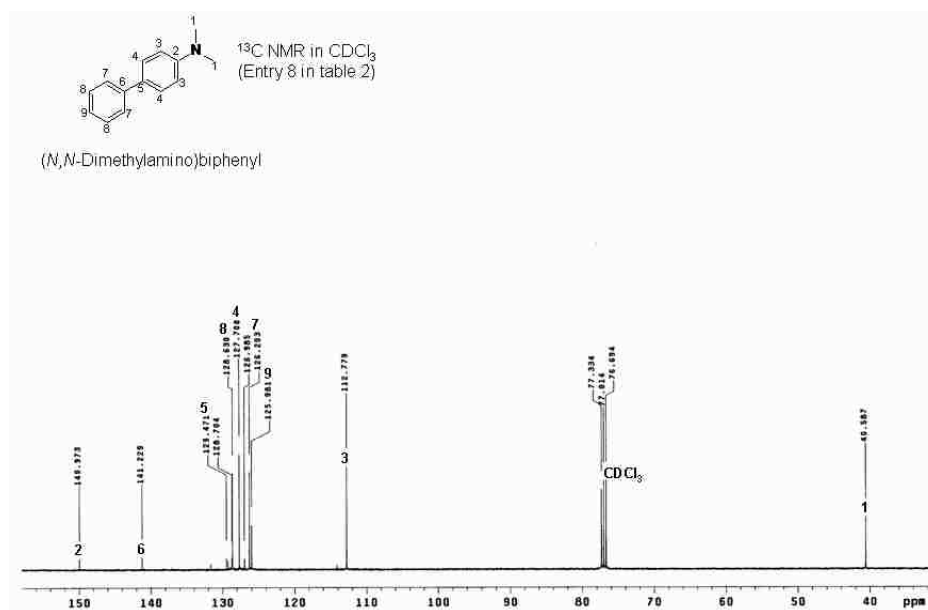


Figure 2.22. ¹³C NMR spectrum of (*N,N*-dimethylamino)biphenyl (20 mg/mL in CDCl₃ at 25 °C) (Entry 8 of Table 2.4).

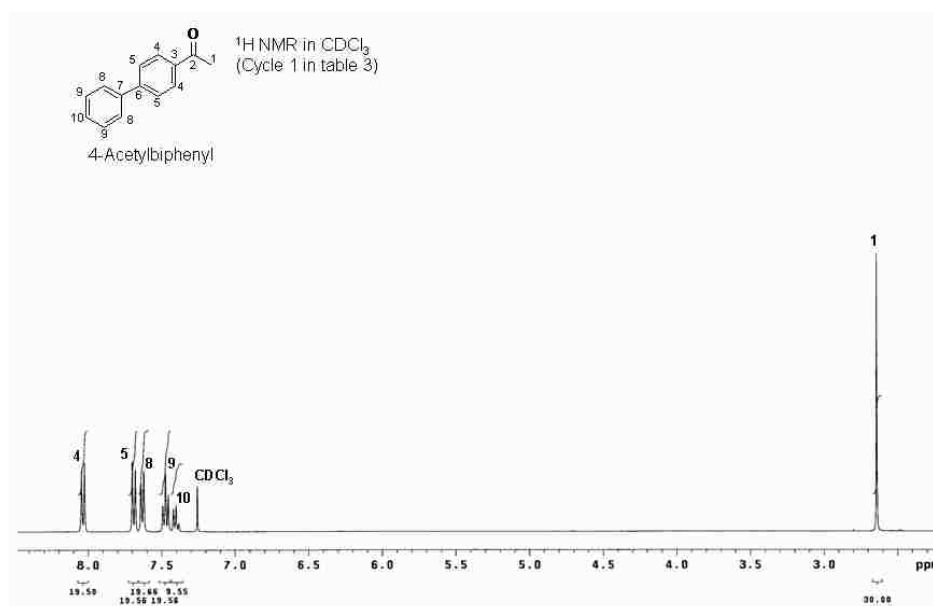


Figure 2.23. ¹H NMR spectrum of 4-acetylbiphenyl (10 mg/mL in CDCl₃ at 25 °C) (Cycle 1 of Table 2.5).

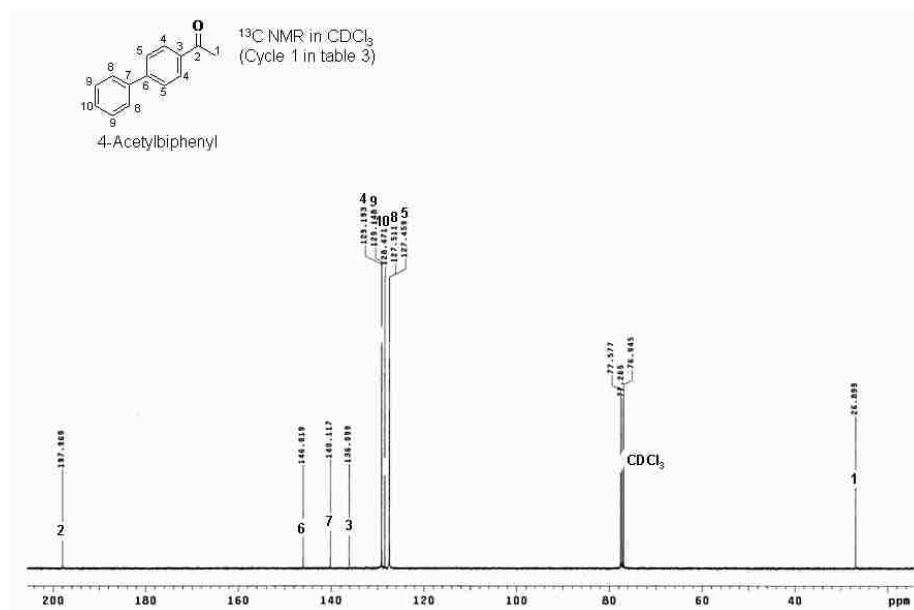


Figure 2.24. ¹³C NMR spectrum of 4-acetylbiphenyl (20 mg/mL in CDCl₃ at 25 °C) (Cycle 1 of Table 2.5).

2.5. Conclusion

In summary, a soluble sPS-supported phosphine ligand was prepared by reacting sPS–B(pin) with TPP-Br. The loading of the polymer support can be easily tuned by changing the boronate ester concentration in the C–H borylation of sPS. The sPS–TPP-supported palladium catalyst showed excellent catalytic activity in Suzuki–Miyaura coupling of aryl halides. Moreover, it could be recovered quantitatively through a simple precipitation/filtration process and reused multiple times without significant loss of activity.

CHAPTER 3

CONTROLLED FUNCTIONALIZATION OF SYNDIOTACTIC POLYSTYRENE BY A COMBINATION AND SUZUKI–MIYAJIMA REACTION

3.1. Abstract

Controlled functionalization of a high-molecular-weight syndiotactic polystyrene (sPS) was performed via combination of electrophilic aromatic bromination and Suzuki–Miyajima cross-coupling reactions. The mol % of the brominated styrene repeating unit in sPS was easily controlled by changing the ratio of added bromine (Br₂) relative to the polymer repeating unit. The crystalline polystyrene was brominated up to 78 mol %. The brominated styrene unit in 8.5 mol % brominated sPS (sPS–Br) was converted to other useful functional groups by Suzuki–Miyajima reactions with *para*- and *meta*-substituted phenyl boronic acids. The conversions of the coupling reactions were always quantitative and afforded various functionalized sPS materials.

3.2. Introduction

Due to good physical properties, chemical stability, processability, and low production cost, the development of new materials based on polyolefin has been actively researched in academia and industry. Stereoregular syndiotactic polystyrene (sPS) has attracted a great deal of attention not only as an interesting polyolefin and but also as a

novel engineering thermoplastic since its first synthesis by Idemitsu Kosan Co. Ltd. in 1985.⁵⁹ Due to its crystalline nature, physical properties of sPS are significantly different from those of amorphous atactic polystyrene materials which are prepared by either radical or anionic polymerization of styrene. They include good chemical and moisture resistance, as well as robust mechanical strength even at elevated temperatures.⁶⁰ Despite these favorable properties, there are a few disadvantages that are limiting further applications of sPS; inherent brittleness, excessively high melt processing temperature (>300 °C) which is near to the polymer degradation temperature, and a lack of compatibility with polar materials. In order to overcome these drawbacks of sPS, the synthesis of functionalized sPS has been pursued as a way to address the limited end-uses of sPS.

Incorporation of a polar moiety into sPS can be conducted by either syndiospecific copolymerization with a functionalized styrene monomer^{61,62} or direct chemical modification (post-functionalization) of sPS. In the former approach, achieving comparable average molecular weight and yields to those of unfunctionalized sPS has been difficult because of the catalyst poisoning effect caused by a polar group present in functionalized styrene comonomer. In the latter approach, because preparation of sPS materials with a variety of molecular weights has been well documented, this method in principle can yield functionalized sPS with different molecular weights and overcome the low molecular weight problem of the copolymerization method. Another important advantage of the latter method is capability to tune the level of functional group concentration by simple stoichiometric considerations. Examples of direct post-functionalization of sPS reported so far include sulfonated sPS,^{63,64,65,66} acetylated sPS,⁶⁷

free radical initiated bromination at the benzylic position of sPS backbone,⁶⁸ and maleic anhydride-functionalized sPS.⁶⁹ Unfortunately, these post-functionalizations of sPS based on reactive carbon intermediates such as free radical or carbocation usually induce competitive side reactions such as chain scission, chain transfer and coupling reactions, which can alter the mechanical properties of the starting polymer as a result of changes in tacticity and/or molecular weight properties.

In our effort to develop functionalized sPS materials, we have recently reported a controlled post-functionalization of sPS via transition metal-catalyzed aromatic C–H activation/borylation under homogenous reaction.⁷⁰ The C–H borylation of sPS allowed incorporation of a high level of a boronate ester group (up to 42 mol %) to the *meta*- and *para*-positions of the aromatic ring. The size-exclusion chromatography (SEC) and NMR spectra confirmed that the iridium-catalyzed borylation of arene C–H bonds of sPS did not negatively affect the molecular weight and the tacticity of the starting polymer.

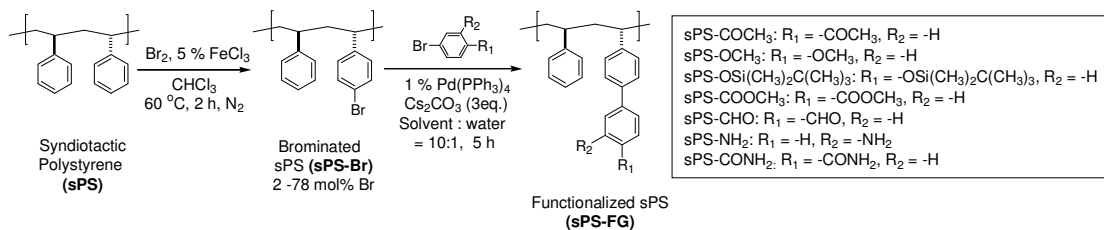
Bromination of the aromatic ring of atactic polystyrene (aPS) via electrophilic aromatic substitution is a well-known chemical modification method of the amorphous material.^{71,72,73,74} The brominated aPS is known to serve as a versatile intermediate polymer in extensive applications such as catalyst supports, chromatographic stationary phases, polymeric reagents.⁷⁵ Because aPS is readily soluble in most organic solvents, it is easy to carry out the bromination in homogenous conditions. In the case of sPS, however, reports of sPS halogenation were very rare due to its poor solubility in most organic solvents.⁷⁶ Thus, except a free radical initiated bromination of benzylic position of sPS under heterogeneous condition,⁶⁸ most literatures of bromination of polystyrene

were concerned with bromination of aPS. Here, we report a synthetic procedure of electrophilic aromatic bromination of sPS via homogenous organic reaction.

Cross-coupling reaction of aryl halides and aryl boron compounds, called Suzuki–Miyaura cross-coupling,⁷⁷ is one of the most powerful biaryl C–C bond formation reactions and aryl boronic acids are very useful reagents in the coupling reaction. Since aryl boronic acids containing various polar functional groups are readily accessible, the Suzuki–Miyaura coupling reactions of brominated sPS and the functionalized aryl boronic acids would offer preparation of functionalized sPS materials that contain a wide range of functionalities.

3.3. Results and Discussion

Scheme 3.1 shows our strategy of sPS post-functionalization; electrophilic aromatic bromination at the *para*-position of the aromatic ring in sPS side chain followed by palladium-catalyzed Suzuki–Miyaura coupling reactions phenyl boronic acids having different functional groups.



Scheme 3.1. Electrophilic bromination and subsequent Suzuki–Miyaura coupling of syndiotactic polystyrene.

3.3.1. Electrophilic Aromatic Bromination of sPS

We first examined different solvents that would be able to dissolve syndiotactic polystyrene at a reasonable concentration for effective bromination of sPS under homogeneous conditions. Solubility of sPS in dichloromethane (CH_2Cl_2), tetrahydrofuran (THF), chloroform (CHCl_3), and carbon tetrachloride (CCl_4) was tested to identify appropriate solvent for the reaction conditions. A mixture of sPS and chloroform in 50 mg/mL concentration became a homogeneous solution at 60 °C. The other solvents did not dissolve sPS completely at this temperature. When we also tested two Lewis acid catalysts—ferric chloride (FeCl_3) and ferrocene [$\text{Fe}(\text{C}_5\text{H}_5)_2$ —for the bromination of sPS under the above condition and found ferric chloride was more effective than ferrocene. Thus, we decided to use ferric chloride (5 mol %) in chloroform at 60 °C for the standard bromination condition of sPS, which has a number average molecular weight (M_n) of 48.6 kg/mol and a polydispersity index ($\text{PDI} = M_w/M_n$) of 2.90. The bromination of sPS was performed in the absence of light to prevent light-catalyzed free radical bromination at the benzylic C–H bonds of the polymer backbone.^{72,73,74}

^1H NMR spectra of all brominated syndiotactic polystyrenes (sPS–Br) showed a new distinctive resonance at 1.71 ppm for $-\text{CH}-$ of the polystyrene main chain that has a brominated phenyl ring (H_2 , of Figure 3.1). Two resonances of the methylene groups of the polymer main chain and the combined methine groups of the brominated and non-brominated polymer main chain maintained an integral ratio of 2:1, proving that there was no side reaction in sPS backbone during the bromination. The ^1H NMR spectrum also displayed two new doublets at 6.30–6.37 and 7.10–7.18 ppm for the *ortho*-positioned and the *meta*-positioned protons of the brominated aromatic moiety (H_b and H_c of Figure

3.1). As more Br₂ was added relative to the polymer repeating unit in the bromination, the intensities of the brominated aromatic protons increased. This indicates that more bromine has been incorporated into the polymer at *para*-position of the phenyl ring.

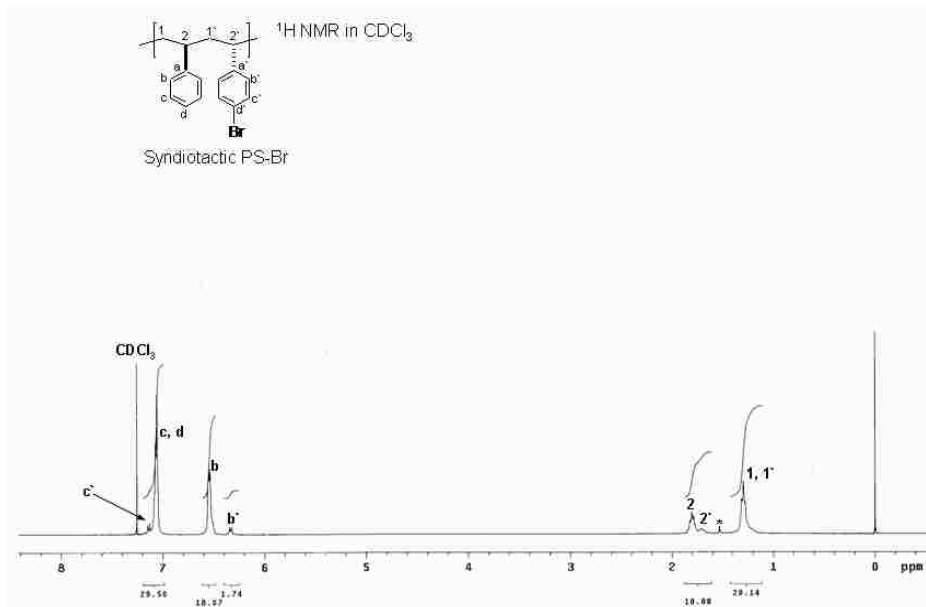


Figure 3.1. ¹H NMR spectrum [delay time = 1 s, number of transients = 16] of brominated sPS [10 mg/mL in CDCl₃ at 25 °C] (An asterisk indicates H₂O from CDCl₃).

The brominated aromatic moiety of sPS showed new sharp resonances at 119.4, 129.6, 131.1, and 114.2 ppm in the ¹³C NMR spectrum (Figure 3.2). The ¹³C attached proton test (APT) NMR spectroscopy of sPS–Br confirmed that these resonances corresponded to the tertiary (C_{b'} at 129.6 and C_{c'} at 131.1 ppm of Figure 3.2) and quaternary (C_{d'} at 119.4 and C_{a'} at 144.2 ppm of Figure 3.2) carbons of the brominated phenyl ring in polymer side chain. These ¹³C NMR spectrum assignments of sPS–Br are consistent with those of brominated atactic polystyrene (aPS–Br).⁷¹ From the ¹³C APT spectrum of sPS–Br, we

did not detect any deshielded resonances corresponding to $\text{—}\overset{\text{Br}}{\text{C}}\text{H—}$ and $\text{—}\overset{\text{Br}}{\text{C}}\text{—}$ that could have resulted from the bromination at the sPS backbone.

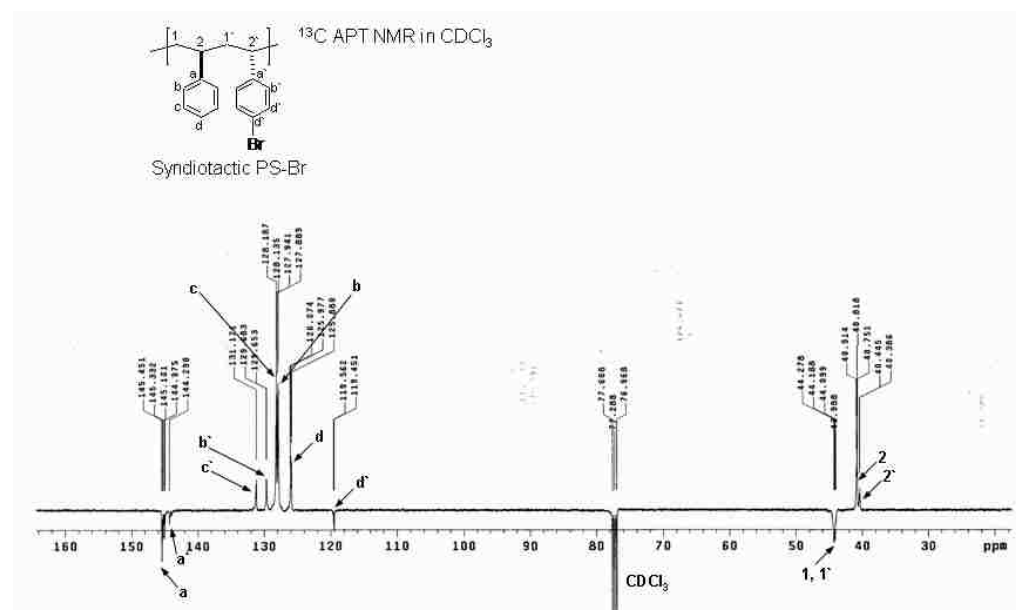


Figure 3.2. ¹³C APT NMR spectrum [delay time = 4 s, number of transients = 8000] of brominated sPS [40 mg/mL in CDCl₃ at 25 °C].

The mol % of brominated styrene repeating unit in sPS-Br was calculated from the ¹H NMR spectrum by comparing the integral ratio of the combined methine protons of sPS main chain (H₂ and H_{2'} at 1.71 and 1.81 ppm in Figure 3.1) and the *ortho* proton of brominated aromatic moiety (H_{b'} at 6.30–6.37 ppm in Figure 3.1). As can be in the results of Table 3.1, sPS could be efficiently brominated with varying degrees. The results also show that the efficiency of bromination, which is defined as the ratio of brominated styrene repeating unit relative to Br₂ added, generally increased as more Br₂ was added (entries 1–9 of Table 3.1). Up to 78 mol % of styrene units of sPS can be easily

brominated using 5 mol % ferric chloride, a traditional Lewis acid catalyst. Bromination of sPS conducted in a larger scale required a little extended reaction time (6–8 h) to achieve the similar mol % of brominated unit (see entries 3 and 10 of Table 3.1).

Table 3.1. Bromination of syndiotactic polystyrene^a with bromine (Br₂)^b.

Entry	M_n^c	PDI (M_w/M_n) ^c	[Br ₂]/ [monomer]	sPS–Br			
				M_n^c	PDI (M_w/M_n) ^c	Br (%) ^d	Effic. (%) ^e
1	48.6	2.90	0.10	37.2	2.76	2.2	11
2	48.6	2.90	0.15	— ^g	— ^g	4.7	16
3	48.6	2.90	0.20	35.0	2.71	8.5	21
4	48.6	2.90	0.25	— ^g	— ^g	10.6	21
5	48.6	2.90	0.30	35.3	2.94	15.5	26
6	48.6	2.90	0.40	— ^g	— ^g	17.9	22
7	48.6	2.90	0.50	33.9	2.61	28.1	28
8	48.6	2.90	0.70	32.1	2.89	48.9	35
9	48.6	2.90	1.00	31.2	2.78	77.8	39
10 ^f	48.6	2.90	0.20	— ^g	— ^g	7.2	18

^a Syndiotactic polystyrene (sPS) [$M_n = 48.6$ kg/mol, PDI = 2.90]. ^b Bromination was conducted with 100 mg of the polymer with 5 mol % of ferric chloride relative to bromine in chloroform at 60 °C for 2 h. ^c M_n in kg/mol and PDI measured with high-temperature size exclusion chromatography in 1,2,4-trichlorobenzene at 160 °C with polystyrene standards. ^d Mol % of Br-functionalized styrene unit calculated from ¹H NMR spectrum. ^e Efficiency of functionalization (i.e., the percentage of brominated styrene unit relative to added Br₂). ^f Bromination was conducted with 900 mg of the

polymer with 10 mol % of ferric chloride relative to bromine in chloroform at 60 °C for 8 h. ^g Not detected.

We also investigated bromination of aPS under the identical reaction condition. As shown in Table 3.2, the bromination of aPS afforded comparable mol % of brominated polymer, suggesting that this post-functionalization process is efficient regardless of the tacticity of polystyrene.

Table 3.2. Bromination of monodisperse atactic polystyrene^a with bromine (Br₂)^b.

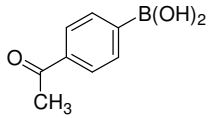
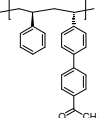
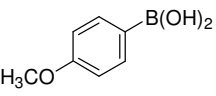
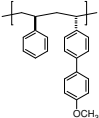
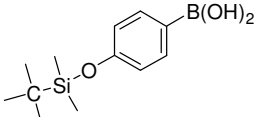
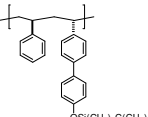
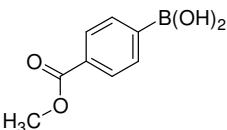
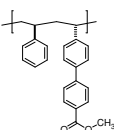
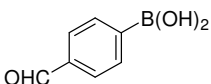
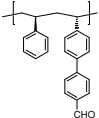
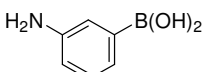
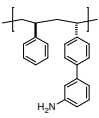
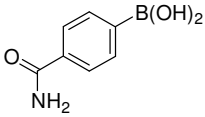
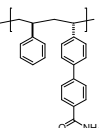
Entry	M_n^c	PDI (M_w/M_n) ^c	[Br ₂]/ [monomer]	aPS-Br			
				M_n^c	PDI (M_w/M_n) ^c	Br (%) ^d	Effic. (%) ^e
1	37.5	1.03	0.10	34.3	1.04	1.2	6
2	37.5	1.03	0.20	32.8	1.05	8.9	22
3	37.5	1.03	0.30	31.8	1.08	17.0	28
4	37.5	1.03	0.50	31.1	1.09	29.3	29
5	37.5	1.03	0.70	31.5	1.09	40.2	29
6	37.5	1.03	1.00	31.1	1.10	51.2	26

^a Atactic polystyrene (aPS) [$M_n = 37.5$ kg/mol, PDI = 1.03]. ^b Bromination was conducted with 100 mg of the polymer with 5 mol % of ferric chloride relative to bromine in chloroform at 60 °C for 2 h. ^c M_n in kg/mol and PDI measured with size exclusion chromatography in THF at 40 °C with polystyrene standards. ^d Mol % of Br-functionalized styrene unit calculated from ¹H NMR spectrum. ^e Efficiency of functionalization (i.e., the percentage of brominated styrene unit relative to added Br₂).

3.3.2. Suzuki–Miyaura Coupling Reactions of sPS-Br

Suzuki–Miyaura cross-coupling reaction is a very powerful biaryl C–C bond formation method owing to its good compatibility with a range of functional groups. Thus, the coupling reaction of functionalized arylboronic acid and sPS–Br using a palladium catalyst would offer installation of various functional groups to the polymer in a convenient way. To explore this possibility, seven examples of *para*- and *meta*-substituted phenyl boronic acids were reacted with 8.5 mol % bromine-functionalized sPS–Br. Phenyl boronic acids containing acetyl, methoxy, siloxy, methoxycarbonyl, formyl, amino, and carbamoyl groups were coupled with sPS–Br using 1 mol % Pd(PPh₃)₄ to form its corresponding functionalized sPS (sPS–FG in Scheme 3.1 and Table 3.3). When sPS–FG were analyzed with ¹H NMR spectroscopy, their spectra showed an appearance of the corresponding functional group with a similar concentration (~8.5 mol %), which suggests that the conversion of each coupling reaction was always quantitative regardless of the location of the substituent at *para*- or *meta*-position of the aromatic ring. The methine resonance main chain at 1.71 ppm and two doublet aromatic proton resonances of sPS–Br at 6.30–6.37 and 7.10–7.18 ppm disappeared completely in ¹H NMR spectra after the Suzuki–Miyaura couplings (see Section 3.4.4. NMR Spectra of Functionalized Polymer Products). The proton resonances of methylene groups and methine groups of sPS–FG were maintained in ratio of 2:1, indicating that the polymer main chain was intact.

Table 3.3. Suzuki–Miyaura reactions of brominated sPS^a with phenyl boronic acid^b.

Entry	Phenyl boronic acid	Product sPS–FG	FG (mol %) ^e /Conversion (%)	$M_n \times 10^{-3}$ (PDI) ^f
1 ^c			8.5 / >99	33.3 (2.78)
2 ^c			8.5 / >99	37.4 (2.56)
3 ^c			8.5 / >99	42.4 (2.56)
4 ^d			8.5 / >99	34.3 (3.89)
5 ^d			8.5 / >99	32.5 (2.99)
6 ^d			8.5 / >99	37.6 (1.83)
7 ^d			8.3 / 98	— ^g

^a Brominated syndiotactic polystyrene (sPS–Br) (8.5 mol % Br, $M_n = 35.0$ kg/mol, PDI =

2.71). ^b Suzuki–Miyaura reaction was conducted with 40 mg of polymer and 1 mol % of

Pd(PPh₃)₄ in toluene at 100 °C (or THF at 80 °C) for 5 h. ^c Reaction was conducted in toluene at 100 °C. ^d Reaction was conducted in THF at 80 °C. ^e Mol % of functionalized styrene unit calculated from ¹H NMR spectra. ^f *M_n* in kg/mol and PDI measured with high-temperature size exclusion chromatography in 1,2,4-trichlorobenzene at 160 °C with polystyrene standards. ^g Not detected.

3.3.3. Molecular Weight Studies with Size Exclusion Chromatography

To study any changes of molecular weight parameters of sPS as a result of bromination process, high-temperature SEC analysis of sPS and sPS–Br was conducted. As can be seen in Table 3.1 and Figure 3.3, a decrease in *M_n* values of sPS–Br (from 48.6 kg/mol of sPS to 31.2 kg/mol of 78 mol % sPS–Br) and their SEC traces suggest a small percentage of polymer chain degradation during the bromination. All PDI values in the brominated polymers, however, remained similar at approximately 2.7 (entries 1, 3, 5, 7, 8, 9 of Table 3.1 and Figure 3.3).

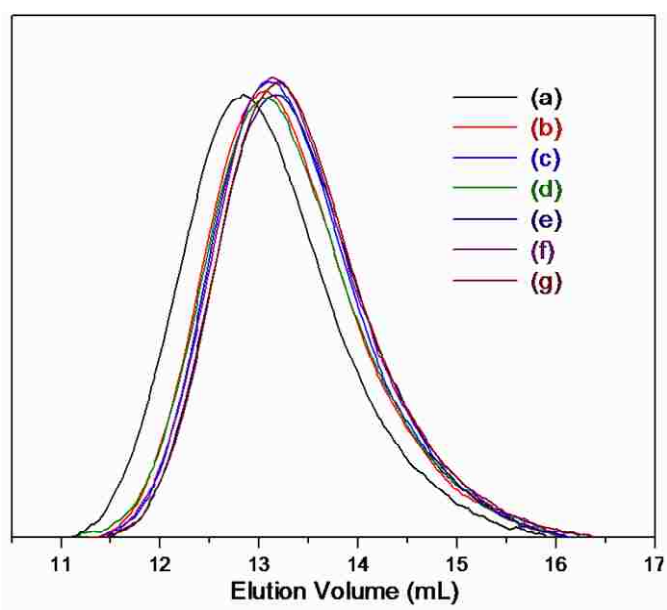


Figure 3.3. High-temperature size exclusion chromatography [1 mg/mL in 1,2,4-trichlorobenzene at 160 °C] of (a) sPS [$M_n = 48.6$ kg/mol; PDI = 2.90]; (b) 2.2 mol % sPS-Br [$M_n = 37.2$ kg/mol; PDI = 2.76] (entry 1 of Table 3.1); (c) 8.5 mol % sPS-Br [$M_n = 35.0$ kg/mol; PDI = 2.71] (entry 3 of Table 3.1); (d) 15.5 mol % sPS-Br [$M_n = 35.3$ kg/mol; PDI = 2.94] (entry 5 of Table 3.1); (e) 28.1 mol % sPS-Br [$M_n = 33.9$ kg/mol; PDI = 2.61] (entry 7 of Table 3.1); (f) 48.9 mol % sPS-Br [$M_n = 32.1$ kg/mol; PDI = 2.89] (entry 8 of Table 3.1); (g) 77.8 mol % sPS-Br [$M_n = 31.2$ kg/mol; PDI = 2.78] (entry 9 of Table 3.1). M_n relative to polystyrene standards.

To study the polymer chain reduction from bromination reaction in detail, a model aPS having narrow molecular weight distribution (M_n of 37.5 kg/mol with a PDI of 1.03) was brominated with the same condition of sPS-Br (Table 3.2 and Figure 3.4). As increasing the amount of added Br_2 , the M_n of aPS-Br also decreased gradually from 37.5 kg/mol of aPS to 31.1 kg/mol of 51.2 mol % aPS-Br. All aPS-Br showed similar PDI values, approximately 1.10, to that of aPS (entries 1–6 of Table 3.2 and Figure 3.4). From the molecular weight results of sPS-Br and aPS-Br, we suspect that the electrophilic aromatic bromination process induces a slight degradation of polymer chain lengths and the extent of the degradation increases as more Br_2 is added. A similar decrease in M_n values as a result of bromination of (atactic) polystyrene has also been reported in literatures.^{78,79}

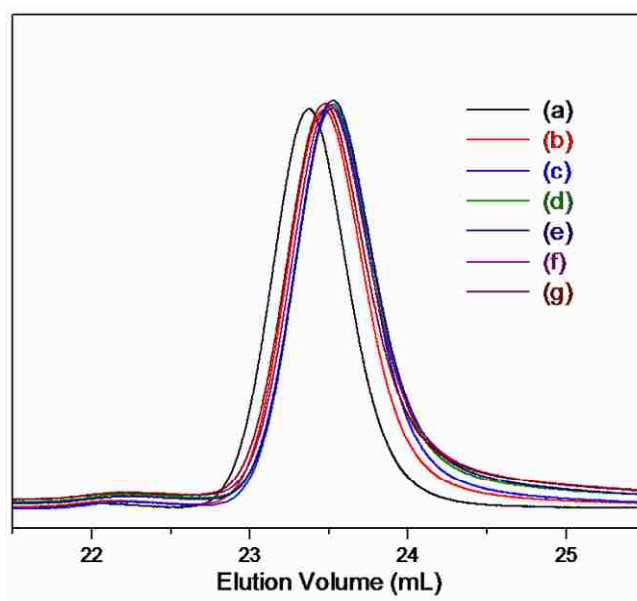


Figure 3.4. Size exclusion chromatography [1.0 mg/mL in THF at 40 °C] of (a) aPS [M_n = 37.5 kg/mol; PDI = 1.03]; (b) 1.2 mol % aPS–Br [M_n = 34.3 kg/mol; PDI = 1.04] (entry 1 of Table 3.2); (c) 8.9 mol % aPS–Br [M_n = 32.8 kg/mol; PDI = 1.05] (entry 2 of Table 3.2); (d) 17.0 mol % aPS–Br [M_n = 31.8 kg/mol; PDI = 1.08] (entry 3 of Table 3.2); (e) 29.3 mol % aPS–Br [M_n = 31.1 kg/mol; PDI = 1.09] (entry 4 of Table 3.2); (f) 40.2 mol % aPS–Br [M_n = 31.5 kg/mol; PDI = 1.08] (entry 5 of Table 3.2); (g) 51.2 mol % aPS–Br [M_n = 31.1 kg/mol; PDI = 1.10] (entry 6 of Table 3.2). M_n relative to polystyrene standards.

As shown in Table 3.3 and Figure 3.5, the molecular weight properties (M_n and PDI) of the Suzuki–Miyaura coupling products were not unchanged significantly from that of 8.5 mol % sPS–Br (M_n = 35.0 kg/mol, PDI = 2.71). This result means that the Suzuki–Miyaura coupling reaction did not induce any side reactions such as chain cleavage and cross-linking in the polymer chains.

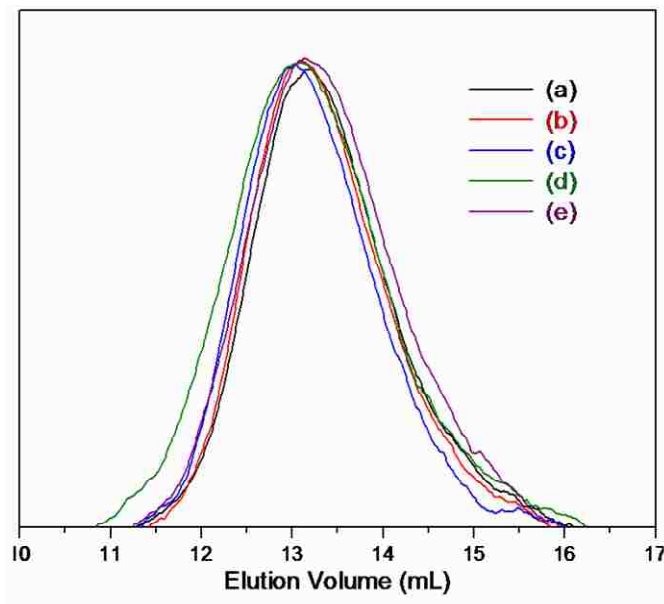


Figure 3.5. High-temperature size exclusion chromatography [1 mg/mL in 1,2,4-trichlorobenzene at 160 °C] of (a) 8.5 mol % 4-acetyl-functionalized sPS [$M_n = 33.3$ kg/mol; PDI = 2.78] (entry 1 of Table 3.3); (b) 8.5 mol % 4-methoxy-functionalized sPS [$M_n = 37.4$ kg/mol; PDI = 2.56] (entry 2 of Table 3.3); (c) 8.5 mol % 4-(*tert*-butyldimethylsilyloxy)-functionalized sPS [$M_n = 42.4$ kg/mol; PDI = 2.56] (entry 3 of Table 3.3); (d) 8.5 mol % 4-(methoxycarbonyl)-functionalized sPS [$M_n = 34.3$ kg/mol; PDI = 3.89] (entry 4 of Table 3.3); (e) 8.5 mol % 4-formyl-functionalized sPS [$M_n = 32.5$ kg/mol; PDI = 2.99] (entry 5 of Table 3.3). M_n relative to polystyrene standards.

3.3.4. Thermal Properties

Thermal properties of unfunctionalized sPS and sPS–Br with a wide range of bromine groups were studied with differential scanning calorimetry (DSC) (Figure 3.6 and Table 3.4). A complex polymorphism of sPS is known to induce similar melting temperatures of two most stable crystalline forms.^{80,81,82} Thus, unfunctionalized sPS possessed more than one melting transition at approximately 270 °C and T_g of 102 °C (Figure 3.6a; entry 1 of

Table 3.4). The 2.2 mol % sPS–Br exhibited a DSC scan similar to that of sPS with a slightly decreased enthalpy and 30% crystallinity (Figure 3.6b; entry 2 of Table 3.4). However, sPS–Br with higher than 4.7 mol % bromine started to lose crystallinity sharply and showed lower melting temperatures because the higher concentration of bromine group disrupted the crystallization process of the polymer extensively (Figure 3.6c–e; entries 3–5 of Table 3.4). Above 15.5 mol % of bromine incorporation, no endothermic response was detected in sPS–Br (Figure 3.6f–j; entries 6–10 of Table 3.4). These sPS–Br samples lost crystallinity completely and showed only T_g at 105 °C.

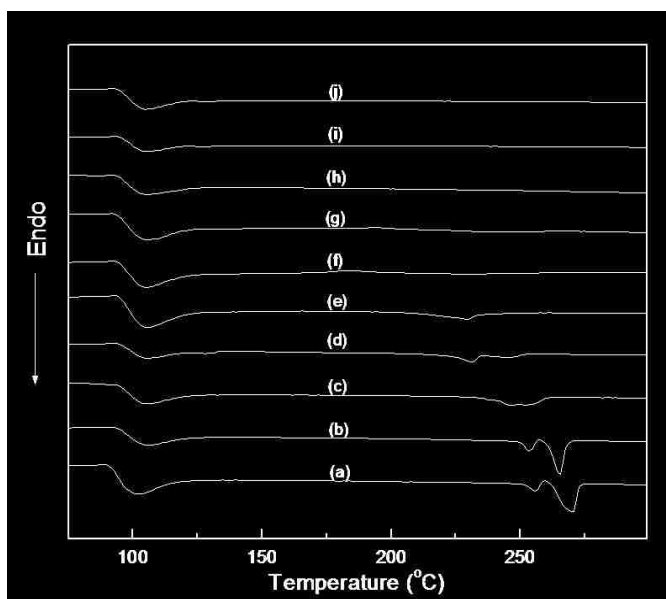


Figure 3.6. DSC scans of (a) sPS, (b) sPS–Br (2.2 mol % Br), (c) sPS–Br (4.7 mol % Br), (d) sPS–Br (8.5 mol % Br), (e) sPS–Br (10.6 mol % Br), (f) sPS–Br (15.5 mol % Br), (g) sPS–Br (17.9 mol % Br), (h) sPS–Br (28.1 mol % Br), (i) sPS–Br (48.9 mol % Br), and (j) sPS–Br (77.8 mol % Br).

Table 3.4. Thermal properties of syndiotactic polystyrene and brominated sPS^a

Entry	Polymer	T_g (°C) ^b	T_m (°C) ^c	ΔH_f (J/g) ^d	Crystallinity ^e (%)
1	sPS	101.6	269.9	19.4	36.5
2	2.2 mol % sPS–Br	106.1	265.3	15.9	29.9
3	4.7 mol % sPS–Br	106.6	246.2	10.9	20.5
4	8.5 mol % sPS–Br	106.4	231.7	5.9	11.0
5	10.6 mol % sPS–Br	105.8	230.0	3.8	7.1
6	15.5 mol % sPS–Br	104.5	— ^f	— ^g	— ^g
7	17.9 mol % sPS–Br	106.1	— ^f	— ^g	— ^g
8	28.1 mol % sPS–Br	105.6	— ^f	— ^g	— ^g
9	48.9 mol % sPS–Br	105.3	— ^f	— ^g	— ^g
10	77.8 mol % sPS–Br	105.7	— ^f	— ^g	— ^g

^a Differential scanning calorimetry (DSC) measurements conducted using heating/cooling rates of 10 °C/min. ^b Glass transition temperature in °C. ^c Melting point of polymer in °C. ^d Heat of fusion of polymer in J/g. ^e The percent of crystallinity based on the theoretical heat of fusion calculated for 100% crystalline sPS (i.e., $\Delta H_f^0 = 53.3$ J/g). ^f Not detected. ^g Cannot be calculated due to absence of endothermic peak.

3.3.5. Water Contact Angles

Water contact angles of sPS, sPS–Br, 4-formyl-functionalized sPS, 3-amino-functionalized sPS, and 4-carbamoyl-functionalized sPS were measured to investigate the change of the surface energy (Figure 3.7). The unfunctionalized sPS has a contact angle of 102.5°. Bromination of sPS did not change the hydrophilicity of the polymer (101.4° of sPS–Br). Although the functionalized polymers have the same concentration of functional group to that of sPS–Br (i.e., 8.5 mol %), their water contact angles were much lower

than that of sPS-Br indicating that the incorporation of polar functionality by Suzuki–Miyaura reaction greatly increased hydrophilicity in the polymer (93.7–95.6°).

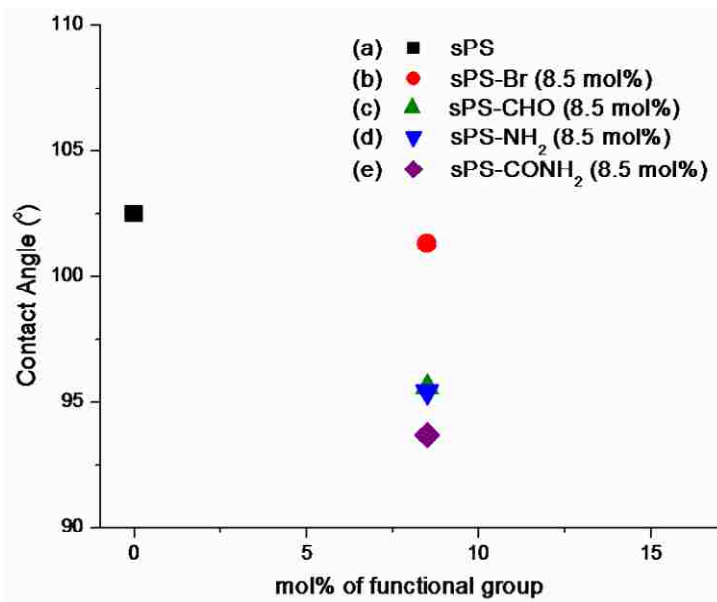


Figure 3.7. Water contact angles of (a) sPS (102.5°); (b) 8.5 mol % sPS–Br (101.4°) (entry 3 of Table 3.1); (c) 8.5 mol % sPS–CHO (95.6°) (entry 5 of Table 3.3); (d) 8.5 mol % sPS–NH₂ (95.4°) (entry 6 of Table 3.3); (e) 8.5 mol % sPS–CONH₂ (93.7°) (entry 7 of Table 3.3).

3.4. Experimental

3.4.1. General Comments

Bromine (Br₂), anhydrous ferric chloride (FeCl₃), chloroform, tetrakis(triphenylphosphine) palladium(0) [Pd(PPh₃)₄], cesium carbonate (Cs₂CO₃), 4-(*tert*-butyldimethylsilyloxy)phenyl boronic acid, 4-acetylphenyl boronic acid, 4-methoxyphenyl boronic acid, 4-(methoxycarbonyl)phenyl boronic acid, 4-formylphenyl boronic acid, 3-aminophenyl boronic acid, and 4-carbamoylphenyl boronic acid were

purchased from commercial vendors (Sigma Aldrich Co., Alfa Aesar, Frontier Scientific, and Acros Organics) and used without further purification. Anhydrous tetrahydrofuran (THF) and toluene were obtained from EMD Chemicals (EM Recycler[®] Container System) and collected from the containers using a positive pressure of nitrogen. Syndiotactic polystyrene (sPS, $M_n = 48.6$ kg/mol with PDI = 2.90) was obtained from LG Chem Ltd., Daejeon, South Korea. To improve the solubility of sPS in the bromination medium, the following procedure was performed. One gram of the polymer was placed in a two-neck round-bottom flask, and then the flask was evacuated and backfilled with nitrogen three times. 1,2-Dichlorobenzene (30 ml) was added to this flask and the mixture was refluxed at 180 °C under nitrogen for 30 min to dissolve sPS. The solution was then cooled to 140 °C and poured into cold methanol (300 mL). The precipitate was filtered and dried under vacuum at 60 °C.

¹H and ¹³C NMR spectra were obtained using 400 and 100 MHz Varian NMR spectrometer at room temperature. All chemical shifts were referenced to tetramethylsilane (TMS). The NMR samples were prepared by applying gentle heat to dissolve the polymer in CDCl₃. ¹H NMR and ¹³C NMR samples were prepared at a concentration of 10 mg/mL and 40 mg/mL, respectively. The molecular weight measurement of sPS and sPS-Br was conducted using a Polymer Laboratory GPC-220 high-temperature size exclusion chromatography at 160 °C. 1,2,4-Trichlorobenzene was the mobile phase and the flow rate was set at 1.0 mL/min. This instrument was calibrated using polystyrene standards. Differential scanning calorimetry (DSC) was performed using a NETZSCH STA 449C instrument under a helium atmosphere. Polymer samples were heated to 300 °C, held there for 1 min to remove the influence of thermal history,

cooled to $-0\text{ }^{\circ}\text{C}$, held there for 1 min, and then reheated to $300\text{ }^{\circ}\text{C}$. The rates of heating and cooling were $10\text{ }^{\circ}\text{C}/\text{min}$. All DSC curves in Figure 3.6 were obtained from the second heating. Glass transition and melting temperatures (T_g and T_m) and enthalpy of fusion (ΔH_f) were obtained after calibration with high-purity indium and zinc standards. The static water contact angles of polymers using a contact angle goniometer (Dataphysics OCA15) at room temperature. The measurement was repeated at ten different positions on the same glass plate, and reported data were the average of the measurements.

sPS: ^1H NMR (400 MHz, CDCl_3 , ppm) $\delta = 1.30$ (2H, $-\text{CH}_2-$), 1.81 (1H, $-\text{CH}-$), 6.55 (2H, $\text{C}_6\text{H}_5\text{-}H_b$), 7.06 (3H, $\text{C}_6\text{H}_5\text{-}H_{c,d}$). ^{13}C NMR (100 MHz, CDCl_3 , ppm) $\delta = 40.5$ ($-\text{CH}-$), 43.8 ($-\text{CH}_2-$), 125.6 ($\text{C}_6\text{H}_5\text{-}C_d$), 127.6 ($\text{C}_6\text{H}_5\text{-}C_b$), 127.9 ($\text{C}_6\text{H}_5\text{-}C_c$), 145.2 ($\text{C}_6\text{H}_5\text{-}C_a$).

3.4.2. Representative Synthesis of sPS-Br (Entry 5 of Table 3.1)

A mixture of sPS (100 mg, 0.960 mmol polystyrene repeating unit), FeCl_3 (2.3 mg, 5 mol % iron based on the amount of sPS) and a magnetic stirring bar were placed in a vial and capped with a Teflon-lined septum. The vial was evacuated and backfilled with nitrogen three times. Chloroform (1.8 mL) was added to the vial with a syringe. The vial was placed in an oil bath at $60\text{ }^{\circ}\text{C}$ and sPS was dissolved completely after 30 min. A bromine stock solution (0.2 mL, 0.288 mmol Br_2) prepared from Br_2 (730 μL) and chloroform (10 mL) was transferred to the vial containing the polymer solution using a microsyringe. A nitrogen balloon was connected to the vial and the mixture was stirred at $60\text{ }^{\circ}\text{C}$ for 2 h in the absence of light. Methanol (2 mL) was added to precipitate the polymer as a white solid, which was filtered and washed with additional methanol (2×10 mL). The polymer product was dried under vacuum at $60\text{ }^{\circ}\text{C}$ for 12 h (98.0 mg, 98%

yield based on polymer weight). ^1H NMR (400 MHz, CDCl_3 , ppm) δ = 1.30 (2H, $-\text{CH}_2-$ of sPS main chain), 1.71 (1H, $-\text{CH}-$ of sPS main chain having brominated aromatic ring), 1.81 (1H, $-\text{CH}-$ of sPS main chain), 6.33 (d, 2H, $\text{C}_6\text{H}_4\text{Br}-H_b$, J = 8.4 Hz), 6.55 (2H, C_6H_5-H_b), 7.06 (3H, $\text{C}_6\text{H}_5-H_{c,d}$), 7.14 (d, 2H, $\text{C}_6\text{H}_4\text{Br}-H_c$, J = 8.2 Hz). ^{13}C NMR (100 MHz, CDCl_3 , ppm) δ = 40.4 ($-\text{CH}-$ of sPS main chain having brominated aromatic rings), 40.8 ($-\text{CH}-$ of sPS main chain), 44.3 ($-\text{CH}_2-$ of sPS main chain), 119.5 ($\text{C}_6\text{H}_4\text{Br}-C_d$), 126.0 (C_6H_5-C_d), 127.9 (C_6H_5-C_b), 128.2 (C_6H_5-C_c), 129.7 ($\text{C}_6\text{H}_4\text{Br}-C_b$), 131.2 ($\text{C}_6\text{H}_4\text{Br}-C_c$), 144.3 ($\text{C}_6\text{H}_4\text{Br}-C_a$), 145.5 (C_6H_5-C_a).

4.4.3. General Suzuki–Miyaura Cross-Coupling Procedure for the Synthesis of sPS–FG

In a nitrogen glovebox, a mixture of 8.5 mol % sPS–Br [40.0 mg, 0.0310 mmol Br] (from entry 3 of Table 3.1), aryl boronic acid (0.310 mmol, 10 equiv based on the amount of bromine concentration of sPS–Br), and Cs_2CO_3 (30.3 mg, 0.0930 mmol, 3 equiv based on the amount of bromine concentration of sPS–Br), and a magnetic stirring bar were placed in a vial. A palladium catalyst stock solution (0.8 mL) prepared from $\text{Pd}(\text{PPh}_3)_4$ (3.6 mg) and toluene (or THF) (8 mL) was transferred to the vial containing the polymer mixture in the glovebox [The amount of added $\text{Pd}(\text{PPh}_3)_4$ is 1 mol % based on the amount of bromine concentration of sPS–Br]. The vial was capped with a Teflon-lined septum and removed from the glovebox. Deionized water (80 μL) was added to the vial with a microsyringe. The vial was placed in an oil bath at 100 $^\circ\text{C}$ (or 80 $^\circ\text{C}$ if THF was used) for 5 h. After cooling, the reaction mixture was diluted with chloroform (10 mL), dried over magnesium sulfate and filtered through a short plug of Celite. The filtrate was concentrated to approximately 1 mL using a rotary evaporator, and cold methanol (1 mL) was added to precipitate the polymer. The process of dissolution in chloroform and

precipitation with methanol was repeated one more time to ensure complete removal of any small molecules trapped in the polymer. The precipitated polymer was filtered and dried under vacuum at 60 °C for 12 h.

4-Acetyl-functionalized sPS (entry 1 of Table 3.3). Yield: 82% based on polymer weight from sPS-Br. ¹H NMR (400 MHz, CDCl₃, ppm) δ = 1.29 (2H, -CH₂- of sPS main chain), 1.80 (1H, -CH- of sPS main chain), 2.64 (s, COCH₃), 6.54 (2H, C₆H₅-H_b), 6.60 (2H, C₆H₄Ar-H_b), 7.06 (3H, C₆H₅-H_{c,d}), 7.28 (2H, C₆H₄Ar-H_c), 7.61 (2H, C₆H₄COCH₃-H_f), 8.02 (2H, C₆H₄COCH₃-H_g). ¹³C NMR (100 MHz, CDCl₃, ppm) δ = 26.7 (COCH₃), 40.3 (-CH- of sPS main chain having functionalized aromatic ring), 40.6 (-CH- of sPS main chain), 43.9 (-CH₂- of sPS main chain), 125.6 (C₆H₅-C_d), 126.7 (C₆H₄Ar-C_c), 126.9 (C₆H₄COCH₃-C_f), 127.7 (C₆H₅-C_b), 127.9 (C₆H₅-C_c), 128.3 (C₆H₄Ar-C_b), 128.9 (C₆H₄COCH₃-C_g), 135.5 (C₆H₄Ar-C_d), 136.9 (C₆H₄COCH₃-C_h), 145.0 (C₆H₄Ar-C_a), 145.2 (C₆H₅-C_a), 145.7 (d, C₆H₄COCH₃-C_e, J = 16.5 Hz), 197.7 (COCH₃)

4-Methoxy-functionalized sPS (entry 2 of Table 3.3). Yield: 85% based on polymer weight from sPS-Br. ¹H NMR (400 MHz, CDCl₃, ppm) δ = 1.29 (2H, -CH₂- of sPS main chain), 1.81 (1H, -CH- of sPS main chain), 3.84 (s, OCH₃), 6.54 (2H, C₆H₅-H_b), 6.97 (2H, C₆H₄OCH₃-H_g), 7.06 (3H, C₆H₅-H_{c,d}), 7.22 (2H, C₆H₄Ar-H_c), 7.48 (2H, C₆H₄OCH₃-H_f). ¹³C NMR (100 MHz, CDCl₃, ppm) δ = 40.5 (-CH- of sPS main chain having functionalized aromatic ring), 40.8 (-CH- of sPS main chain), 44.1 (-CH₂- of sPS main chain), 55.6 (OCH₃), 114.4 (C₆H₄OCH₃-C_g), 125.9 (C₆H₅-C_d), 126.4 (C₆H₄Ar-C_c), 127.9 (C₆H₅-C_b), 128.1 (C₆H₅-C_c), 128.3 (C₆H₄Ar-C_b), 134.1 (C₆H₄OCH₃-C_e), 138.2 (C₆H₄Ar-C_d), 144.0 (C₆H₄Ar-C_a), 145.5 (C₆H₅-C_a), 159.1 (C₆H₄OCH₃-C_h).

4-(*tert*-Butyldimethylsilyloxy)-functionalized sPS (entry 3 of Table 3.3). Yield: 83% based on polymer weight from sPS-Br. ^1H NMR (400 MHz, CDCl_3 , ppm) δ = 0.24 (s, $\text{Si}(\text{CH}_3)_2\text{C}(\text{CH}_3)_3$), 1.02 (s, $\text{Si}(\text{CH}_3)_2\text{C}(\text{CH}_3)_3$), 1.29 (2H, $-\text{CH}_2-$ of sPS main chain), 1.81 (1H, $-\text{CH}-$ of sPS main chain), 6.54 (2H, $\text{C}_6\text{H}_5\text{-}H_b$), 6.90 (2H, $\text{C}_6\text{H}_4\text{OSi}(\text{CH}_3)_2\text{C}(\text{CH}_3)_3\text{-}H_g$), 7.05 (3H, $\text{C}_6\text{H}_5\text{-}H_{c,d}$), 7.21 (2H, $\text{C}_6\text{H}_4\text{Ar-}H_c$), 7.40 (2H, $\text{C}_6\text{H}_4\text{OSi}(\text{CH}_3)_2\text{C}(\text{CH}_3)_3\text{-}H_f$). ^{13}C NMR (100 MHz, CDCl_3 , ppm) δ = -4.1 ($\text{Si}(\text{CH}_3)_2\text{C}(\text{CH}_3)_3$), 18.5 ($\text{Si}(\text{CH}_3)_2\text{C}(\text{CH}_3)_3$), 26.0 ($\text{Si}(\text{CH}_3)_2\text{C}(\text{CH}_3)_3$), 40.5 ($-\text{CH}-$ of sPS main chain having functionalized aromatic ring), 40.8 ($-\text{CH}-$ of sPS main chain), 44.1 ($-\text{CH}_2-$ of sPS main chain), 120.5 ($\text{C}_6\text{H}_4\text{OCH}_3\text{-}C_g$), 125.9 ($\text{C}_6\text{H}_5\text{-}C_d$), 126.4 ($\text{C}_6\text{H}_4\text{Ar-}C_c$), 127.9 ($\text{C}_6\text{H}_5\text{-}C_b$), 128.1 ($\text{C}_6\text{H}_5\text{-}C_c$), 134.7 ($\text{C}_6\text{H}_4\text{OSi-}C_e$), 138.3 ($\text{C}_6\text{H}_4\text{Ar-}C_d$), 144.0 ($\text{C}_6\text{H}_4\text{Ar-}C_a$), 145.5 ($\text{C}_6\text{H}_5\text{-}C_a$), 155.2 ($\text{C}_6\text{H}_4\text{OSi-}C_h$).

4-(Methoxycarbonyl)-functionalized sPS (entry 4 of Table 3.3). Yield: 80% based on polymer weight from sPS-Br. ^1H NMR (400 MHz, CDCl_3 , ppm) δ = 1.29 (2H, $-\text{CH}_2-$ of sPS main chain), 1.80 (1H, $-\text{CH}-$ of sPS main chain), 3.94 (s, COOCH_3), 6.54 (2H, $\text{C}_6\text{H}_5\text{-}H_b$), 6.60 (2H, $\text{C}_6\text{H}_4\text{Ar-}H_b$), 7.05 (3H, $\text{C}_6\text{H}_5\text{-}H_{c,d}$), 7.28 (2H, $\text{C}_6\text{H}_4\text{Ar-}H_c$), 7.60 (2H, $\text{C}_6\text{H}_4\text{COOCH}_3\text{-}H_f$), 8.11 (2H, $\text{C}_6\text{H}_4\text{COOCH}_3\text{-}H_g$). ^{13}C NMR (100 MHz, CDCl_3 , ppm) δ = 40.3 ($-\text{CH}-$ of sPS main chain having functionalized aromatic ring), 40.6 ($-\text{CH}-$ of sPS main chain), 43.9 ($-\text{CH}_2-$ of sPS main chain), 51.5 (COOCH_3 , J = 121.9 Hz), 125.6 ($\text{C}_6\text{H}_5\text{-}C_d$), 126.6 ($\text{C}_6\text{H}_4\text{Ar-}C_c$), 126.7 ($\text{C}_6\text{H}_4\text{COOCH}_3\text{-}C_f$), 127.7 ($\text{C}_6\text{H}_5\text{-}C_b$), 127.8 ($\text{C}_6\text{H}_5\text{-}C_c$), 128.2 ($\text{C}_6\text{H}_4\text{Ar-}C_b$), 128.5 ($\text{C}_6\text{H}_4\text{COOCH}_3\text{-}C_h$), 130.0 ($\text{C}_6\text{H}_4\text{COOCH}_3\text{-}C_g$), 137.1 ($\text{C}_6\text{H}_4\text{Ar-}C_d$), 145.0 ($\text{C}_6\text{H}_4\text{Ar-}C_a$), 145.2 ($\text{C}_6\text{H}_5\text{-}C_a$), 145.6 (d, $\text{C}_6\text{H}_4\text{COOCH}_3\text{-}C_e$, J = 15.8 Hz), 167.1 (COOCH_3).

4-Formyl-functionalized sPS (entry 5 of Table 3.3). Yield: 83% based on polymer weight from sPS-Br. ^1H NMR (400 MHz, CDCl_3 , ppm) δ = 1.29 (2H, $-\text{CH}_2-$ of sPS main chain), 1.80 (1H, $-\text{CH}-$ of sPS main chain), 6.54 (2H, $\text{C}_6\text{H}_5\text{-}H_b$), 6.61 (2H, $\text{C}_6\text{H}_4\text{Ar-}H_b$), 7.05 (3H, $\text{C}_6\text{H}_5\text{-}H_{c,d}$), 7.30 (2H, $\text{C}_6\text{H}_4\text{Ar-}H_c$), 7.69 (2H, $\text{C}_6\text{H}_4\text{CHO-}H_f$), 7.95 (2H, $\text{C}_6\text{H}_4\text{CHO-}H_g$), 10.05 (s, CHO). ^{13}C NMR (100 MHz, CDCl_3 , ppm) δ = 40.3 ($-\text{CH}-$ of sPS main chain having functionalized aromatic ring), 40.6 ($-\text{CH}-$ of sPS main chain), 43.9 ($-\text{CH}_2-$ of sPS main chain), 125.6 ($\text{C}_6\text{H}_5\text{-}C_d$), 126.8 ($\text{C}_6\text{H}_4\text{Ar-}C_c$), 127.3 ($\text{C}_6\text{H}_4\text{CHO-}C_f$), 127.7 ($\text{C}_6\text{H}_5\text{-}C_b$), 127.9 ($\text{C}_6\text{H}_5\text{-}C_c$), 128.3 ($\text{C}_6\text{H}_4\text{Ar-}C_b$), 130.2 ($\text{C}_6\text{H}_4\text{CHO-}C_g$), 134.9 ($\text{C}_6\text{H}_4\text{CHO-}C_d$), 136.8 ($\text{C}_6\text{H}_4\text{Ar-}C_h$), 145.0 ($\text{C}_6\text{H}_4\text{Ar-}C_a$), 145.2 ($\text{C}_6\text{H}_5\text{-}C_a$), 146.6 (d, $\text{C}_6\text{H}_4\text{CHO-}C_e$, $J = 128.0$ Hz), 191.9 (CHO).

3-Amino-functionalized sPS (entry 6 of Table 3.3). Yield: 87% based on polymer weight from sPS-Br. ^1H NMR (400 MHz, CDCl_3 , ppm) δ = 1.29 (2H, $-\text{CH}_2-$ of sPS main chain), 1.81 (1H, $-\text{CH}-$ of sPS main chain), 3.67 (s, NH_2), 6.54 (2H, $\text{C}_6\text{H}_5\text{-}H_b$), 6.62 (1H, $\text{C}_6\text{H}_4\text{NH}_2\text{-}H_i$), 6.84 (1H, $\text{C}_6\text{H}_4\text{NH}_2\text{-}H_j$), 6.94 (1H, $\text{C}_6\text{H}_4\text{NH}_2\text{-}H_f$), 7.06 (3H, $\text{C}_6\text{H}_5\text{-}H_{c,d}$), 7.20 (1H, $\text{C}_6\text{H}_4\text{NH}_2\text{-}H_g$), 7.30 (2H, $\text{C}_6\text{H}_4\text{Ar-}H_b$). ^{13}C NMR (100 MHz, CDCl_3 , ppm) δ = 40.6 ($-\text{CH}-$ of sPS main chain having functionalized aromatic ring), 40.9 ($-\text{CH}-$ of sPS main chain), 44.2 ($-\text{CH}_2-$ of sPS main chain), 114.0 ($\text{C}_6\text{H}_4\text{NH}_2\text{-}C_{i,j}$), 117.8 ($\text{C}_6\text{H}_4\text{NH}_2\text{-}C_f$), 125.9 ($\text{C}_6\text{H}_5\text{-}C_d$), 126.8 ($\text{C}_6\text{H}_4\text{Ar-}C_c$), 128.0 ($\text{C}_6\text{H}_5\text{-}C_b$), 128.1 ($\text{C}_6\text{H}_5\text{-}C_c$), 128.3 ($\text{C}_6\text{H}_4\text{NH}_2\text{-}C_g$), 138.8 ($\text{C}_6\text{H}_4\text{Ar-}C_d$), 142.7 ($\text{C}_6\text{H}_4\text{NH}_2\text{-}C_e$), 144.6 ($\text{C}_6\text{H}_4\text{Ar-}C_a$), 145.5 ($\text{C}_6\text{H}_5\text{-}C_a$), 146.9 ($\text{C}_6\text{H}_4\text{NH}_2\text{-}C_h$).

4-Carbamoyl-functionalized sPS (entry 7 of Table 3.3). Yield: 80% based on polymer weight from sPS-Br. ^1H NMR (400 MHz, CDCl_3 , ppm) δ = 1.29 (2H, $-\text{CH}_2-$ of sPS main chain), 1.81 (1H, $-\text{CH}-$ of sPS main chain), 6.55 (2H, $\text{C}_6\text{H}_5\text{-}H_b$), 6.61 (2H, $\text{C}_6\text{H}_4\text{Ar-}$

H_b), 7.06 (3H, $C_6H_5-H_{c,d}$), 7.29 (2H, $C_6H_4Ar-H_c$), 7.61 (2H, $C_6H_4CONH_2-H_f$), 7.89 (2H, $C_6H_4CONH_2-H_g$). ^{13}C NMR (100 MHz, $CDCl_3$, ppm) δ = 40.3 ($-CH-$ of sPS main chain having functionalized aromatic rings), 40.6 ($-CH-$ of sPS main chain), 43.9 ($-CH_2-$ of sPS main chain), 125.6 ($C_6H_5-C_d$), 126.6 ($C_6H_4Ar-C_c$), 127.0 ($C_6H_4CONH_2-C_f$), 127.7 ($C_6H_5-C_b$), 127.9 ($C_6H_5-C_e$), 128.3 ($C_6H_4Ar-C_b$), 131.5 ($C_6H_4CONH_2-C_h$), 137.0 ($C_6H_4Ar-C_d$), 145.0 ($C_6H_4Ar-C_a$), 145.2 ($C_6H_5-C_a$), 145.2 (d, $C_6H_4CONH_2-C_e$, J = 60.6 Hz), 169.1 ($CONH_2$).

3.4.4. NMR Spectra of Functionalized Polymer Products

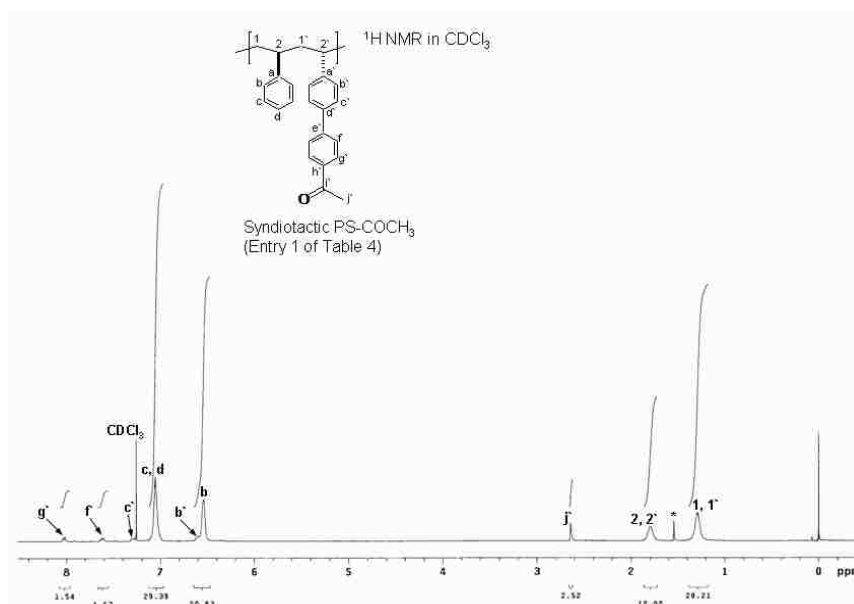


Figure 3.8. 1H NMR spectrum [delay time = 1 s, number of scans = 16] of sPS- $COCH_3$ [10 mg/mL in $CDCl_3$ at 25 °C] (An asterisk indicates H_2O from $CDCl_3$).

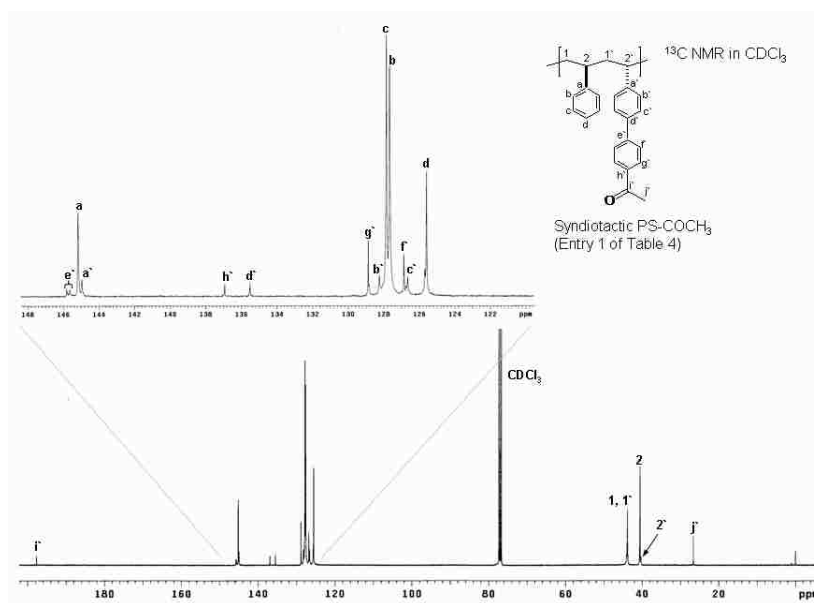


Figure 3.9. ^{13}C NMR spectrum [delay time = 4 s, number of scans = 8000] of sPS-COCH₃ [40 mg/mL in CDCl₃ at 25 °C].

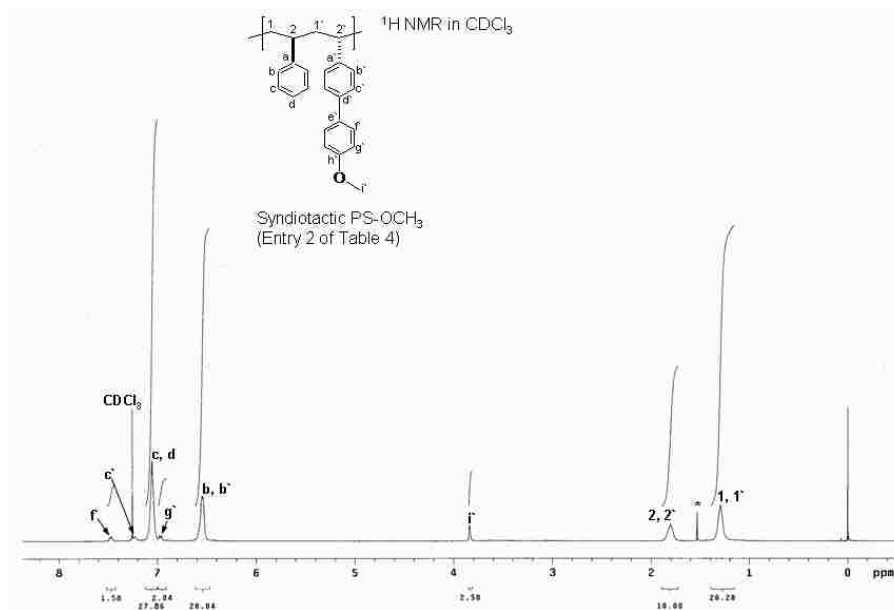


Figure 3.10. ^1H NMR spectrum [delay time = 1 s, number of scans = 16] of sPS-OCH₃ [10 mg/mL in CDCl₃ at 25 °C] (An asterisk indicates H₂O from CDCl₃).

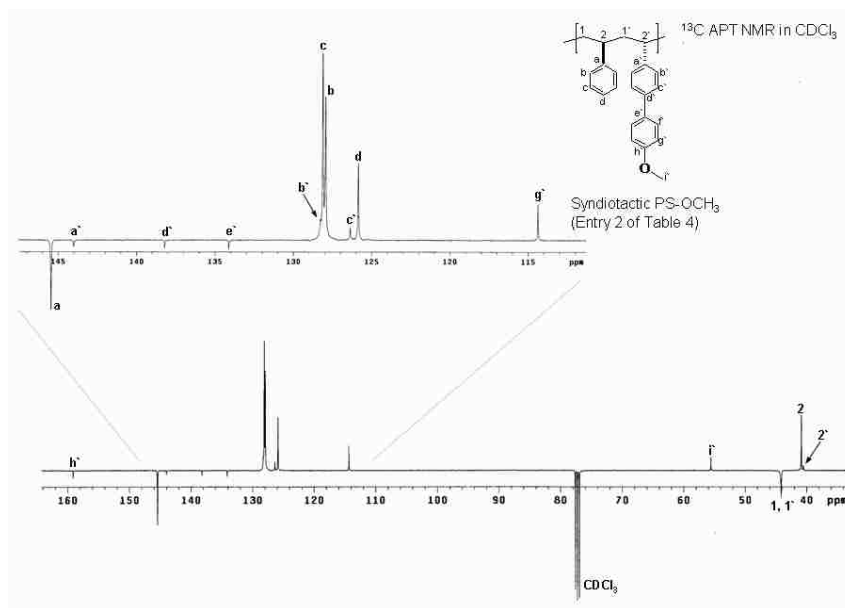


Figure 3.11. ^{13}C APT NMR spectrum [delay time = 4 s, number of scans = 8000] of sPS- OCH_3 [40 mg/mL in CDCl_3 at 25°C].

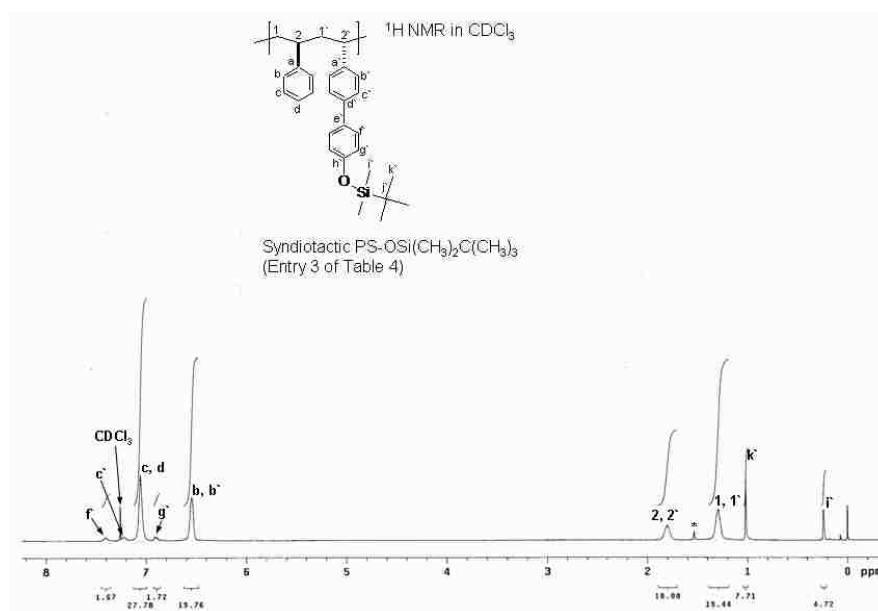


Figure 3.12. ^1H NMR spectrum [delay time = 1 s, number of scans = 16] of sPS- $\text{OSi}(\text{CH}_3)_2\text{C}(\text{CH}_3)_3$ [10 mg/mL in CDCl_3 at 25°C] (An asterisk indicates H_2O from CDCl_3).

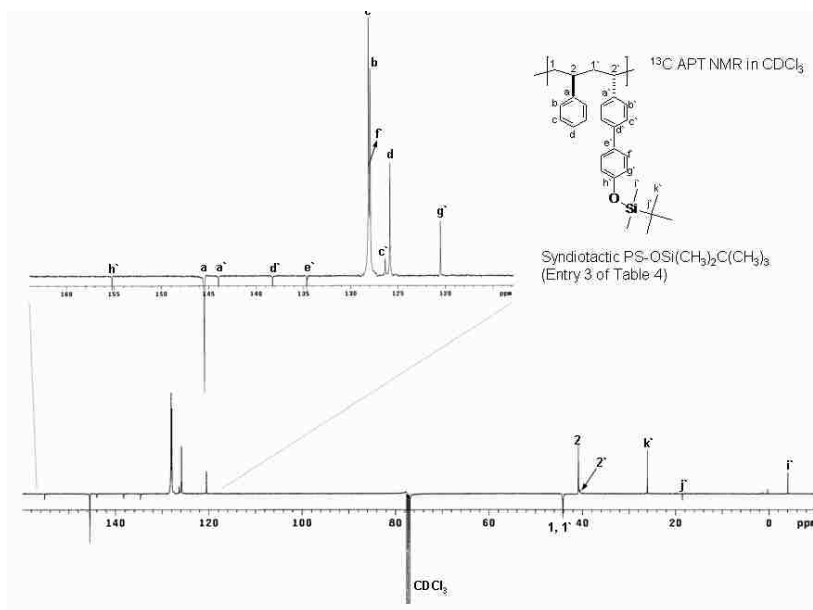


Figure 3.13. ¹³C APT NMR spectrum [delay time = 4 s, number of scans = 8000] of sPS–OSi(CH₃)₂C(CH₃)₃ [40 mg/mL in CDCl₃ at 25 °C].

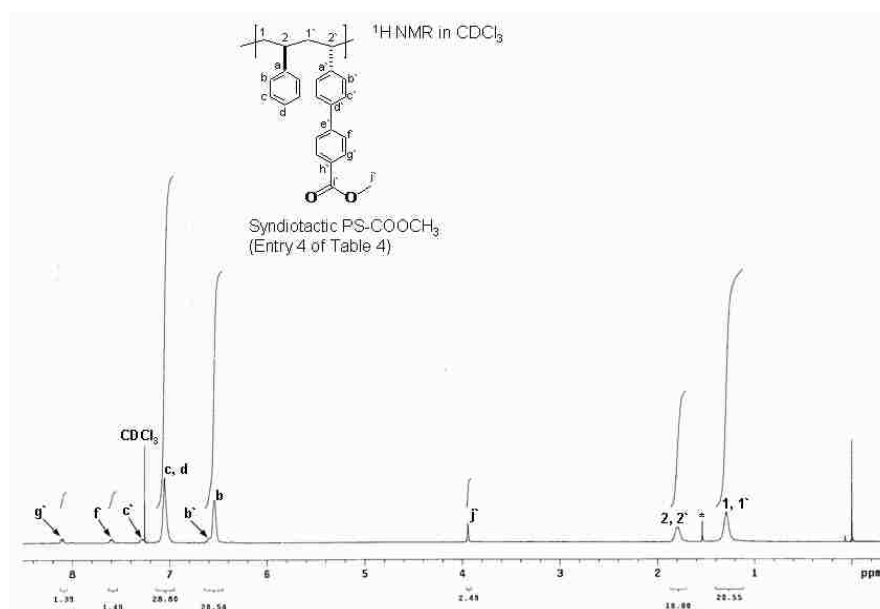


Figure 3.14. ¹H NMR spectrum [delay time = 1 s, number of scans = 16] of sPS–COOCH₃ [10 mg/mL in CDCl₃ at 25 °C] (An asterisk indicates H₂O from CDCl₃).

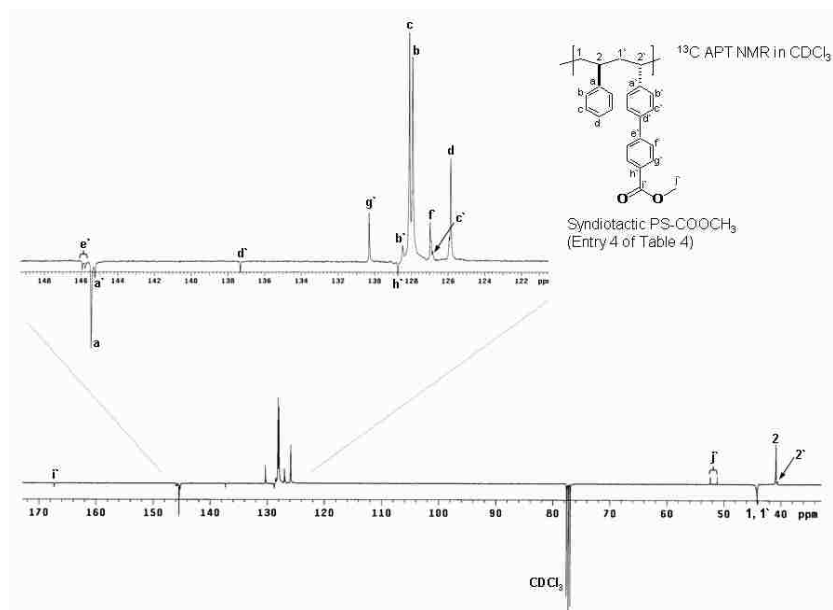


Figure 3.15. ^{13}C APT NMR spectrum [delay time = 4 s, number of scans = 8000] of sPS-COOCH₃ [40 mg/mL in CDCl₃ at 25 °C].

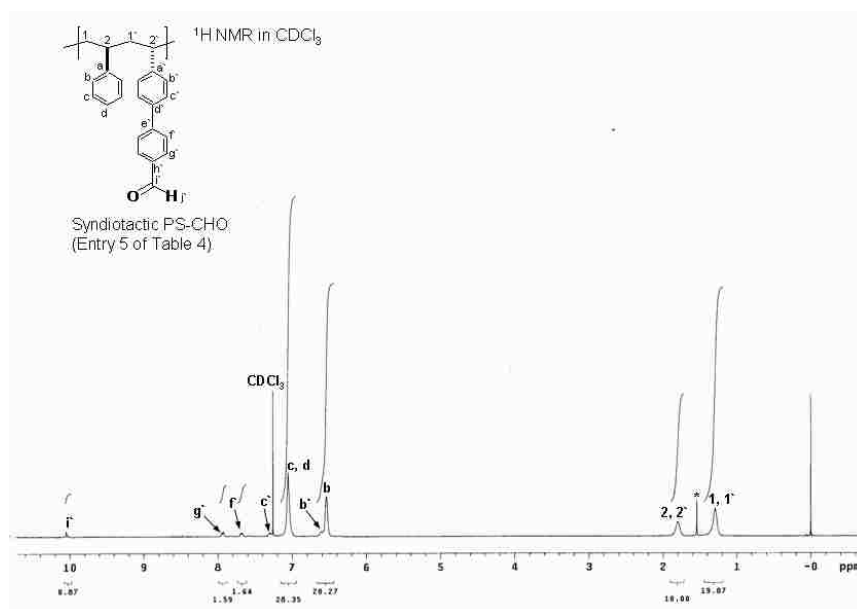


Figure 3.16. ^1H NMR spectrum [delay time = 1 s, number of scans = 16] of sPS-CHO [10 mg/mL in CDCl₃ at 25 °C] (An asterisk indicates H₂O from CDCl₃).

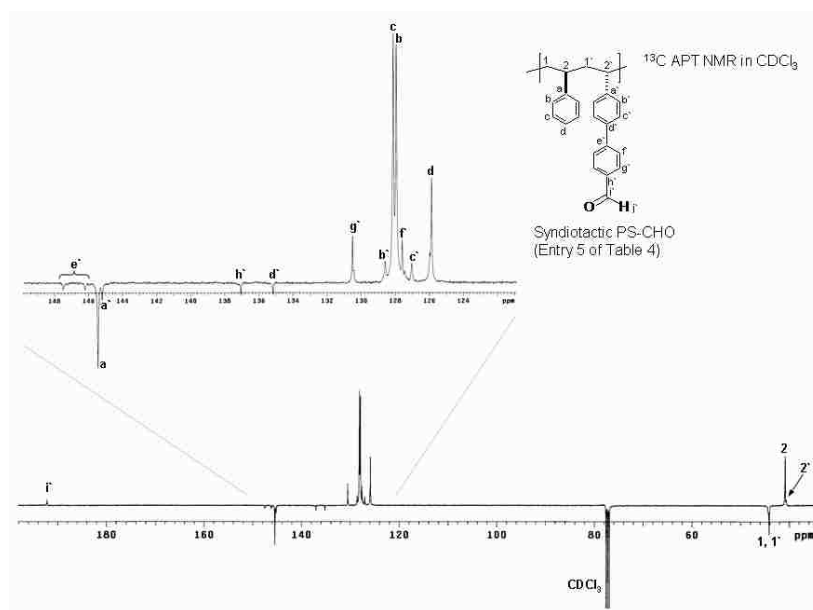


Figure 3.17. ^{13}C APT NMR spectrum [delay time = 4 s, number of scans = 8000] of sPS-CHO [40 mg/mL in CDCl_3 at 25°C].

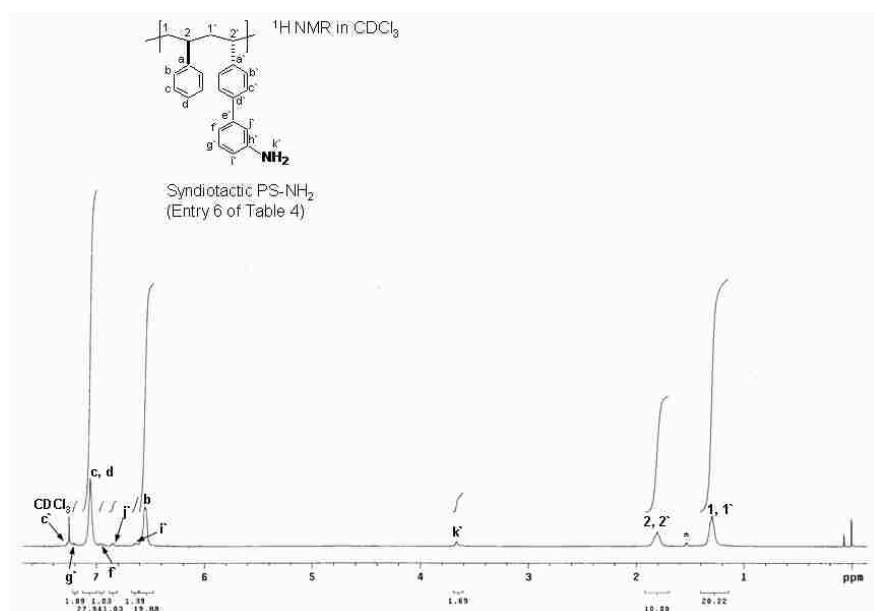


Figure 3.18. ^1H NMR spectrum [delay time = 1 s, number of scans = 16] of sPS- NH_2 [10 mg/mL in CDCl_3 at 25°C] (An asterisk indicates H_2O from CDCl_3).

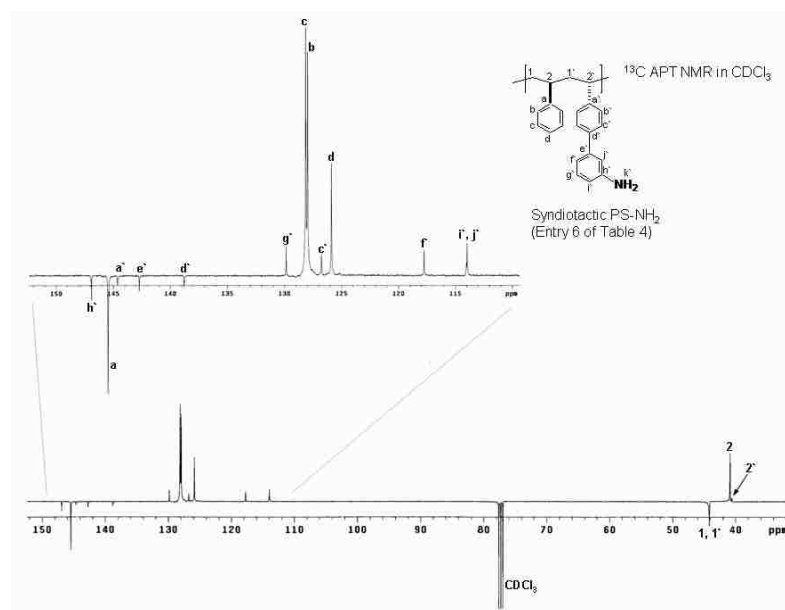


Figure 3.19. ¹³C APT NMR spectrum [delay time = 4 s, number of scans = 8000] of sPS-NH₂ [40 mg/mL in CDCl₃ at 25 °C].

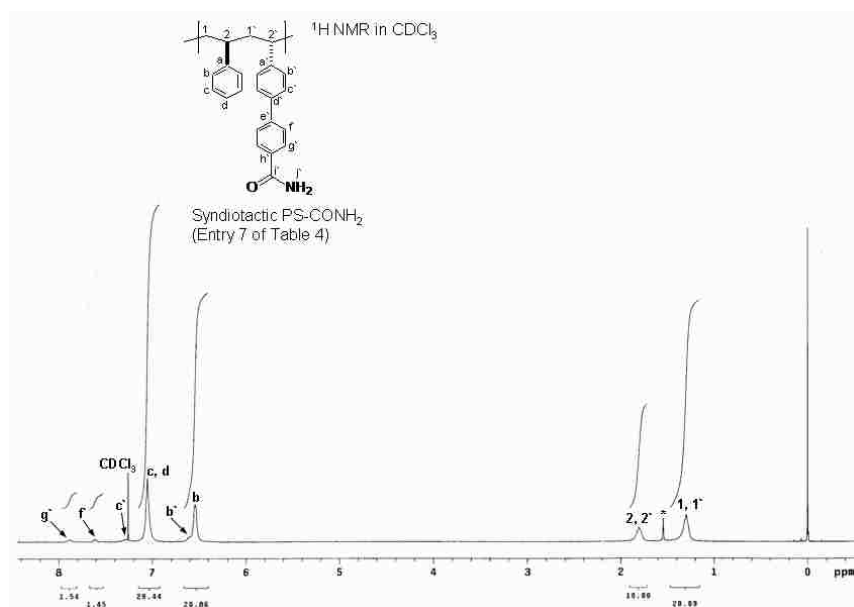


Figure 3.20. ¹H NMR spectrum [delay time = 1 s, number of scans = 16] of sPS-CONH₂ [10 mg/mL in CDCl₃ at 25 °C] (An asterisk indicates H₂O from CDCl₃).

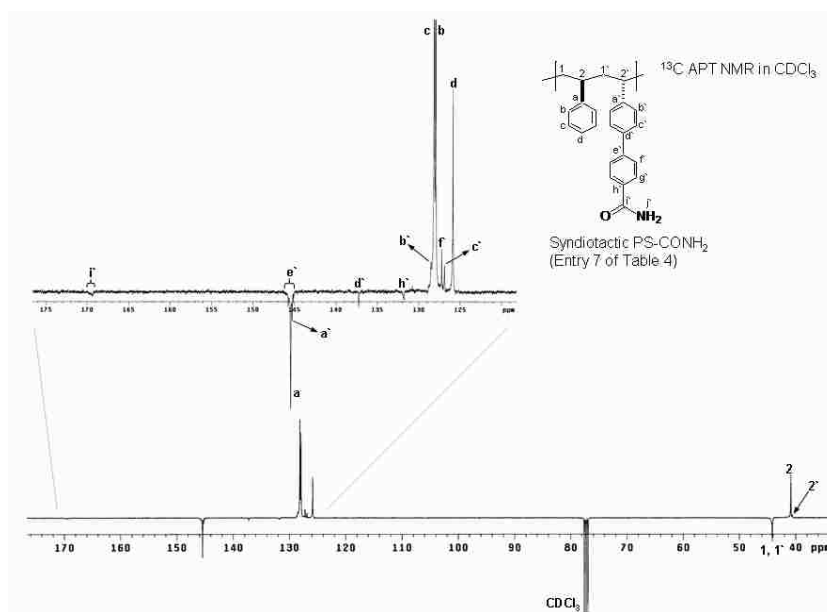


Figure 3.21. ^{13}C APT NMR spectrum [delay time = 4 s, number of scans = 8000] of sPS- CONH_2 [40 mg/mL in CDCl_3 at 25 $^\circ\text{C}$].

3.5. Conclusion

In summary, we have described a new incorporation method of a wide range of functional groups into high-molecular-weight sPS via a combination of electrophilic aromatic bromination at the *para*-position of the polymer and subsequent Suzuki–Miyaura cross-coupling reactions of the brominated polymer with functionalized aryl boronic acid. The controlled bromination of the crystalline polystyrene allowed introduction of bromine group up to 78 mol %, although there was a slight degradation of the polymer chain length. Suzuki–Miyaura cross-coupling reactions with functionalized phenyl boronic acids afforded quantitative replacement of the attached bromine group in sPS to other versatile functional groups. This easy-to-perform post-functionalization method provides a convenient alternative way to install various functional groups with desired concentration into aromatic polymers.

CHAPTER 4

HYDROPHILIC GRAFT MODIFICATION OF A COMMERCIAL CRYSTALLINE POLYOLEFIN

4.1. Abstract

We report a novel approach to synthesize hydroxy-functionalized isotactic poly(1-butene) using rhodium-catalyzed *regioselective* C–H activation at the side chain of the commercial polyolefin and subsequent oxidation of boronic ester group. The introduction of a hydroxy group was accomplished up to ~19 mol % without any significant side reactions that could alter the molecular weight properties. The functionalization was controllable by changing the ratio of the boron reagent to the polymer repeating unit. A side chain-functionalized polyolefin macroinitiator was prepared by esterification of the hydroxy group in the polymer with 2-bromoisobutyl bromide.

Atom Transfer Radical Polymerization of methyl methacrylate and *tert*-butyl acrylate from the macroinitiator generated high molecular-weight graft copolymers of the polyolefins, isotactic poly(1-butene)-*graft*-poly(methyl methacrylate) (PB-*g*-PMMA) and isotactic poly(1-butene)-*graft*-poly(*tert*-butyl acrylate) (PB-*g*-PtBA). Finally, hydrolysis of the *tert*-butoxy ester group of PB-*g*-PtBA created an amphiphilic polyolefin containing a short carboxylic acid-functionalized polymer block at the side chain, isotactic poly(1-butene)-*graft*-poly(acrylic acid) (PB-*g*-PAA).

4.2. Introduction

Because polyolefins provide excellent mechanical property, chemical stability, processability and low production cost, they are ubiquitously used around the world as commercial polymers.⁸³ In spite of their large-scale production and favorable properties, the saturated polymers have some limitations for wider application. These include incompatibility with polar materials due to low surface energy which is resulted from the lack of polar functional groups in the polymers. Selective functionalization of polyolefins even with low concentration of polar group can be sufficient to change surface properties and improve compatibility with other materials. Thus, synthesis of such a polar group-incorporated polyolefins has attracted much interest from the research community of academia and industry.⁸⁴⁻¹²⁵

Several olefin copolymerization approaches of α -olefins with vinyl monomers containing pendant boranes⁸⁷ or protected polar group⁸⁸ have been attempted to obtain functionalized polyolefin. Copolymerization with polar chain transfer agents such as phosphines,⁸⁹ silanes,⁹⁰ boranes,⁹¹ and vinyl chloride⁹² have also been reported. These catalysts, however, showed much reduced activity in the copolymerization compared with those in homopolymerization of α -olefin, and the polar monomer-incorporated copolymers had much lower molecular weight. In addition, less oxophilic late metal catalysts have been used for copolymerization of olefin with polar vinyl monomers.⁹³⁻⁹⁷ However, the microstructures of polymers generated by late transition metal catalysts are different from those of crystalline polyolefins.^{96,97} Controlled radical copolymerization of α -olefins with methyl acrylate has been recently reported for randomly functionalized polyolefins. However, the functionalized polymers were mostly composed of

poly(methyl acrylate) instead of polyolefin.^{98,99}

As an alternative approach, direct chemical modification of polyolefin can introduce polar functionality into the polymer. Since a diverse spectrum of polyolefins having different molecular weight properties are easily obtainable, a successful postfunctionalization of the polymers could readily afford a variety of uniformly functionalized polyolefins.¹⁰⁰ Because the saturated C–C and C–H bonds in polyolefin are very inert, however, this approach typically uses a highly reactive free radical to activate the polymer functionalization. The radical intermediate generally accompanies side reactions such as chain scission and cross-linking and alters the length and properties of the polymer in the chemical modification process.

Recently, polymer modification by transition metal-catalyzed C–H activation has attracted attention as a new methodology of polyolefin functionalization.¹⁰⁰⁻¹⁰⁷ Unlike typical polyolefin modification via a highly reactive free radical or a carbocation intermediate, this new method allowed incorporation of functional group into polyolefins with small or negligible changes in molecular weight from the starting polymers. Unfortunately, these methods were mostly adopted for functionalization of amorphous polyolefins and generated only a low concentration of polar functionality when high-molecular-weight crystalline polymers were used.

Atom Transfer Radical Polymerization (ATRP) is a useful polymerization method to prepare various vinyl polymers having controllable molecular weight. It was reported that a combination of a transition metal catalyzed polymerization of olefin and subsequent ATRP of vinyl monomers generated several examples of functionalized polyolefin block or graft copolymers.^{108-112,115,116,118,120} Given that the most of the block/graft copolymers

prepared from low-molecular weight macroinitiator were made up of a polyacrylate segment in place of polyolefin segment,^{111,112} they were far different from real commercial polyolefin. Direct functionalization of commercial polyolefins for the creation of well-defined graft copolymers has not been studied much.^{105,109,110,119}

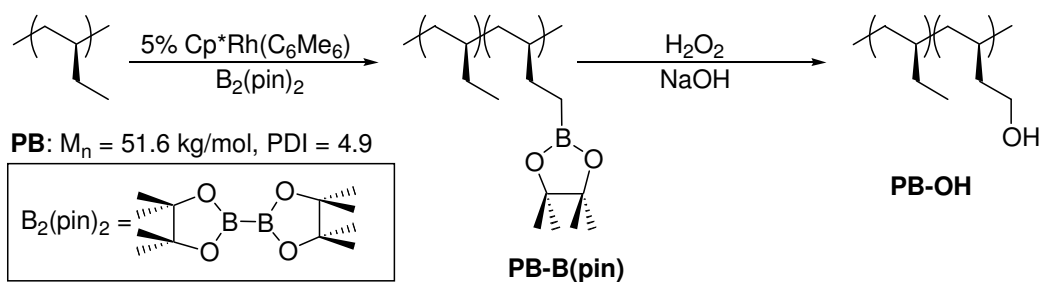
It has recently been reported by us that the regiospecific functionalization of the C–H bond of isotactic poly(1-butene) (PB), a commercial high-molecular-weight crystalline polyolefin, through a rhodium catalyzed terminal C–H activation/borylation with bis(pinacolato)diboron [B₂(pin)₂] can be achieved.¹²⁶ We herein demonstrated that the concentration of (hydroxy-)functionalized side chains in the polymer could be easily controlled up to ~19 mol % by changing the percentage of the boron reagent to that of the polymer repeating unit in C–H borylation and subsequently oxidizing the pinacolboronic ester [B(pin)] group. Furthermore, using a functionalized macroinitiator prepared from the hydroxylated PB, we report ATRP of methyl methacrylate (MMA) and *tert*-butyl acrylate (*t*BA) and synthesis of polar block-grafted polyolefins, isotactic poly(1-butene)-graft-poly(methyl methacrylate) (PB-*g*-PMMA) and isotactic poly(1-butene)-*graft*-poly(*tert*-butyl acrylate) (PB-*g*-*Pt*BA). Finally, an amphiphilic graft copolymer, isotactic poly(1-butene)-*graft*-poly(acrylic acid) (PB-*g*-PAA), was synthesized from the hydrolysis of the *tert*-butoxy ester group in PB-*g*-*Pt*BA.

4.3. Results and Discussion

4.3.1. Borylated and Hydroxylated Isotactic Poly(1-butene)

Scheme 4.1 shows the synthetic route for the preparation of hydroxylated isotactic poly(1-butene) (PB–OH). A commercial high-molecular-weight crystalline polyolefin,

isotactic poly(1-butene) (PB in Scheme 4.1), was functionalized regiospecifically at the terminal methyl groups of the polymer's side chain. The C–H activation/borylation was conducted using variable amounts of $B_2(\text{pin})_2$ and 5 mol % $\text{Cp}^*\text{Rh}(\eta^4\text{-C}_6\text{Me}_6)$ (based on the amount of $B_2(\text{pin})_2$) in cyclooctane solvent at 150 °C. Because of the steric effect, only the terminal methyl group is known to react with $B_2(\text{pin})_2$ in the rhodium-catalyzed C–H activation of alkane containing methyl, methylene and methine groups.¹²⁶ Thus, cyclooctane, a high boiling solvent composed only of methylene groups, was chosen as the solvent. After the functionalization, the crude borylated polymer [PB–B(pin)] was dissolved in toluene and precipitated in cold methanol for purification. To explore the possibility of introducing a polar group into the nonpolar polymer, the isolated B(pin)-functionalized polymer was then oxidized with a solution of $\text{NaOH}/\text{H}_2\text{O}_2$ in THF to give the corresponding PB–OH. The boronic ester group at the terminal side chain was completely converted into a hydroxy group.



Scheme 4.1. Regioselective functionalization of isotactic poly(1-butene).

The ^1H NMR spectrum of PB–B(pin) showed a new resonance at 1.24 ppm for the four methyl groups of the B(pin) moiety ($-\text{BOC}(\text{CH}_3)_2$) (Figure 4.1). The ^{13}C NMR spectrum of PB–B(pin) showed two new resonances from the B(pin) group: 83.0 ppm for

$-\text{BOC}(\text{CH}_3)_2$ and 25.0 ppm for $-\text{BOC}(\text{CH}_3)_2$ (Figure 4.2). The successful incorporation of the B(pin) group was also verified by ^{11}B NMR spectrum, which revealed a broad resonance at 34.0 ppm (Figure 4.3).

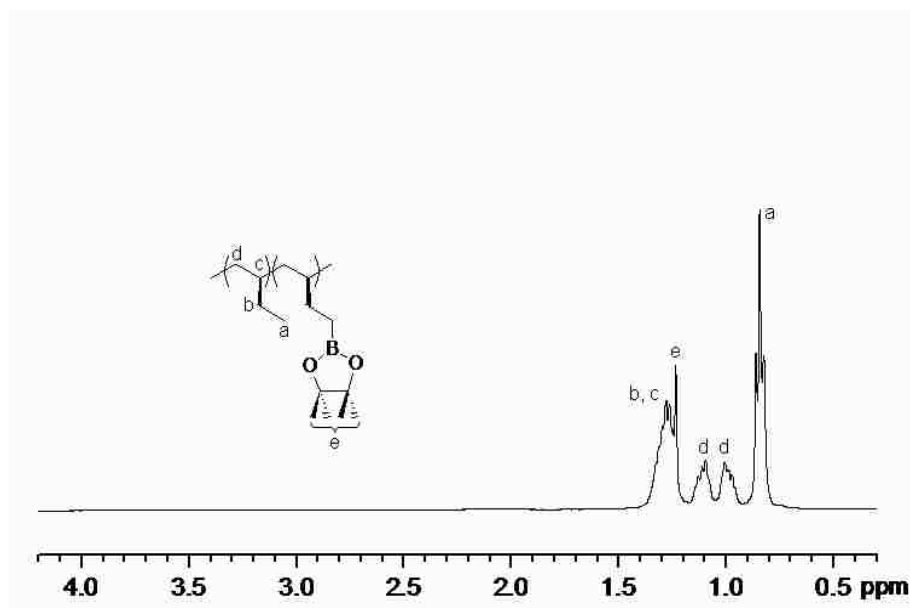


Figure 4.1. ^1H NMR spectrum of PB-B(pin) (Entry 2 of Table 4.1; 10 mg/mL in CDCl_3).

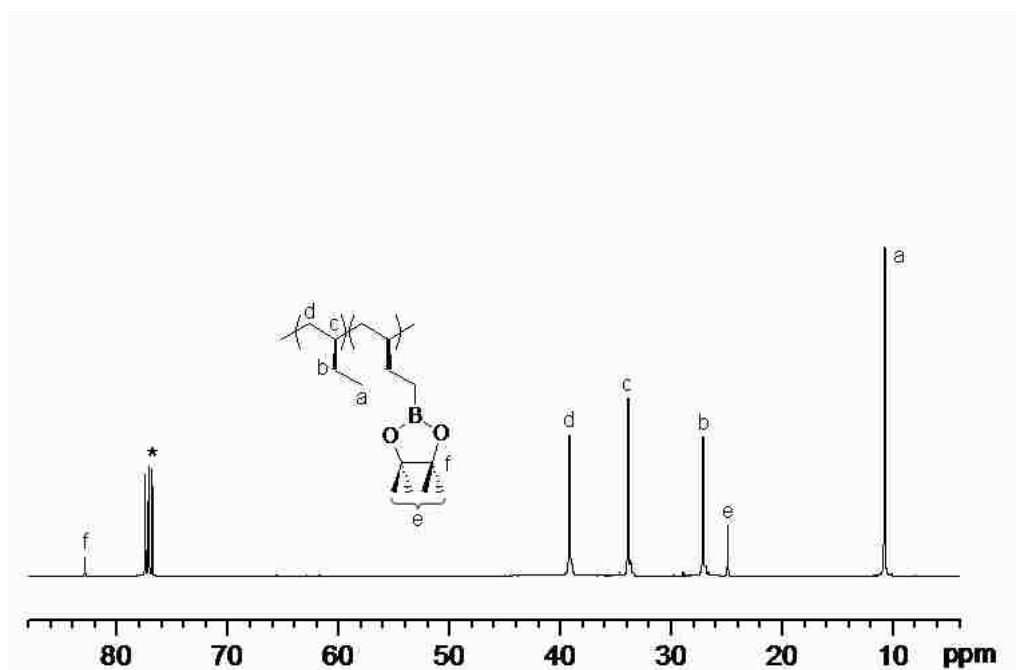


Figure 4.2. ^{13}C NMR spectrum of PB-B(pin) (Entry 2 of Table 4.1; 30 mg/mL in CDCl_3).

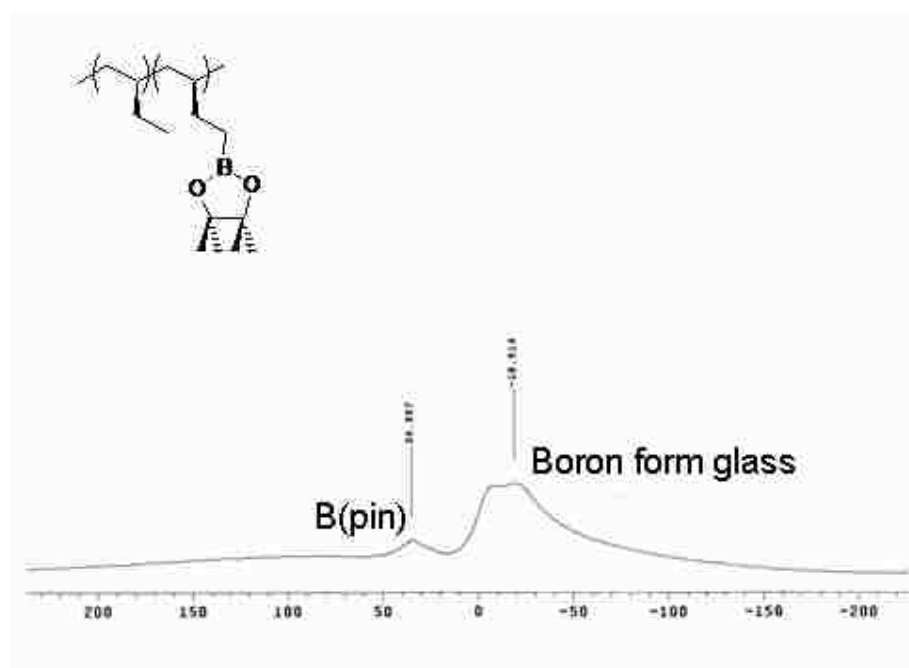


Figure 4.3. ^{11}B NMR spectrum of PB-B(pin) (Entry 3 of Table 4.1; 30 mg/mL in CDCl_3).

Upon oxidation the FT-IR spectrum supports the presence of hydroxy group in PB-OH, which showed a broad O-H bond stretching band at 3330 cm^{-1} (Figure 4.4). The ^1H and ^{13}C NMR spectra of PB-OH showed a triplet resonance at 3.67 ppm and a resonance at 61.4 ppm, respectively, for the methylene group of $-\text{CH}_2\text{OH}$ (Figures 4.5 and 4.6). The resonance at 61.4 ppm in the ^{13}C NMR spectrum was confirmed as a methylene group using ^{13}C attached proton test (APT) NMR spectroscopy (Figure 4.7). The complete disappearance of resonances at 25.0 and 83.0 ppm of the B(pin) group in the ^{13}C NMR spectrum of PB-OH demonstrated successful oxidation in the polymer chain. In the ^{13}C

APT NMR spectrum of PB-OH, no resonances corresponding to $-\overset{\text{OH}}{\underset{|}{\text{C}}}-$ or $-\overset{\text{OH}}{\text{C}}-$ resulting from hydroxylation of the backbone methylene or methine positions were detected. Based on this analysis, it was concluded that the rhodium-catalyzed C-H borylation occurred selectively at the terminal methyl group of the side chain. Furthermore, the absence of resonances corresponding to $-\text{C}(=\text{O})\text{H}$ or $-\text{CO}_2\text{H}$ in the ^1H and ^{13}C NMR spectra of PB-OH indicates that the oxidation of the B(pin) group in the side chain was not over-oxidized.

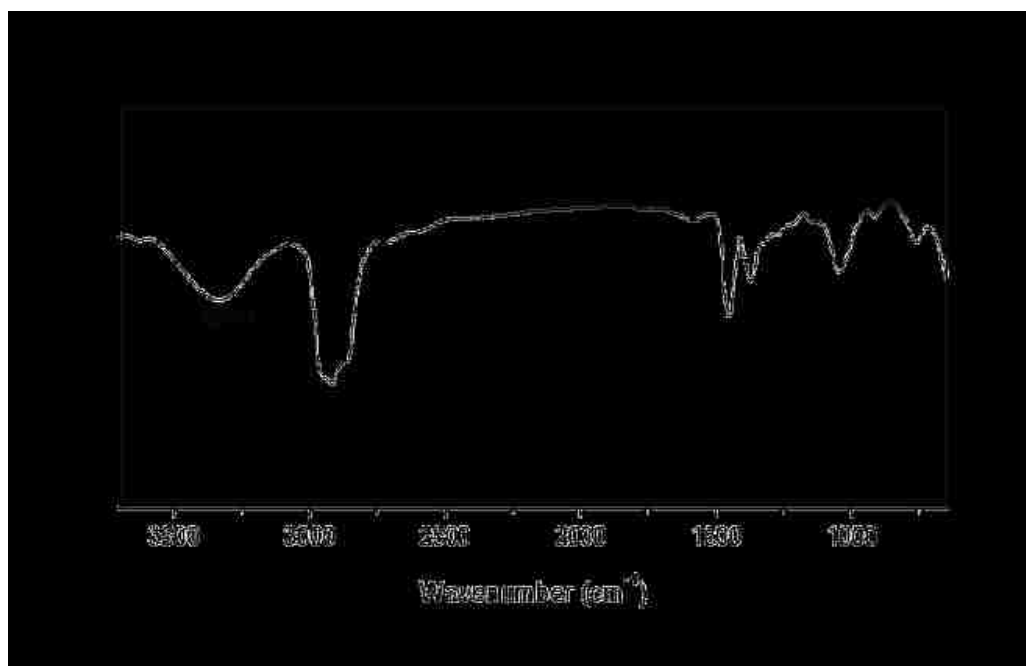


Figure 4.4. FT-IR spectrum of PB-OH (11.0 mol % OH, Entry 6 of Table 4.1).

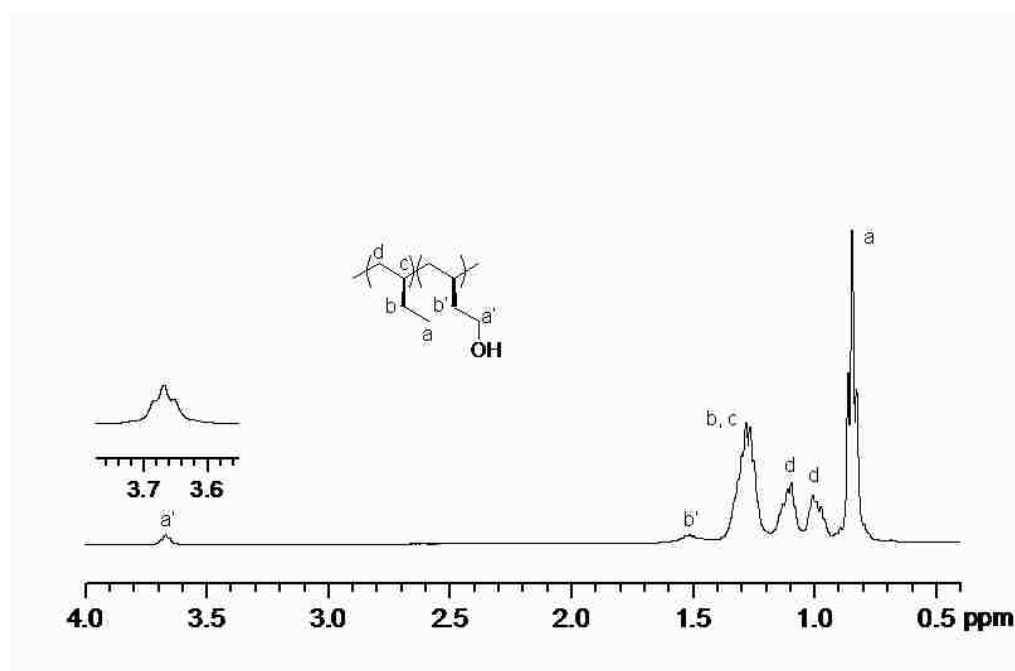


Figure 4.5. ¹H NMR spectrum of PB-OH (Entry 4 of Table 4.1; 10 mg/mL in CDCl₃).

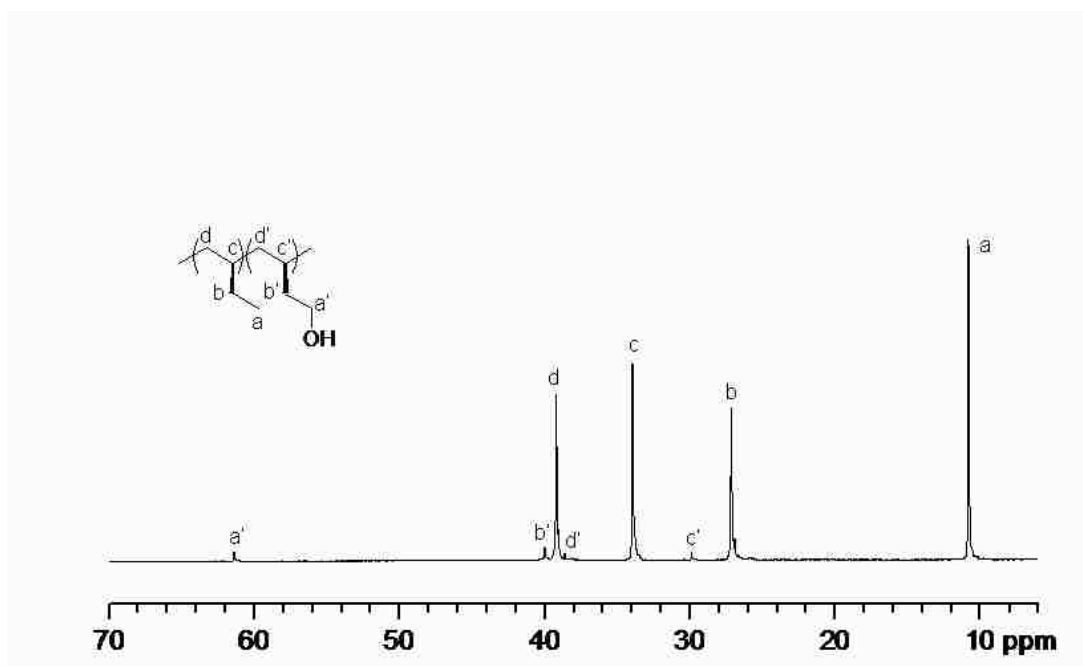


Figure 4.6. ^{13}C NMR spectrum of PB-OH (Entry 4 of Table 4.1; 30 mg/mL in CDCl_3).

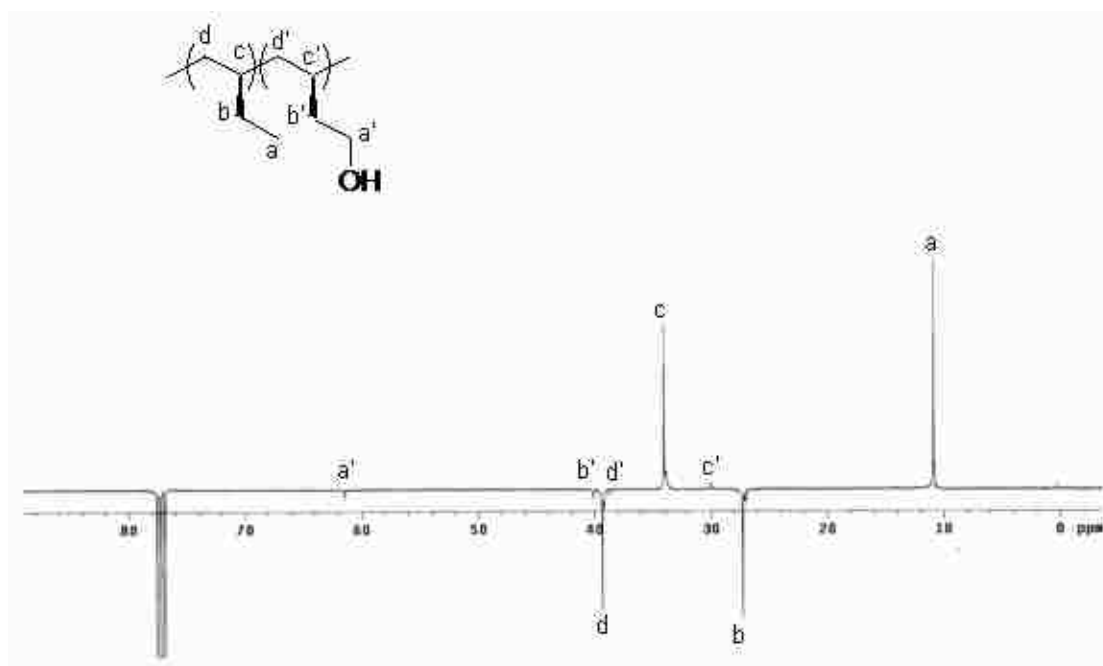


Figure 4.7. ^{13}C APT NMR spectrum of PB-OH (Entry 4 of Table 4.1 in CDCl_3).

The relative intensities of the triplet resonance of $-CH_2OH$ at 3.67 ppm and the triplet resonance of $-CH_3$ at 0.85 ppm in the 1H NMR spectrum of PB-OH allowed the calculation of the mol % of $-CH_2OH$ group in the polymer and their values are provided in Table 4.1. With increasing amounts of $B_2(pin)_2$ added relative to the polymer repeating unit in the C-H borylation, the intensity of the resonance increases, indicating that more of the B(pin) group was incorporated into the polymer. Based on assumption that all of the $-CH_2B(pin)$ groups of PB-B(pin) were converted to $-CH_2OH$ groups of PB-OH without deborylation or over-oxidation, we determined the percentage of $-CH_2OH$ group relative to the added $B_2(pin)_2$ as the efficiency of the C-H bond functionalization, which is included in Table 4.1.

The relationship of the ratio of $B_2(pin)_2$ to the polymer repeating unit in the borylation condition and the concentration of functionalized side chain in PB-OH was studied using 5 mol % of $Cp^*Rh(\eta^4-C_6Me_6)$ as the catalyst. Although the relationship of the ratio and hydroxymethyl group concentration was nonlinear, increasing the ratio generally resulted in more functionalized side chains of the polymer (Table 4.1). Because the terminal methyl group of the side chain of PB is sterically less hindered than that of isotactic polypropylene, both the maximum mol % of hydroxymethyl group (i.e., 19 mol %) and the efficiency of C-H functionalization of PB-OH were substantially higher than those of crystalline hydroxy-functionalized isotactic polypropylene, where the maximum concentration of hydroxy-functionalized methyl side chain was ~1 mol %.¹⁰⁵

We also attempted C-H borylation of PB using pinacolborane as a boron reagent. It resulted in a significantly lower concentration of functionalized side chain (i.e., ~1 mol % of $-CH_2OH$ group in the functionalized polymer) under the experimental conditions.

Table 4.1. Regioselective C–H functionalization of isotactic poly(1-butene) with bis(pinacolato)diboron^a.

Entry	Ratio ^b	PB–B(pin)	PB–OH	PB–OH	Effic. (%) ^e	PB–OH
		$M_n \times 10^{-3}$ (PDI) ^c	$M_n \times 10^{-3}$ (PDI) ^c	OH mol % ^d		Contact Angle ^f
1	0.02	51.5 (5.6)	55.0 (5.0)	1.8	90	104.4°
2	0.03	53.9 (5.1)	61.9 (5.6)	2.7	90	102.7°
3	0.05	58.7 (4.7)	61.6 (5.3)	3.5	70	102.0°
4	0.07	64.9 (5.9)	63.1 (5.4)	4.6	66	100.5°
5	0.15	70.2 (5.9)	69.0 (5.6)	7.7	51	100.4°
6	0.03	68.9 (5.3)	68.9 (5.6)	11.0	37	93.9°
7	0.45	73.0 (4.6)	74.4 (5.9)	15.3	34	92.2°
8	0.60	75.4 (3.7)	77.6 (5.9)	18.6	31	90.9°

^a Starting material: isotactic poly(1-butene) (PB) ($M_n = 51.6$ kg/mol, PDI = 4.9). ^b Initial ratio of bis(pinacolato)diboron [B₂(pin)₂]/polymer repeating unit. ^c M_n in kg/mol and PDI measured using size exclusion chromatography at 40 °C relative to polystyrene standards. THF was used as eluent. ^d Mol % of –CH₂OH relative to the terminal methyl group of the side chains of PB–OH. ^e Efficiency of functionalization = the percentage of –CH₂OH groups in the final polymer relative to the B₂(pin)₂ added. ^f Contact angles of other polymers: PB (105.7°), 6.4% *t*BA-grafted PB-*g*-*Pt*BA (100.8°), 6% acrylic acid-grafted PB-*g*-PAA (96.9°).

When a higher-molecular weight isotactic poly(1-butene) (*h*PB) ($M_w = \sim 570$ kg/mol by GPC in Aldrich[®]) was subjected to the same condition of the C–H functionalization, it generated similar concentrations of hydroxy groups in the side chains to those of the lower-molecular-weight isotactic poly(1-butene) (PB; $M_n = 51.6$ kg/mol, PDI = 4.9) (see Tables 4.1 and 4.2). Since *h*PB showed much limited solubility in the eluent of SEC, (i.e.

THF), molecular weight properties of *hPB* and functionalized *hPB* [*hPB*-B(pin) and *hPB*-OH] were not studied.

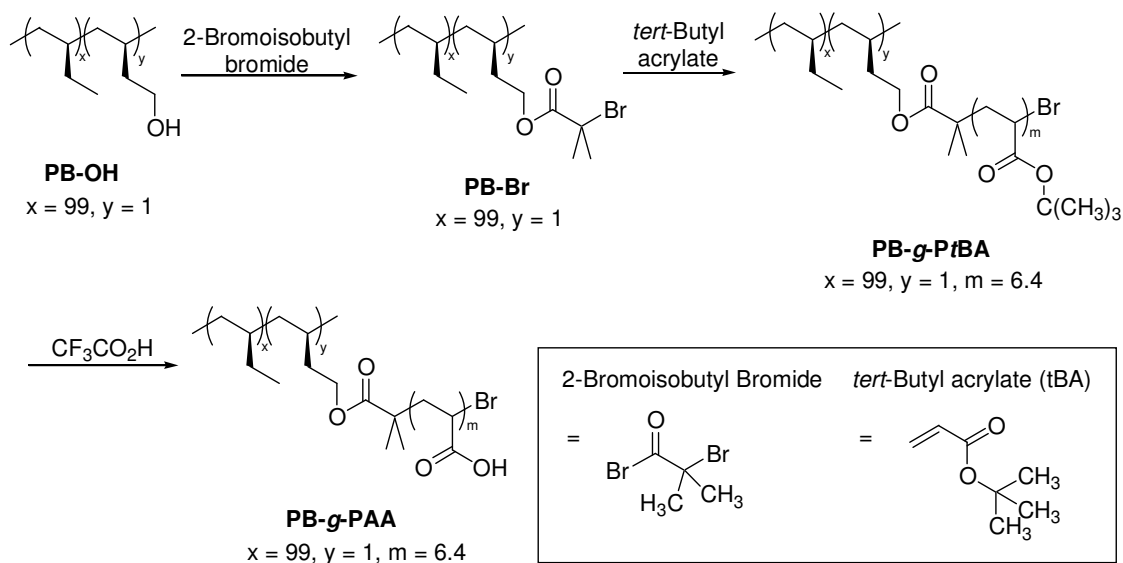
Table 4.2. Regioselective C–H functionalization of higher-molecular-weight isotactic poly(1-butene) (*hPB*) with bis(pinacolato)diboron^a.

Entry	Ratio ^b	PB–OH		Effic. (%) ^d
		OH mol % ^c		
1	0.02	0.7		35
2	0.03	2.1		70
3	0.05	3.7		74
4	0.07	4.4		63
5	0.15	6.7		45
6	0.03	11.4		38

^a Starting material (*hPB*), isotactic poly(1-butene): $M_w = \sim 580$ kg/mol in Aldrich[®]. ^b Initial ratio of B₂(pin)₂/repeating units. ^c Mol % of CH₂OH of *hPB*-OH relative to methyl side chains. ^d Efficiency of functionalization [the percentage of –CH₂OH groups in the final polymer relative to the B₂(pin)₂ added].

4.3.2. Macroinitiator of Isotactic Poly(1-butene): PB-Br

The synthetic procedure of isotactic poly(1-butene) macroinitiator (PB–Br) using ~1 mol % hydroxy-functionalized PB–OH (Table 4.1, entry 1) is shown in Scheme 4.2.



Scheme 4.2. Preparation of macroinitiator (PB-Br), PB-g-PtBA, and PB-g-PAA.

The esterification of the primary alcohol of PB-OH with 2-bromoisobutyl bromide gave PB-Br, which could be used as a macroinitiator for the graft polymerization of a polar vinyl monomer. To remove HBr by-product from the reaction, triethylamine was added and the resulting triethylamine hydrobromide was removed via filtration. The ^1H NMR spectrum of PB-Br showed a triplet at 4.20 ppm and a singlet at 1.93 ppm corresponding to $-\text{CH}_2\text{CH}_2\text{OC}(=\text{O})-$ and $-\text{C}(\text{CH}_3)_2\text{Br}$, respectively (Figure 4.8). Their integral ratio was approximately 1:3, which was consistent with the structure. The ^1H NMR spectrum also showed complete disappearance of the triplet at 3.67 ppm, confirming the absence of unreacted $-\text{CH}_2\text{OH}$ from PB-OH. The relative intensities of the triplet resonance of the $-\text{CH}_2\text{CH}_2\text{OC}(=\text{O})$ at 4.20 ppm and the triplet resonance of $-\text{CH}_3$ at 0.85 ppm in the ^1H NMR spectrum of PB-Br indicated that ~1 mol % of the a bromoester group is attached to the polymer side chain. The ^{13}C NMR spectrum of PB-Br showed new resonances at 31.0 ppm for the two methyl carbons of $-\text{CH}_2$

OC(=O)C(CH₃)₂Br, at 55.9 ppm for the alpha carbon of -CH₂OC(=O)C(CH₃)₂Br, at 64.5 ppm for the methylene carbon of -CH₂OC(=O)C(CH₃)₂Br, and at 171.9 ppm for the carbonyl carbon of -CH₂OC(=O)C(CH₃)₂Br (Figure 4.9).

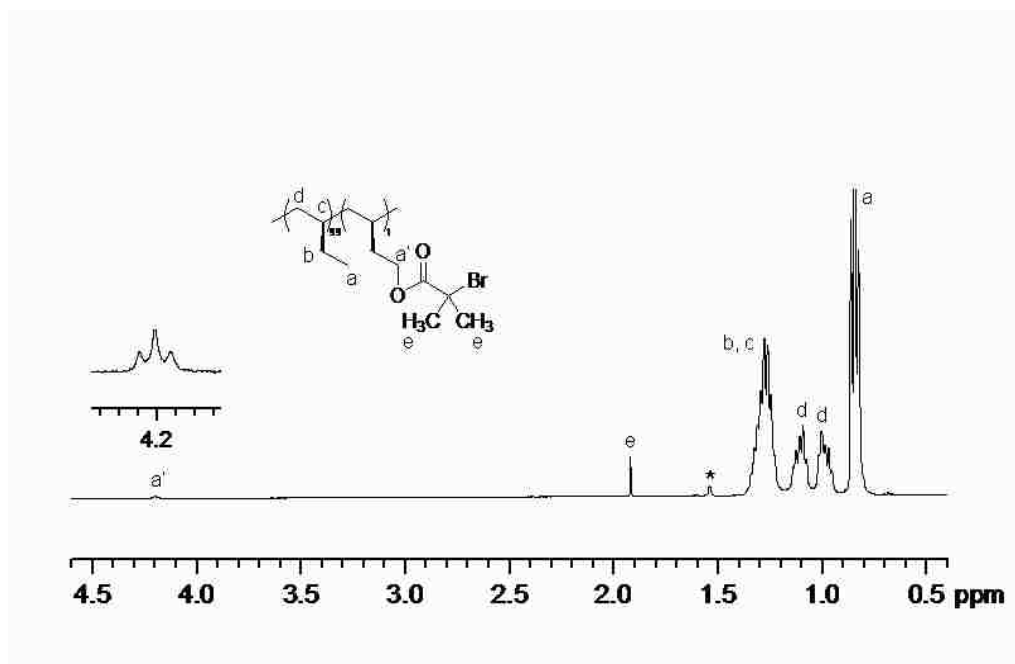


Figure 4.8. ¹H NMR spectrum of PB-Br (from Entry 1 of Table 4.1).

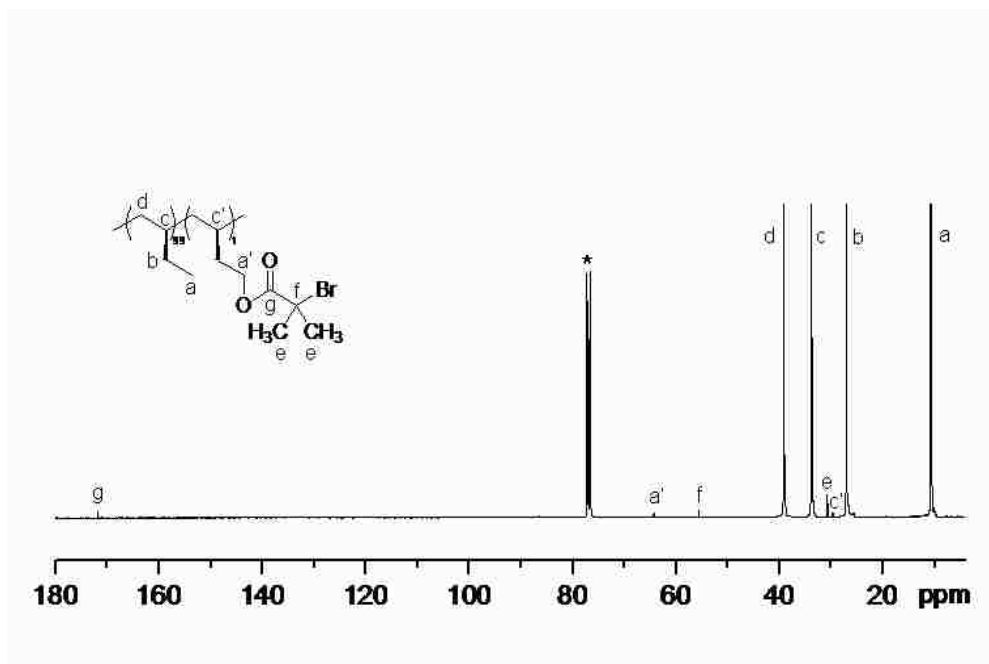


Figure 4.9. ^{13}C NMR spectrum of PB-Br (from Entry 1 of Table 4.1).

4.3.3. Graft Copolymer PB-*g*-PtBA

ATRP of *t*BA from the macroinitiator PB-Br was conducted to prepare a polar block-grafted polyolefin, PB-*g*-PtBA, using Cu(I)Br and N,N,N',N'',N'''-pentamethyldiethylenetriamine (PMDETA) at 90 °C in toluene (Scheme 4.2). When we screened various solvents and reaction times to optimization of ATRP condition, we found that toluene was the most effective solvent showing higher activity than other solvents such as *o*-xylene and anisole. Increasing the graft polymerization time from 10 to 20 h in toluene did not result in significant improvement in the graft chain length. The FT-IR spectrum of PB-*g*-PtBA showed a new absorption at 1710 cm^{-1} , which corresponded to the C=O stretching of the ester group of the *t*BA unit (Figure 4.10). The ^1H NMR spectrum of the polymer displayed a resonance at 1.46 ppm for the methyl protons of the tertiary butoxy group, $-\text{OC}(\text{CH}_3)_3$ (Figure 4.11).

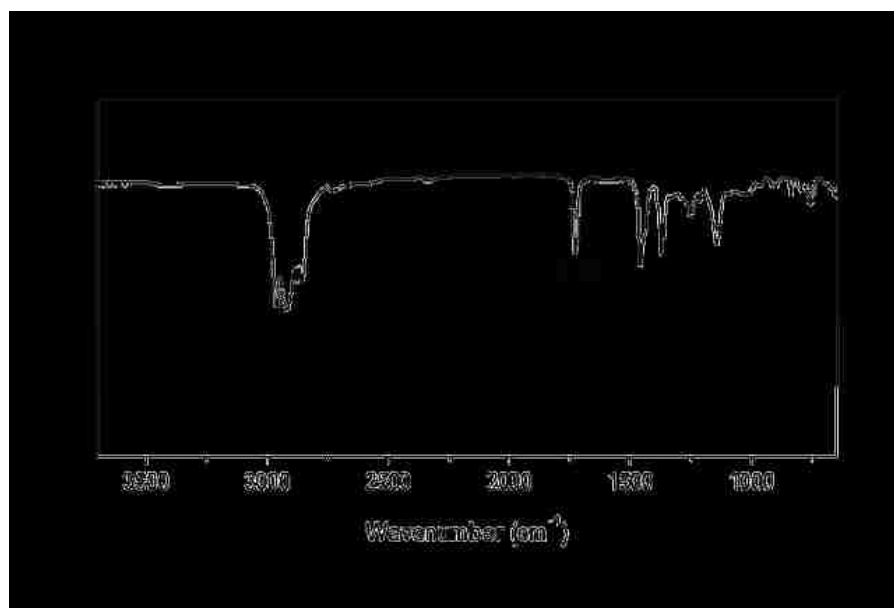


Figure 4.10. FT-IR spectrum of PB-g-PtBA (6.4 mol % PtBA, Entry 6 of Table 4.3).

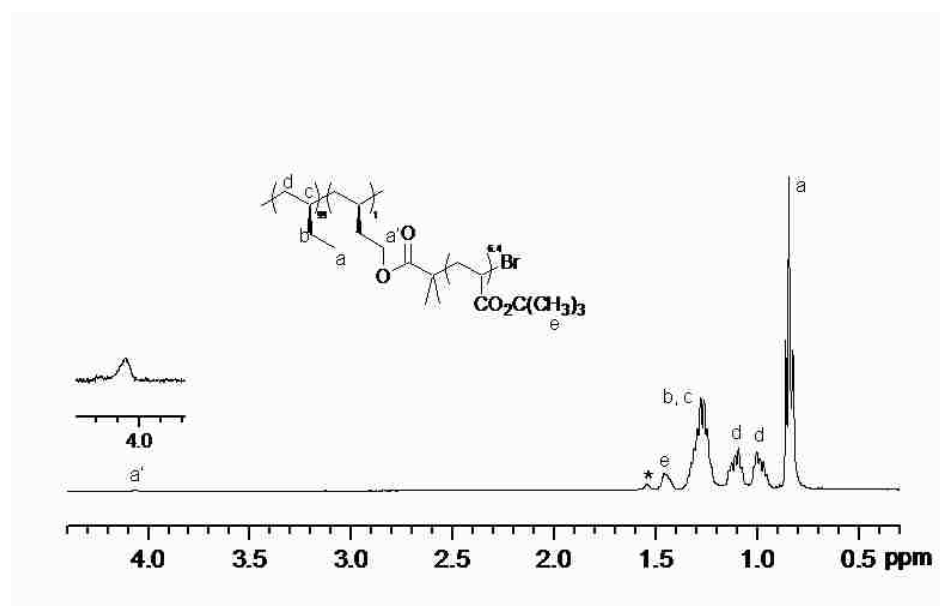


Figure 4.11. ^1H NMR spectrum of PB-g-PtBA (6.4 mol % PtBA, Entry 6 of Table 4.3).

*Resonance from H_2O .

It was found that the mol % of PtBA blocks in the graft copolymers ranged from 2.4 to 6.4 mol % based on the relative intensity ratio of the tertiary butoxy group resonance at 1.46 ppm to the resonance of the terminal methyl group of side chain in the PB segment at 0.85 ppm. The mol % of the polar block in the graft copolymer can be controlled by changing the amount of *t*BA relative to the bromine concentration of the macroinitiator (Table 4.3, Entries 4–6). Because the conversion of *t*BA was quite low under the ATRP condition and we were interested in preparation of a low concentration of polar block functionalized polyolefins that preserve good properties of the unfunctionalized polymer, we used the 6.4 mol % PB-*g*-PtBA (Entry 6 of Table 4.3) for the next hydrolysis reaction.

Table 4.3. Analytical results of poly(1-butene)-*graft*-poly(*t*-butyl acrylate)s and their precursor polymers.

Entry	Polymer ^a	Functional Group (mol %) ^b	$M_n \times 10^{-3}$ (PDI) ^c
1	PB	None	51.6 (4.9)
2	PB–OH	–OH (1%)	55.0 (5.0)
3	PB–Br	–OC(=O)C(CH ₃) ₂ Br (1%)	57.7 (4.6)
4 ^d	PB- <i>g</i> -PtBA	–CH ₂ CH(CO ₂ <i>t</i> -Bu)– (2.4%)	– ^e
5 ^f	PB- <i>g</i> -PtBA	–CH ₂ CH(CO ₂ <i>t</i> -Bu)– (4.0%)	– ^e
6 ^g	PB- <i>g</i> -PtBA	–CH ₂ CH(CO ₂ <i>t</i> -Bu)– (6.4%)	69.5 (5.2)

^a Graft polymerization condition: toluene (3.5 g); initiator = poly(1-butene) macroinitiator PB–Br (50 mg, 1 mol % Br); temperature = 90 °C; time = 10 h. ^b Functional group incorporated into the side chain of isotactic PB. Mol % of the functional group is based on calculation from ¹H NMR spectrum. ^c M_n in kg/mol and PDI measured using SEC with THF as eluent at 40 °C. ^d Molar ratio of *t*BA/Br = 50. ^e Not measured. ^f Molar ratio of *t*BA/Br = 100. ^g Molar ratio of *t*BA/Br = 150.

4.3.4. Amphiphilic Graft Copolymer PB-*g*-PAA

An amphiphilic graft copolymer of the polyolefin, PB-*g*-PAA, was synthesized from the hydrolysis of the *tert*-butoxy ester group in PB-*g*-PtBA (Scheme 4.2). The amphiphilic graft copolymer consisted of a nonpolar PB block at the main chain and polar poly(acrylic acid) block at the side chains. The hydrolysis was conducted in dichloromethane at room temperature, and the resulting PB-*g*-PAA was precipitated from the reaction mixture due to the solubility differences. The carboxylic acid-containing polymer was insoluble in CHCl₃, methanol and toluene but was soluble in THF. The FT-IR spectrum of PB-*g*-PAA showed a C=O stretching peak at 1730 cm⁻¹ corresponding to the carbonyl group of the carboxylic acid (Figure 4.12). The ¹H NMR spectrum of PB-*g*-PAA in THF-*d*₈ showed a new deshielded resonance at 10.9 ppm from the proton of the carboxylic acid group (Figure 4.13). The relative intensities of the singlet resonance of the -CO₂H at 10.9 ppm and the triplet resonance of -CH₃ at 0.88 ppm in the ¹H NMR spectrum of the graft copolymer indicated the presence of ~6 mol % of the carboxylic acid group in the polymer side chain, which indicates the hydrolysis reaction did not result in degrafting of PtBA blocks. The absence of the three methyl groups of *t*-butoxy ester at 1.46 ppm in the ¹H NMR spectrum suggested that the ester group in the polymer was completely hydrolyzed.

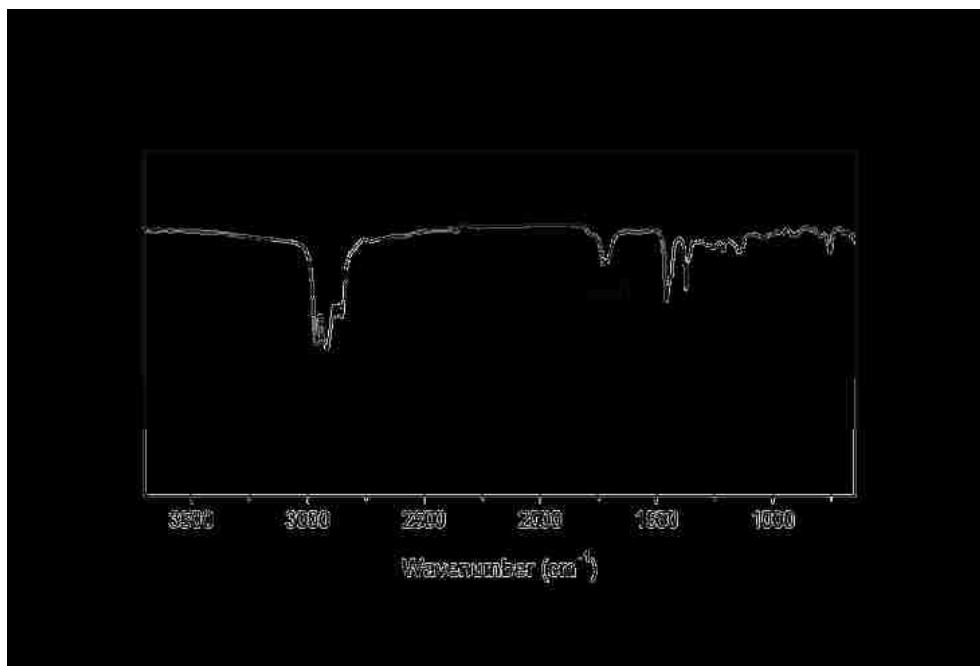


Figure 4.12. FT-IR spectrum of PB-g-PAA (6.0 mol % PAA).

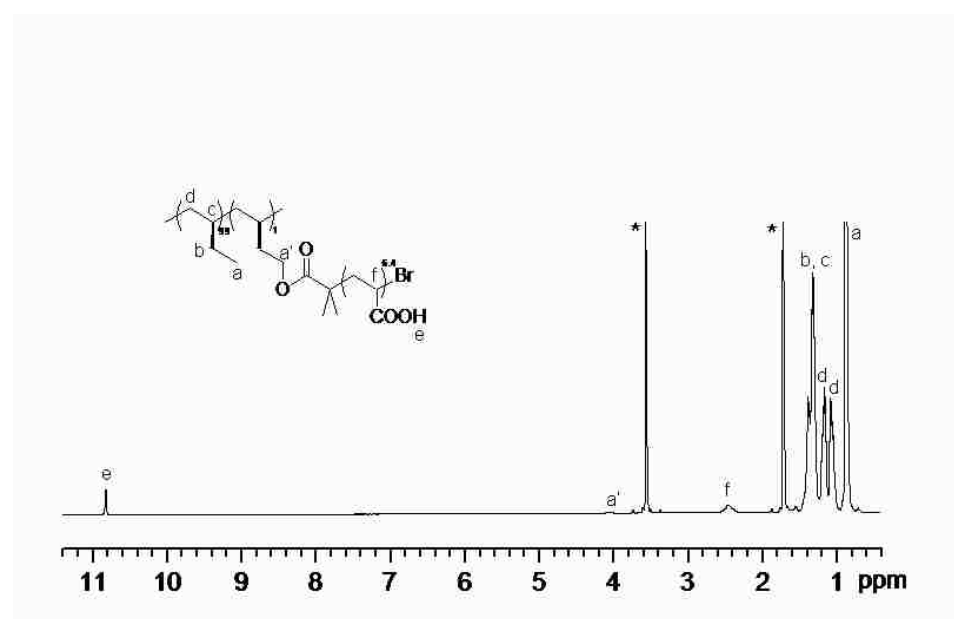


Figure 4.13. ^1H NMR spectrum of PB-g-PAA (6.4 mol % PAA) in $\text{THF-}d_8$. *Resonance from solvents.

4.3.5. Size Exclusion Chromatography

M_n and PDI of PB–B(pin) and PB–OH were investigated using size exclusion chromatography (SEC) to see whether their molecular weight properties changed as a result of the functionalization process. In contrast to typical postfunctionalization of polyolefin via a free radical method, the sequence of C–H borylation and oxidation did not change M_n and PDI significantly from those of the starting parent polymer (PB: $M_n = 51.6$ kg/mol, PDI = 4.9), indicating that these reactions underwent without significant chain scission or coupling between polymer chains (Table 4.1; Figure 4.14). M_n and PDI of PB–Br measured using SEC with THF as the eluent were 57.7 kg/mol and 4.6, respectively, which were again close to those of PB ($M_n = 51.6$ kg/mol; PDI = 4.9) (Figure 4.14). Since the PB block was assumed to contain an average of 921 repeating units (i.e., degree of polymerization = 921) based on the SEC analysis of PB ($M_n = 51.6$ kg/mol; PDI = 4.9), the average degree of polymerization and M_n of the combined PtBA segment in the longest copolymer (Entry 6 of Table 4.3) were calculated to be 63 and 8.1 kg/mol, respectively. The combination of the M_n of PB–Br (57.7 kg/mol measured using SEC analysis) and the M_n of combined PtBA segments (8.1 kg/mol estimated using ^1H NMR spectrum) gives the estimated M_n of PB-*g*-PtBA as 65.8 kg/mol. An SEC trace of the graft copolymer also revealed that the synthesized copolymer had a slightly higher average molecular weight than that of the macroinitiator while maintaining a similar molecular weight distribution ($M_n = 69.5$ kg/mol; PDI = 5.2; see Figure 4.14e; Entry 6 of Table 4.3). Although PB-*g*-PAA was soluble in THF, it did not provide a reasonable signal on SEC measurement possibly owing to the strong interaction between column packing material and the polar group in the polymer.

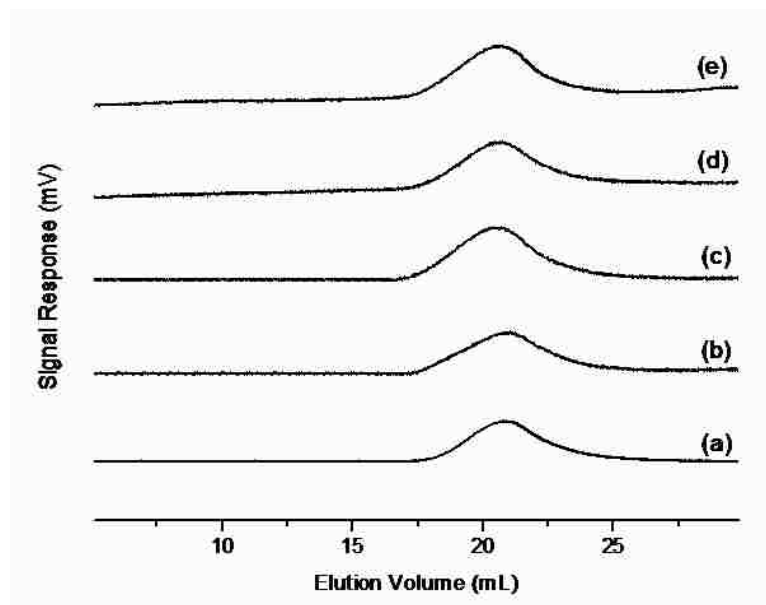


Figure 4.14. Size exclusion chromatography [1.0 mg/ mL THF] for (a) PB [$M_n = 51.6$ kg/mol, PDI = 4.9], (b) PB-B(pin) (Entry 5 of Table 4.1) [$M_n = 70.2$ kg/mol, PDI = 5.9], (c) PB-OH (Entry 5 of Table 4.1) [$M_n = 69.0$ kg/mol, PDI = 5.6], (d) PB-Br (Entry 3 of Table 4.3) [$M_n = 57.7$ kg/mol, PDI = 4.6], (e) PB-*g*-PtBA (Entry 6 of Table 4.3) [$M_n = 69.5$ kg/mol, PDI = 5.2]. M_n relative to polystyrene standards.

4.3.6. Thermal Properties

Thermal properties of unfunctionalized PB, PB-OH with different concentrations of hydroxy group, PB-Br, and the graft polymers (PB-*g*-PtBA and PB-*g*-PAA) were investigated using differential scanning calorimetry (DSC) (Figures 4.15 and 4.16). Based on the data shown in Table 4.1, we demonstrated that the rhodium-catalyzed C-H borylation and subsequent oxidation process can convert a fraction of the terminal methyl group of the polymer side chain selectively to a hydroxymethyl group without altering the structure or the chain length of the polymer main chain. Thus, this method can, in principle, generate a functionalized polyolefin material that still preserves the physical

properties of starting material, such as tacticity, molecular weight, and crystallinity. The unfunctionalized PB has a T_m of 115 °C and a T_g of -20 °C (Figure 4.15a). Up to 5 mol % of the polymer side chain contained hydroxy group, the PB-OH samples showed almost the same T_m of PB with a slightly decreased enthalpy of change in DSC data (Figure 4.15b-e) and had little effect on crystallinity. When more than 7 mol % of the polymer side chain contains hydroxy group, however, the PB-OH materials display an endothermic peak with a lower temperature and a sharply decreased enthalpy of change (Figure 4.15f-g) because the higher concentration of hydroxy group starts to interfere with the crystallization process of the polymer chain significantly.

Thermal properties of unfunctionalized PB, PB-OH with different concentrations of hydroxy group, PB-Br, and the graft polymers (PB-*g*-PtBA and PB-*g*-PAA) were investigated using differential scanning calorimetry (DSC) (Figures 4.15 and 4.16). Based on the data shown in Table 4.1, we demonstrated that the rhodium-catalyzed C-H borylation and subsequent oxidation process can convert a fraction of the terminal methyl group of the polymer side chain selectively to a hydroxymethyl group without altering the structure or the chain length of the polymer main chain. Thus, this method can, in principle, generate a functionalized polyolefin material that still preserves the physical properties of starting material, such as tacticity, molecular weight, and crystallinity. The unfunctionalized PB has a T_m of 115 °C and a T_g of -20 °C (Figure 4.15a). Up to 5 mol % of the polymer side chain contained hydroxy group, the PB-OH samples showed almost the same T_m of PB with a slightly decreased enthalpy of change in DSC data (Figure 4.15b-e) and had little effect on crystallinity. When more than 7 mol % of the polymer side chain contains hydroxy group, however, the PB-OH materials display an

endothermic peak with a lower temperature and a sharply decreased enthalpy of change (Figure 4.15f-g) because the higher concentration of hydroxy group starts to interfere with the crystallization process of the polymer chain significantly.

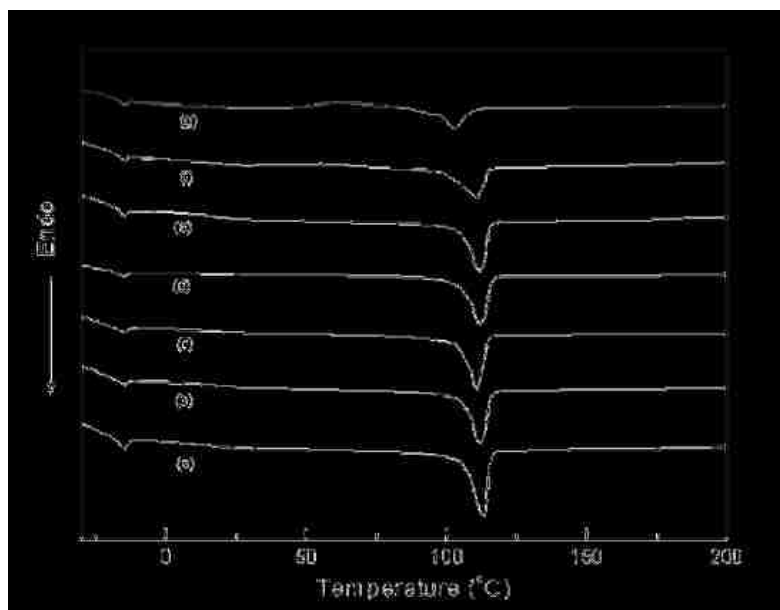


Figure 4.15. DSC scans of (a) PB, (b) PB–OH (1.4 mol % OH), (c) PB–OH (2.7 mol % OH), (d) PB–OH (3.5 mol % OH), (e) PB–OH (4.6 mol % OH), (f) PB–OH (7.7 mol % OH), and (g) PB–OH (11 mol % OH).

In the case of PB–Br, even though the concentration of functionalized side chain is very low (~1 mol %), the macroinitiator shows a slightly reduced melting point (i.e., 100 °C) owing to the bulky size of the α -bromoester group in the side chain (Figure 4.16c). After graft polymerization of *t*BA, the T_m of the graft copolymer shifted to a lower temperature because the relatively short poly(*tert*-butyl acrylate) block in the side chain of the graft copolymer suppressed the crystallization of isotactic PB main chain instead of forming a separate phase (Figure 4.16d). A similar melting point depression was

observed during DSC analysis of PB-g-PAA (Figure 4.16e).

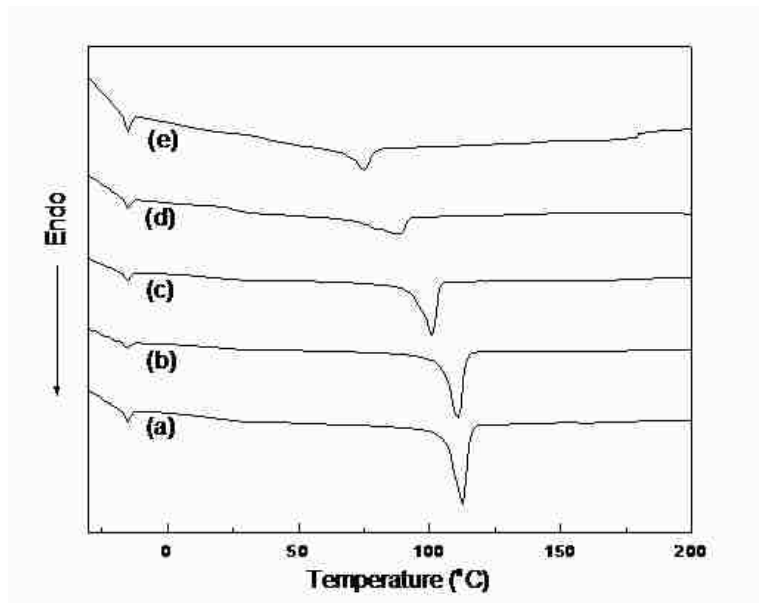


Figure 4.16. DSC scans of (a) PB, (b) PB-OH (1 mol % OH), (c) PB-Br (1 mol % Br), (d) PB-*g*-*Pt*BA (6.4 mol % *Pt*BA), and (e) PB-*g*-PAA (6 mol % PAA).

4.3.7. Water Contact Angles

As discussed in the Introduction, one of the major drawbacks of polyolefins is low surface energy, which can be indirectly studied by measuring water contact angles of the polymers. Contact angle measurement of water on the surface of functionalized PB on glass plate is summarized in Table 4.1 and plotted in Figure 4.17. The unfunctionalized PB has a contact angle of 105.6°. As shown in Figure 4.17, the water contact angles of PB-OHs were lower than that of PB, and the more incorporation of hydroxy group into the polymer side chain resulted in a systematic decrease of contact angle in a series of PB-OH. This result indicates that the hydroxy functionalization led to an increase of hydrophilicity of the polymer. The 6.4 mol % *t*BA-grafted PB-*g*-*Pt*BA has a contact

angle of 100.7° , which is smaller than that of PB, 105.6° . Compared with the contact angle of PB, the 6 mol % acrylic acid-grafted PB-g-PAA exhibited a much smaller contact angle (96.8°), also indicating the creation of a more hydrophilic surface in the polymer.

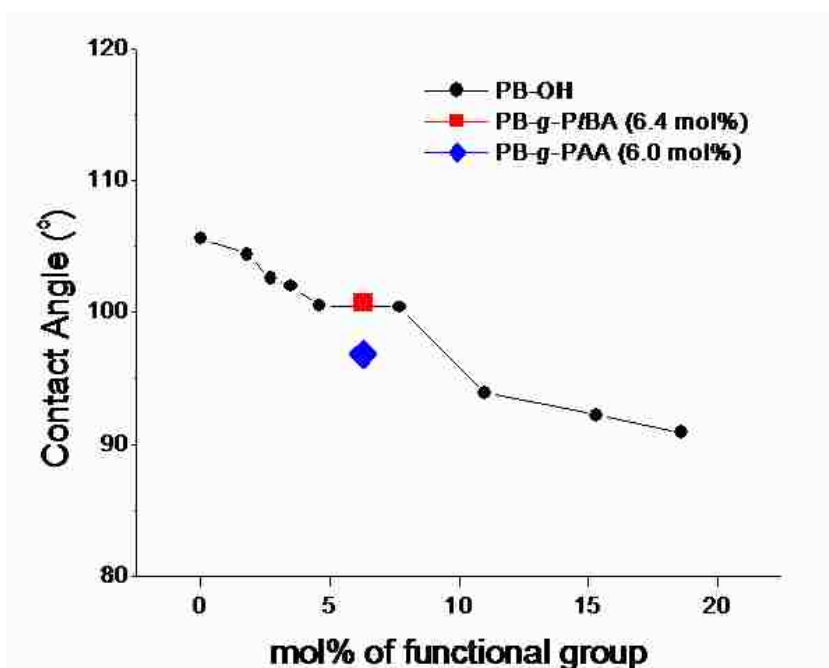
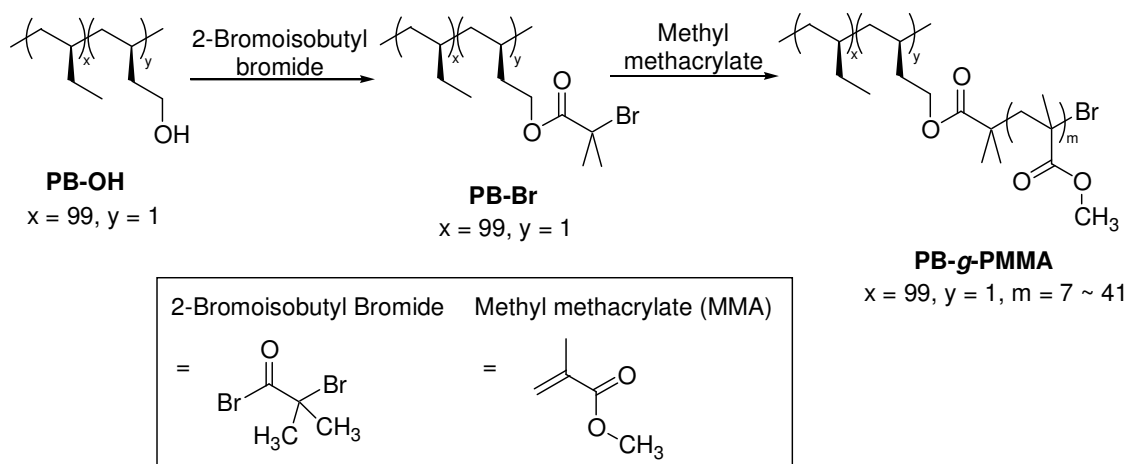


Figure 4.17. Water contact angles of a series of hydroxy-functionalized isotactic poly(1-butene)s and graft copolymers.

4.3.8. Graft Copolymer PB-g-PMMA

ATRP of MMA from the macroinitiator was also conducted to prepare poly(methyl methacrylate)-grafted polyolefin, PB-g-PMMA. As shown in Scheme 4.3, the same polymerization condition of ATRP of PB-g-PtBA (CuBr and PMDETA at 90°C in toluene) was used.



Scheme 4.3. Preparation of a graft copolymer of isotactic poly(1-butene), PB-g-PMMA.

The FT-IR spectrum of PB-g-PMMA confirmed grafting of MMA units into PB. The C=O stretching of PMMA block was clearly visible at 1740 cm^{-1} (Figure 4.18). As more MMA was introduced into the graft copolymer, the intensity of the C=O stretching of the PMMA block was increased in the FT-IR spectra of the graft copolymer.

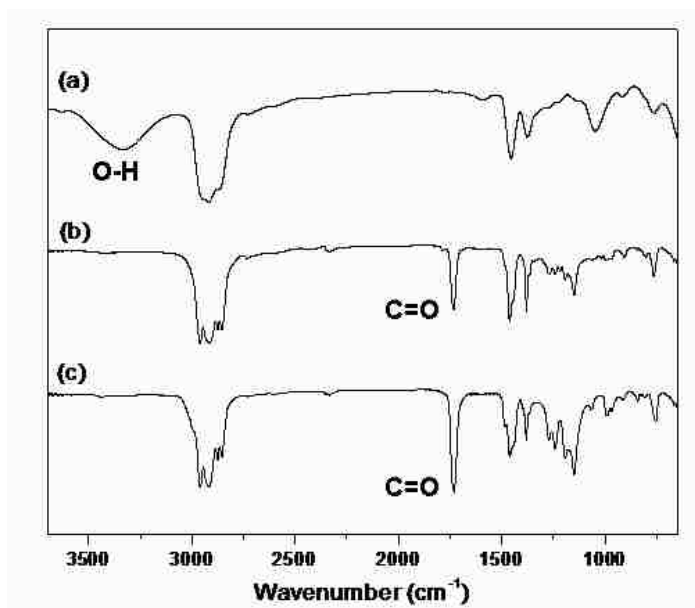


Figure 4.18. FT-IR spectra of PB-OH (a) poly(1-butene)-*graft*-poly(methyl methacrylate) copolymers containing (b) 6, and (c) 29 mol % PMMA content.

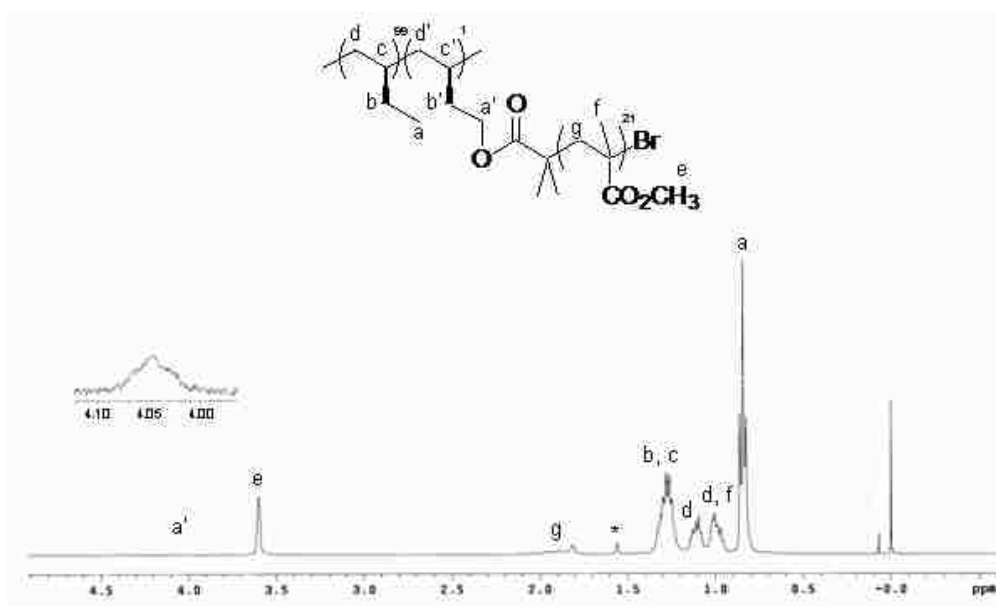


Figure 4.19. ^1H NMR spectrum of PB-*g*-PMMA (21 mol % PMMA, Entry 4 of Table 4.4).

*Resonance from H_2O .

The ^1H NMR spectrum of PB-*g*-PMMA showed a distinct resonance at $\delta = 3.59$ for $-\text{OCH}_3$ of the PMMA block (Figure 4.19). As more MMA was introduced into the polymer, the intensity of the resonance from the PMMA block was increased. This change in the composition of PMMA block relative to PB main-chain in the graft copolymer as a result of different amounts of MMA addition is summarized in Table 4.3. Based on the relative intensity ratio of the methoxy resonance at 3.59 ppm to the resonance of the terminal methyl group of side chain in the PB segment at 0.85 ppm, it was concluded that the mol % of PMMA blocks in the graft copolymers could be controlled 6–29 mol % by changing the amount of MMA relative to bromine concentration of the macroinitiator.

Table 4.4. Analytical results of poly(1-butene)-*graft*-poly(methyl methacrylate)s and their precursor polymers^a.

Entry	Polymer ^b	Functional Group (mol %) ^b	$M_n \times 10^{-3}$ (PDI) ^c
1	PB	None	67.4 (3.5)
2	PB-Br	$-\text{OC}(=\text{O})\text{C}(\text{CH}_3)_2\text{Br}$ (1 mol %)	67.9 (4.0)
3 ^d	PB- <i>g</i> -PMMA	$-\text{CH}_2(\text{CH}_3)(\text{CO}_2\text{CH}_3)-$ (6.3 mol %)	90.7 (7.9)
4 ^e	PB- <i>g</i> -PMMA	$-\text{CH}_2(\text{CH}_3)(\text{CO}_2\text{CH}_3)-$ (21.1 mol %)	102.5 (10.5)
5 ^f	PB- <i>g</i> -PMMA	$-\text{CH}_2(\text{CH}_3)(\text{CO}_2\text{CH}_3)-$ (28.9 mol %)	102.2 (7.6)

^a Graft polymerization condition: toluene (3.5 g); initiator = poly(1-butene) macroinitiator PB-Br (50 mg, 1 mol % Br); temperature = 90 °C; time = 10 h. ^b Functional group incorporated into the side chain of isotactic poly(1-butene). Mol % of the functional group is based on calculation from ^1H NMR spectrum. ^c Number-average molecular weight (M_n) in kg/mol and polydispersity index (PDI, M_w/M_n) measured using high temperature SEC using 1,2,4-trichlorobenzene as eluent at 160 °C. ^d Molar ratio of MMA/Br = 50. ^e Molar ratio of MMA/Br = 150. ^f Molar ratio of MMA/Br = 200.

Because the PMMA-grafted copolymer exhibited much low solubility in THF, their M_n and PDI were obtained from high temperature SEC at 160 °C using 1,2,4-trichlorobenzene as eluent. To evaluate the effect of grafting on M_n and PDI of graft copolymers, the M_n values of PB and PB-Br were also obtained with high temperature SEC (Entries 1 and 2 of Table 4.4; 67.7 kg/mol and PDI = 3.5 for PB; 67.9 kg/mol and PDI = 4.0 for PB-Br) and they were found to be a little higher than those from SEC measured at 40 °C using THF as eluent (Entries 1 and 3 of Table 4.3; 51.6 kg/mol and PDI = 4.9 for PB; 57.7 kg/mol and PDI = 4.6 for PB-Br). The differences in M_n and PDI of PB and PB-Br are believed to derive from hydrodynamic volume change under the different SEC measurement conditions. Upon grafting, the PMMA graft copolymers showed higher M_n and broader PDIs than those of the macroinitiator (Entries 3–5 of Table 4.4). This broad molecular weight distribution of the graft copolymer was also confirmed in the SEC traces of PB-*g*-PMMA which showed bimodal distribution of molecular weight (Figure 4.20). Because ATRP reactivity of MMA is known to be much higher than that of *t*BA, it is believed that non-quantitative graft initiation of MMA that occurred at the macroinitiator resulted in fast growing of PMMA along the side chain while leaving some polymer chains un-grafted.

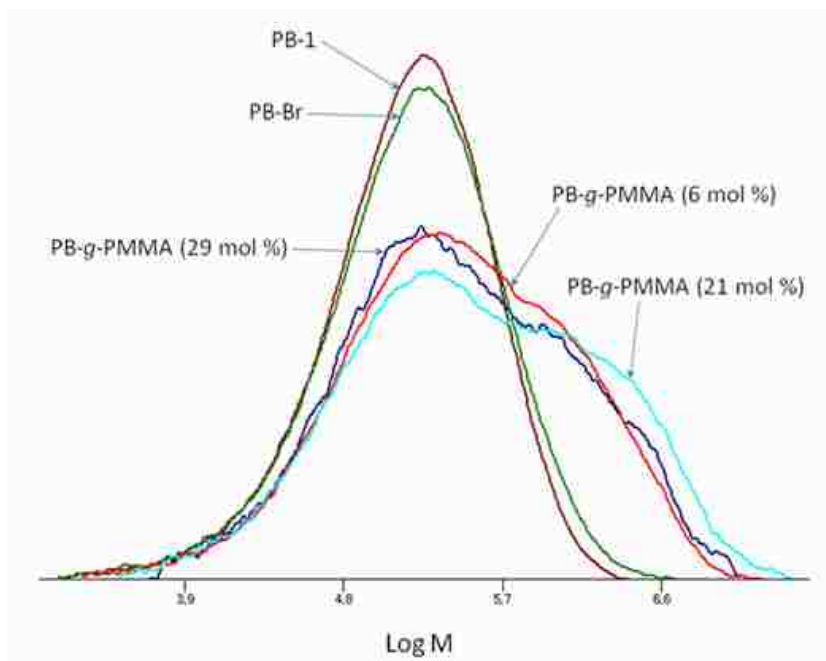


Figure 4.20. High-temperature size exclusion chromatography [1,2,4-trichlorobenzene at 160 °C] for PB, PB-Br, and PB-g-PMMA. M_n relative to polystyrene standards.

4.4. Experimental

4.4.1. General Comments

Hydrogen peroxide (30%), sodium hydroxide, tetrahydrofuran (THF), trifluoroacetic acid (TFA), triethylamine, 2-bromoisobutyl bromide, copper bromide, and PMDETA were purchased from commercial vendors (Sigma Aldrich Co., Alfa Aesar, and Acros) and used without further purification. The unfunctionalized isotactic poly(1-butene) with a number-average molecular weight (M_n) of 51.6 kg/mol and a polydispersity index (PDI, M_w/M_n) of 4.9, measured using size exclusion chromatography (SEC) with THF as the eluent, was purchased from Aldrich and used as received. $B_2(\text{pin})_2$ was donated by Frontier Scientific and used after recrystallization from hexane. $\text{Cp}^*\text{Rh}(\eta^4\text{-C}_6\text{Me}_6)$ was prepared according to literature methods.^{127,128} Cyclooctane and toluene were dried using

sodium and benzophenone, distilled under reduced pressure, and stored in a nitrogen-filled glove box. *t*BA (98% from Aldrich) was passed through a disposable alumina column (Sigma Aldrich Co.) to remove the inhibitor, dried over calcium chloride, and distilled under reduced pressure. ^1H NMR spectra were recorded using a 400 MHz Varian NMR spectrometer at room temperature. All chemical shifts were referenced to tetramethylsilane. The ^1H NMR samples were prepared at a concentration of 10 mg/mL by applying gentle heat to dissolve the polymer in deuterated NMR solvents. The OH mol % of PB-OH was determined based on the relative intensity of resonances of $-\text{CH}_2\text{OH}$ at 3.67 ppm and $-\text{CH}_3$ of the side chain at 0.85 ppm in the ^1H NMR spectrum (Table 4.1). SEC analysis of both unfunctionalized and functionalized polymers was conducted using a VISCOTEK chromatograph equipped with three Visco-GEL I series columns and a tetra detector array (UV/visible, low and right angle light scattering, refractive index, and viscometer) at 40 °C. The SEC traces of polymers displayed in Figure 4.14 were obtained from the signals of refractometer. THF was the mobile phase, and the flow rate was set at 1.0 mL/min. The instrument was calibrated using polystyrene standards. The unfunctionalized polymer PB was received as semicrystalline pellets and has a limited solubility in THF at room temperature. To decrease the crystallinity of PB and improve the solubility in THF for the SEC measurement, the following procedure was performed: One gram of the polymer was placed in a two neck round-bottom flask, and then the flask was evacuated and backfilled with nitrogen three times. Toluene (50 mL) was added to this flask and the mixture was refluxed at 110 °C under nitrogen for 30 min to dissolve all PB. The solution was then cooled to room temperature and poured into cold methanol (100 mL). The precipitate was filtered and dried under vacuum at 60 °C.

DSC measurement was conducted on a NETZSCH STA 449C under a helium atmosphere. The polymer samples were heated to 200 °C, held there for 1 min to avoid the influence of thermal history, cooled to -50 °C, held there for 1 min, and then reheated to 200 °C. The rates of heating and cooling were 10 °C/min. All DSC curves in Figures 4.15 and 4.16 were obtained from the second heating. The glass transition and melting temperatures (T_g and T_m) and enthalpy of change (ΔH_f) were obtained after calibration with high-purity indium and zinc standards. The static contact angle measurement of water on polymer film was carried using a contact angle goniometer (Dataphysics OCA15) at room temperature. To prepare a polymer film, the polymer was dissolved in a small amount of chloroform and was cast on a glass plate. After the solvent was slowly evaporated at room temperature, the polymer film was dried under vacuum at 50 °C. A droplet of pure water (10 μ L) was placed on the polymer film for 30 s, and the static contact angle was measured. Each reported contact angle value in Table 4.1 is the average of 10 measurements.

4.4.2. Synthesis of $(Cp^*RhCl_2)_2$

Rhodium (III) chloride hydrate (40% Rh, 500 mg, 1.94 mmol) and absolute methanol (15 mL) were placed in a round bottom flask fitted with a reflux condenser under nitrogen. 1,2,3,4,5-Pentamethylcyclopentadiene (317 mg, 2.33 mmol) was added using a syringe under a nitrogen flow. The mixture was gently refluxed for 20 h. The reaction mixture was allowed to cool to room temperature, and the dark brown precipitate was filtered. The collected reddish brown solid was washed with diethyl ether (3 \times 2 mL) and dried under vacuum (470 mg, Yield: 78%). 1H NMR (400 MHz, $CDCl_3$) δ = 1.65 (s, $-CH_3$). ^{13}C NMR (100 MHz, $CDCl_3$) δ = 9.7 (s, $-CH_3$), 94.4 (d, C_{arom}).

4.4.3. Synthesis of $[\text{Cp}^*\text{Rh}(\text{C}_6\text{Me}_6)](\text{PF}_6)_2$

$[\text{Cp}^*\text{RhCl}_2]_2$ (580 mg, 0.94 mmol) and hexamethylbenzene (679 mg, 4.45 mmol) were combined with trifluoroacetic acid (12 mL) in a nitrogen filled round bottom flask fitted with a reflux condenser. The mixture was refluxed for 14 h. Trifluoroacetic acid was evaporated using a rotary evaporator. Addition of water (30 mL) produced an off-white precipitate that was filtered and washed with water (3×15 mL). The filtrate solution was concentrated to ~ 20 mL using a rotary evaporator. The addition of ammonium hexafluorophosphate (1.03 g, 6.30 mmol) to the filtrate solution caused formation of an off-white precipitate that was filtered and washed with water (3×8 mL) and diethyl ether (3×8 mL). The solid was dried at 100°C under vacuum for 10 h (969 mg, Yield: 75%). The product was consumed to synthesize the final product, $\text{Cp}^*\text{Rh}(\eta^4\text{-C}_6\text{Me}_6)$, without further analysis.

4.4.4. Synthesis of $\text{Cp}^*\text{Rh}(\eta^4\text{-C}_6\text{Me}_6)$

$[\text{Cp}^*\text{Rh}(\text{C}_6\text{Me}_6)](\text{PF}_6)_2$ (969 mg, 1.40 mmol) and hexane (40 mL) were placed in a Schlenk flask in a nitrogen filled glove box. Cobaltocene (477 mg, 2.52 mmol) was added to the flask in the glove box, and the reaction mixture was stirred at room temperature for 14 h during which a yellow precipitate was formed. The solution was filtered through a short pack of celite inside the glove box, and the filtrate was evaporated under reduced pressure. The reddish-brown solid was dried at 60°C under vacuum (412 mg, Yield: 74 %). ^1H NMR (400 MHz, C_6D_6) $\delta = 1.27$ (s, CH_3 , 6H), 1.41 (s, CH_3 , 6H), 1.64 (s, CH_3 , 15H), 2.05 (s, CH_3 , 6H). ^{13}C NMR (100 MHz, C_6D_6) $\delta = 10.1, 14.5, 18.6, 64.8, 89.7, 93.0, 134.1$

4.4.5. Synthesis of Pinacol Boronic Ester-Functionalized Isotactic Poly(1-butene) [PB–B(pin)] (Table 4.1, Entry 5)

In a nitrogen-filled glove box, a mixture of PB (157 mg), B₂(pin)₂ (107 mg), Cp*Rh(η^4 -C₆Me₆) (8.4 mg, 5 mol % based on the amount of the boron reagent), cyclooctane (300 mg), and a magnetic stirring bar were placed into a vial and capped with a Teflon-lined septum. The vial was removed from the glove box and the reaction mixture was stirred in an oil bath at 150 °C for 24 h. The mixture was cooled to room temperature, diluted with toluene (20 mL), and filtered through a short plug of silica to remove the catalyst. The filtrate was concentrated using a rotary evaporation to ~5 mL, and cold methanol (20 mL) was added to precipitate the polymer as a white solid. The precipitated solid was filtered and dried under vacuum at 60 °C for 12 h. Yield: 158.0 mg (101% based on polymer weight). ¹H NMR (400 MHz, CDCl₃, ppm): 0.85 (t, 3H, CH₃ of the PB unit side chain), 1.01 and 1.10 (m, 2H, –CH₂– of the PB unit backbone), 1.24 (s, BOC(CH₃)₂), 1.27 (m, 3H, –CH– of the PB unit backbone and –CH₂– of the PB unit side chain). ¹³C NMR (100 MHz, CDCl₃, ppm): 10.8 (CH₃ of the PB unit side chain), 25.0 (BOC(CH₃)₂), 27.2 (–CH₂– of the PB unit side chain), 34.0 (–CH– of the PB unit backbone), 39.3 (–CH₂– of the PB unit backbone), 82.9 (BOC(CH₃)₂). ¹¹B NMR (128.3MHz, CDCl₃, ppm): 34.3 (–BOC(CH₃)₂)

4.4.6. Synthesis of Hydroxylated Isotactic Poly (1-butene) (PB–OH)

PB–B(pin) (100 mg) (Table 4.1, entry 4) was dissolved in THF (50 mL) in a 250-mL flask by applying gentle heat and then cooled to room temperature. A mixture of aqueous 3 N NaOH solution (1 mL) and 30% H₂O₂ (1 mL) was slowly added to the PB–B(pin) solution, and the solution was vigorously stirred at room temperature for 12 h. The

solution was concentrated using a rotary evaporator to approximately 3 mL, and a mixture of water/methanol (40 mL/10 mL) was added. The heterogeneous suspension was stirred for 20 min and filtered. The collected white solid was washed with methanol (3 × 5 mL), dissolved in toluene, and filtered. The filtrate was concentrated using a rotary evaporation to approximately 5 mL, and cold methanol (10 mL) was added to precipitate the polymer as a white solid. The precipitated solid was filtered and dried under vacuum at 60 °C for 12 h. Yield: 85.0 mg (85% based on polymer weight). ¹H NMR (400 MHz, CDCl₃, ppm): 0.85 (t, 3H, -CH₃ of the PB unit side chain), 1.01 and 1.10 (m, 2H, -CH₂- of the PB unit backbone), 1.27 (m, 3H, -CH- of the PB unit backbone and -CH₂- of the PB unit side chain), 1.52 (2H, -CH₂CH₂OH), 3.67 (t, 2H, -CH₂OH). ¹³C NMR (100 MHz, CDCl₃, ppm): 10.8 (-CH₃ of the PB unit side chain), 27.2 (-CH₂- of the PB unit side chain), 30.0 (-CH₂CH(CH₂CH₂OH)-), 34.0 (-CH- of the PB unit backbone), 38.7 (-CH₂CH(CH₂CH₂OH)-), 39.3 (-CH₂- of the PB unit backbone), 40.1 (-CH₂CH(CH₂CH₂OH)-), 61.4 (-CH₂OH). FT-IR (film) $\nu = 3333\text{ cm}^{-1}$ (O-H).

4.4.7. Synthesis of the Macroinitiator (PB-Br)

PB-OH (200 mg with 1.4 mol % OH; 5×10^{-2} mmol hydroxy group) was placed in a Schlenk flask equipped with a magnetic stirring bar, and the flask was evacuated and backfilled with nitrogen three times. Toluene (3 mL) was added to the flask, and the mixture was stirred at 90 °C for 20 min to dissolve the polymer. Triethylamine (70 μ L, 0.5 mmol) and 2-bromoisobutyryl bromide (62 μ L, 0.5 mmol) were added to the solution, and the reaction mixture was stirred at 90 °C for 8 h. After cooling the reaction mixture, additional toluene (15 mL) was added. The heterogeneous suspension was filtered. The dark brown filtrate was concentrated using a rotary evaporator to approximately 5 mL

and 2% HCl-acidified cold methanol (10 mL) was added to precipitate the polymer as a pale brown solid. The solid was collected via filtration, washed with methanol (3×10 mL), and dried under vacuum at 60 °C for 12 h. Yield: 200.0 mg (100% yield based on polymer weight). ^1H NMR (400 MHz, CDCl_3 , ppm): 0.85 (t, 3H, CH_3 of the PB unit side chain), 1.01 and 1.10 (m, 2H, $-\text{CH}_2-$ of the PB unit backbone), 1.27 (m, 3H, $-\text{CH}-$ of the PB unit backbone and $-\text{CH}_2-$ of the PB unit side chain), 1.93 (s, 6H, $-\text{OCOC}(\text{CH}_3)_2\text{Br}$), 4.20 (t, 2H, $-\text{CH}_2\text{CH}_2\text{OC}(=\text{O})-$). ^{13}C NMR (100 MHz, CDCl_3 , ppm): 10.8 (CH_3 of the PB unit side chain), 27.2 ($-\text{CH}_2-$ of the PB unit side chain), 30.0 ($-\text{CH}_2\text{CH}(\text{CH}_2\text{CH}_2\text{OC}(=\text{O}))-$), 31.0 ($-\text{C}(\text{CH}_3)_2\text{Br}$), 34.00 ($-\text{CH}-$ of the PB unit backbone), 39.3 ($-\text{CH}_2-$ of the PB unit backbone), 55.9 ($-\text{C}(\text{CH}_3)_2\text{Br}$), 64.5 ($-\text{CH}_2\text{CH}_2\text{OC}(=\text{O})-$), 171.9 ($-\text{CH}_2\text{CH}_2\text{OC}(=\text{O})-$). $M_n = 57.7$ kg/mol, PDI = 4.6 (SEC using THF as the eluent at 40 °C); $M_n = 67.9$ kg/mol, PDI = 4.0 (SEC using 1,2,4-trichlorobenzene at 160 °C).

4.4.8. Synthesis of PB-*g*-PtBA (Entry 6 in Table 3.2)

In a nitrogen-filled glove box, PB-Br (50.0 mg, 7.0×10^{-3} mmol Br concentration), toluene (2.1 g), and a magnetic stirring bar were placed in a 25-mL vial. The vial was removed from the glove box, and PB-Br was dissolved with gentle heating. A catalyst solution (1.7 mL) composed of Cu(I)Br (1.0 mg, 7.0×10^{-3} mmol), PMDETA (2.4 mg, 1.4×10^{-2} mmol), toluene (1.4 g), and *t*BA (134.6 mg, 1.05 mmol) was placed in a vial in the glove box and transferred to the vial containing the PB-Br solution. The mixture was stirred at room temperature for 5 min and at 90 °C for 10 h. After cooling the reaction mixture, toluene (15 mL) was added, and the solution was filtered through a short plug of celite to remove the metal catalyst. The filtrate was concentrated to approximately 3 mL using a rotary evaporator, and cold methanol (10 mL) was added to precipitate the

polymer as a white solid. The solid was filtered and dried under vacuum at 60 °C for 12 h. Yield: 48.0 mg (96% based on polymer weight). ¹H NMR (400 MHz, CDCl₃, ppm): 0.85 (t, 3H, CH₃ of the PB unit side chain), 1.01 and 1.10 (m, 2H, -CH₂- of the PB unit backbone), 1.28 (m, 3H, -CH- of the PB unit backbone and -CH₂- of the PB unit side chain), 1.46 (9H, -OC(CH₃)₃), 2.25 (1H, -CH₂CH(CO₂*t*-Bu)-), 4.07 (2H, -CH₂CH₂OC(=O)-). ¹³C NMR (100 MHz, CDCl₃, ppm): 10.8 (CH₃ of the PB unit side chain), 27.2 (-CH₂- of the PB unit side chain), 28.2 (-OC(CH₃)₃), 34.0 (-CH- of the PB unit backbone), 39.3 (-CH₂- of the PB unit backbone), 42.3 (-CH₂CH(CO₂*t*-Bu)-), 80.5 (-OC(CH₃)₃), 174.4 (-C(=O)O*t*-Bu). FT-IR (film) ν = 1731 cm⁻¹ (C=O). M_n = 69.5 kg/mol, PDI = 5.2 (SEC using THF as eluent at 40 °C).

4.4.9. Synthesis of PB-*g*-PAA

PB-*g*-PtBA (25.0 mg of 6.4 mol % *t*BA-grafted polymer, 0.025 mmol *t*BA concentration) and a magnetic stirring bar were placed into a vial and capped with Teflon-lined septum. The vial was evacuated and backfilled with nitrogen three times. Dichloromethane (1 mL) was added to the vial, and the polymer was dissolved by applying gentle heating. TFA (37 μ L, 0.5 mmol, 20 equiv to *t*BA concentration) was added to the polymer solution, and it was then stirred for 24 h at room temperature under nitrogen. Cold methanol (4 mL) was added to precipitate the polymer as a white solid which was filtered and washed with additional methanol (3 \times 10 mL). The polymer product was dried under vacuum and dissolved in THF (3 mL). After filtration through a short plug of celite, the THF solution was concentrated to approximately 2 mL using a rotary evaporator and added to cold methanol (4 mL) to precipitate the polymer as a white solid. The solid product was filtered, washed with methanol (3 \times 10 mL), and dried

under vacuum at 60 °C for 12 h. Yield: 15.0 mg (60% based on polymer weight). ¹H NMR (400 MHz, THF-*d*₈, ppm): 0.88 (t, 3H, CH₃ of the PB unit side chain), 1.09 and 1.17 (m, 2H, –CH₂– of the PB unit backbone), 1.32 (m, 3H, –CH– of the PB unit backbone and –CH₂– of the PB unit side chain), 2.48 (br, –CH₂CH(CO₂H)–), 4.06 (br, –CH₂CH₂OC(=O), 10.85 (s, –CO₂H). FT-IR (film) ν = 1715 (C=O).

4.4.10. Synthesis of PB-*g*-PMMA (Entry 3 of Table 3.4)

In a nitrogen-filled glove box, PB–Br (50.0 mg, 7.0×10^{-3} mmol Br concentration), toluene (2.1 g), and a magnetic stirring bar were placed in a 25-mL vial. The vial was removed from the glove box, and PB–Br was dissolved with gentle heating. A catalyst solution (1.7 mL) composed of Cu(I)Br (1.0 mg, 7.0×10^{-3} mmol), PMDETA (2.4 mg, 1.4×10^{-2} mmol), toluene (1.4 g), and MMA (70.0 mg, 0.70 mmol) was placed in a vial in a glove box and transferred to the vial containing the PB–Br solution. The mixture was stirred at room temperature for 5 min and at 90 °C for 10 h. After cooling the reaction mixture, toluene (15 mL) was added, and the solution was filtered through a short plug of celite to remove the metal catalyst. The filtrate was concentrated to ca. 3 mL using a rotary evaporator, and cold methanol (10 mL) was added to precipitate the polymer as a white solid. The solid was filtered and dried under vacuum at 60 °C for 12 h. Yield: 64.0 mg (128% based on polymer weight). ¹H NMR (400 MHz, CDCl₃, ppm): 0.85 (t, 3H, CH₃ of the PB unit side chain), 1.01 and 1.10 (m, 2H, –CH₂– of the PB unit backbone), 1.28 (m, 3H, –CH– of the PB unit backbone and –CH₂– of the PB unit side chain), 1.78–1.99 (m, 2H, –CH₂C(CH₃)(CO₂CH₃)–), 3.60 (s, 1H, –CH₂C(CH₃)(CO₂CH₃)–), 4.04 (2H, –CH₂CH₂OC(=O)–). FT-IR (film) ν = 1740 cm⁻¹ (C=O). M_n = 102.5 kg/mol, PDI = 10.5 (SEC using 1,2,4-trichlorobenzene as eluent at 160 °C).

4.5. Conclusion

The regioselective rhodium-catalyzed borylation of C–H bonds introduced a boronic ester functionality at the terminal methyl group of side chain of a commercial high-molecular-weight crystalline polyolefin, isotactic poly(1-butene). The boronic ester group of the polymer was selectively converted into hydroxy group by subsequent oxidation at the side chain termini. The functionalization did not disturb the M_n or the molecular weight distribution significantly compared with those of the parent material. The concentration of functionalized side chains could easily be controlled by changing the ratio of diboron reagent to polymer repeating units in the rhodium-catalyzed borylation. Esterification of the hydroxylated polymer generated a macroinitiator that has an α -bromoester group at the end of side chain of the polymer. We successfully synthesized high-molecular-weight polar block grafted polyolefins, PB-*g*-PMMA and PB-*g*-PtBA, by ATRP of polar vinyl monomers from the macroinitiator. Hydrolysis of PB-*g*-PtBA created an amphiphilic graft copolymer of the polyolefin, PB-*g*-PAA. Development of the amphiphilic graft copolymer from an easily accessible commercial polyolefin offers a convenient alternative way to synthesize new polyolefin-based functionalized materials and expand their potential applications.

REFERENCES

1. Malanga, M. "Syndiotactic polystyrene materials." *Adv. Mater.* **2000**, *12*, 1869–1872.
2. Boffa, L. S.; Novak, B. M. "Copolymerization of polar monomers with olefins using transition-metal complexes." *Chem. Rev.* **2000**, *100*, 1479–1493.
3. Kim, K. H.; Jo, W. H.; Kwak, S.; Kim, K. U.; Kim, J. "Synthesis of 4-*tert*-butyldimethylsilyloxystyrene and its copolymerization with styrene using (η^5 -indenyl) trichlorotitanium in the presence of methylaluminumoxane." *Macromol. Rapid Commun.* **1999**, *20*, 175–178.
4. Dong, J. Y.; Manias, E.; Chung, T. C. "Functionalized syndiotactic polystyrene polymers prepared by the combination of metallocene catalyst and borane comonomer." *Macromolecules* **2002**, *35*, 3439–3447.
5. Boen, N. K.; Hillmyer, M. A. "Post-polymerization functionalization of polyolefins." *Chem. Soc. Rev.* **2005**, *34*, 267–275.
6. Cheung, W. K. Modification of Polystyrene. In *Polymer Modification*; Meister, J. J., Ed.; Marcel Dekker: New York 2000; Chapter 8.
7. Orlor, E. B.; Moore, R. B. "Influence of ionic interactions on the crystallization of lightly sulfonated syndiotactic polystyrene ionomers." *Macromolecules* **1994**, *27*, 4774–4780.
8. Orlor, E. B.; Yontz, D. J.; Moore, R. B. "Sulfonation of syndiotactic polystyrene for model semicrystalline ionomer investigations." *Macromolecules* **1993**, *26*, 5157–5160.

9. Su, Z.; Li, X.; Hsu, S. L. "Spectroscopic and thermal studies of sulfonated syndiotactic polystyrene." *Macromolecules* **1994**, *27*, 287–291.
10. Li, H.-M.; Liu, J.-C.; Zhu, F.-M.; Lin, S.-A. "Synthesis and physical properties of sulfonated syndiotactic polystyrene ionomers." *Polym. Int.* **2001**, *50*, 421–428.
11. Gao, Y.; Li, S.; Li, H.; Wang, X. "Synthesis of syndiotactic-polystyrene-*graft*-poly(methyl methacrylate) and syndiotactic-polystyrene-*graft*-atactic-polystyrene by atom transfer radical polymerization." *Eur. Polym. J.* **2005**, *41*, 2329–2334.
12. Liu, S.; Sen, A. "Syntheses of syndiotactic-polystyrene-*graft*-poly(methyl methacrylate), syndiotactic-polystyrene-*graft*-poly(methyl acrylate), and syndiotactic-polystyrene-*graft*-atactic-polystyrene with defined structures by atom transfer radical polymerization." *Macromolecules* **2000**, *33*, 5106–5110.
13. Among refs 7-12, sulfonation of sPS was conducted under homogeneous conditions.
14. Chung, T. C.; Janvikul, W. "Borane-containing polyolefins: synthesis and applications." *J. Organomet. Chem.* **1999**, *581*, 176–187.
15. Paetzold, P.; Hoffmann, J. "Eine neue Methode zur Borylierung von Alkylbenzol und Polystyrol." *Chem. Ber.* **1980**, *113*, 3724–3733.
16. Farrall, M. J.; Fréchet, J. M. J. "Bromination and lithiation: two important steps in the functionalization of polystyrene resins." *J. Org. Chem.* **1976**, *41*, 3877–3882.
17. Qin, Y.; Cheng, G.; Sundararaman, A.; Jäkle, F. "Well-defined boron-containing polymeric lewis acids." *J. Am. Chem. Soc.* **2002**, *124*, 12672–12673.
18. Qin, Y.; Cheng, G.; Achara, O.; Parab, K.; Jäkle, F. "A new route to organoboron polymers via highly selective polymer modification reactions." *Macromolecules* **2004**, *37*, 7123–7131.

19. Ray, A.; Zhu, K.; Kissin, Y. V.; Cherian, A. E.; Coates, G. W.; Goldman, A. S. "Dehydrogenation of aliphatic polyolefins catalyzed by pincer-ligated iridium complexes." *Chem. Commun.* **2005**, 3388–3390.
20. Boen, N. K.; Hillmyer, M. A. "Selective and mild oxyfunctionalization of model polyolefins." *Macromolecules* **2003**, *36*, 7027–7034.
21. Kondo, Y.; García-Cuadrado, D.; Hartwig, J. F.; Boen, N. K.; Wagner, N. L.; Hillmyer, M. A. "Rhodium-catalyzed, regiospecific functionalization of polyolefins in the melt." *J. Am. Chem. Soc.* **2002**, *124*, 1164–1165.
22. Bae, C.; Hartwig, J. F.; Harris, N. K. B.; Long, R. O.; Anderson, K. S.; Hillmyer, M. A. "Catalytic hydroxylation of polypropylenes." *J. Am. Chem. Soc.* **2005**, *127*, 767–776.
23. Bae, C.; Hartwig, J. F.; Chung, H.; Harris, N. K.; Switek, K. A.; Hillmyer, M. A. "Regiospecific side-chain functionalization of linear low-density polyethylene with polar Groups." *Angew. Chem., Int. Ed.* **2005**, *44*, 6410–6412.
24. Díaz-Requejo, M. M.; Wehrmann, P.; Leatherman, M. D.; Trofimenko, S.; Mecking, S.; Brookhart, M.; Pérez, P. J. "Controlled, copper-catalyzed functionalization of polyolefins." *Macromolecules* **2005**, *38*, 4966–4969.
25. Ishiyama, T.; Takagi, J.; Ishida, K.; Miyaura, N.; Anastasi, N. R.; Hartwig, J. F. "Mild iridium-catalyzed borylation of arenes. High turnover numbers, room temperature reactions, and isolation of a potential intermediate." *J. Am. Chem. Soc.* **2002**, *124*, 390–391.
26. Ishiyama, T.; Takagi, J.; Hartwig, J. F.; Miyaura, N. "A stoichiometric aromatic C–H borylation catalyzed by iridium(I)/2,2'-bipyridine complexes at room temperature."

- Angew. Chem., Int. Ed.* **2002**, *41*, 3056–3058.
27. Cho, J.-Y.; Tse, M. K.; Holmes, D.; Maleczka, R. E., Jr.; Smith, M. R., III. “Remarkably selective iridium catalysts for the elaboration of aromatic C–H bonds.” *Science* **2002**, *295*, 305–308.
28. Tse, M. K.; Cho, J.-Y.; Smith, M. R., III. “Regioselective aromatic borylation in an inert solvent.” *Org. Lett.* **2001**, *3*, 2831–2833.
29. Cho, J.-Y.; Iverson, C. N.; Smith, M. R., III. “Steric and chelate directing effects in aromatic borylation.” *J. Am. Chem. Soc.* **2000**, *122*, 12868–12869.
30. Miyaura, N.; Suzuki, A. “Palladium-catalyzed cross-coupling reactions of organoboron compounds.” *Chem. Rev.* **1995**, *95*, 2457–2483.
31. De Rosa, C.; Ruiz de Ballesteros, O.; Di Gennaro, M.; Auriemma, F. “Crystallization from the melt of α and β forms of syndiotactic polystyrene.” *Polymer* **2003**, *44*, 1861–1870.
32. Guerra, G.; Vitagliano, V. M.; De Rosa, C.; Petraccone, V.; Corradini, P. “Polymorphism in melt crystallized syndiotactic polystyrene samples.” *Macromolecules* **1990**, *23*, 1539–1544.
33. Lin, R. H.; Woo, E. M. “Melting behavior and identification of polymorphic crystals in syndiotactic polystyrene.” *Polymer* **2000**, *41*, 121–131.
34. Song, C. E.; Lee, S.-G. “Supported chiral catalysts on inorganic materials.” *Chem. Rev.* **2002**, *102*, 3495–3524.
35. (a) Merrifield, R. B. “Solid phase peptide synthesis. I. the synthesis of a tetrapeptide.” *J. Am. Chem. Soc.* **1963**, *85*, 2149–2154. (b) Wang, S.-S. “*p*-Alkoxybenzyl alcohol resin and *p*-alkoxybenzyloxycarbonylhydrazide resin for solid phase synthesis of

- protected peptide fragments.” *J. Am. Chem. Soc.* **1973**, *95*, 1328–1333.
36. Seki, M. “Recent advances in Pd/C-catalyzed coupling reactions.” *Synthesis* **2006**, 2975–2992.
37. Djakovitch, L.; Rollet, P. “Sonogashira cross-coupling reactions catalysed by copper-free palladium zeolites.” *Adv. Synth. Catal.* **2004**, *346*, 1782–1792.
38. Köhler, K.; Wagner, M.; Djakovitch, L. “Supported palladium as catalyst for carbon–carbon bond construction (Heck reaction) in organic synthesis.” *Catal. Today* **2001**, *66*, 105–114.
39. Goyal, P.; Zheng, X.; Weck, M. “Enhanced cooperativity in hydrolytic kinetic resolution of epoxides using poly(styrene) resin-supported dendronized Co-(salen) catalysts.” *Adv. Synth. Catal.* **2008**, *350*, 1816–1822.
40. Shiels, R. A.; Venkatasubbaiah, K.; Jones, C. W. “Polymer and silica supported tridentate schiff base vanadium catalysts for the asymmetric oxidation of ethyl mandelate –activity, stability and recyclability.” *Adv. Synth. Catal.* **2008**, *350*, 2823–2834.
41. Van Heerbeek, R.; Kamer, P. C. J.; Van Leeuwen, P. W. N. M.; Reek, J. N. H. “Dendrimers as support for recoverable catalysts and reagents.” *Chem. Rev.* **2002**, *102*, 3717–3756.
42. (a) Kuang, Y.-Q.; Zhang, S.-Y.; Wei, L.-L. “A simple and effective soluble polymer-bound ligand for the asymmetric dihydroxylation of olefins: DHQD-PHAL-OPEG-OMe.” *Tetrahedron Lett.* **2001**, *42*, 5925–5927. (b) Flood, R. W.; Geller, T. P.; Petty, S. A.; Roberts, S. M.; John S.; Volk, M. “Efficient asymmetric epoxidation of α,β -unsaturated ketones using a soluble triblock polyethylene glycol-polyamino acid

- catalyst.” *Org. Lett.* **2001**, *3*, 683–686. (c) Bergbreiter, D. E.; Osburn, P. L.; Liu, Y.-S. “Tridentate SCS palladium(II) complexes: new, highly stable, recyclable catalysts for the Heck reaction.” *J. Am. Chem. Soc.* **1999**, *121*, 9531–9538.
43. (a) Bergbreiter, D. E.; Blanton, J. R. “Functionalized ethylene oligomers as phase-transfer catalysts.” *J. Org. Chem.* **1985**, *50*, 5828–5833. (b) Bergbreiter, D. E.; Weatherford, D. A. “Polyethylene-bound soluble recoverable palladium(0) catalysts.” *J. Org. Chem.* **1989**, *54*, 2726–2730. (c) Bergbreiter, D. E.; Chandran, R. “Polyethylene-bound rhodium(I) hydrogenation catalysts.” *J. Am. Chem. Soc.* **1987** *109*, 174–179.
44. (a) Doherty, S.; Robins, E. G.; Pál, I.; Newman, C. R.; Hardacre, C.; Rooney, D.; Mooney, D. A. “Polymer-supported phosphoramidites: highly efficient and recyclable catalysts for asymmetric hydrogenation of dimethylitaconate and dehydroamino acids and esters.” *Tetrahedron: Asymmetry* **2003**, *14*, 1517–1527. (b) Datta A.; Plenio, H. “Nonpolar biphasic catalysis: Sonogashira and Suzuki coupling of aryl bromides and chlorides.” *Chem. Comm.* **2003**, 1504–1505. (c) Giffels, G.; Beliczey, J.; Felder, M.; Kragl, U. “Polymer enlarged oxazaborolidines in a membrane reactor: enhancing effectivity by retention of the homogeneous catalyst.” *Tetrahedron: Asymmetry* **1998**, *9*, 691–696.
45. There have been reports on the recovery yield of soluble polymer supports. See, for example: (a) Lau, K. C. Y.; He, H. S.; Chiu, P.; Toy, P. H. “Polystyrene-supported triphenylarsine reagents and their use in suzuki cross-coupling reactions.” *J. Comb. Chem.* **2004**, *6*, 955–960. (b) Manzotti, R.; Tang, S.-Y.; Janda, K. D. “Improved synthesis of prostanoids on a non-cross-linked polystyrene soluble support.”

- Tetrahedron* **2000**, *56*, 7885–7892. (c) Enholm, E. J.; Gallagher, M. E.; Moran, K. M.; Lombardi, J. S.; Schuttle, J. P., II. “An allylstannane reagent on non-cross-linked polystyrene support.” *Org. Lett.* **1999**, *1*, 689–691.
46. (a) Malanga, M. “Syndiotactic polystyrene materials.” *Adv. Mater.* **2000**, *12*, 1869–1872. (b) Su, Z.; Li, X.; Hsu, S. L. “Spectroscopic and thermal studies of sulfonated syndiotactic polystyrene.” *Macromolecules* **1994**, *27*, 287–291. (c) Dong, J. Y.; Manias, E.; Chung, T. C. “Functionalized syndiotactic polystyrene polymers prepared by the combination of metallocene catalyst and borane comonomer.” *Macromolecules* **2002**, *35*, 3439–3447.
47. Shin, J.; Jensen, S. M.; Ju, J.; Lee, S.; Xue, Z.; Noh, S. K.; Bae, C. “Controlled functionalization of crystalline polystyrenes via activation of aromatic C-H bonds.” *Macromolecules* **2007**, *40*, 8600–8608.
48. (a) Harrison, C. R.; Hodge, P.; Hunt, B. J.; Khoshdel, E.; Richardson, G. “Preparation of alkyl chlorides, acid chlorides, and amides using polymer-supported phosphines and carbon tetrachloride: mechanism of these reactions.” *J. Org. Chem.* **1983**, *48*, 3721–3728. (b) Charette, A. B.; Boezio, A. A.; Janes, M. K. “Synthesis of a triphenylphosphine reagent on non-cross-linked polystyrene support: application to the Staudinger/aza-Wittig Reaction.” *Org. Lett.* **2000**, *2*, 3777–3779. (c) Wentworth, P., Jr.; Vandersteen, A. M.; Janda, K. D. “Poly(ethylene glycol) (PEG) as a reagent support: the preparation and utility of a PEG–triarylphosphine conjugate in liquid-phase organic synthesis (LPOS).” *Chem. Commun.* **1997**, 759–760. (d) Bergbreiter, D. E.; Blanton, J. R. “Diphenylphosphinated ethylene oligomers as polymeric reagents for synthesis of alkyl chlorides from alcohols.” *J. Chem. Soc. Chem.*

- Commun.* **1985**, 337–338. (e) Bergbreiter, D. E.; Li, C. “Poly(4-*tert*-butylstyrene) as a soluble polymer support in homogeneous catalysis.” *Org. Lett.* **2003**, *5*, 2445–2447.
49. Miyaura, N.; Suzuki, A. “Palladium-catalyzed cross-coupling reactions of organoboron compounds.” *Chem. Rev.* **1995**, *95*, 2457–2483.
50. (a) Pham, N. T. S.; Van Der Sluys, M.; Jones, C. W. “On the nature of the active species in palladium catalyzed Mizoroki–Heck and Suzuki–Miyaura couplings – homogeneous or heterogeneous catalysis, a critical review.” *Adv. Synth. Catal.* **2006**, *348*, 609–679. (b) Lee, D.-H.; Kim, J.-H.; Jun, B.-H.; Kang, H.; Park, J.; Lee, Y.-S. “Macroporous polystyrene-supported palladium catalyst containing a bulky N-heterocyclic carbene ligand for suzuki reaction of aryl chlorides.” *Org. Lett.* **2008**, *10*, 1609–1612. (c) Schweizer, S.; Becht, J.-M.; Le Drian, C. “Highly efficient and reusable supported Pd catalysts for Suzuki-Miyaura reactions of aryl chlorides.” *Org. Lett.* **2007**, *9*, 3777–3780. (d) Yang, Q.; Ma, S.; Li, J.; Xiao, F.; Xiong, H. “A water-compatible, highly active and reusable PEG-coated mesoporous silica-supported palladium complex and its application in Suzuki coupling reactions.” *Chem. Commun.* **2006**, 2495–2497. (e) Nishio, R.; Sugiura, M.; Kobayashi, S. “Novel polymer incarcerated palladium with phosphinated polymers: active catalyst for Suzuki-Miyaura coupling without external phosphines.” *Org. Lett.* **2005**, *7*, 4831–4834. (f) Phan, N. T. S.; Brown, D. H.; Styring, P. “A polymer-supported salen-type palladium complex as a catalyst for the Suzuki–Miyaura cross-coupling reaction.” *Tetrahedron Lett.* **2004**, *45*, 7915–7917. (g) Parrish, C. A.; Buchwald, S. L. “Use of polymer-supported dialkylphosphinobiphenyl ligands for palladium-catalyzed amination and Suzuki Reactions.” *J. Org. Chem.* **2001**, *66*, 3820–3827.

51. (a) Sommera, W. J.; Weck, M. "Poly(norbornene)-supported N-heterocyclic carbenes as ligands in catalysis." *Adv. Synth. Catal.* **2006**, *348*, 2101–2113. (b) Leyva, A.; García, H.; Corma, A. "A soluble polyethyleneglycol-anchored phosphine as a highly active, reusable ligand for Pd-catalyzed couplings of aryl chlorides: comparison with cross and non-crosslinked polystyrene and silica supports." *Tetrahedron* **2007**, *63*, 7097–7111. (c) Stevens, P. D.; Li, G.; Fan, J.; Yen, M.; Gao, Y. "Recycling of homogeneous Pd catalysts using superparamagnetic nanoparticles as novel soluble supports for Suzuki, Heck, and Sonogashira cross-coupling reactions." *Chem. Commun.* **2005**, 4435–4437.
52. (a) Joshaghani, M.; Faramarzi, E.; Rafiee, E.; Daryanavard, M.; Xiao, J.; Baillie, C. "Efficient Suzuki cross-coupling reactions using bulky phosphines." *J. Mol. Catal. A: Chem.* **2006**, *259*, 35–40. (b) Grushin, V. V.; Alper, H. "Transformations of chloroarenes, catalyzed by transition-metal complexes." *Chem. Rev.* **1994**, *94*, 1047–1062.
53. (a) Thomas, C. M.; Peters, J. C. "Coordinating anions: (phosphino)tetraphenyl borate ligands as new reagents for synthesis." *Inorg. Chem.* **2004**, *43*, 8–10. (b) Tunney, S. E.; Stille, J. K. "Palladium-catalyzed coupling of aryl halides with (trimethylstannyl) diphenylphosphine and (trimethylsilyl)diphenylphosphine." *J. Org. Chem.* **1987**, *52*, 748–753.
54. Desmarets, C.; Omar-Amrani, R.; Walcarious, A.; Lambert, J.; Champagne, B.; Fort, Y.; Schneider, R. "Naphthidine di(radical cation)s-stabilized palladium nanoparticles for efficient catalytic Suzuki–Miyaura cross-coupling reactions." *Tetrahedron* **2008**, *64*, 372–381.

55. Mu, B.; Li, T.; Xu, W.; Zeng, G.; Liu, P.; Wu, Y. "Synthesis, characterization, and applications in Heck and Suzuki coupling reactions of amphiphilic cyclopalladated ferrocenylimines." *Tetrahedron* **2007**, *63*, 11475–11488.
56. Zhang, L.; Meng, T.; Wu, J. "Palladium-catalyzed Suzuki-Miyaura cross-couplings of aryl tosylates with potassium aryltrifluoroborates." *J. Org. Chem.* **2007**, *72*, 9346–9349.
57. Mao, J.; Guo, J.; Fang, F.; Ji, S.-J. "Highly efficient copper(0)-catalyzed Suzuki-Miyaura cross-coupling reactions in reusable PEG-400." *Tetrahedron*, **2008**, *64*, 3905–3911.
58. Tao, B.; Boykin, D. W. "Simple amine/Pd(OAc)₂-catalyzed Suzuki coupling reactions of aryl bromides under mild aerobic conditions." *J. Org. Chem.* **2004**, *69*, 4330–4335.
59. Hermanson, N. J.; Wessel T. E. "Syndiotactic polystyrene: a new polymer for high-performance medical applications." *Medical Plastics and Biomaterials* **1998**, 10–15.
60. Malanga, M. "Syndiotactic polystyrene materials." *Adv. Mater.* **2000**, *12*, 1869–1872.
61. Kim, K. H.; Jo, W. H.; Kwak, S.; Kim, K. U.; Kim, J. "Synthesis of 4-*tert*-butyldimethylsilyloxystyrene and its copolymerization with styrene using (η^5 -indenyl) trichlorotitanium in the presence of methylaluminumoxane." *Macromol. Rapid Commun.* **1999**, *20*, 175–178.
62. Dong, J. Y.; Manias, E.; Chung, T. C. "Functionalized syndiotactic polystyrene polymers prepared by the combination of metallocene catalyst and borane comonomer." *Macromolecules* **2002**, *35*, 3439–3447.

63. Orlor, E. B.; Moore, R. B. "Influence of ionic interactions on the crystallization of lightly sulfonated syndiotactic polystyrene ionomers." *Macromolecules* **1994**, *27*, 4774–4780.
64. Orlor, E. B.; Yontz, D. J.; Moore, R. B. "Sulfonation of syndiotactic polystyrene for model semicrystalline ionomer investigations." *Macromolecules* **1993**, *26*, 5157–5160.
65. Su, Z.; Li, X.; Hsu, S. L. "Spectroscopic and thermal studies of sulfonated syndiotactic polystyrene." *Macromolecules* **1994**, *27*, 287–291.
66. Li, H.-M.; Liu, J.-C.; Zhu, F.-M.; Lin, S.-A. "Synthesis and physical properties of sulfonated syndiotactic polystyrene ionomers." *Polym. Int.* **2001**, *50*, 421–428.
67. Gao, Y.; Li, S.; Li, H.; Wang, X. "Synthesis of syndiotactic-polystyrene-graft-poly(methyl methacrylate) and syndiotactic-polystyrene-graft-atactic-polystyrene by atom transfer radical polymerization." *Eur. Polym. J.* **2005**, *41*, 2329–2334.
68. Liu, S.; Sen, A. "Syntheses of syndiotactic-polystyrene-graft-poly(methyl methacrylate), syndiotactic-polystyrene-graft-poly(methyl acrylate), and syndiotactic-polystyrene-graft-atactic-polystyrene with defined sStructures by atom transfer radical polymerization." *Macromolecules* **2000**, *33*, 5106–5110.
69. Li, H.-M.; Chen, H.-B.; Shen, Z.-G.; Lin, S. "Preparation and characterization of maleic anhydride-functionalized syndiotactic polystyrene." *Polymer* **2002**, *43*, 5455–5461.
70. Shin, J.; Jensen, S. M.; Ju, J.; Lee, S.; Xue, Z.; Noh, S. K.; Bae, C. "Controlled Functionalization of Crystalline Polystyrenes via Activation of Aromatic C–H Bonds." *Macromolecules* **2007**, *40*, 8600–8608.

71. Farrall, M. J.; Fréchet, J. M. J. "Functionalization of polystyrene resins by chemical modification: characterization of halogenated polystyrenes by carbon-13 Nuclear magnetic resonance spectroscopy." *Macromolecules* **1979**, *12*, 426–428.
72. Kambour, R. P.; Bendler, J. T.; Bopp, R. C. "Phase behavior of polystyrene, poly(2,6-dimethyl-1,4-phenylene oxide), and Their Brominated Derivatives." *Macromolecules* **1983**, *16*, 753–757.
73. Genzer, J.; Faldi, A.; Oslanec, R.; Composto, R. J. "Surface enrichment in a miscible polymer blend: an experimental test of self-consistent field and long-wavelength approximation models." *Macromolecules* **1996**, *29*, 5438–5445.
74. Lukey, C. A.; Tymichova, M.; Brown, H. R. "Novel route to styrene/*p*-aminostyrene copolymers." *J. Polym. Sci., Polym. Chem.* **2007**, *45*, 1282–1286.
75. (a) Thomas, G. L.; Ladlow, M.; Spring, D. R. "Complete functionalisation of small and large diameter bromopolystyrene beads; applications for solid-supported reagents, scavengers and diversity-oriented synthesis." *Org. Biomol. Chem.* **2004**, *2*, 1679–1681. (b) Thomas, G. L.; Böhner, C.; Ladlow, M.; Spring, D. R. "Synthesis and utilization of functionalized polystyrene resins." *Tetrahedron* **2005**, *61*, 12153–12157. (c) Farrall, M. J.; Fréchet, J. M. J. "Bromination and lithiation: two important steps in the functionalization of polystyrene resins." *J. Org. Chem.* **1976**, *41*, 3877–3882. (d) O'Brien, R. A.; Rieke, R. D. "Direct metalation of *p*-bromopolystyrene using highly reactive copper and preparation and reaction of highly reactive copper bound to an insoluble polymer." *J. Org. Chem.* **1990**, *55*, 788–790. (e) Chen, Y.; Huang, Z.-E.; Cai, R.-F.; Kong, S.-Q.; Chen, S.; Shao, Q.; Yan, X.; Zhao, F.; Fu, D. "Synthesis and characterization of soluble C₆₀-chemically modified poly(*p*-bromostyrene)." *J.*

- Polym. Sci., Polym. Chem.* **1996**, *34*, 3297–3302.
76. De Girolamo Del Mauro, A.; Loffredo, F.; Venditto, V.; Longo, P.; Guerra, G. “Polymorphic Behavior of Syndiotactic Poly(*p*-chlorostyrene) and styrene/*p*-chlorostyrene cosyndiotactic random copolymers.” *Macromolecules* **2003**, *36*, 7577–7584.
77. Miyaura, N.; Suzuki, A. “Palladium-catalyzed cross-coupling reactions of organoboron compounds.” *Chem. Rev.* **1995**, *95*, 2457–2483.
78. Bertini, F.; Audisio, G.; Kiji, J. “Thermal behavior and degradation mechanism of brominated polystyrenes.” *J. Anal. Appl. Pyrolysis* **1995**, *33*, 213–230.
79. Boinon, B.; Abboud, W.; Bouras, A.; Ainad-Tabet, D. “Kinetics of the thermal degradation of partially *para*-brominated polystyrenes.” *Polym. Deg. Stab.* **1993**, *42*, 75–80.
80. De Rosa, C.; Ruiz de Ballesteros, O.; Di Gennaro, M.; Auriemma, F. “Crystallization from the melt of α and β forms of syndiotactic polystyrene.” *Polymer* **2003**, *44*, 1861–1870.
81. Guerra, G.; Vitagliano, V. M.; De Rosa, C.; Petraccone, V.; Corradini, P. “Polymorphism in melt crystallized syndiotactic polystyrene samples.” *Macromolecules* **1990**, *23*, 1539–1544.
82. Lin, R. H.; Woo, E. M. “Melting behavior and identification of polymorphic crystals in syndiotactic polystyrene.” *Polymer* **2000**, *41*, 121–131.
83. Albizzati, E.; Galimberti, M. “Catalysts for olefins polymerization.” *Catal. Today* **1998**, *41*, 159–168.
84. Boffa, L. S.; Novak, B. M. “Copolymerization of polar monomers with olefins using

- transition-metal complexes.” *Chem. Rev.* **2000**, *100*, 1479–1493.
85. Ittel, S. D.; Johnson, L. K.; Brookhart, M. “Late-metal catalysts for ethylene homo- and copolymerization.” *Chem. Rev.* **2000**, *100*, 1169–1203.
86. Chung T. C. “Synthesis of functional polyolefin copolymers with graft and block structures.” *Prog. Polym. Sci.* **2002**, *27*, 39–85.
87. Chung T. C.; Rhubright D. “Synthesis of functionalized polypropylene.” *Macromolecules* **1991**, *24*, 970–972.
88. Kesti, M. R.; Coates, G. W.; Waymouth, R. M. “Homogeneous Ziegler-Natta polymerization of functionalized monomers catalyzed by cationic Group IV metallocenes.” *J. Am. Chem. Soc.* **1992**, *114*, 9679–9680.
89. Kawaoka, A. M.; Marks, T. J. “Organolanthanide-catalyzed synthesis of phosphine-terminated polyethylenes. Scope and mechanism.” *J. Am. Chem. Soc.* **2005**, *127*, 6311–6324.
90. Koo, K.; Fu, P.-F.; Marks, T. J. “Organolanthanide-mediated silanolytic chain transfer processes. Scope and mechanism of single reactor catalytic routes to silapolyolefins.” *Macromolecules* **1999**, *32*, 981–988.
91. Xu, G.; Chung, T. C. “Borane chain transfer agent in metallocene-mediated olefin polymerization. Synthesis of borane-terminated polyethylene and diblock copolymers containing polyethylene and polar polymer.” *J. Am. Chem. Soc.* **1999**, *121*, 6763–6764.
92. Boone, H. W.; Athey, P. S.; Mullins, M. J.; Philipp, D.; Muller, R.; Goddard, W. A. “Copolymerization studies of vinyl chloride and vinyl acetate with ethylene using a transition-metal catalyst.” *J. Am. Chem. Soc.* **2002**, *124*, 8790–8791.

93. Younkin, T. R.; Connor, E. F.; Henderson, J. I.; Friedrich, S. K.; Grubbs, R. H.; Bansleben, D. A. "Neutral, single-component nickel(II) polyolefin catalysts that tolerate heteroatoms." *Science* **2000**, *287*, 460–462.
94. Connor, E. F.; Younkin, T. R.; Henderson, J. I.; Hwang, S.; Grubbs, R. H.; Roberts, W. P.; Litzau, J. J. "Linear functionalized polyethylene prepared with highly active neutral Ni(II) complexes." *J. Polym. Sci. Part A: Polym. Chem.* **2002**, *40*, 2842–2854.
95. Gibson, V. C.; Tomov, A. "Functionalized polyolefin synthesis using [P,O]Ni catalysts." *Chem. Commun.* **2001**, 1964–1965.
96. Johnson, L. K.; Mecking, S.; Brookhart, M. "Copolymerization of ethylene and propylene with functionalized vinyl monomers by palladium(II) catalysts." *J. Am. Chem. Soc.* **1996**, *118*, 267–268.
97. Chen, G.; Ma, X. S.; Guan, Z. "Synthesis of functional olefin copolymers with controllable topologies using a chain-walking catalyst." *J. Am. Chem. Soc.* **2003**, *125*, 6697–6704.
98. Liu, S.; Elyashiv, S.; Sen, A. "Copper-mediated controlled copolymerization of methyl acrylate with 1-alkenes under mild conditions." *J. Am. Chem. Soc.* **2001**, *123*, 12738–12739.
99. Liu, S.; Gu, B.; Rowlands, H. A.; Sen, A. "Controlled random and alternating copolymerization of methyl acrylate with 1-alkenes." *Macromolecules* **2004**, *37*, 7924–7929.
100. Boen, N. K.; Hillmyer, M. A. "Post-polymerization functionalization of polyolefins." *Chem. Soc. Rev.* **2005**, *34*, 267–275.
101. Kondo, Y.; García-Cuadrado, D.; Hartwig, J. F.; Boen, N. K.; Wagner, N. L.;

- Hillmyer, M. A. "Rhodium-catalyzed, regiospecific functionalization of polyolefins in the melt." *J. Am. Chem. Soc.* **2002**, *124*, 1164–1165.
102. Boen, N. K.; Hillmyer, M. A. "Selective and mild oxyfunctionalization of model polyolefins." *Macromolecules* **2003**, *36*, 7027–7034.
103. Ray, A.; Zhu, K.; Kissin, Y. V.; Cherian, A. E.; Coates, G. W.; Goldman, A. S. "Dehydrogenation of aliphatic polyolefins catalyzed by pincer-ligated iridium complexes." *Chem. Commun.* **2005**, 3388–3390.
104. Díaz-Requejo, M. M.; Wehrmann, P.; Leatherman M. D.; Trofimenko, S.; Mecking, S.; Brookhart, M.; Pérez, P. J. "Controlled, copper-catalyzed functionalization of polyolefins." *Macromolecules* **2005**, *38*, 4966–4969.
105. Bae, C.; Hartwig J. F.; Harris, N. K. B.; Long, R. O.; Anderson, K. S.; Hillmyer, M. A. "Catalytic hydroxylation of polypropylenes." *J. Am. Chem. Soc.* **2005**, *127*, 767–776.
106. Bae, C.; Hartwig J. F.; Chung, H.; Harris, N. K.; Switek, K. A.; Hillmyer, M. A. "Regiospecific side-chain functionalization of linear low-density polyethylene with polar groups." *Angew. Chem., Int. Ed.* **2005**, *44*, 6410–6413.
107. Shin, J.; Jensen, S. M.; Ju, J.; Lee, W.; Xue, Z.; Noh, S. K.; Bae, C. "Controlled functionalization of crystalline polystyrenes via activation of aromatic C-H bonds." *Macromolecules* **2007**, *40*, 8600–8608.
108. Inoue, Y.; Matsugi, T.; Kashiwa, N.; Matyjaszewski, K. "Graft copolymers from linear polyethylene via atom transfer radical polymerization." *Macromolecules* **2004**, *37*, 3651–3658.
109. Liu, S.; Sen, A. "Syntheses of *syndiotactic*-polystyrene-*graft*-poly(methyl

- methacrylate), *syndiotactic*-polystyrene-*graft*-poly(methyl acrylate), and *syndiotactic*-polystyrene-*graft*-*atactic*-polystyrene with defined structures by atom transfer radical polymerization.” *Macromolecules* **2000**, *33*, 5106–5110.
110. Liu, S.; Sen, A. “Synthesis of novel linear polyethylene-based graft copolymers by atom transfer radical polymerization.” *Macromolecules* **2001**, *34*, 1529–1532.
111. Kaneyoshi, H.; Inoue, Y.; Matyjaszewski, K. “Synthesis of block and graft copolymers with linear polyethylene segments by combination of degenerative transfer coordination polymerization and atom transfer radical polymerization.” *Macromolecules* **2005**, *38*, 5425–5435.
112. Hong, S. C.; Jia, S.; Teodorescu, M.; Kowalewski, T.; Matyjaszewski, K.; Gottfried, A. C.; Brookhart, M. “Polyolefin graft copolymers via living polymerization techniques: Preparation of poly(*n*-butyl acrylate)-*graft*-polyethylene through the combination of Pd-mediated living olefin polymerization and atom transfer radical polymerization.” *J. Polym. Sci. Part A: Polym. Chem.* **2002**, *40*, 2736–2749.
113. Inoue, Y.; Matyjaszewski, K. “Preparation of polyethylene block copolymers by a combination of postmetallocene catalysis of ethylene polymerization and atom transfer radical polymerization.” *J. Polym. Sci. Part A: Polym. Chem.* **2004**, *42*, 496–504.
114. Matyjaszewski, K.; Teodorescu, M.; Miller, P. J.; Peterson, M. L. “Graft copolymers of polyethylene by atom transfer radical polymerization.” *J. Polym. Sci. Part A: Polym. Chem.* **2000**, *38*, 2440–2448.
115. Hwu, J.-M.; Chang, M.-J.; Lin, J.-C.; Cheng, H.-Y.; Jiang, G.-J. “Synthesis and application of functional polyethylene graft copolymers by atom transfer radical

- polymerization.” *J. Organometallic Chem.* **2005**, *690*, 6300–6308.
116. Cao, C.; Zou, J.; Dong, J.-Y.; Hu, Y.; Chung, T. C. “Synthesis of polypropylene graft copolymers by the combination of a polypropylene copolymer containing pendant vinylbenzene groups and atom transfer radical polymerization.” *J. Polym. Sci. Part A: Polym. Chem.* **2005**, *43*, 429–437.
117. Baughman, T. W.; Chan, C. D.; Winey, K. I.; Wagener, K. B. “Synthesis and morphology of well-defined poly(ethylene-*co*-acrylic acid) copolymers.” *Macromolecules* **2007**, *40*, 6564–6571.
118. Matsugi, T.; Kojoh, S.-I.; Kawahara, N.; Matsuo, S.; Kaneko, H.; Kashiwa, N. J. “Synthesis and morphology of polyethylene-*block*-poly(methyl methacrylate) through the combination of metallocene catalysis with living radical polymerization.” *Polym. Sci. Part A: Polym. Chem.* **2003**, *41*, 3965–3973.
119. Yamamoto, K.; Tanaka, H.; Sakaguchi, M.; Shimada, S. “Well-defined poly(methyl methacrylate) grafted to polyethylene with reverse atom transfer radical polymerization initiated by peroxides.” *Polymer* **2003**, *44*, 7661–7669.
120. Biswas, A.; Bandyopadhyay, A.; Singha, N. K.; Bhowmick, A. K. “Chemical modification of metallocene-based polyolefinic elastomers by acrylic acid and its influence on physico-mechanical properties: Effect of reaction parameters, crystallinity and pendant chain length.” *J. Polym. Sci. Part A: Polym. Chem.* **2007**, *45*, 5529–5540.
121. Badel, T.; Beyou, E.; Bounor-Legaré, V.; Chaumont, P.; Flat, J. J.; Michel, A. “Melt grafting of polymethyl methacrylate onto poly(ethylene-*co*-1-octene) by reactive extrusion: Model compound approach.” *J. Polym. Sci. Part A: Polym. Chem.* **2007**,

- 45, 5215–5226.
122. Bryaskova, R.; Willet, N.; Degée, P.; Dubois, P.; Jérôme, R.; Detrembleur, C. “Copolymerization of vinyl acetate with 1-octene and ethylene by cobalt-mediated radical polymerization.” *J. Polym. Sci. Part A: Polym. Chem.* **2007**, *45*, 2532–2542.
123. Caporaso, L.; Oliva, L. “Synthesis of hydrophilic isotactic polypropylenes promoted by metallocene catalysts.” *J. Polym. Sci. Part A: Polym. Chem.* **2006**, *44*, 7008–7013.
124. Berda, E. B.; Baughman, T. W.; Wagener, K. B. “Precision branching in ethylene copolymers: Synthesis and thermal behavior.” *J. Polym. Sci. Part A: Polym. Chem.* **2006**, *44*, 4981–4989.
125. Carlini, C.; De Luise, V.; Martinelli, M.; Raspolli Galletti, A. M.; Sbrana, G. “Homo- and copolymerization of methyl methacrylate with ethylene by novel Ziegler-Natta-Type nickel catalysts based on N,O-nitro-substituted chelate ligands.” *J. Polym. Sci. Part A: Polym. Chem.* **2006**, *44*, 620–633.
126. Chen, H.; Schlecht, S.; Semple, T. C.; Hartwig, J. F. “Thermal, catalytic, regiospecific functionalization of alkanes.” *Science* **2000**, *287*, 1995–1997.
127. White, C.; Yates, A.; Maitlis, P. M. In *Inorganic Synthesis*; Grimes, R. N., Ed.; Wiley: New York, 1992; Vol. 29, pp 228–230.
128. Bowyer, W. J.; Merkert, J. W.; Geiger, W. E.; Rheingold A. L. “Structural consequences of electron-transfer reactions. Part 18. Redox-induced hapticity changes: effect of substituents on arene bending in a series of rhodium complex.” *Organometallics* **1989**, *8*, 191–198.

VITA

Graduate College
University of Nevada Las Vegas

Jihoon Shin

Local Address:

11000 S. Eastern Ave. #1226
Henderson, Nevada 89052

Home Address:

101-708 Poonglim APT. 214 Gajwa-dong Seo-Gu
Incheon, South Korea, 404-250

Degree:

Bachelor of Engineering, Biological Engineering, 1995
Inha University, Incheon, South Korea

Master of Engineering, Chemical Engineering, 1999
Inha University, Incheon, South Korea

Special Honors and Awards:

Graduate Access Scholarship Award (UNLV) – 2009

Publications:

Jihoon Shin, Julie Bertoia, Kenneth R. Czerwinski, and Chulsung Bae “A New Homogeneous Polymer Support Based on Syndiotactic Polystyrene and Its Application in Palladium–Catalyzed Suzuki–Miyaura Cross–Coupling Reactions” *Green Chemistry*, **2009**, Accepted.

Tae Soo Jo, Se Hye Kim, Jihoon Shin, and Chulsung Bae “Highly Efficient Incorporation of Functional Groups into Aromatic Main-Chain Polymer Using Iridium-Catalyzed C–H Activation and Suzuki–Miyaura Reaction” *J. Am. Chem. Soc.* **2009**, *131*, 1656–1657.

Jihoon Shin, Andrew Y. Chang, Lacie V. Brownell, Ira O. Racoma, Coreen H. Ozawa, Ho-Yong Chung, Shufu Peng, Chulsung Bae “Hydrophilic Graft Modification of a Commercial Crystalline Polyolefin” *J. Polym. Sci. Part A: Polym. Chem.* **2008**, *46*, 3533–3545.

Jihoon Shin, Stephen M. Jensen, Jinhun Ju, Sunwoo Lee, Zhigang Xue, Seok Kyun Noh, and Chulsung Bae “Controlled functionalization of Crystalline Polystyrenes via Activation of Aromatic C–H bonds” *Macromolecules* **2007**, *40*, 8600–8608.

Jihoon Shin, Lacie V. Brownell, and Chulsung Bae “Synthesis of Graft Copolymer of Syndiotactic Polystyrene and PMMA via Activation of Inert C–H Bonds and Atoms Transfer Radical Polymerization” *Polym. Prep. (American Chemical Society, Division of Polymer Chemistry)*, **2007**, *48*, 139–140.

Geon-Joong Kim, and Ji-Hoon Shin “The Catalytic Activity of New Chiral Salen Complexes Immobilized on MCM-41 by Multi-step Grafting in the Asymmetric Epoxidation” *Tetrahedron Lett.* **1999**, *40*, 6827–6830.

Geon-Joong Kim, and Ji-Hoon Shin “Symmetric Borohydride Reduction of Ketones by Unsymmetrical Co(II) Chiral Salen Complexes” *React. Kinet. Catal. Lett.* **2000**, *69*, 183–190.

Geon-Joong Kim, and Ji-Hoon Shin “Applications of New Unsymmetrical Chiral Mn(III), Co(II,III) and Ti(IV) Salen Complexes in Enantioselective Catalytic Reaction” *Catal. Lett.* **1999**, *63*, 83–90.

Geon-Joong Kim, and Ji-Hoon Shin “The Synthesis of New Salen Complexes Immobilized on MCM-41 by Grafting and their Catalytic Activity in the Asymmetric Borohydride Reduction of Ketones” *Cata. Lett.* **1999**, *63*, 205–212.

Dissertation: Controlled Functionalization of Crystalline Polyolefins and Their Application in Soluble Polymer Support

Dissertation Examination Committee:

Chairperson, Dr. Chulsung Bae, Ph. D.

Committee Member, Dr. Ernesto Abel-Santos, Ph. D.

Committee Member, Dr. Dong-Chan Lee, Ph. D.

Graduate Faculty Representative, Dr. James C. Selser, Ph. D.